

**SIMULATION OF THE HYDROLOGICAL IMPACTS OF
CLIMATE AND LAND USE/COVER CHANGE ON TIKUR
WUHA WATERSHED IN ETHIOPIA**

Thesis

Submitted in partial fulfilment of the requirement for the degree of

DOCTOR OF PHILOSOPHY

By

ABIOT KETEMA DEMMSIE



DEPARTMENT OF WATER RESOURCES AND OCEAN
ENGINEERING
NATIONAL INSTITUTE OF TECHNOLOGY KARNATAKA,
SURATHKAL, MANGALORE – 575025
AUGUST 2021

**SIMULATION OF THE HYDROLOGICAL IMPACTS OF
CLIMATE AND LAND USE/COVER CHANGE ON TIKUR
WUHA WATERSHED IN ETHIOPIA**

Thesis

Submitted in partial fulfilment of the requirement for the degree of

DOCTOR OF PHILOSOPHY

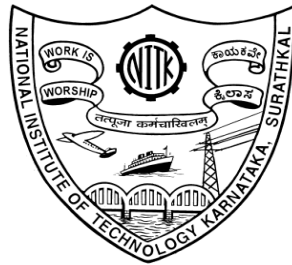
By

ABIOT KETEMA DEMMSIE

165085AM16F01

Under the Guidance of

Prof. Dwarakish G.S.



**DEPARTMENT OF WATER RESOURCES AND OCEAN
ENGINEERING**

**NATIONAL INSTITUTE OF TECHNOLOGY KARNATAKA,
SURATHKAL, MANGALORE – 575025**

AUGUST 2021

DECLARATION

I hereby declare that the Research Thesis entitled "**Simulation of the hydrological impacts of climate and land use/cover change on Tikur Wuha watershed in Ethiopia**" which is being submitted to the National Institute of Technology Karnataka, Surathkal in partial fulfilment of the requirements for the award of the Degree of Doctor of Philosophy in **Department of Water Resources and Ocean Engineering** is a *bonafide report of the research work carried out by me*. The material contained in this Research Thesis has not been submitted to any University or Institution for the award of any degree.



Abiot Ketema

(Registration Number: 165085AM16F01)

Department of Water Resources and Ocean Engineering

Place: Surathkal

Date: 26/08/2021

CERTIFICATE

This is to certify that the Research Thesis entitled " **Simulation of the hydrological impacts of climate and land use/cover change on Tikur Wuha watershed in Ethiopia** " submitted by **Abiot Ketema** (Register Number: 165085AM16F01) as the record of the research work carried out by him, is *accepted as the Research Thesis submission* in partial fulfilment of the requirements for the award of the degree of Doctor of Philosophy.

Research Guide

Prof. Dwarakish G.S.

Department of Water Resources and Ocean Engineering

Chairman – DRPC

Prof. Dodamani B M

Department of Water Resources and Ocean Engineering

ACKNOWLEDGEMENTS

Above all, I am thankful to the Almighty GOD for blessing and guiding my direction. Next, I would like to express my genuine appreciation to Hawassa University and Ethiopia's science and higher education ministry for full sponsorship to pursue the Ph. D. research work in India.

My heartfelt thanks go to Professor Dwarakish G.S. (the research supervisor) for his valuable guidance, support, encouragement, patience, and understanding throughout the research work. His overall supervision, experience, and knowledge make this Ph. D. study complete. Thank you so much, Sir; you have taught me a lot.

Next, special gratitude to the members of the Research Progress Assessment Committee (RPAC) panel: Professor Lakshman Nandagiri (Department of Water Resources and Ocean Engineering) and Professor A.C. Hedge (Department of Chemistry) for their insightful comments and suggestions in all steps of the progress, which enhanced the quality of the thesis. Thank you for your valuable contribution to shaping this study.

Special thanks to Head of Department (HoD) professor Dodamani B M and former HoD Prof. Amba Shetty for their kind help and support. I want to thank all the department members (faculties and staff), research scholars, and MTech students for always solving technical problems.

I express sincere gratitude to my respectable spouse, Genet Fekadu, for her care, help, and patience, all the time. You encourage me against all difficulties and helping me by taking our family's full responsibilities during the study period. I am grateful to my lovely kids, Hemen and Kal. You are a source of motivation and purpose in my life. I wish to thank my parents, sisters, brothers, and friends for their care, cooperation, and moral support throughout the study. Your significant contributions are highly appreciated and led to the successful completion of the study. Finally, I would like to express my gratitude to Amina Jemal for her considerable assistance in my life.

NITK-Surathkal, Mangalore, India

Date:

Abiot Ketema



DEDICATION

**This thesis is dedicated to my mother Azalech Ali
and my father Ketema Demmsie**

ABSTRACT

The study was carried out on the Tikur Wuha watershed (TWW) in Ethiopia with four specific objectives: simulation of the potential impact of climate change on hydro-meteorological variables, evaluation of the hydrological impacts of land use/cover (LU/LC) change, examination of the trend and variability of hydro-meteorological variables, and prioritisation of the sub-watersheds for soil and water conservation (SWC) measures based on soil loss rate (SLR). The LU/LC map was developed using a supervised classification method. The impact of LU/LC and climate change on streamflow was assessed using the Soil and Water Assessment Tools (SWAT) hydrological model. The Mann-Kendall trend test and Sen's slope estimator were employed for the trend and size of the trend, respectively. A Universal Soil Loss Equation (USLE) was used to estimate the SLR. The result revealed that the Bega, Kiremt, and annual rainfall increased for all scenarios. In contrast, the Belg rainfall decreased in all cases except for RCP8.5 at the end of the century. Both the minimum and maximum temperatures increased for all scenarios. The annual average streamflow in TWW increased in all cases except a slight reduction in the RCP4.5 scenario in mid-century. Climate change affects the streamflow in the study watershed by increasing the wet season flow and reducing the dry season flow. The LU/LC detection shows a steady expansion of cropland and built-up areas and the withdrawal of shrubland, swampy, water bodies, and grassland during the 1978 to 2017 periods. The LU/LC changes increased the average annual streamflow by 14.77% from 1978 to 2017. The LU/LC change had a dominant role in the hydrological responses of the TWW. The trend analysis discovered that the average annual rainfall exhibited an insignificant declining trend of 20.8 mm/decade at a watershed scale. The temperature showed a statistically significant rising trend, with the minimum temperature rising faster than the maximum temperature. The Tikur Wuha River's streamflow increased at 21.16 MCM/decade from 1980 to 2002. The average SLR of the watershed is 14.13 t ha⁻¹yr⁻¹. It is larger than the maximum soil loss tolerance of the watershed and higher than the country's average SLR. The SWC measures should be implemented rapidly in the TWW, consistent with the priority watersheds' rank.

Keywords: Climate change; LU/LC; Mann–Kendall; Soil loss rate; SWAT; Trend analysis; USLE

Table of Contents

ABSTRACT	III
LIST OF FIGURES	VIII
LIST OF TABLES	XI
LIST OF ABBREVIATION	XIV
CHAPTER 1: INTRODUCTION	1
1.1. GENERAL.....	1
1.2. CLIMATE CHANGE IMPACTS ON WATER RESOURCE.....	1
1.3. LAND USE/COVER CHANGE IMPACTS ON STREAMFLOW	3
1.4. VARIABILITY AND TREND ANALYSIS OF HYDRO-METEOROLOGICAL VARIABLES.....	4
1.5. WATERSHED PRIORITIZATION BASED ON THE SOIL LOSS RATE.....	5
1.6. STATEMENT OF THE PROBLEM	7
1.7. OBJECTIVES OF THE STUDY	12
1.8. THE SCOPE OF THE STUDY.....	12
1.9. THE ORGANISATION OF THE THESIS	13
CHAPTER 2: REVIEW OF LITERATURE.....	15
2.1 GENERAL.....	15
2.2 CLIMATE CHANGE IMPACTS ON WATER RESOURCES IN ETHIOPIA	15
2.2.1 <i>Water resources of Ethiopia</i>	15
2.2.2 <i>Ethiopian contribution to global greenhouse emission</i>	17
2.2.3 <i>Climate change impacts on water resources in Ethiopia</i>	17
2.2.3.1 Observed (historical) impacts.....	17
2.2.3.2 Potential impacts	18
2.2.4 <i>State reaction to threats of climate change in Ethiopia</i>	22
2.2.5 <i>Other climate change impact studies</i>	24
2.3 LU/LC CHANGE IMPACTS ON WATER AVAILABILITY	28
2.4 VARIABILITY AND TREND ANALYSIS STUDIES	31
2.5 SOIL LOSS RATE	36
2.5.1 <i>Soil loss rate studies</i>	37
2.5.2 <i>Water erosion assessment methods</i>	42
2.5.2.1 Qualitative approaches based on expert Knowledge.....	43
2.5.2.2 A quantitative approach based on the measurement.....	44
2.5.3 <i>Erosion models</i>	44
2.5.3.1 Empirical models (Statistical model)	44
2.5.3.2 Physical-based models (Deterministic model)	47
2.5.4 <i>Selection of water erosion models</i>	48
2.6 SUMMARY AND KEY POINTS FROM THE LITERATURE.....	51

CHAPTER 3: STUDY AREA, DATASETS, AND RESEARCH METHODOLOGY	55
3.1 DESCRIPTION OF THE STUDY AREA	55
3.2 DATASETS FOR THE STUDY.....	57
3.3 RESEARCH METHODOLOGY	60
3.3.1 <i>Methods for hydro-meteorological impacts of climate change</i>	62
3.3.1.1 Selection and evaluation of climate scenarios	62
3.3.1.2 Description and applicability of the SWAT hydrological model	64
3.3.1.4 Preparation of LU/LC map.....	66
3.3.1.4 Calibration and validation of the model	67
3.3.1.5 Model performance evaluation	67
3.3.2 <i>Methods for land use/land cover change impacts</i>	71
3.3.2.1 LU/LC change detection	71
3.3.3 <i>Methods for variability and trend analysis of hydro-meteorological variables</i>	75
3.3.4 <i>Methods for prediction of the soil loss rate</i>	82
3.3.4.1 Rainfall erosivity factor (R-factor)	83
3.3.4.2 Soil erodibility factor (K- factor).....	84
3.3.4.3 Slope length and slope steepness (LS-factor)	85
3.3.4.4 Cover and management factor (C-factor)	85
3.3.4.5 Support practice factor (P-factor)	86
CHAPTER 4: HYDRO-METEOROLOGICAL IMPACT ASSESSMENT OF CLIMATE CHANGE	87
4.1 GENERAL	87
4.2 VALIDATION OF CORDEX DATA WITH OBSERVED DATA	87
4.3 DESCRIPTION OF STATISTICAL PARAMETERS OF SEASONAL AND ANNUAL CLIMATE VARIABLES.....	88
4.3.1 <i>Description of statistical parameters of seasonal and annual climate variables of historical CORDEX outputs</i>	88
4.3.2 <i>Description of statistical parameters of seasonal and annual climate variables of mid-century CORDEX outputs</i>	90
4.3.3 <i>Description of statistical parameters of seasonal and annual climate variables of end century CORDEX outputs</i>	92
4.4 CLIMATE CHANGE IMPACTS ON PRECIPITATION, MINIMUM AND MAXIMUM TEMPERATURE	94
4.4.1 <i>Climate change impacts on precipitation</i>	94
4.4.2 <i>Climate change impacts on the minimum and maximum temperature</i>	98
4.5 CALIBRATION VALIDATION AND MODEL PERFORMANCE EVALUATION	101
4.6 CLIMATE CHANGE IMPACTS ON STREAMFLOW	104
4.7 CLOSURE	109
CHAPTER 5: HYDROLOGICAL RESPONSES TO LAND USE/LAND COVER CHANGE.....	111
5.1 GENERAL	111
5.2 LU/LC CHANGE DETECTION	111
5.2.1 <i>Classification accuracy assessment</i>	111
5.2.2 <i>The magnitude of LU/LC changes</i>	112
5.2.3 <i>Rate, per cent, and trend of LU/LC change</i>	117

5.3	HYDROLOGICAL RESPONSES TO LAND USE/LAND COVER CHANGE	119
5.4	CLOSURE	122
CHAPTER 6:TREND AND VARIABILITY OF HYDRO-METEOROLOGICAL VARIABLES.....		123
6.1	GENERAL.....	123
6.2	RAINFALL VARIABILITY AND TREND	123
6.3	TEMPERATURE VARIABILITY AND TREND	134
6.4	STREAMFLOW VARIABILITY AND TREND	140
6.5	PET VARIABILITY AND TREND	143
6.6	CLOSURE	146
CHAPTER 7: WATERSHED PRIORITIZATION FOR CONSERVATION ACTIVITIES		147
7.1	GENERAL.....	147
7.2	USLE FACTORS DETERMINED.....	147
7.2.1	<i>R-factor</i>	147
7.2.2	<i>K-factor</i>	149
7.2.3	<i>LS-factor</i>	151
7.2.4	<i>C-factor</i>	152
7.2.5	<i>P-factor</i>	154
7.3	THE SOIL LOSS RATE OF TIKUR WUHA WATERSHED.....	155
7.4	PRIORITIZATION OF SUB-WATERSHEDS FOR SWC BASED ON SLR	160
7.5	CLOSURE	163
CHAPTER 8: CONCLUSIONS AND RECOMMENDATIONS.....		165
REFERENCES		171
LIST OF PUBLICATIONS		195

LIST OF FIGURES

Figure No.	Title	Page No.
Figure 3.1:	Location of Tikur Wuha watershed	56
Figure 3.2:	The 40 years average monthly rainfall and temperature of the TWW	56
Figure 3.3:	Digital elevation model of Tikur Wuha watershed	59
Figure 3.4:	Soil class map of the Tikur Wuha watershed	59
Figure 3.5:	General methodology framework of the study	61
Figure 3.6:	Methodology flow chart for climate change impact on hydro-meteorological variables in TWW	70
Figure 3.7:	Methodology flow chart for LU/LC impacts on streamflow	75
Figure 3.8:	Methodology flow chart for trend and variability analysis of hydro-meteorological variables in TWW	77
Figure 3.9:	The framework for the modelling of SLR and prioritisation of watersheds using the USLE	83
Figure 4.1:	Intra annual variation of precipitation in TWW in the historical, mid and end century for RCP4.5 and RCP8.5 climate change scenario	96
Figure 4.2:	Per cent of change in precipitation in TWW in the mid and end century for RCP4.5 and RCP8.5 climate change scenario compared to the Historical period	96
Figure 4.3:	Monthly, seasonal, and yearly average maximum temperature of historical, mid and end century for RCP4.5 and RCP8.5 climate change scenarios	100
Figure 4.4:	Monthly, seasonal, and yearly average minimum temperature of historical, mid and end century for RCP4.5 and RCP8.5 climate change scenarios	101
Figure 4.5:	Yearly average minimum and maximum temperature in the future for RCP4.5 and RCP8.5 climate change scenario	101
Figure 4.6:	Simulated and observed streamflow for calibration and validation period	103

Figure 4.7:	Scatter plots of simulated and observed monthly average daily flow for the calibration period.	103
Figure 4.8:	Scatter plots of simulated and observed monthly average daily flow for the validation period.	104
Figure 4.9:	The monthly variation of average streamflow in historical, mid, and end century	105
Figure 4.10:	Per cent of change of average streamflow in the future compared to the reference period	106
Figure 5.1:	LU/LC map of the Tikur Wuha watershed in 1978	113
Figure 5.2:	LU/LC map of the Tikur Wuha watershed in 1988	114
Figure 5.3:	LU/LC map of the Tikur Wuha watershed in 1998	114
Figure 5.4:	LU/LC map of the Tikur Wuha watershed in 2017	115
Figure 5.5:	LCLU change trend from the year 1978 to 2017 in Tikur Wuha watershed	118
Figure 5.6:	Rate of change of LU/LC (km ² /yr) in Tikur Wuha watershed	120
Figure 5.7:	Intra annual variation of streamflow for the year 1978 to 2017	122
Figure 6.1:	Average annual rainfall (mm) of each rain gauge station in TWW (1978-2017)	124
Figure 6.2:	Seasonal distribution of rainfall in the watershed (1978-2017)	125
Figure 6.3:	Trend and interannual variability of annual rainfall Hawassa (1978 -2017)	127
Figure 6.4:	Trend and interannual variability of annual rainfall Haisawita	128
Figure 6.5:	Trend and interannual variability of annual rainfall Shashemene	130
Figure 6.6:	Trend and interannual variability of annual rainfall Wondogenet	131
Figure 6.7:	Trend and interannual variability of the areal weighted	

	average annual rainfall of TWW	134
Figure 6.8:	Trend and intra-annual variability of temperature in TWW	137
Figure 6.9:	Trend and Interannual variability of temperature in TWW	137
Figure 6.10:	Trend and inter-annual variability of streamflow and runoff in TWW	143
Figure 6.11:	Trend and interannual variability of PET in TWW	146
Figure 7.1:	Annual rainfall map of TWW	148
Figure 7.2:	Rainfall erosivity map of TWW	149
Figure 7.3:	K-factor map of TWW	150
Figure 7.4:	LS-factor map of TWW	152
Figure 7.5:	Cover and management factor map of the TWW	153
Figure 7.6:	Supporting practice factor map	155
Figure 7.7:	SLR class map of TWW based on severity class	157
Figure 7.8:	Soil loss rate class based on SLT of the area	159
Figure 7.9:	Soil loss rate class based on Ethiopia average SLR	160
Figure 7.10:	The average SLR of sub-watersheds in TWW	162
Figure 7.11:	Priority watersheds for planning and implementation SWC practices in TWW	163

LIST OF TABLES

Table No.	Title	Page No.
Table 3.1:	The characteristics of Landsat images used for LU/LC change detection	58
Table 3.2:	The type, source, and the purpose data	60
Table 3.3:	List of RCMs from multiple GCMs used in the study	63
Table 3.4:	Overall performance ratings for a simulation with a monthly time step	69
Table 3.5:	Description LU/LC classes in Tikur Wuha watershed	74
Table 3.6:	Relationship between slope in per cent and m-values	85
Table 4.1:	The NSE values of the five selected and the weighted average of the RCMs	88
Table 4.2:	Summary of statistical parameters for all variables of the weighted average historical CORDEX outputs (1960 to 1999)	88
Table 4.3:	Summary of statistical parameters for all variables of the weighted average mid-century CORDEX outputs (2020 to 2059)	90
Table 4.4:	Summary of statistical parameters for all variables of the weighted average of end century CORDEX outputs (2060 to 2099)	92
Table 4.5:	Summaries of the average values and per cent of change of precipitation in mid and end century compared to the historical period	95
Table 4.6:	Summaries of the change in minimum and maximum temperature in mid and end century for RCP4.5 and RCP8.5 climate change scenario compared to the historical period	98
Table 4.7:	Statistical performance indicator of SWAT for TWW with the different objective function	102
Table 4.8:	Summaries of the average values and per cent of change of streamflow in mid and end century compared to the historical period	104
Table 5.1:	Summary of accuracy assessment of LU/LC	111

Table 5.2:	The areal extent of LU/LC classes in the Tikur Wuha watershed in 1978, 1988, 1998 and 2017	115
Table 5.3:	LU/LC per cent of changes with respect to the original area of each class and rate of changes from 1978 to 2017 in the Tikur Wuha watershed	117
Table 5.4:	The monthly, seasonal, and yearly average and per cent of change in streamflow (m ³ /s) in different LU/LC	119
Table 6.1:	Features of stations for measured rainfall	124
Table 6.2:	Summary statistics of Hawassa rainfall (1978-2017)	126
Table 6.3:	Summary statistics of Haisawita rainfall (1978-2017)	127
Table 6.4:	Summary statistics Shashemene rainfall (1978-2017)	129
Table 6.5:	Summary statistics of Wondogenet Precipitation (1978-2017)	131
Table 6.6:	Summary statistics of the areal weighted average annual rainfall of TWW (1978-2017)	133
Table 6.7:	Summary statistics of Hawassa minimum temperature (1978-2017)	138
Table 6.8:	Summary statistics of Hawassa maximum temperature (1978-2017)	138
Table 6.9:	Summary statistics of Haisawita minimum temperature (1978-2017)	139
Table 6.10:	Summary statistics of Haisawita maximum temperature	140
Table 6.11:	Summary statistics of streamflow TWW (1978-2017)	142
Table 6.12:	Summary statistics Hawassa PET (1978-2017).	144
Table 6.13:	Summary statistics of Haisawita PET (1978-2017)	145
Table 7.1:	Annual rainfall and the R-factor of TWW	148
Table 7.2:	K-factor values in SI unit and the corresponding area	150
Table 7.3:	The LS-factor values and the corresponding area	151
Table 7.4:	Adopted cover and management factor values for different LU/LC in the TWW	153
Table 7.5:	P-factor values	154
Table 7.6:	SLR class of TWW based on severity class	157

Table 7.7:	Soil loss rate class based on soil loss tolerance (SLT) of the TWW	159
Table 7.8:	Soil loss rate class based on the average value of soil erosion of Ethiopia	160
Table 7.9:	Priority watersheds for SWC based on the SLR	161

LIST of ABBREVIATION

Abbreviations	Description
AGNPS:	Agricultural Non-Point Source Pollution Model
AR5:	Fifth Assessment Report of the IPCC
CanESM2	Second generation Canadian Earth System Model
CCCma:	Canadian Centre for Climate Modelling and Analysis
CLHMS:	Coupled Land Surface and Hydrological Model System
CMIP3:	Coupled Model Intercomparison Project Phase 3
CMIP5:	Coupled Model Intercomparison Project Phase 5
CN :	Curve Number
CORDEX:	Coordinated Regional Climate Downscaling Experiment
CREAMS:	Chemical Runoff and Erosion from Agricultural Management Systems
CRGE:	Climate Resilience Green Economy
CV:	Coefficient of Variation
DEM:	Digital Elevation Model
DMI:	Danish Meteorological Institute
EPCC:	Ethiopian Panel on Climate Change
ETM+:	Enhanced Thematic Mapper Plus
EUROSEM:	European Soil Erosion Model
FAO:	Food and Agricultural Organization
GCM:	General Circulation Model/ General Climate Model
GDP:	Gross Domestic Product
GERD:	Great Ethiopian Renaissance Dam
GFDL:	Geophysical Fluid Dynamics Laboratory
GIS:	Geographic Information System
GHG:	Greenhouse Gases
GTP:	Growth and Transformation Plan
GW-MATE:	Groundwater Management Advisory Team
HadCM3:	Hadley Centre Coupled Model version 3
HBV:	Hydrologiska Byråns Vattenbalansavdelning

HIRHAM5	High-Resolution Limited Area Model-version 5
HLPE:	High-Level Panel of Experts
HRU:	Hydrological Response Unit
ICHEC	Irish Centre for High-End Computing
IHA:	International Hydropower Association
IPCC:	Intergovernmental Panel on Climate Change
KNMI:	Koninklijk Netherlands Meteorological Institute
LU/LC:	Land Use Land Cover
MCE:	Multi-Criteria Evaluation
MMF:	Morgan-Morgan-Finney
MODFLOW:	Modular Finite-Difference Groundwater Flow Model
MoWIE:	Ministry of Water Resources, Irrigation and Energy
MoWR:	Ministry of Water Resources
MPI-M:	Max Planck Institute for Meteorology
MPI-HM:	Max Planck Institute for Meteorology-Hydrology Model
MPI-ESM	Max Planck Institute for Meteorology Earth System Model
MSS:	Multispectral Scanner
MUSLE:	Modified Universal Soil Loss Equation
NAMA:	Nationally Appropriate Mitigation Actions
NAPA:	National Adaptation Programs of Action
NMSA:	National Meteorological Service Agency
NSE:	Nash and Sutcliffe simulation efficiency
PBIAS:	Per cent Bias
PET:	Potential Evapotranspiration
PRECIS:	Providing REgional Climates for Impacts Studies
PSNP:	Productive Safety Net Program
RACMO	Regional Atmospheric Climate Model
RCP:	Representative Concentration Pathways
RCM:	Regional Climate Model
RSR:	The ratio of root mean square error to measured Standard deviation
RUSLE:	Revised Universal Soil Loss Equation

RVLB:	Refit Valley Lake Basin
SCRP:	Soil Conservation Research Project
SCS :	Soil Conservation Service
SDR:	Sediment Delivery Ratio
SLR:	Soil Loss Rate
SLT:	Soil Loss Tolerance
SMHI:	Swedish Meteorological and Hydrological Institute
SNNPRS:	Southern Nation Nationalities Peoples Regional State
SRES:	Special Report on Emission Scenarios
SRTM:	Shuttle Radar Topography Mission
SUF12:	Sequential Uncertainty Fitting Version2
SWAT:	Soil and Water Assessment Tool
SWAT–CUP:	Soil and Water Assessment Tool – Calibration and Uncertainty
SWC:	Soil and Waterer Conservation
SY:	Sediment Yield
TM:	Thematic Mapper
TWW:	Tikur Wuha Watershed
UBNRB:	Upper Blue Nile River Basin
UNFCCC:	United Nations Framework Convention on Climate Change
USA:	United States of America
USAID:	United States Agency for International Development
USDA:	United States Department of Agriculture
USGS:	United States Geological Survey
USLE:	Universal Soil Loss Equation
UTM:	Universal Transverse Mercator
WCED:	World Commission for Environment and Development
WEAP:	Water Evaluation and Planning
WEPP:	Water Erosion Prediction Project
WFP:	World Food Program
WWDSE:	Water Works Design and Supervision Enterprise

CHAPTER 1: INTRODUCTION

1.1. General

Climate change, Land Use/Cover (LU/LC) change, soil erosion, and poor management of water resources are challenging to sustainable development (Food and Agriculture Organization [FAO] 2011; Intergovernmental Panel on Climate Change [IPCC] 2014). Sustainable development meets the present's needs without compromising upcoming generations' capacity to meet their own needs (World Commission on Environment and Development [WCED] 1987; Holden et al. 2014). The impacts of climate change on development are already observed. The first chapter of the thesis has briefly presented the background, statement of the problem, objectives, and scope of the study.

1.2. Climate Change Impacts on Water Resource

Water is an essential natural resource for all forms of life. It is vital in almost all human activities. It is the lifeblood of the environment, on which the food security of current and upcoming generations depends. The climate, water, biophysical, and socio-economic systems are all intricately linked. Accordingly, altering one of these elements influences the others (Bates et al. 2008; High-Level Panel of Experts [HLPE] 2015). The effects of climate change on the water are of high significance since all natural and socio-economic systems critically depend on water. Hence, the relationship between water resources and climate change is of primary interest and concern.

A warmer climate will speed up the hydrological cycle, varying rainfall and runoff amount and timing. Increased rainfall variability and intensity are projected to enhance the possibility of drought and flooding in many areas (Bates et al. 2008). The direct effects of climate change are the rise in temperature and sea level, the change in the pattern of precipitation and water availability, and extreme hydrological events such as floods, droughts, and heatwaves (Bates et al. 2008; IPCC 2014). It has many indirect effects on agriculture, energy production, and overall water infrastructure. Global change is likely to amend the temperature, precipitation, and streamflow patterns upon which agriculture depends (FAO 2011).

Climate change impacts are location specific. Its magnitude varies from region to region throughout the world. The severity of climate change's undesirable effects will differ notably across regions, countries, and socio-economic groups (IPCC 2014; Mamuye and Kebebewu 2018). Usually, developing countries like Ethiopia are more likely vulnerable to climate extremes than developed countries because of their ability to implement adaptation and mitigation measures to alleviate the harmful impacts of global change (Ringler et al. 2011; IPCC 2014). A climate-associated natural hazard such as drought and flood happens everywhere globally; however, its consequences are not as severe as in Africa in general and Ethiopia in particular (National Meteorological Service agency [NMSA] 2007).

Africa is highly vulnerable to the potential impacts of climate change. According to Hallegatte et al. (2016), the consequences of climate change for Africa are shocking and threaten to push millions of people into severe poverty by 2030. It is mainly due to reducing crop yields, increased food costs, and harmful health impacts. By mid-century (2050), 300 to 360 million people in Africa are anticipated to be prone to water stress caused by climate change (IPCC 2007). African communities face double impacts (direct and indirect) of climate change. The direct effects of increases in extreme weather events (flood and drought) induce a decline of crop yields and livestock productivity, drinking water shortage, the spread of diseases such as malaria, possible migration, social conflict, and increased cost of infrastructure development and maintenance. The indirect impacts are declining land productivity due to soil erosion, desertification, deforestation, and biodiversity loss (World Bank 2009). Accordingly, it is vital to understand the effects of global change on natural resources in Africa to recognise up to date and practical adaptation measures and investment priorities that can be implemented to alleviate the adverse impacts of global change in the future (Ringler et al. 2011).

Ethiopia is one of the developing countries in Africa, and its major economy is heavily reliant on rain-fed agriculture (NMSA 2007; Setegn et al. 2011; Robinson et al. 2013; Ethiopian Panel on Climate Change [EPCC] 2015a). In a country with a predominantly rain-fed agricultural system like Ethiopia, variation in rainfall and follow-on changes in soil moisture may unfavourably affect crop yield, and the livelihood of millions of people as rainfall is one of the most critical climatic

determinants of food production (NMSA 2007; Ringler et al. 2011). Although the country contributes little to Green House Gas (GHG) emissions, Ethiopians already suffer from climate change events like drought and flood (NMSA 2007).

Although Ethiopia has considerable water resource potential, the spatial and temporal distribution of water is highly uneven (EPCC 2015a), and people face water-related problems. Ethiopia is often cited as one of the most vulnerable and with a minor capability to respond and adapt (Robinson et al. 2013). Yearly, many people in Ethiopia are exposed to famine, serious health problems, flood hazards, and drought due to rainfall variability in response to ongoing climate change (NMSA 2007; EPCC 2015a). Current climate change is already imposing a significant challenge to Ethiopia by affecting food security, energy and water supply, poverty reduction, and sustainable socio-economic development efforts (Robinson et al. 2013; EPCC 2015a). Therefore, it is vital to implement adaptation and mitigation measures to decrease the potential impact of climate change in Ethiopia. Since adaptation measures are implemented at the watershed level, it is indispensable to recognise the detailed climate change impact at the watershed level. This study focused on examining the potential effects of climate change on streamflow at the watershed level to help respective water resource managers plan watershed specific water resource management strategies to adapt to climate change.

1.3. Land Use/Cover Change Impacts on Streamflow

The impact of climate change and LU/LC change on hydrological processes can not be distinguished or is still a challenge in hydrology. Climate and LU/LC are the leading causes that affect the hydrological response of a watershed. LU/LC change has become a global concern due to its diverse environmental impacts (Bewket 2002). LU/LC change is an essential factor that directly affects watershed hydrology (Setegn et al. 2009; Wagner et al. 2013; Gashaw et al. 2018). LU/LC has many influences on the hydrological cycle. Changes in LU/LC affect the partitioning of precipitation into interception, infiltration, evapotranspiration, surface runoff, and groundwater recharge. LU/LC changes can increase water scarcity, flood risk, and erosion rate. Understanding the impacts of LU/LC change on water resources is, therefore, of decisive importance.

Globally, expansions of cultivated land and pastureland in the forest, grassland, and shrubland have been observed. However, the direction of LU/LC change was not uniform across the world. LU/LC change is one of the fundamental environmental problems in Ethiopia. There was a rapid expansion of cropland at the expense of forests in the country. Cultivation is stretched to highly steep areas (Zelege and Hurni 2001). Ethiopia's forest cover fell from 16% in the 1950s to 2.7% by the early 1990s (Shiferaw and Holden 2001). Dessie and Christiansson (2008) report that Ethiopia's forest area declined from about 40% at the end of the nineteenth century to less than 3% in 2000.

LU/LC change is responsible for altering the hydrological response of watersheds in Ethiopia (Setegn et al. 2009; Gashaw et al. 2018). According to several reports, LU/LC changes impact water resources in Ethiopia (Bewket and Sterk 2005; Getachew and Melesse 2012; Getahun and Van Lanen 2015; Tufa et al. 2015; Chakilu and Moges 2017; Welde and Gebremariam 2017; Gashaw et al. 2018). This study aims to detect the LU/LC change and its impacts on streamflow in the Tikur Wuha watershed (TWW).

1.4 Variability and Trend Analysis of Hydro-meteorological Variables

The Gross Domestic Product (GDP) of Ethiopia is reliant on agriculture. The agriculture of Ethiopia is mainly dependent on rainfall. Ethiopia is among the most susceptible nations to the undesirable effects of climate change (NMSA 2007; EPCC 2015a). Rainfall variability has considerable adverse effects on agricultural production in Ethiopia (Rosell and Holmer 2007; Alemayehu and Bewket 2017). Analysis of the spatiotemporal variability and trend of hydro-meteorological variables has paramount importance for securing sustainable agricultural production in Ethiopia (NMSA 2007). Recognition of patterns of hydro-meteorological elements is required to notice a historical change. It helps to make predictions of the future and for better preparedness (Raju and Nandagiri 2017). Tabari et al. (2011) have noted that researchers recently gave great attention to analysing the weather elements trend.

The trend analysis of historical hydro-meteorological variables contributes to projecting likely future trends and planning adaptation and mitigation measures to tackle climate change impacts (Raju and Nandagiri 2017). The exploration of rainfall

trends is critical for adaptation to future effects and development planning, as natural rainfall variability has always been a significant problem for the Ethiopian economy. Rainfall and temperature trend analysis often recognises the magnitude and extent of climate change (IPCC 2007 2014).

In Africa, average precipitation and temperature have shown declining and increasing trends, respectively. In the future, the temperature in Africa is likely to grow more rapidly than in other regions, which could exceed four °C at the end of the 21st century (IPCC 2014). Simultaneously, the East African highlands will experience a high degree of spatial and temporal variability. Studies in Ethiopia have also discovered that rainfall variability has considerable adverse effects on agricultural production (Rosell and Holmer 2007; Alemayehu and Bewket 2017).

Trend analysis studies in Ethiopia to date are not conclusive. Though some studies are carried out at macro levels, more research is warranted in this direction. There is a need to do trend analysis and variability at the microscale. The effect of ongoing climate change on rainfall in Ethiopia is more on its variability than on the amount. For crop production, seasonal reliability is essential than annual reliability (NMSA 2007; Asfaw et al. 2018). There is high spatiotemporal variability of rainfall in Ethiopia. So it must be analysed in clusters rather than as a whole (Gissila et al. 2004). Local-scale trend analysis is highly recommended. Analysis of the variation of temperature and rainfall at the macro level is not valid for local agricultural production. Also, watershed-scale trend examination is vigorous for site specific planning and executing mitigation and adaptation techniques (Gebre et al. 2013; Alemayehu and Bewket 2017).

1.5 Watershed Prioritization Based on the Soil Loss Rate

Soil erosion is unquestionably the trickiest land degradation on the globe (Bridges and Oldeman 1999). Soil erosion influences about one billion people globally, of which about 50% of the affected population is concerted in Africa (Lal and Humberto 2008). In Ethiopia, soil erosion by water is the most critical environmental threat that adversely affects agricultural productivity, economic growth, and food security (Hurni 1985; Taddese 2001; Gashaw et al. 2017). Rapid population growth, cultivation on steep slopes, clearing of vegetation, and overgrazing are the main factors that

accelerate soil erosion in Ethiopia. Rill and inter-rill erosions account for the major impact of soil erosion on land productivity in Ethiopia.

Erosion has both onsite and off-site effects. As Morgan (2005) elucidated, onsite effects are mainly significant on farming land where the relocation and loss of soil within/from a field, a decline in organic matter, soil structure, nutrient, soil depth, and soil fertility consequences in a decline of soil productivity, crop yield, and food security. Moreover, erosion results in various associated off-site effects such as sedimentation downstream and pollution. Soil erosion affects the capacity of drainage ditches and rivers, clogs up irrigation canals, raises the risk of flooding, and affects the intended use and life of reservoirs (Morgan 2005). Soil erosion also affected the water quality due to the chemicals (nutrients, pesticides) adsorbed by it, raising the nitrogen and phosphorus in water bodies and resulting in eutrophication and pollution (Bekele 2003; Morgan 2005; Kothyari 2012). Soil erosion may also enhance the release of soil organic content into the atmosphere as CO₂. Accordingly, it contributes to global warming, as rising CO₂ content increases the greenhouse effect (Lal and Humberto 2008). Reports from Ethiopia (Hurni 1988) show that the average soil erosion rate nationwide was estimated to be 12 t ha⁻¹yr⁻¹, from cropland was 42 t ha⁻¹yr⁻¹, degraded land was 70 t ha⁻¹yr⁻¹, and in the highlands of the country, it extends up to 300 t ha⁻¹yr⁻¹; which is beyond any tolerable soil loss.

The consequence of soil erosion in Ethiopian reservoirs is serious (Wolanchu 2012). Reports from different parts of Ethiopia show that many reservoirs have already lost their storage capacity and intended service because of heavy sedimentation (Setegn et al. 2010; Haregeweyn et al. 2012; Berhane et al. 2016; Gelagay 2016). As Tamene et al. (2006) stated, most micro-irrigation dams in the Tigray region of northern Ethiopia will be closed due to siltation in less than half of the design period. Lake Haramaya (Senti et al. 2014) in eastern Ethiopia and Lake Cheleleka (WWDSE 2001) in southern Ethiopia were filled with sediment and vanished due to soil erosion.

It is imperative to plan and implement appropriate soil and water conservation (SWC) measures to reduce onsite and off-site soil erosion and sedimentation impacts. Scientific planning for SWC to counteract the erosion problems requires sufficient knowledge of areas susceptible to erosion risk (spatial pattern of soil erosion), the extent of areas affected, and their magnitude in the area. It may not be feasible to cope

with the whole watershed area with SWC measures at a time. Since resources are scarce in developing countries like Ethiopia, implementing SWC practice at a time on the entire watershed is not practical. Thus, the whole watershed is divided into several smaller units, as sub-watersheds, since a watershed is an excellent unit for planning and executing the SWC practices. Therefore, recognising erosion-prone areas for prioritising sub-watershed based on the magnitude of SLR is indispensable for planning and implementing sustainable watershed management and wise use of resources. Prioritising a sub-watershed for the execution of SWC practices involves ranking different sub-watershed based on the magnitude of SLR (Adinarayana 2003). Therefore, a comprehensive study is highly needed, and the issue has to be addressed at a scale relevant to practising watershed management. The present study predicted the spatial variation of SLR and prioritised the sub-watersheds of TWW.

1.6 Statement of the Problem

Countries like Ethiopia, with low economic development levels, insufficient infrastructure, and lack of institutional competence, are more susceptible to climate change (NMSA 2007). Ethiopia has previously been prone to extreme climate events. Recurrent floods, drought, and soil erosion are listed along with the country's main environmental problems, and these are the leading causes of loss of life, property, and migration of many people in Ethiopia (NMSA 2007). The rise in temperature and the change in precipitation patterns are prominent features of climate change. These two factors affect almost all other hydrological processes. The long-term climate change impacts in Ethiopia are mainly linked to these two climate elements (EPCC 2015a). So recognition and analysis of their pattern in the watershed are highly needed.

Although Ethiopia has executed some water development programs, watershed management activities, and mitigation and adaptation measures to protect the country from the undesirable outcomes of climate change and enhance water security, water scarcity is one of the country's most significant challenges (NMSA 2007). The nature and magnitude of how global change will affect the Ethiopian water resources are not yet adequately understood, and there are many knowledge gaps related to climate and water interface (EPCC 2015a). This gap is a current challenge for planners and policy-makers to develop long-term water resource management and climate change

adaptation strategies in the water sector. Therefore, a comprehensive study is highly needed, and the issue has to be addressed at a scale relevant to decision making to improve the level of water security and the planning for climate change adaptation and mitigation practices in the country.

Previously, most climate change impact studies in Ethiopia were done based on Coupled Model Intercomparison Project Phase 3 (CMIP3) climate change models under Special Report on Emission Scenarios (SRES) (Zeray et al. 2006; Setegn et al. 2011; Dile et al. 2013; Wagesho et al. 2013; Chaemiso et al. 2016; Nigatu et al. 2016). The scientific community has developed a set of new emission scenarios termed Representative Concentration Pathways (RCPs). The RCPs include a strict mitigation scenario, RCP2.6 that aims to keep global warming below two °C above pre-industrial temperatures, two intermediate scenarios (RCP4.5 and RCP6.0), and one scenario with high GHG emission, RCP8.5 (IPCC 2014). The studies have been based on a single or a limited number of Global Climate Models (GCMs) (Dile et al. 2013; Nigatu et al. 2016; Serur and Sarma 2016). Concluding the effect of climate change on watershed hydrology using a particular GCM may not give an exact representation of future changes (IPCC 2007). High uncertainty is expected in climate change impact studies if the simulation results of a single GCM are relied upon, and it will likely mislead the decision-makers and policy developers. Researchers suggested uncertainty minimisation by employing an ensemble of relevant models. The mean ensemble forecast is generally more accurate than an individual ensemble member (Vano et al. 2015; Jose and Dwarakish 2020; Kundzewicza et al. 2018). Thus, predicting climate change impacts based on multiple GCMs under Coupled Model Intercomparison Project Phase 5 (CMIP5) is quite crucial in Ethiopia for a better understanding of the potential climate change impacts, informed decision making for proper water resource management, and effectively respond and adapt to projected changes; otherwise, the consequences becoming awful.

Even though the impact of climate change scenarios is examined globally, the exact magnitude of the effects at a watershed level is not examined in most parts of Ethiopia. Water-related climate change impacts in the TWW are poorly understood. Since climate change impacts are location specific and adaptation measures are implemented at the watershed level, recognising local climate change effects at a

watershed level is sensibly imperative. Hence, this study has examined the potential impacts of climate change on hydro-meteorological variables of the Tikur Wuha watershed using multiple Regional Climate Models (RCMs) from multiple GCMs under CMIP5 RCP4.5 and RCP8.5 emission scenarios until 2099.

Tikur Wuha watershed suffers from human-induced land degradation mainly due to unregulated LU/LC change. A significant change in LU/LC has been reported in the watershed during the last few decades. For example, Lake Cheleleka (11.3 km²) in 1973 in TWW was changed first to a swampy area (WWDSE 2001) and subsequently dried up and changed to grassland in 2011 (Dadi 2013; Wondrade 2014). Also, recently, the grassland near Tikur Wuha village has been converted into cultivation. A vast expansion of industrialisation and urbanisation in the TWW (expansion of Hawassa town and recently introduced industrial park (300ha)) is observed. The impacts of such changes on hydrology are poorly understood. Although the exact reason needs further assessment, the TWW stream discharge has recently increased (Dadi 2013; Kebede et al. 2014). As a result, floods repeatedly damage the town of Hawassa and the farms near the lake during extreme wet seasons (Gebreegziabher 2004). Hence, thorough analyses and understanding of the effects of LU/LC changes on hydrology are critically crucial for planning watershed management. It is vital to capture the hydrological impacts of the past LU/LC changes in the TWW and translate the results into a management decision to overcome the negative consequences of such changes on the hydrology of the TWW.

There are many studies on rainfall and temperature trends and variabilities in Ethiopia at different spatiotemporal scales (Osman and Sauerborn 2002; Seleshi and Zanke 2004; Admassu and Seid 2006; Rosell and Holmer 2007; Cheung et al. 2008; Resoll 2011; Funk et al. 2012; Gebre et al. 2013; Jury and Funk 2013; Wagesho et al. 2013; Mekasha et al. 2014; Mengistu et al. 2014; Abrha and Simhadri 2015; Kiros et al. 2016; Alemayehu and Bewket 2017; Asfaw et al. 2018; Eshetu et al. 2018). Studies on temperature generally report warming trends, with the minimum temperature more often rising rapidly than the maximum temperature (NMSA 2007). Studies on rainfall do not show clear directions for the country; the change patterns are mixed. Some studies reported a decreasing/downward trend in seasonal and annual rainfall totals in their respective study areas (Osman and Sauerborn 2002; Admassu and Seid 2006;

Funk et al. 2012; Gebre et al. 2013; Jury and Funk 2013; Wagesho et al. 2013; Asfaw et al. 2018). On the other hand, other studies reported a lack of clear trends (mixed results) in precipitation (Seleshi and Zanke 2004; Rosell and Holmer 2007; Cheung et al. 2008; Resoll 2011; Mengistu et al. 2014; Mekasha et al. 2014; Abrha and Simhadri 2015; Kiros et al. 2016; Alemayehu and Bewket 2017; Eshetu et al. 2018). The rational inference from those previous studies is that rainfall trends are sensitive to local scale climatic controls such as topography (Mengistu et al. 2014). Kiros et al. (2016) mentioned that some of the reasons for such controverting outcomes had been reported for a similar region. These are differences in the temporal and spatial scale, quality of the data set, presence of outliers, different delineations of seasons, and variations in the techniques employed for trend testing.

Although a trend study of hydro-meteorological variables in Ethiopia is common, previous studies focused only on rainfall and temperature. They have not been providing complete information about the hydrology of the watershed. Also, no previous research was conducted in the TWW. This study attempts to fill this gap. This study integrates annual, seasonal, and monthly variability examination and trend analysis of hydro-meteorological variables in TWW. The trend and variability of rainfall were analysed at individual rain-gauge stations and weighted average rainfall depths for the watershed. The variables analysed were minimum temperature and maximum temperature, rainfall depth, Potential Evapotranspiration (PET), and streamflow recorded at stations located within and near the TWW.

The issue of soil erosion is severe in the TWW. Lake Cheleleka (11.3 km²) in 1973 in TWW was changed first to a swampy area and subsequently dried up and changed to grassland in 2011 (WWDSE 2001; Dadi 2013; Wondyrad 2014) as a result of soil erosion and sedimentation. After Lake Cheleleka was filled with silt, the sediment is now directly entering Lake Hawassa, and the consequences are a rise of the lake level and expansion of the surface area of the Lake (Gebreegziabher 2004). Also, grasses are growing in the lake and expanding yearly due to the deposition of nitrogen and phosphorus from agricultural fields due to soil erosion. The implication is that the problem of soil erosion is severe in the study area.

Previous studies point out that, within the watershed, small erosion hot spot areas are the source of a large amount of soil erosion and sediment load. Besides, the factors

controlling soil loss vary from place to place (Maryam and Biswajeet 2014; Adriyanto et al. 2015; Gelagay and Minale 2016; Markose and Jayappa 2016, Yuan et al. 2016; Setegn et al. 2009; Rejari et al. 2016). Managing this small portion of the watershed can significantly reduce soil erosion's onsite and off-site impacts. Therefore, it is crucial to identify potential erosion areas for appropriate management interventions to tackle the main causative factors at their specific locations from an economic, management, and sustainability perspective. However, the spatial variation of SLR in TWW is not understood well. It is a current challenge for planners and policy-makers to develop long-term SWC strategies.

Most soil erosion assessment studies for watershed prioritisation in Ethiopia are not presented at the sub-watershed level. They are given the finding at the watershed level. It may not help to identify hot spot areas for implementing soil and water conservation activities in the top priority area. The present study was carried out to predict the spatial variation of SLR and prioritise the sub-watersheds of TWW using universal soil loss equation (USLE) and Geographic Information System (GIS) techniques.

The international application of the USLE needs adaptation to local conditions and the changing of USA units to the SI metric system. However, users of the USLE are unaware of the considerations necessary to develop metric conversion factors. K-factor values in the SI units will be about 0.1317 times those of US customary units (Foster et al. 1981). The maximum K-factor value will be comparable to 0.10 (Foster et al. 1981). Panagos et al. (2012) assessed the K-factor for Europe, relying on 22,000 soil samples collected within Europe. They found that the K-factor of USLE ranges from 0.013 to 0.087, with a mean of 0.041 in the SI unit. The K-factor values in China are concentrated in the ranges between 0.0229 and 0.0457, with a mean of 0.0321 (Wang et al. 2016). Studies in Ethiopia for predicting soil erosion using USLE misused K-factor values (Bewket and Teferi 2009; Brhane and Mekonen 2009; Amsalu and Mengaw 2014; Ayalew 2015). They used the K-factor values without converting them into the metric system. These are relatively high values and seriously affect the result and may mislead the decision-makers. Corrected K-factor values were used in this study.

1.7 Objectives of the Study

1. To simulate the potential impacts of climate change on the hydro-meteorological variables in the Tikur Wuha watershed.
2. To evaluate the hydrological impacts of LU/LC changes in the Tikur Wuha watershed using the hydrological model.
3. To examine the trend and variability of hydro-meteorological variables in the Tikur Wuha watershed.
4. To prioritise the watersheds for soil and water conservation measures based on soil loss rate.

1.8 The Scope of the Study

This research was accentuated to investigate how the medium (RCP4.5) and high (RCP8.5) emission scenarios affect future temperature, precipitation, and streamflow up to 2099. The medium emission scenario provides an average future climate condition. The high emission scenario (RCP8.5) represents the business as usual scenario. Besides, the study assessed the LU/LC change impacts on the hydrology of TWW in Ethiopia. Moreover, trend and variability analysis of hydro-meteorological variables were evaluated. Finally, the spatial variation of the SLR was estimated for the prioritisation of sub-watershed for conservation activities. The map that indicates the spatial variation of SLR in the watersheds was developed. The research outputs will help recognise soil erosion risk zones and allow the planning and implementation of location-specific SWC measures in high erosion risk areas to reduce the sediment load in Lake Hawassa and improve the agricultural productivity of the TWW in the future. Also, it provides a wide range of helpful information about the potential impact of climate change on water resources in the context of TWW. It helps planners and decision-makers to plan site-specific and appropriate adaptation and mitigation measures to reduce the various adverse effects of global change in the watershed. Spatially, the study delimited its scope at the watershed level in Ethiopia.

1.9 The Organisation of the Thesis

This thesis is segregated into eight chapters, and information about the chapters is as follows. The background, problem statements, objectives, and scope of the study were presented in the **first chapter**.

Chapter Two: This chapter has five major sections. The impacts of climate change on Ethiopian water resources, state responses to climate change threats, and studies regarding climate change impacts on water resources were addressed in the first part. The second part addressed how LU/LC change affects water availability. The third part summarises studies regarding the trend and variability of hydro-meteorological variables. In the fourth section, soil erosion studies were presented. Lastly, the major findings from the review works are highlighted, and major literature gaps are identified.

Chapter Three: This chapter provides a detailed description of the study area, data products used, and a comprehensive methodology framed to complete the research work. It also provides a brief description of SWAT and USLE models.

Chapter Four: This section provides a wide range of helpful information about the potential impact of climate change on water resources in the context of TWW.

Chapter Five: This chapter provides insight into the LU/LC change dynamics over the study period in TWW. Besides, the impact of LU/LC change on streamflow is provided.

Chapter Six: In this section, the trend and variability of hydro-meteorological variables of TWW in southern Ethiopia have been given and discussed.

Chapter Seven: In this section, the priority watersheds are recognised for SWC activities based on the magnitude of the SLR.

Chapter Eight: This chapter summarises and concludes the findings of this research work. The next chapter presents a review of related literature.

CHAPTER 2: REVIEW OF LITERATURE

2.1 General

This chapter has five parts. The first part elaborates on the water resources of Ethiopia, the impacts of climate change on Ethiopian water resources, state reaction to climate change threats, and studies regarding climate change impacts on water resources. The second part is about how the LU/LC change affects water availability. The third part summarises studies regarding the trend and variability of hydro-meteorological variables. In the fourth section, soil erosion studies were presented. Soil erosion assessment methods are reviewed. Lastly, critical points from the review were stated.

2.2 Climate Change Impacts on Water Resources in Ethiopia

2.2.1 Water resources of Ethiopia

Ethiopia is located in East Africa between 3° - 15° north and 33° - 48° east just north of the equator. Its area is around 1.13×10^6 km² (Berhanu et al. 2014). Ethiopia's climate ranges from temperate in the highlands to tropical in the lowlands (Fazzini et al. 2015). The yearly average rainfall of the country is about 744mm (Awulachew et al. 2007). Lowlands are vulnerable to increasing temperatures and prolonged droughts, whereas highlands are prone to intense and irregular rainfall (USAID 2016). In terms of rainfall occurrence, Bega, Belg, and Kiremt are the three seasons in Ethiopia. The Bega is the period from October to January. It is a dry and harvesting period for various parts of Ethiopia. The Belg corresponds to a short rainy period from February to May, and during this season, the rainfall patterns are very erratic in nature. The Kiremt is the main rainy period from June to September. 50 to 80 per cent of the country's annual rainfall is measured in this period (NMSA 2007; NMSA 2013; Fazzini et al. 2015; USAID 2016).

Ethiopia has copious surface water resources, with estimated yearly average flows from the country's 12 river basins being 122 billion cubic meters per annum (MoWR 2002), and lake water from 12 Lakes is 70 billion cubic meters (Berhanu et al. 2014). The real potential of the country's groundwater is not yet known. However, it is reported that Ethiopia has a groundwater potential of approximately up to 30 billion

cubic meters (MoWR and GW-MATE 2011). Although Ethiopia has considerable water resource potential, the spatiotemporal water distribution is highly uneven (EPCC 2015a), and Ethiopians face water-related problems. Despite plenty in some parts, Ethiopia is highly water scarce due to poor water management and a shortage of storage infrastructure.

The availability of surface water and rainfall in Ethiopia is erratic and varies with space and time (Robinson et al. 2013; EPCC 2015a). Spatially, 80 to 90% of the water resources are found in Ethiopia's western parts, where no more than 30 to 40 per cent of Ethiopia's population lives. In contrast, more than 60% of the population lived in Ethiopia's eastern and central regions, where surface water resources are just 10 to 20% of the total. Temporally, most of the rivers in Ethiopia become full in June, July, and August within the duration of the Kiremt season (Berhanu et al. 2014). The amount of rainfall varies spatially within the country and within different regions in the country. For example, within the Amhara national regional state, yearly precipitation ranges from 770mm in the eastern part to greater than 1660mm in the western part of the region (Bewket and Conway 2007). An increment in rainfall from the northeast to the west portion of the Tigray region was also recorded. According to Gebrehiwot and Van der Veen (2013), annual rainfall in Tigray ranges from 300mm in the northeast to 1260mm in the west.

Too little has been done to date in utilising the water resources in Ethiopia as engines to boost the country's socio-economic development. Even though the country's water resources can develop an irrigation area of $3.8 * 10^6$ ha (Berhanu et al. 2014), less than 5% is developed (World Bank 2006). Hydropower potential has been estimated at 45,000MW per annum (Berhanu et al. 2014), of which the country developed only 3813MW (International Hydropower Association [IHA] 2017). Currently, the government pays more attention to generating electric energy from hydropower. For example, a 5225 MW hydropower project is under construction from the Great Ethiopian Renaissance Dam (GERD) project. Inadequate finance for investment to control water, a technical challenge like having few numbers of hydrological gauging stations, hydro-politics, and lack of competent authority and skilled experts in the water sector are some of the reasons for not fully utilised the water resource potential in Ethiopia (Berhanu et al. 2014; Mosello et al. 2015).

2.2.2 Ethiopian contribution to global greenhouse emission

Ethiopia's contribution to global annual GHG emissions is negligible. According to the EPCC report, GHG emissions from the country were 48 Mt CO₂e (0.9 tone CO₂e per capita) in 1994, 150 MtCO₂e in 2010 (1.8 tone CO₂e per capita), and will increase to 400 MtCO₂e (3 tone CO₂e per capita) by 2030. The primary GHG-emission sector in Ethiopia is agriculture. In 2010, 87 per cent of national emissions were accounted for by agriculture and land-use change. The rest, 13 per cent, comes from the sectors of industry, transport, and energy (EPCC 2015b). Although the country contributes little to GHG emissions, Ethiopians already suffer from climate change events like drought and flood (NMSA 2007).

2.2.3 Climate change impacts on water resources in Ethiopia

2.2.3.1 Observed (historical) impacts

In Ethiopia, floods and droughts occur repetitively due to climate change (Robinson et al. 2013; EPCC 2015a). These events can lead to famine and disruption of socio-economic well-being. Yearly, the country loses up to 6% of crop yield due to rainfall variability (EPCC 2015b). In some parts of Ethiopia, too much surface water results in floods, and at the same time, other parts of the country suffer from drought.

The principal and direct consequence of climate change would be the changes in water availability. Some of the adverse effects observed in Ethiopia due to rising temperatures and changing rainfall amounts and patterns include a decrease in soil moisture, decreased freshwater availability, repeated droughts, and floods (USAID 2016). According to the USAID report, floods and drought have increased since 1960 in Ethiopia (USAID 2016). As the Ethiopian socio-economic development is dependent on rain-fed agriculture, Ethiopia suffers a lot from climate variability and weather extremes. Global warming has resulted in repeated droughts and heavy rainfall in different parts of Ethiopia and decreasing crop productivity. Yearly, many Ethiopians are exposed to famine, serious health problems, flood hazards, and drought due to rainfall variability in response to ongoing climate change (NMSA 2007; EPCC 2015a). Drought is a very critical climate-associated disaster in Ethiopia. For example, due to drought, 7.75 million people in 1983, 2.1million in 1996, 13.2 million in 2003, and 7.1 million in 2004 were exposed to famine (Dorosh and Rashid

2013; EPCC 2015b). A few years back, in 2015/16, more than 10,000,000 people were affected by drought in Ethiopia (Cochrane and Singh 2017). Like drought, floods have a considerable impact in different parts of Ethiopia. For instance, the 2006 flood in Gambella regional state damaged 1650ha of maize and decreased agricultural production by 20% (Gambella Region Disaster Prevention and Preparedness Agency 2007). Besides, 364 people were killed, and 6000-10,000 people were displaced in the South nation nationality people region (South Omo zone) (World Food Program [WFP] 2006). In the same year, due to the flash flood, 256 people died, more than 9956 people were displaced, and more than 1000 traders' property was damaged in Dire Dawa city (Alemu 2015). The spatiotemporal variability of rainfall is more important than total rainfall deficits for water-related problems in Ethiopia.

2.2.3.2 Potential impacts

Long-term climate change impacts in Ethiopia are primarily linked to the rise in temperature and rainfall variability (EPCC 2015a). So recognition and analysis of their pattern in the country are highly needed. Future predictions of temperature and rainfall patterns in Ethiopia show a high degree of uncertainty.

Most GCMs and regional projections of climate models agreed that the yearly average temperature is estimated to rise by between 1-2°C (USAID 2016), between 1.4 and 2.9°C (Cochrane and Singh 2017) by 2050. It is uncertain whether rainfall will rise/drop in Ethiopia, and its projections vary between -25% and +30% by 2050s. The percentage of extreme total rainfall increases to 18%. Studies suggest a 30% decrease in the runoff on several Nile tributaries by 2050 (USAID 2016). The increase in temperature results in increased water stress, whereas an increase in extreme rainfall results in an increasing flood. As an outcome, climate change affects the country's development by reducing Ethiopia's GDP by nearly 10% in the upcoming (2045) (USAID 2016). The following section lists a relevant summary of prior studies in Ethiopia related to the futuristic impact of climate change on water resources.

Serur and Sarma (2016) studied the climate change effects on the water resources of the Weyib watershed, Ethiopia. They used CanESM2 of the CMIP5 climate change model with three RCP emission scenarios to predict future rainfall and temperature; SWAT to estimate water availability until 2100. They detected that both precipitation and temperature showed an increasing trend in the upcoming periods. As well, they

identified a rising trend of yearly average daily water availability in the ranges of 11.82-12.68% (RCP 2.6), 3.98-20.40% (RCP4.5), and 9.18-24.49% (RCP8.5), and a decreasing trend of PET in all the three RCPs climate change scenarios compared to the reference period (1984-2004). They also estimated the seasonal variation of water availability in the basin. The result showed an increase in water availability in the rainy and transitional seasons, whereas a decline in the dry season. Gebre and Ludwing (2015) used five GCM outputs of CMIP5 based on high and stabilisation scenarios to appraise climate change impacts on water resources of Giligel Abay, Ribb, Gummer, and Megech catchments of Lake Tana watershed in Ethiopia. The result revealed that both temperature and PET increased in all months and seasons and all five GCMs. Although it varies in both magnitude and direction, precipitation shows an increasing trend in the future. The average yearly runoff may rise about +55.7% (RCP4.5) and +74.8% (RCP8.5) for the period of (2035-2064), and by +73.5% (RCP4.5) and +127.4% (RCP8.5) for the period (2071-2100) as compared to the baseline period (1960 to 2005). They conclude that the increase in runoff may positively contribute to existing development projects and crop productivity based on rain-fed agriculture in the basin on the condition that appropriate mitigation and adaptation measures are applied to diminish possible harmful impacts. The effect of climate change on the water availability in Lake Tana watershed in Ethiopia for early (2010 to 2039), mid (2040 to 2069), and late (2070 to 2099) 21st century was studied by Nigatu et al. (2016) using HadCM3 GCM output of A2 and B2 emission scenarios under SRES. Their result revealed that for both emission scenarios and all three future periods, Lake Tana's water storage constantly increases relative to the baseline period (1981 to 2010) due to the increase in rainfall noticeably from 9 to 11%. Kim and Kaluarachchi (2009) study showed that the Upper Blue Nile River Basin (UBNRB) in northern Ethiopia might not be adversely affected by climate change. They used the ensemble mean of six GCMs under A2 of SRES. The result revealed that both rainfall and runoff showed an increasing trend (2040 to 2069) compared to (1961 to 1990). The rising precipitation trend in the UBNRB implies water availability for crop production, reduced severe drought events, and a slight increase in flood risk by 2050s.

According to Dile et al. (2013), both rainfall and discharge of the Gilgel Abay River basin in Ethiopia decreased in 2010-2039 and increased in 2070-2100. They used HadCM3 GCM output based on A2 and B2 scenarios of SRES to project the future temperature and precipitation and SWAT for simulation of its effect on discharge. They concluded that the rise in rainfall in the wet period (Belg and Kiremt) enhances crop production in the basin, which is rainfall dependent even though the increase in evapotranspiration (ET) is expected due to the temperature rise. Depending on adaptation measures implemented in the area, the increase in flow may positively impact (water development projects) or negative impact (recurrent flooding problems). Mekonnen and Disse (2018) examined the effect of climate change on the Blue Nile River basin's water resources in Ethiopia based on CMIP3 and CMIP5 GCMs. The ensemble results showed an increasing rainfall pattern ranging from 1.0% to 14.4%, maximum temperature from 0.4°C to 4.3°C, and minimum temperature from 0.3°C to 4.1°C. Wagesho et al. (2013) examined the climate change impacts on the Blate and Hare watersheds runoff in Ethiopia. They used two GCM outputs under CMIP3 based on A2 and A1B emission scenarios input to the SWAT hydrological model. Results revealed that extreme events of daily rainfall and temperature would be increasing in the future compared to observed events. During the simulation period (2081 to 2090), the streamflow in the Hare and Blate River basins ranges from -4% to 18% and -4 % to 14%, respectively, compared to the baseline period (1990-1999). Setegn et al. (2011) analysed future temperature and precipitation in Ethiopia's Lake Tana basin using A1B, A2, and B1 emission scenarios. Then, they applied the temperature and precipitation generated from the 15 GCMs as an input to the SWAT model to predict streamflow and other hydrological components in the two future periods. They found that from 2070 to 2100 and for the three emission scenarios, the temperature increased 2°C-4.4°C and 2.2°C-4.9°C in the wet and dry periods, respectively. For the same period, the precipitation varies from -13% to +12% and -14% to +16%, respectively. They also observed a statistically significant decline in streamflow magnitude following the same direction as rainfall compared to the baseline period (1980-2000). Both soil moisture and groundwater also show a reduction in the future. They concluded that the basin might be exposed to agricultural drought unless ample irrigation water is available. A study was carried out by

Chaemiso et al. (2016) in the Omo-Gibe basin in southern Ethiopia to spot the impact of global change on water resources. They used the ArcSWAT model and the A1B emission scenario under SRES. The result indicated that both temperature and the annual PET would increase in the 2030s and 2090s. The rainfall varies considerably relative to the base period (1980 to 2005). The surface water availability is declining within the dry period and rising within the basin's wet period.

Abraham et al. (2018) revealed a high water availability reduction in the future in the Katar and Meki sub-watersheds of Lake Ziway, Ethiopia. They applied the outputs of multiple/three GCMs under stabilisation (RCP4.5) and high (RCP8.5) climate change emission scenarios and HBV. They reported that temperatures (maximum and minimum) would rise for the above scenarios. Rainfall shows a decreasing trend by up to 51.19% within the 2050s (2041 to 2070). Annual runoff depth was reduced by up to 19.45% and 20.28% in the Katar and Meki sub-watersheds, respectively, by the 2080s (2071 to 2099) compared to the base period (1980 to 2005). Another study in the same watershed by Zeray et al. (2006) indicates that the water resources in the watershed will be significantly affected by climate change in the future. They used B2A and A2A scenarios and SWAT to analyse the future interaction between climate change and water resources in the Lake Ziway watershed. They reported that average inflow volume to Lake Ziway decreased notably by about 19.47% and 27.43% for A2A and B2A scenarios, respectively, for the time from 2001 to 2099 relative to 1981 to 2000, even though the average monthly and annual rainfall will increase in Lake Zeway watershed by up to 29% and 9.4%, respectively. The rise in the rain is concealed by the increase in temperature (minimum and maximum) in the region.

Previously, most climate change studies in Ethiopia were based on CMIP3 climate change models (Zeray et al. 2006; Setegn et al. 2011; Dile et al. 2013; Wagesho et al. 2013; Chaemiso et al. 2016; Nigatu et al. 2016) and had been relying on a particular/finite number of climate models (Dile et al. 2013; Serur and Sarma 2016; Nigatu et al. 2016). The results will be highly uncertain if the simulation is based on a particular/finite number of GCMs. It will also most likely mislead decision-makers and policy developers (IPCC 2007; Taye et al. 2011). Thus, predicting climate change impacts based on multiple GCMs under CMIP5 is essential in Ethiopia for well perceptible of the potential climate change effects, informed decision making for

proper water resource management, and effectively responding and adapting to projected changes; otherwise, the consequences become awful.

2.2.4 State reaction to threats of climate change in Ethiopia

In Ethiopia, several strategies were implemented to reduce climate change's detrimental outcomes and maximise the country's adaptive capability. The government has signed some of the global and regional environmental agreements associated with global warming. Ethiopia also approved the UNFCCC (United Nations Framework Convention on Climate Change) and the Kyoto Protocol on 31th May 1994 and 21st February 2005. The 1992 Rio Convention on Environment and Development guide to designing of its conservation strategy in 1993 (EPCC 2015b). The 1995 Constitution of Ethiopia provides for environmental rights and a policy of promoting sustainable development. The constitution stipulated the environmental right under Article 44 (1), which states that "the citizens have the right to a clean and healthy environment".

Ethiopia prepared the National Adaptation Programs of Action (NAPA) in June 2007 (Tadege 2007). The NAPA includes the following 11 projects: Encouraging crop/drought coverage package, reinforcement of flood and drought timely caution structures, implementation of small-scale irrigation techniques and wise utilisation of water, pasture management measures, sustainable usage of wetlands, capacity building program for climate change adaptation, multipurpose large-scale water development project, community-based carbon sequestration project, establishing of a state research centre for climate change, strengthening malaria control package and upgrade of agroforestry practices in selected parts of the country. In addition to NAPA, based on Copenhagen's agreement, Ethiopia submitted Nationally Appropriate Mitigation Actions (NAMAs) to UNFCCC. The document lists about 88 projects (EPCC 2015b).

For a long time, emergency food aid was the first response to food insecurity in the country. However, emergency support delivery repeatedly as food for work had not solved the hitch. This observation influenced the launching of a Productive Safety Net Program (PSNP) in 2005. PSNP is credited for improvements in natural resource management and the environment through the conservation measures (watershed

management techniques) executed by the beneficiary households. PSNP builds households' resilience to climate variability and weather extremes (EPCC 2015b). On the other hand, (Weldegebriel and Prows 2013) reported that although the PSNP has effectively protected farmers from malnutrition and safeguarded farmers for the squat period, it is not developing resilience to hazards lastingly (Cochrane and Singh 2017). Presently, it is supported by the climate-smart initiative project to enhance its contribution to climate resilience.

Ethiopia launched a Sustainable Land Management Program in 2008. The second phase of the program introduces methods to tackle climate variability/change interrelated hazards and reduce GHG emissions to meet the GTP (Growth and Transformation Plan) and CRGE (Climate Resilience Green Economy) targets. The current GTP has a section entitled "Environment and Climate Change." The CRGE predates GTP II, provides a blueprint for achieving middle-income status by 2025 with no net increases in greenhouse gas emissions relative to 2010 levels (USAID 2016). The CRGE approach concentrates on both climate change adaptation and mitigation objectives. Having a policy framework is essential, but it is also equally noteworthy to monitor policies' implementation. In this regard, it is reported that there is a problem with implementation and enforcement capacity. The country has already started the implementation of some of the vital CRGE components. The policy framework is not yet complete. Literature and studies on the country's policy and institutional response to ongoing climate change threats are limited.

There are two general approaches to controlling the undesirable impacts of ongoing climate change: mitigation and adaptation, slowing down GHG emissions, and reducing their consequences, respectively. Concerning water resources and crop production, adaptation measures consist of using varieties and drought-resistant crops, using water-efficient irrigation techniques like drip irrigation, implementing water harvesting technology, and adjusting crop calendars (Bates et al. 2008). Hadgu et al. (2015) point out that alteration in crop type/variety, watershed management measures, crop diversifications, an adjustment in planting calendar, and water-efficient irrigation practices are adaptation measures that have been implemented in Tigray regional state in Northern Ethiopia. Another report by Ahmed (2016) showed that the above-listed

adaptations strategies are commonly implemented by farmers in Ethiopia's central Rift valley.

2.2.5 Other climate change impact studies

The followings are the summaries of the studies related to future climate change impact on water resources.

Chaturvedi et al. (2012) used eighteen GCMs and all the four climate change emission scenarios (RCP8.5, RCP6.0, RCP4.5, and RCP2.6) under CMIP5 to project surface temperature and rainfall for overall India. They found that, under no policy scenario (between RCP6.0 and RCP8.5), the mean surface temperature increases in the range of 1.7 to 2 °C and 3.3 to 4.8 °C for the period of (2021 to 2050) and (2070 to 2099), respectively compared to baseline time (1961 to 1900). Even if there is a more considerable spatial variation, rainfall rises by 4 to 5% and 6 to 14%, respectively, from 2021 to 2050 and 2070 to 2099, compared to the reference period. Their findings conclude that the ensemble mean closer to the observed climate rather than individual climate models. They recommended that the new RCP climate change emission scenarios under CMIP5 be used for climate change impacts and vulnerability estimation for adaptation planning by considering extreme projection.

In Kerala, India's humid tropics, Raneesh and Santosh (2011) assessed the climate change effects on streamflow at the watershed level. They used the Providing Regional Climates for Impacts Studies (PRECIS) regional climate model under A2 and B2 emission scenarios to project future temperature and precipitation and the SWAT hydrological model to simulate streamflow. They found that, for the southwestern monsoon period in the A2 emission scenario, there is an increase in temperature and ET by 2°C and 1.14%, respectively. Whereas rainfall and streamflow decreased by 11.5% and 7.53% from 2071 to 2100 compared to the baseline period (1981-2010). For the same period in the B2 scenario, temperature and ET increased by 1% and 1.12%, respectively. In contrast, rainfall and streamflow decreased by 8.79% and 4.62%, respectively. A similar trend was projected in the northeast monsoon also.

Basheer et al. (2016) used four GCMs under CMIP5 combined with SWAT to examine the potential climate change effects on future streamflow magnitude and

ecosystem habitats in the Dinder river basin in Sudan based on RCP4.5 and RCP8.5 climate change scenarios. Their studies concluded that the prevalent climate over the basin deciphers drying and warming trends. The streamflow has increased in the 2020s, 2050s, and 2080s relative to the baseline period (1961 to 1990). Also, the projected climate supports the ecological restoration of the habitats of flora and fauna in the Dinder national park in the basin on the condition that strong consideration will be given to extreme events to evade the undesirable impacts on the park's ecosystem habitat.

Leta et al. (2017) used SWAT and assessed the effect of precipitation, temperature, and CO₂ concentration changes on the water budget components of the Heeia watershed in Hawaii, USA. Due to the changes in projected temperature and rainfall, they observed that an overall decrease in all water budget components in general and groundwater (up to 15%) in particular by 2100 might have severe water availability implications in the area.

Vicuña et al. (2012) used three GCMs based on SRES, namely B1 (low), A1B (medium), and A2 (high) emission scenarios under CMIP3 combined with the Water Evaluation and Planning (WEAP) hydrological model to recognize the impact of upcoming temperature and precipitation changes on water resources and irrigated agriculture in Limari basin in Chile for two future periods (2010-2040) and (2070-2100). They had concluded that the climate in the basin demonstrates drying and warming trends. In turn, it reduces the amount of water availability and soil moisture in the basin (precipitation effect). Furthermore, due to enhanced ET at the plot scale, the demand for water in the basin increases (temperature effect), leading to a complicated situation for water resource management unless integrated water resource management practice is implemented to adapt to climate change.

A study carried out in the Mekong Delta in Vietnam by Shretha et al. (2016) revealed that groundwater level and storage are projected to decline at the end of the 21st century due to the rise in temperature by 1.5°C (RCP4.5) and 4.9°C (RCP8.5). The rainfall variability increases in the wet and decreases in the dry season. They have used five GCMs based on RCP4.5 and RCP8.5 climate change emission scenarios under CMIP5 to project the future temperature and precipitation. Groundwater level and storage were estimated by MODFLOW, whereas WESPASS hydrological models

estimated groundwater recharge and its spatial variation to examine the climate change impacts on groundwater resources in the study area.

Adhikari and Nejadhashemi (2016a) used six GCMs combined with the SWAT model to assess the impact of global change on water resource components such as potential ET, soil moisture content, surface runoff, and water yield in Malawi at the sub-basin, watershed, and country levels. They found a significant variation of -5.4% to 24.6% in annual rainfall, -5% to 3% in annual ET, 7.5% to 50% in runoff and water yield, and up to an 11.5% increase in yearly soil water at the country level. At the sub-basin level, the annual rainfall, runoff, and soil water increase in the north and declines in the south part of the country by 2050s (2041 to 2060) compared to the 1990s (1981–2000). Since all the models projected a distinct spatial pattern with an increase in annual rainfall in the north and a progressive reduction towards the south, they concluded that a significant increase in precipitation in the north part of Malawi enhanced agricultural productivity or induced flood hazards. In contrast, the southern region was found to be more prone to droughts.

Furthermore, Adhikari and Nejadhashemi (2016b) used the same GCMs, hydrological model, methods, and emission scenarios to evaluate the effect of global warming on water resources in Tanzania by the 2050s. In contrast to Malawi, although no distinct spatial trends were recognized in Tanzania, the result showed a seasonal trend. At the country's level, annual rainfall increases (4.3 to 30.7%) during the wet seasons but decreases during the dry seasons (-31.5 to 6.3%). In both seasons, both PET and soil moisture content increased. A significant increase in surface runoff (18.3 to 104.8%) was reported for the wet seasons. Overall, the sub-basin, watershed, and country levels revealed an increase in Tanzania's water resources during the wet seasons in the 2050s (2040–2059) compared to the 1990s (1980 to 1999). Depending on the level of water management technologies implemented in the country, a significant increase in surface runoff may have a positive (improve crop production) or negative (increase soil erosion and flood risk) impact.

The climate change influence on streamflow and sediment yield in the Gorganroud basin in Iran was studied by Mahmood et al. (2016) using three GCMs output for three emission scenarios: B1, A1, and A1F1 combined with the SWAT hydrological model. They found that an increase in sediment yield of 35.9%, 44.5%, and 47.7%

and an increase in discharge of 9.5%, 2.8% and 5.8% for the B1, A2, and A1F1 emission scenarios, respectively, by 2050s (2040–2069) compared to the baseline period (1971 to 2000). They concluded that climate change has more effect on sediment yield than streamflow. Besides, the increase in discharge and sediment yield is more marked in wet seasons, and the decrease is more significant in summer.

Zhu et al. (2016) used the coupled land surface and hydrological model system (CLHMS) based on RCP2.6, RCP4.5, and RCP8.5 emission scenarios under CMIP5 to predict the influence of climate change on water resources of the Yellow river basin in China. They found a considerable reduction of water resources up to 30% in the early and mid-21st century (up to 2080) relative to the reference period (1962 to 2005). Nevertheless, after 2080, the RCP8.5 scenario simulation increased extreme flood events due to increased rainfall.

In West Africa (upper Senegal basin), Mbaya et al. (2015) investigated the impact of climate change on hydrological variables and water resources availability by using the Max Planck Institute for Meteorology-Hydrology Model (MPI-HM) output data based on RCP4.5 and RCP8.5 emission scenarios as an input to the hydrological model to predict ET, soil moisture content, runoff and streamflow for the period of 2071 to 2100. In most of the basin, a general reduction of ET, soil moisture content, runoff, and streamflow was identified due to the decline in the magnitude of rainfall in the area for both emission scenarios compared to the baseline period (1971 to 2000). However, there are some localized increases in highland parts of the basin, particularly for uncorrected data. The reduction in water availability is more severe in the case of the RCP8.5 scenario pathway than RCP4.5.

Dumenu and Obeng (2016) investigated the repeatedly observed climate change impacts, socioeconomic factors contributed to vulnerability, and adaptation strategies implemented by rural communities in Guana. They reported a decline in crop yield, unpredictable rainfall, changing crop season, and extreme events like recurrent floods and prolonged drought are the most observed climate change impacts in Guana. For instance, socioeconomic aspects, such as heavy reliance on climate change susceptible livelihood, less diversified income source, high illiteracy level, and inadequate access to climate change information, contribute to climate change's high vulnerability level. Furthermore, the most dominant forms of adaptation strategies engaged by rural

communities in Guana based on indigenous knowledge and experience are crop diversification, farm size expansion, migration to urban areas, and engaging in non-climate sensitive occupation. Guana's situation is just a reflection of the condition of the African continent.

Changkun et al. (2015) examined the effect of climate change on streamflow in the Chu river basin, Central Asia, using five GCMs from CMIP5 under RCP8.5, RCP4.5, and RCP2.6 emission scenarios, along with the SWAT hydrological model. They found that, for all emission scenarios, precipitation showed a decreasing trend, although the difference is noted among scenarios. As well, under all scenarios and both short (1916-2045) and far future (2066-2096) periods, a general reduction trend was recognized in mean annual runoff in streamflow (-27.7% to -6.6%), snow (-21.4% to 1.1%) and glacier (-26.6% to -1%) compared to the reference period (1966-1995). They concluded that the climate would become drier and warmer, and the maximum streamflow will happen one month in advance in the future compared to the reference period in the study area.

Shrestha et al. (2016) estimated the potential climate change effect on temperature, precipitation, and streamflow of Nepal's Indrawati river basin. They used RCP4.5 and RCP8.5 scenarios under one regional climate model and two GCMs coupled with SWAT. It is found that the average ensemble temperature of the area will continuously rise and increase by 2.5⁰C to 4.9⁰C by the end of the 21st century compared to the reference period (1981 to 2005). Whereas the precipitation shows no distinct trends, its magnitude varies with time and RCPs. The annual streamflow will increase in the future, but the change is not consistent during the year.

2.3 LU/LC Change Impacts on Water Availability

Land cover covers the surface of the Earth, such as water, grassland, and forest, whereas land use refers to how the land cover is modified. Land use includes agricultural land, recreation areas, and built-up land. Due to its diverse environmental impacts, LU/LC change has become a global concern (Bewket 2002).

LU/LC changes and socio-economic dynamics have a strong relationship (Maitima et al. 2009). Socio-economic development drives LU/LC changes, potentially impacting water resources (Wagner et al. 2013). As the population increases, the need for cultivated land, grazing land, fuelwood, settlement areas also increases to meet the

growing demand for food and energy. Population growth, lack of awareness, and weak management are the leading causes of LU/LC change in Ethiopia (Bewket 2002).

LU/LC change is responsible for altering the hydrological response of watersheds in Ethiopia (Setegn et al. 2009; Gashaw et al. 2018). Several studies have reported the impacts of LU/LC changes on water availability. The conversion of forest to agriculture between the 1985 and 2011 periods in the Angereb watershed in Ethiopia has increased the mean wet flow by 39% and decreased the dry average flow by 46% (Getachew and Melesse 2012). It is also evident that surface runoff is lower, and groundwater flow is higher in vegetative lands due to the greater infiltration of rainfall into the shallow and deep aquifers. On bare land, where vegetation is absent, surface runoff is higher, and groundwater flow is lower (Bewket and Sterk 2005).

Gashaw et al. (2018) detected the hydrological impacts of LU/LC changes in the Adanssa watershed in Ethiopia. They found that the expansion of a cultivated and urban area, and the forest, scrubland, and grassland withdrawal during the 1985 to 2015 periods had increased the annual and wet season flow, surface runoff, and water yield. The LU/LC changes, on the other hand, reduced dry season flow, groundwater flow, lateral flow, and evapotranspiration. They concluded that the LU/LC change in the watershed significantly impacts the area's hydrology. These impacts will continue in the future. The increase in wet season flow will result in a flood, and a decrease in dry season flow will affect crop production unless proper watershed management measures are implemented in the area. Welde and Gebremariam (2017) identified the impact of LU/LC change on the hydrological responses of the Tekeze Dam watershed in Ethiopia. The discharge was increased in the watershed because of increased agricultural land and bare land at the expense of shrubland and grassland. The annual average discharge was increased by 6.20% due to LU/LC change in the study period (1986 to 2008). Chakilu and Moges (2017) assessed the effect of LU/LC change on the low flow of the Gumara watershed in Ethiopia. The result revealed that the bushland and forest had been changed into croplands. As a result, the low flow was reduced by 18.87% in the study area from 1973 to 2013. Tufa et al. (2015) evaluated the hydrological impact of LU/LC change in the Ketar watershed, Ethiopia. The expansion of cropland and settlement and reduction of grassland and forest in the

watershed increased monthly average wet flow by 3.8% for 2010 compared to 1986. In contrast, the monthly average dry season flow was reduced by 12.3% at the same time. Getahun and Van Lanen (2015) identified the hydrological effect of LU/LC dynamics of the Melka Kuntrie watershed in Ethiopia. Cultivated land has been stretched, whereas forest, grass, and shrublands are contracted in the study period (1986 to 2003).

The change in LU/LC increases wet season streamflow by up to 25%, even though dry season streamflow was inconsistent from month to month. Due to the decrease in forest and the increase in bare land and build-up areas in the metropolitan district of Mansehra in Pakistan, river discharge increased by 33.61% from the year 2000 to 2010 (Younis and Ammar 2018). Yira et al. (2016) assessed LU/LC change impacts on the Dano watershed streamflow in West Africa. A decrease in Savannah and an increase in cultivated land and build-up areas resulted in an increment of streamflow by 17%. Yang et al. (2014) assessed the hydrological response of LU/LC change in China's Laohahe basin. A significant reduction in streamflow up to 64% was exhibited within a short period (1999 to 2009) in the study area. Human water consumption appeared to be the most likely factor contributing to the significant reduction in streamflow in addition to increased build-up areas and cropland and decreased grassland in the watershed. Petchprayoon et al. (2010) studied the impact of LU/LC change on the Yom watershed streamflow in Thailand. A significant expansion of urban areas within a short period (1990 to 2006) was observed in the watershed. The change in LU/LC significantly increased the streamflow; more specifically, the peak flows at most measurement stations.

Pokhrel (2018) predicted the hydrological response for LU/LC change in the Khokana outlet of the Bagmati River, Nepal. Built-up areas increased by 6%, whereas the forest, shrubland, grassland, cropland, open fields, and waterbody decreased from 2000 to 2010. As a result, surface runoff has increased by 27%. In contrast, lateral flow and groundwater flow are reduced by 25% and 21%, respectively.

2.4 Variability and Trend Analysis Studies

Many trend analysis studies have been done in Ethiopia at different spatiotemporal scales and came up with mixed results. The following are the summaries of the studies related to the trend and variability of hydro-meteorological variables.

Asfaw et al. (2018) analyzed the spatiotemporal dynamics of meteorological variables of the Woleka watershed in Ethiopia based on 114 years (1901 to 2014). They employed a Mann-Kendall (M-K) trend test and Sen's slope estimator to identify the trend and magnitude of the trend, respectively. They found that the main rain season (Kiremt) and annual rainfall have decreased significantly with a rate of 15 and 13mm per decade, respectively, at a 0.05 level of significance. A highly variable and erratic but insignificant (1.93mm per decade) decrease in Belg rain was recorded. The temperature trend analysis revealed that the maximum temperature exhibited an insignificant increasing trend, whereas the minimum temperature exhibited a significant increasing trend for all months. They conclude that rainfall in the study area is erratic, unreliable, and concentrated into two months (July and August). The variability and change in onset and cessation periods, rather than the total amount, are the main challenges of rainfall distribution in the study area. The rain onsets late and ends up very early-which makes the cropping calendar shorter than before. Moreover, erratic rainfall and prolonged dry-spell periods during the primary rain season have been significant phenomena that adversely affect agricultural activity. Therefore, it is vital to adjust the agriculture activity to the variable situation and design planned climate change adaptation strategies to enhance rain-fed dependent smallholder farmers' adaptive capacity and resilience.

Kiros et al. (2016) analyzed the trend and variability of rainfall in the Geba river basin in Ethiopia's semi-arid climate. They used 43 years (1971-2013) measured rainfall data of seven stations and employed a non-parametric M-K test and Sen's slope estimator to identify the trend and magnitude of the trend. They came up with a mixed result. The Geba river basin's rainfall pattern exhibited a very high variability over time, with a peak value in July and August. Annual and seasonal rainfall upstream showed a non-significant decreasing trend, while downstream showed an increasing

trend. They concluded that seasonal and annual rainfall's temporal variability might affect water availability and crop production in the study area.

Chakraborty et al. (2013) applied both parametric and non-parametric tests to study the trend and variability of rainfall of the Seonath sub-basin in India from 1960 to 2008. They used the M-K trend test and Sen's slope estimator to detect the trend and size of the trend, respectively. The results showed that rainfall decreased seasonally and annually, with high interannual variability (CV=22.08%) in the northern parts of the watershed, except for a few stations in the southern part of the area, which showed a non-significant increasing trend.

Raju and Nandagiri (2017) evaluated trends and variability of rainfall, streamflow, maximum temperature, and minimum temperature in the upper Cauvery Basin, India, based on 30 years (1981 to 2010) data. They used CV and percentage departure for variability and the seasonal Kendall and Sen's slope estimators to identify the trend and magnitude of the trend. They found that although rainfall varies largely from during the winter season (December to March) up to 71%, its variability is less than 10% during the other months, including the Basin's monsoon season. Maximum temperature showed less variability (5-10%) across all stations and months, whereas minimum temperature exhibits more variation at all stations, particularly during winter. Streamflow also showed slight variation. Rainfall indicates no statistically significant trend at any of the stations in the basin during the study period. Concerning the trend of temperature, they found mixed results. Streamflow showed no significant trend, except for one station in the Basin.

Wagesho et al. (2013) examined the spatiotemporal variability of seasonal and annual rainfall over Ethiopia based on 0.5° resolution gridded monthly rainfall data from 1951 to 2000. They employed the M-K test and Moran spatial autocorrelation method for the analysis. The annual and summer (primary rainy season) rainfall data show significant decreasing trends in northern and western parts of the country, whereas an increasing trend in annual rainfall was observed in a small area in eastern parts of Ethiopia. Statistically, insignificant trends were observed in most regions (77%) of Ethiopia.

The spatiotemporal dynamics of rainfall in Ethiopia were investigated by Cheung et al. (2008). They used historical rain gauge data from 134 stations in 13 basins from

1960 to 2002. They reported no significant change/trend in annual rainfall at the country and watershed level in Ethiopia. Although there is a significant decline in Kiremt season (June to September) rainfall in the country's central and southwestern parts, the Belg (the primary source of rain for the south and southeast of the country) rainfall shows an insignificant increment with higher variability. The rise in Belg rainfall compensated for the dwindling in Kiremt rain.

Based on the comprehensive review of climate variability in Ethiopia, Conway (2000) concluded that spatially, average annual rainfall generally increases from the northeast to the southwest with increasing elevation. Temporally, there is no evidence for the overall trend or regime change in annual rainfall in the northeast Ethiopian highlands. However, a slight increase in Belg rainfall (in 1980s and 1996s) and a very slight decrease in Kiremt rain until the mid of the 1980s are reported. Osman and Sauerborn (2002) investigated the 100 years (1898 to 2097) trend of summer rainfall of the central highlands of Ethiopia. They concluded that summer rainfall had shown a decreasing trend statistically significant at a 1% level throughout Ethiopia's central highlands.

Gebre et al. (2013) analyzed the variability and trend of rainfall in the Tigray regional state in Ethiopia. They used 30 years (1980-2009) of daily rainfall data from five meteorological stations in the region. The M-K test and Sen's estimator were employed for trend and size of trend detection, respectively. They reported that rainfall in the area is highly unpredictable. Sizeable interannual variability of rainfall is observed in the area. Both the onset and cessation dates have changed significantly over time. The Kiremt precipitation has ended earlier in the northeast than in the southeast part of the region. Farmers' perception in the area strongly supports these results. The M-K test showed statistically a non-significant ($P > 0.05$) decreasing trend in annual and seasonal rainfall amounts over time in the region. However, these disagree with the farmers' perception of the area.

The space-time variability and trend of rainfall in Ethiopia's central highlands were investigated by Resoll (2011). He used 20 years (1987-2007) of daily rainfall data from seven meteorological stations to analyse. The result revealed that annual and Kiremt season (July to October) rainfall showed an increasing trend in the region while the Belg season (February to May) rainfall declined. Also, high rainfall

fluctuation was observed in Kiremt, whereas a shorting of the Belg season and an increase in temperature and PET were recognized in the Belg season.

Trend and space-time variability of annual and seasonal rainfall and temperature of UBNRB in Ethiopia were investigated from 1981 to 2010 by Mengistu et al. (2014). They employed slopes of regression lines using the list square method and the *F*-distribution test to appraise trends and significance. They come up with mixed results. In all seasons, minimum temperature showed a statistically significant increasing trend in a large portion of the basin, while declining trends were observed in the Basin's western and north-eastern parts. Annually, both the minimum and maximum temperatures showed a statistically significant warming trend in the area except in the small western side part of the basin. Rainfall in the area is highly variable, and it shows a non-significant increasing trend (35mm per decade) for the period studied. In general, they concluded that the mean maximum temperature increased at a slower rate than the mean minimum temperature. There was no statistically significant trend in annual rainfall in the basin during the study period.

Jury and Funk (2013) evaluated the long-term trend of historical and future rainfall and temperature over Ethiopia. They used observed data and A1B emission scenarios from Geophysical Fluid Dynamics Laboratory (GFDL) to examine historical (1948-2006) and future (2001-2050) periods, respectively. They observed that historically, temperature shows an increasing trend (0.03°C per year) across most of Ethiopia, and monthly rainfall shows a decreasing trend (-0.4 per year) over Ethiopia's southwestern region. The same trends are projected to continue up to 2050. The historical and future decline in rainfall and the rise of temperature over Ethiopia may reduce agricultural production and cause food insecurity.

Alemayehu and Bewket (2017) measure the spatial and temporal variabilities and trends of monthly temperature (1981 to 2011) and monthly rainfall (1983 to 2013) in the central highlands of Ethiopia. They employed linear regression and the *F*-distribution test to detect trend/change and statistical significance of trends. They found that both the annual and Kiremt rainfall show statistically insignificant rising trends while Belg rainfall shows significant declining trends. Besides, both the minimum and maximum temperatures showed a statistically significant warming trend across the study area. Trends of temperature and precipitation vary significantly

in the region. Thus, site-specific planning and adaptation measures to cope with climate change's adverse impact are highly needed.

Eshetu et al. (2018) investigated local level trends and variability of rainfall of two stations data, namely, Gatira (1983 to 2013) and Setema (1979 to 2011) in southwestern Ethiopia. The M-K test revealed no statistically significant annual and Kiremt rainfall trend in the area for the analysis period. They found a mixed result. The yearly rain showed an increasing and decreasing trend in Gatira and Setema, respectively. Unlike other parts of the country, rainfall in the area has low inter-annual variability, with CV values of 8% and 23% at Gatira and Setema.

In recent days annual and Kiremt rainfall for the southern, eastern, and south-western Ethiopia exhibits a significant reduction since about 1982. Nevertheless, there is no trend in annual, seasonal rain, and rainy days over central, northern, and north-western Ethiopia from 1965 to 2002 (Seleshi and Zanke 2004). Seleshi and Zanke used 11 station data in different agro-climatic zones of Ethiopia and employed the M-K test for the analysis.

Funk et al. (2012) identified a significant drop in rainfall and rising temperatures over time in many parts of Ethiopia. Belg and Kiremt rainfall has declined by 15 to 20% since the mid 1970s in southern, south-eastern, and south-western Ethiopia (Funk et al. 2012).

Shi et al. (2013) investigated the trend and spatial variation of rainfall in an upstream watershed of the Huai River in China. They used 60 years (1951 to 2010) of daily rainfall data from 38 rain gauge stations and employed the M-K test and linear regression for the analysis. They found that the annual rainfall exhibits a slightly increasing trend with 0.042mm/year over the analysis period. Seasonally, they found a mixed result. Both negative (in spring and autumn) and positive (in summer and winter) trends were observed in the region. Spatially, the annual rainfall showed positive and negative trends in the northern and southern regions, respectively.

Admassu and Seid (2006) assessed the trend of rainfall over Ethiopia from 1973 to 2002. They used ten selected station data and the M-K test for the analysis. They found that the annual total rainfall exhibits a statistically significant decreasing trend, while Belg rainfall does not show any significant trend in the analysis period. It is difficult to conclude the trend over the country based on only ten station data.

Abrha and Simhadri (2015) analyzed the monthly, seasonal, and annual rainfall trends in southern Tigray, Ethiopia. They used 34 years (1978 to 2012) rainfall data from three stations in the area and an M-K test for the analysis. They reported a statistically significant increase in Kiremt rainfall in the region at the 0.01 and 0.05 levels, while Belg rainfall exhibits a non-significant decreasing trend. Annual rainfall does not show any significant change/trend in the area due to an increasing and decreasing trend in Kiremt and Belg rain, respectively, in the region.

Rosell and Holmer (2007) analyzed the CV, rainy days, dry spells, and rainfall intensity in South Wollo, Ethiopia. They used 40 years from 1963 to 2013 data for the analysis. They reported that rainfall varies significantly in the area with minor changes in the annual amount. Despite the fact that rainfall in the Belg season has decreased and rainfall in the Kiremt season has increased, both seasons have become shorter. The more considerable precipitation variation in the area affects crop production in the region, particularly Tef (stable crop in Ethiopia) production in the Belg season.

Mekasha et al. (2014) analyzed climate extremes using 42 years (1967 to 2008) daily measured temperature and rainfall data from 11 stations in three different environments in Ethiopia, namely highland, pastoral, and agro-pastoral. They found mixed results. Temperature extremes showed both a negative and a positive trend. There is a general tendency to increase warm extremes and a decrease in cold extremes in the regions. Precipitation extremes showed high variability within stations. They concluded that the local climate's response to global warming could differ in physiographically diverse areas (Mekasha et al. 2014).

2.5 Soil Loss Rate

Soil erosion is a process of losing topsoil particles by erosion agents (Eckelmann et al. 2006). Soil erosion resulting from the natural causes exclusive of man's interference is called geological erosion, which occurs at low rates. When soil loss exceeds the annual soil formation, mainly in agriculture, it will generate accelerated soil erosion, which is more rapid and more destructive than natural erosion (Morgan 2005). Wind and water are the most important agents for causing accelerated soil erosion. Thus, accelerated erosion can further be classified as wind and water erosion. Water erosion is the removal of soil particles from the surface owing to runoff and raindrop impact.

It is unquestionably the trickiest land degradation in the globe (Bridges and Oldeman 1999).

The soil erosion processes due to water are classified into inter rill (splash and sheet), rill, gully, and stream channel erosion. Splash and sheet erosions remove soil by raindrop impact and shallow overland flow, respectively (Morgan 2005; Kothyari 2012). Rill erosion is the soil erosion resulting from runoff whereby several small but well-defined channels are formed. They are differentiated from gullies because they are small enough to be erased easily with conventional tillage methods (Kothyari 2012; USDA 2011). Among different water erosion types, inter rill and rill erosions are the primary reason for reducing soil productivity. Gully erosion is a process of the wearing away of soil by large channels of not less than 0.3m width and 0.3m depth due to concentrated runoff. Streambank erosion removes stream bank soil by water either flowing over the sides of the stream or scouring from the stream bed. Three complex processes in water erosion act in sequence, namely, detachment (the removal of individual soil particles from the soil mass), transport (the movement of soil particles), and deposition (the transfer of soil particles from the sediment load to the soil mass) (Lal and Humberto 2008; USDA 2011). The followings are the summaries of the studies related to soil loss rate.

2.5.1 Soil loss rate studies

Ganasiri and Ramesh (2016) used RUSLE with GIS and RS to assess the soil loss rate of the Nethravathi river basin in the southwestern part of India. They found that the basin's soil loss is 473339 t yr⁻¹ from 3128km², equivalent to 1.51 t ha⁻¹yr⁻¹. The result is comparable with the observed sediment data from 2002 to 2003 water year. They also identified that a slight change in land use from forest to cultivation increases soil loss markedly in the Nathravathi river basin. Gelagay and Minale (2016) evaluated the Koga watershed soil loss rate in Ethiopia using RUSLE combined with RS and GIS. They recognized that the soil erosion in the watershed ranges from 0 to 265 t ha⁻¹yr⁻¹, with an average soil loss of 47 t ha⁻¹yr⁻¹. They also identified that topography and soil are significant soil loss factors in the study area as a large amount (71%) of soil loss is initiated from the steepest slope, and Nitosols and Alisols are dominant.

In India's Kali river basin, Markose and Jayappa (2016) used the RUSLE and GIS tools to predict SLR for prioritizing sub-watershed for watershed management. Even

though a substantial soil loss rate is observed in the basin (up to 6995 t ha⁻¹yr⁻¹ with an average value of 2339.58 t ha⁻¹yr⁻¹), most areas experience SLR between 0 and 38 t ha⁻¹yr⁻¹. Only 6.67%, 3.77%, and 10% of the area are exposed to very high, severe, and extreme erosion hazards, respectively. They also recognized that the downstream part of the basin where a steep slope exists is exposed to excessive soil erosion. Cropland areas show less soil loss than forest land, and rainfall and topography are the main factors of soil erosion in the Kali river basin.

Uddin et al. (2016) identified priority areas of the Koshi basin for soil and water conservation measures using RS data, GIS tools, and RUSLE. They developed a soil erosion risk map and classified the basin into eight erosion hazard classes based on soil loss rate. They recognized that topography is the main factor affecting soil loss in the Kashi basin. The central part of the basin needs a top priority for management as it is exposed to high erosion due to its topography. Rejari et al. (2016) estimated both temporal and spatial variation of soil loss of wet semi-arid Seethagondi watershed cluster in India using RUSLE coupled with ArcGIS. Results showed that 85.3% of the cluster had soil loss below 20 t ha⁻¹yr⁻¹. A small portion of the watershed (20.7%) is prone to severe erosion (> 15 t ha⁻¹yr⁻¹). In drought and high rainfall years, the cropland's soil loss rate varied from 2.9 to 3.6 t ha⁻¹yr⁻¹ and 29.4 to 34.7 t ha⁻¹yr⁻¹, respectively, with an average soil loss of 12.2 t ha⁻¹yr⁻¹. A maximum soil loss is estimated in August due to the high value of erosivity in this month. In terms of LU/LC wise, the soil loss is relatively higher in forest land, followed by wasteland and cropland. Since most of the area is cropland and has a slope of less than 10%, they recommended agronomic SWC measures combined with water harvesting technologies for sustainable watershed management.

Maryam and Biswajeet (2014) used USLE to predict the spatial distribution and temporal variation of soil erosion risk at Kuala Lumpur city in Malaysia. Results revealed that only 3.8% of the area is susceptible to a severe (> 20 t ha⁻¹yr⁻¹) soil loss rate, and it shows a decreasing trend from 2000 to 2010. Adriyanto et al. (2015) evaluated the soil erosion of the Kalikonto watershed of Indonesia by using RS data and the RUSLE. They found that the watershed's soil loss rate varies from 5.5 to 376.67 t ha⁻¹yr⁻¹ with a mean annual value of 72 t ha⁻¹yr⁻¹. They also identified that only 9% of the watershed area is prone to severe and very severe erosion. Besides, a

minimum erosion is observed from forest areas relative to other land covers. Senti et al. (2014) used MUSLE to study Lake Haramaya watershed soil erosion in Ethiopia. Results show that the mean annual sediment yield is $24.32 \text{ t ha}^{-1}\text{yr}^{-1}$ and rainfall is the primary factor affecting soil erosion in the area.

Bewket and Teferi (2009) assessed the spatial variation of soil erosion risk of Ethiopia's Chemago watershed using USLE integrated with RS and GIS. They found that the watershed's annual SLR varied from 0 to $125 \text{ t ha}^{-1}\text{yr}^{-1}$ with a mean annual value of $93 \text{ t ha}^{-1}\text{yr}^{-1}$. They also identified that over 58% of the watershed is prone to severe erosion risk ($> 80 \text{ t ha}^{-1}\text{yr}^{-1}$). In the erosion hot spot area where steep lands are overgrazed or cultivated, the erosion is estimated above $125 \text{ t ha}^{-1}\text{yr}^{-1}$. A study carried out in the Densu River Basin of Ghana by Ashiagbor et al. (2013) predicted the spatial distribution of soil erosion hazards using the RUSLE and GIS tools. Similar to other studies, a small portion of the watershed (6%) is prone to high and very severe erosion risk. Gashaw et al. (2017) assessed the soil erosion rate of the Geleda watershed in Ethiopia by using USLE adopted to Ethiopian conditions. The watershed soil loss rate varied from 0 to $237 \text{ t ha}^{-1}\text{yr}^{-1}$ with a mean annual value of $23.7 \text{ t ha}^{-1}\text{yr}^{-1}$. About 21.25% of the watershed is prone to soil erosion above the country's maximum soil loss tolerance limit.

Ayalew (2015a) used RUSLE adapted to Ethiopian conditions combined with RS and GIS to examine the soil loss rate of the Zingin watershed in the highlands of Ethiopia. He identified that the mean annual soil loss of the watershed is $9.10 \text{ t ha}^{-1}\text{yr}^{-1}$. 21.69% of the area is categorized under moderate to high soil loss rate, which is greater than its maximum soil loss tolerance. Furthermore, Ayalew (2015b) applied the same approach to estimate the soil loss of the Lalen watershed in the highlands of Ethiopia. Nevertheless, in this case, only 5% of the watershed is susceptible to moderate to high soil erosion, which is greater than tolerable soil loss. Brhane and Mokonen (2009) studied the SLR of different land use and landforms of Medego Watershed in Ethiopia's arid and semi-arid zone using USLE adapted and modified to Ethiopian conditions. They found that the mean annual soil erosion of the Medego watershed is $9.63 \text{ t ha}^{-1}\text{yr}^{-1}$. The result showed that in flat plains (slope $< 2\%$) of the watershed, soil loss is about $1.59 \text{ t ha}^{-1}\text{yr}^{-1}$, which is less than the minimum soil loss tolerance of Ethiopia ($2 \text{ t ha}^{-1}\text{yr}^{-1}$). However, from steep mountains (slope 30-50%) landforms, the

soil loss is about 35.43 t ha⁻¹yr⁻¹ which is the highest compared to soil losses of other landforms in the watershed. The soil loss of very steep mountains (slope > 50%) of the watershed is 7.63 t ha⁻¹yr⁻¹, which is less than steep mountains (slope 30-50%), hill landforms (slope 15-30%), and rolling (slope 8-15%) landforms because of more human activities like intensive cultivation and overgrazing in these slope classes compared to very steep slope class in the watershed.

Wolka et al. (2015) used RUSLE to map soil erosion risk areas of the Cheleleka wetland watershed of southern Ethiopia. They recognized a great spatial variation in soil loss's magnitude in the watershed (2.5 to 85.64 t ha⁻¹yr⁻¹). 13.6%, 15.5%, and 17.3% of the area is classified under low (less than 10 t ha⁻¹yr⁻¹), moderate (10 to 20 t ha⁻¹yr⁻¹) and high to very high (20 to 45 t ha⁻¹yr⁻¹) soil loss rate, respectively. However, 53.6% of the watershed is vulnerable to severe to very severe soil loss, which is greater than 45 t ha⁻¹yr⁻¹. Adugna et al. (2015) assessed soil erosion on different land use land cover in northeast Wollega in Ethiopia by using RUSLE. They found that the mean annual soil loss rate from forest, grass, shrub, and cropland is 4.5 t ha⁻¹yr⁻¹, 22 t ha⁻¹yr⁻¹, 37.6 t ha⁻¹yr⁻¹, and 65.9 t ha⁻¹yr⁻¹, respectively. According to Fanta et al. (2016), a significant reduction in soil loss rate is observed due to soil and water conservation measures in the Agula watershed in semi-arid northern Ethiopia. They assessed the temporal variation of soil loss rate from 1990 to 2012 by using RUSLE. The result showed that the soil erosion reduced from 28 t ha⁻¹yr⁻¹ to 12 t ha⁻¹yr⁻¹ from 1990 to 2000. And from 28 t ha⁻¹yr⁻¹ to 10 t ha⁻¹yr⁻¹ from 1990 to 2012. Sisay et al. (2014) employed RUSLE integrated with GIS to identify soil erosion hot spot areas of the mountainous landscape of Abaro Medeo in the Wondo Genet watershed of Ethiopia. They recognized that the area's soil loss rate varies spatially from 2.5 t ha⁻¹yr⁻¹ to over 60 t ha⁻¹yr⁻¹ with a mean annual soil loss of 26 t ha⁻¹yr⁻¹. Moreover, 56.3% of the study area is prone to soil loss greater than 20 t ha⁻¹yr⁻¹ and susceptible to high to severe erosion hazards. Amsalu and Mengaw (2014) assessed soil erosion's spatial distribution in the Jabi Tehinan woreda in Ethiopia using RUSLE and GIS. The result revealed a significant spatial variation of soil loss in the woreda from 0 to 504.6 t ha⁻¹yr⁻¹ with an average value of 30.6 t ha⁻¹yr⁻¹.

Coca and Nilca (2016) used RUSLE to estimate soil loss in the upper catchment of the Bârsa River. They found that the area's annual soil loss ranges from 0 to 263 t ha-

yr^{-1} , and the majority of the site has a soil loss of less than $25 \text{ t ha}^{-1}\text{yr}^{-1}$, whereas soil loss exceeding $100 \text{ t ha}^{-1}\text{yr}^{-1}$ has a little weight. They also identified that the slope and land cover are the primary influencing factors in the study area. In the Lake Tana basin of Ethiopia, Setegn et al. (2009) used the SWAT model to recognize the watershed portion, which contributes a large amount of sediment and GIS integration with Multi-Criteria Evaluation (MCE). Results from SWAT revealed that 18.4% of the area (mainly cultivated areas and areas at a steep slope condition) is identified to be the most vulnerable areas for soil erosion, which has sediment yield ranges from 30 to $65 \text{ t ha}^{-1}\text{yr}^{-1}$, and results from MCE also indicate that only 12-30.5% of the basin is high erosion potential area. Moreover, topography and land cover are the two most dominant factors affecting soil erosion in the Lake Tana basin (Setegn et al. 2009). The maps from the two approaches showed a significant likeness indicating areas that contribute a heavy sediment load.

A study was carried out at the Doviraj watershed of Iran by Fathizad et al. (2014) using RUSLE and SDR to calculate SY. They reported that the mean annual SY of the watershed is $273.6 \text{ t ha}^{-1}\text{yr}^{-1}$, and it is close to observed sediment data ($253.4 \text{ t ha}^{-1}\text{yr}^{-1}$) in the watershed. Gelagay (2016) quantified the spatial variation of the Koga watershed soil loss rate in Ethiopia by using RUSLE with a GIS environment. The result revealed that the annual average sediment yield delivered to the Koga watershed outlet is $25 \text{ t ha}^{-1}\text{yr}^{-1}$. It mainly originated from the very steep upper part of the watershed, and topography and soil are the main factors affecting the soil loss rate in the watershed. They concluded that unless appropriate watershed management is implemented to control the eroded sediment, the Koga irrigation reservoir will lose its intended service due to heavy sedimentation. Yuan et al. (2016) used the USLE to estimate the soil loss rate from China's Lake Poyang watershed. The soil loss rate ranges from 0 to $394.8 \text{ t ha}^{-1}\text{yr}^{-1}$, with a mean value of $1.82 \text{ t ha}^{-1}\text{yr}^{-1}$. The total sediment load in the Lake is $1438 * 10^4 \text{ t yr}^{-1}$ from 62000km^2 . Like other areas, a small portion of the watershed (0.83%) in the northwest and northeast corners is the source of massive soil loss. They concluded that, unless suitable and effective soil erosion measures are practised, the watershed reservoirs are severely affected by soil erosion.

Tamene et al. (2006) carried out a reservoir survey to estimate the sediment load rate for 11 micro-irrigation dams in the Tigray region of Northern Ethiopia. The reservoirs' spatial variation in sediment yield varied from 3.45 to 49.35 t ha⁻¹yr⁻¹, with an average annual sediment yield of 19 t ha⁻¹yr⁻¹. They concluded that most micro-dams would be closed due to soil erosion and sedimentation in less than half the design period. A further study in the same region by Haregeweyn et al. (2006) point out that only 30% of the micro-dams are expected to last for the whole design period. Whereas the rest 70% of irrigation reservoirs lost their proposed purpose before their intended service time due to sediment deposition in the reservoirs. Wolancho (2012) reviewed the problem and effect of sedimentation in Ethiopian reservoirs and concluded that heavy sedimentation was experienced in most Ethiopian existing dams such as Koga, Melke Wakena, Aba-Samuel, Gilgel Gibe I, Angereb, Legedadi, Adrako, and many irrigation micro-dams. The inventory of 92 micro dam reservoirs in the Tigray region in Ethiopia made by Berhane et al. (2016) based on direct field observational method, secondary data, and selected interviews showed that 61% of the sustainability of micro-dams in the region was threatened due to soil erosion. The sustainability of the Angereb water supply dam in north-western Ethiopia is threatened due to highly accelerated sediment deposition (Haregeweyn et al. 2012). They employed a bathymetric survey to recognize the sediment load in the domestic water supply reservoir. Although a relatively decreasing trend is observed due to SWC measures undertaken in the watershed, the annual total capacity loss was estimated at 4.02%, 3.16%, and 3.03% during 1997-2005, 1997-2007, 2005-2007, respectively. Moreover, the specific sediment yield of the watershed ranged from 1,789 to 3,354 t km⁻² yr⁻¹. They concluded that the water supply from the reservoir to Gondar town would diminish under half the designers' design life. The mean annual observed sediment yield in Anjeni gauged watershed in Ethiopia is 24.6 t ha⁻¹ (Setegn et al. 2010). They simulated the sediment yield in the Anjeni watershed using SWAT and found that the mean annual sediment yield was 27.8 t ha⁻¹ during calibration and 29.5 t ha⁻¹ for the validation period.

2.5.2 Water erosion assessment methods

This subtopic describes and discusses various methods and approaches to soil erosion assessment by focusing on water erosion models.

Depending on the intended purpose, data on water erosion and factors affecting it can be gathered from the field or laboratory. For realistic data, field measurements are the most reliable. However, it is not easy to determine the principal causes of soil loss due to conditions that vary in time and space. Since various factors affecting soil erosion can be controlled in the laboratory, measurements intended for explanation are better undertaken. However, due to the artificiality of laboratory experiments, verification of their natural circumstance results is needed (Morgan 2005). Identifying areas at risk of soil erosion is a prerequisite for planning and executing SWC measures to reduce soil erosion effectively. Major approaches to identify areas at risk of soil erosion are a qualitative approach using expert knowledge and a quantitative approach based on measurements and erosion models.

2.5.2.1 Qualitative approaches based on expert Knowledge

Qualitative approaches are the relative indication of areas at risk of soil erosion based on expert knowledge. These approaches use surveys about a complete acquisition of the soil loss data in a particular place as a base for assessing soil erosion risks and their controlling factors (Eckelmann et al. 2006). An example of a qualitative approach based on expert knowledge is the Global Assessment of Human-induced Soil Degradation (GLASOD). GLASOD is intended to give information about soil erosion and create awareness of the importance of soil conservation for decision-makers and governments at a global level to make a suitable plan and set priorities for future investments. The GLASOD survey provides essential data on the spatial variation and severity of soil degradation based on responses to a questionnaire from experts in different parts of the globe (Bridges and Oldeman 1999). Its main advantage is its applicability at all scales, from local to global quickly. However, it is difficult to compare countries because GLASOD relies only on an expert's opinion, exclusive of any field measurements, and some experts even did not reply to the questionnaire. Its reliability and reproducibility remain uncertain. Qualitative approaches revealed the spatial variation of erosion (Bridges and Oldeman 1999). However, they are subjective and do not provide the information needed to plan and appraise SWC measures.

2.5.2.2 A quantitative approach based on the measurement

Conventional soil erosion assessment approaches are centred on quantifying soil erosion from field erosion plots based on actual measurements. This approach gives the most precise SLR. However, they are costly, require a long time, and provide site-specific data, which may be applicable for only that location. Moreover, it is impractical to take measurements at all points in the watershed. It also takes time to perform repeated measurements to build an adequate database to verify that the data is not influenced by a few years of unusually high rainfall and extreme events. Long-time measurements are necessary to evaluate climate, and LU/LC change impacts on SLR and SWC measures' utility. These difficulties can be overcome by soil erosion models (Morgan 2005).

2.5.3 Erosion models

Soil erosion models are the mathematical descriptions used to designate complex erosion processes in a simplified form. They applied to estimate soil loss rates under various conditions for planning and evaluating SWC practices' performance (Tiwari et al. 2000). Besides, modelling soil erosion is vital to clarify the factors controlling soil erosion, understanding the driving processes and their interaction, evaluating onsite and off-site consequences on soil productivity and water quality, and selecting suitable SWC measures (Tiwari et al. 2000; Lal and Humberto 2008). Well developed and accurately calibrated soil erosion models provide reasonable estimates of soil loss rates. Several erosion models of different prediction capabilities and purposes have been developed (Lal and Humberto 2008). There are three main reasons for modelling soil erosion. They are used as a predictive tool for assessing soil loss rate, providing data on spatiotemporal dynamics (where and when) of soil erosion, and models can elucidate erosion processes and their interactions. In general, water erosion models are classified into two types based on the principles used in developing the models. These are empirical and physically-based models.

2.5.3.1 Empirical models (Statistical model)

Empirical models are developed based on relating erosion controlling factors to soil loss through comprehensive field observation and measurement (Beach 1987). Hudson also articulates it similarly. An empirical model is one based on observation or experiment and not derived from theory. It fits observed facts and predicts what

will happen in certain circumstances because we know what has happened before in those situations (Hudson 1995). Empirical models do not consider the fundamental processes involved and how the system functions. These models can only be operated in the designed direction where inputs go into one side of the equation and the output on the other side. Scientist-developed the parameters under particular environmental circumstances, and for that reason, the parameters are appropriate to only those situations. SWC planners often use empirical models in preference to process-based models as they can be implemented in situations with limited data and parameter inputs, primarily for predicting soil erosion and recognizing leading causes of erosion in the area (Merritt et al. 2003). Empirical models are speedy in estimating water erosion, but they need many years' data and are valid only within the boundaries they developed. The use of empirical models in other areas requires an adaptation of the model to local conditions. The USLE model and its derivatives (MUSLE and RUSLE) are the most commonly used empirical water erosion models described in brief below.

Universal Soil Loss Equation (USLE): The USLE is the most commonly applied and widely recognized empirical water erosion model developed in the United States based on measured data on soil loss and its controlling factors from many field erosion plots. SWC planners and decision-makers use this model to predict the long-term average soil loss for possible alternative combinations of vegetative cover and land use in relationship with a specific slope gradient and length, soil, rainfall, and management systems (Wischmeier and Smith 1978). The equation assembled many interconnected physical and management parameters that affect soil loss under six significant erosion controlling factors. Mathematically the equation is denoted as:

$$A = RKLSCP \quad (2.1)$$

Where A is the mean annual soil loss rate ($t \text{ ha}^{-1}\text{yr}^{-1}$), R is the rainfall erosivity factor [$\text{MJ mm ha}^{-1} \text{ hr}^{-1} \text{ yr}^{-1}$], K is the soil erodibility factor [$t \text{ hr MJ}^{-1} \text{ mm}^{-1}$], L is the slope length factor, S is the slope steepness factor, C is the land cover and management factor, and P is the support practice factor. The details of the USLE factors are found in (Wischmeier and Smith 1978).

Revised Universal Soil Loss Equation (RUSLE): Further investigation and practice have improved USLE and led to the development of RUSLE. RUSLE is a water

erosion model intended to estimate the long-term annual soil loss rate by splash, sheet, and rill erosion resulting from raindrop impact and runoff. It is an update of USLE that takes account of the extensive knowledge about the physics of soil erosion and the analysis of data that did not exist when USLE was developed (Renard et al. 1997). RUSLE retains the six factors of USLE. Although the original USLE has been retained, technology for determining these factors' values has been altered. The new data has been introduced, updating the method to calculate the terms in the equation. For example, the cover and management factor (C) is now a product of four subfactors representing crop canopy (CC), surface cover (SC), surface roughness (SR), and prior land use (PLU). To determine the topographic factor (LS), a new equation was developed. The new algorithm helps to estimate water erosion from a wide range of slope gradients. The K-factor in the RUSLE made time-varying, bringing an alternative regression equation for soil erodibility term. RUSLE also includes new isoerodent maps as well as conservation practice values (P). The change in RUSLE made the model suitable for predicting water erosion from agronomic settings and rangelands, disturbed areas, and a situation involving construction sites, mine spoils, and land reclamation. It is also used for a wide range of slope gradients (Renard et al. 1997).

Modified Universal Soil Loss Equation (MUSLE): Researchers have modified the USLE parameters for extended applications. Investigators developed the MUSLE to estimate sediment yield for particular storm runoff events (Williams 1975). Sediment yield is the quantity of eroded soil delivered to an outlet of a watershed or a point in the watershed far from the source of the detached soil particles (Renard et al. 1997). MUSLE is a modified version of USLE and used many readily available parameters and data sets of USLE. The equation of MUSLE can be mathematically expressed as follows:

$$Y = 11.8(Qq_p)^{0.56}KLSCP \quad (2.2)$$

Y is total sediment yield from a storm event in a ton, Q is the volume of storm runoff in m³, q_p is the peak runoff rate in m³/s. K is the soil erodibility factor, L is the slope length factor, S is the slope steepness factor, C is the land cover and management factor, and P is the support practice factor.

In the MUSLE, the factors made up of peak discharge and runoff variables replace the USLE's rainfall erosivity factor. It made the model predict sediment yield, channel erosion, gully erosion, floodplain scour, and deposition, which is not possible by USLE and RUSLE. In contrast to USLE/RUSLE, the MUSLE estimates sediment yield directly without sediment delivery ratio. Moreover, MUSLE has an advantage over USLE/RUSLE due to its capability to predict a single storm sediment yield. The limitation of MUSLE is, it predicts a sediment yield only and is not suited for long-term soil loss estimation.

2.5.3.2 Physical-based models (Deterministic model)

Physically-based water erosion models are derived from understanding the basic erosion processes and considering the laws of conservation of mass and energy (Tiwari et al. 2000; Morgan 2005). These models indicate the natural processes by explaining each physical process/sub-processes of the system relevant to erosion and deposition and combining them into a complex model. Since they require cost-demanding, extensive, and high resolution spatial and temporal input data, the successful implementation of physically-based models is restricted by the availability and quality of data for calibration and validation (Beach 1987). Such problems are noticeable in developing countries where data is limited, not easily accessible, and stored in different formats.

However, they can accommodate the ongoing natural process's spatiotemporal dynamics, which can not be realized through empirical models (Tiwari et al. 2000). Moreover, physical processes do not vary from one environment to another, and therefore, theoretically, these models can be used in new environments. Usually, researchers employ physically-based models to elucidate the mechanics of soil erosion. Examples of physical-based models include Water Erosion Prediction Project (WEPP), Agricultural Non-Point Source (AGNPS), Soil and Water Assessment Tool (SWAT), Areal Nonpoint Source Watershed Environmental Response Simulation Model (ANSWER), Chemical Runoff and Erosion from Agricultural Management Systems (CREAMS), European Soil Erosion Model (EUROSEM).

These physically-based models usually require expensive methods to determine the input parameters. They require extensive data. For example, AGNPS requires 22 input parameters, and EUROSEM needs more than 60 input parameters for implementation.

Most of them (such as AGNPS, ANSWER, and EUROSEM) are single storm event-based, whereas few, like CREAMS, simulate single or long-term sequences. Some of them (for example, SWAT and CREAMS) incorporated MUSLE to estimate water erosion. Physical-based models vary in size of the area they are applicable and can predict water erosion.

2.5.4 Selection of water erosion models

There is no best soil erosion model for all purposes. Erosion models vary in terms of the type of input data requirements, difficulty, the scale, intended use, the types of output they give, and the processes considered (Merritt et al. 2003). It is essential to identify the exact objective and purpose of models designed to estimate soil erosion to select models. Two main divisions are models for prediction and models to assist with an explanation. If the intention is to predict the amounts of soil loss rate under different SWC measures, the empirical models are efficient and effective, whereas the purpose is for explaining the process of erosion, physically-based models are the preference (Hudson 1995). However, it is challenging to execute physically based water erosion models in developing countries because of their extensive data requirements. Therefore, it is vital to recognize models that are not very much simplified and under-represent the physical basis or are too complicated and costly to apply. An assessment of erosion based on the fundamental soil erosion models that best fit with the available resource and data is necessary (Sonneveld et al. 1999).

Among various soil erosion models, USLE and its revised version (RUSLE) coupled with GIS are more prevalent in water erosion estimation and applied worldwide to guide conservation planning, quantify water erosion and estimate sediment yield (Ashiagbor et al. 2013; Maryam and Biswajeet 2014; Adriyanto et al. 2015; Ganasiri and Ramish 2016; Markose and Jayappa 2016; Rejari et al. 2016; Uddin et al. 2016; Yuan et al. 2016). It is due to practicability within logical costs, better accuracy for larger watersheds, easy availability of input data, and the model is relatively easy to use, compatible with incorporating various spatial information such as LU/LC, topography, soil, management, and its capability to predict the many years' average annual soil loss rate and comparing the possible benefits of different SWC measures (Arnold et al. 1998). According to Wischmeier and Smith (1978), USLE enables SWC planners to estimate the mean soil erosion for each possible alternative

combination of conservation measures and crop type in integration with a particular soil, rainfall, and topography. Thus, RUSLE/USLE with the GIS environment has been widely used worldwide.

Despite the above advantages, USLE can not simulate the following (Wischmeier and Smith 1978): Soil loss daily and its variation from storm to storm; gully and stream bank erosion; detailed processes. USLE only predicts soil loss that results from splash, sheet, and rill erosion. Although the model has the above limitations, it is still used most extensively for predicting water erosion as a function of the primary soil erosion controlling factors in data-scarce areas of developing countries.

USLE/RUSLE was mainly developed for conditions in the USA. The use of USLE/RUSLE in other areas requires adaptation to local conditions. For example, in East Africa, Ethiopia, Hurni (1985) simplified the USLE by adapting the factors to conditions in Ethiopia based on long-term measurements and experimental data from a large number of test plots in various slopes, soils, land uses, crops, and under several SWC treatments in different agro-climatic zones. After Hurni (1985), in various agro-climatic regions of Ethiopia, USLE/RUSLE coupled with GIS has been successfully and extensively applied for the estimation of the spatial variation of soil loss and sediment yield, and it has provided good results (Bewket and Teferi 2009; Brhane and Mokonen 2009; Sisay et al. 2014; Adugna et al. 2015; Ayalew 2015a,b; Wolka et al. 2015; Fanta et al. 2016; Gelagay and Minale 2016; Gashaw et al. 2017).

Primary USLE was developed to predict the long-term average annual soil loss rate from agricultural land and predict rill, splash, and sheet erosion. It suits slopes with a low gradient. Therefore, its performance is less in areas where gully erosion is the dominant, a wide range of slope gradients, and other non-agricultural areas like construction sites. Although RUSLE shares the limitations of USLE, the changes in RUSLE make it useful for estimating soil loss for agronomic settings and situations involving construction, mine spoils, land reclamation, and from a wide range of slope gradients. In the MUSLE, the newly developed rainfall-runoff erosivity term of peak discharge and runoff variables makes it the model useful for estimating channel erosion, gully erosion, floodplain scour, and deposition separately. Moreover, the change in MUSLE makes it suitable to predict sediment yield for individual storm runoff events. That is the main limitation of USLE/RUSLE.

If the competition is between USLE and its derivatives (RUSE and MUSLE), it is better to select a water erosion model that simulates the important processes in the study area and is based on the purpose. For instance, if the intention is to estimate the event-based/storm-based sediment yield or the area is dominated by gully erosion, select the MUSLE rather than the USLE/RUSLE. Whereas the intention is to estimate the long-term average soil loss rate to prioritize the subwatershed for soil and water conservation planning, evaluate management practices, or rill and inter-rill water erosion is dominant, select USLE/RUSLE. More specifically, for agricultural land and slopes with a low gradient, select USLE rather than RUSLE, whereas for high gradient and non-agricultural areas, choose RUSLE rather than USLE.

For example, in a non-agricultural area, Spaeth et al. (2003) compared RUSLE and USLE predicted soil loss rate with measured field data on different sets of rangeland vegetation types. They found that RUSLE performs better than USLE in rangelands. Bayramove et al. (2013) compared the performance of USLE with MMF. Their findings showed that USLE has an excellent performance in predicting soil loss rate compared to MMF in all aspects.

Furthermore, According to Tiwari et al. (2000), USLE and RUSLE did show evidence of better model efficiency than WEPP. Mondal et al. (2018) compared USLE, RUSLE, and MMF water erosion models' performance in central India. They compared the models' output with measured sediment data. They found that RUSLE has better performance than other models in that specific area. Ubierna et al. (2009) compared the suitability of USLE, RUSLE, and WEPP to estimate soil loss in non-agricultural areas. They compared the model output with field data. They found that USLE is overestimated, and WEPP underestimates soil loss on restored mining slopes, whereas RUSLE estimates are close to field data. They concluded that RUSLE is more suitable for estimating soil loss than USLE and WEPP on restoring mining slopes. Sadeghi and Mizuyama (2007) evaluated the performance of MUSLE to assess storm event sediment yield in the Khanmirza watershed, Iran. The MUSLE output is compared with measured sediment data. The result revealed that the MUSLE had performed well enough ($R^2 = 0.99$) to predict storm event sediment yield in the study area.

No particular model is best for each application. Each model has strengths and weaknesses, data requirements, and purposes. Therefore, a model's choice should be mainly based on the reason for which it is intended (prediction or explanation) and the availability of data, money, and time.

2.6 Summary and Key Points from the Literature

The followings are some of the main points concluded from the literature review.

- Climate change and LU/LC change impacts on hydrological processes are the leading causes that affect the hydrological response of a watershed. Hydrological processes are very sensitive to change in temperature and precipitation. The rise in temperature and the variability of rainfall are the major features of climate change. Those climate elements affect almost all other hydrological processes, and the long-term climate change impacts in Ethiopia is mainly linked to these two climate elements. So recognition and analysis of their pattern in the watershed are highly needed.
- Climate change impacts are location specific. Adaptation measures are implemented at the watershed level. As a result, recognizing the effects of climate change at a watershed level is sensibly imperative. However, the exact impacts at the watershed level in Ethiopia are poorly understood. The potential impacts of these changes on water resources at the appropriate level are not examined in most Ethiopian parts and particularly in the southern region. Ethiopia's climate change studies are concentrated on the UBNRB, or Lake Tana watershed, and other areas were neglected.
- Previous climate change studies in Ethiopia are based on old emission scenarios under SRES and a single or finite number of GCMs. Forming an inference regarding climate change impacts on water resources based on a single GCM may not provide a clear picture of the coming changes.
- The nature and magnitude of global change affecting Ethiopian water resources are not yet adequately understood. Despite the fact that the water sector is one of Ethiopia's most vulnerable, there are many knowledge gaps regarding the climate-water interface. This gap is a current challenge for planners and policymakers to develop long-term water resource management and climate change adaptation strategies in the water sector. Therefore, a

comprehensive study is highly needed, and the issue has to be addressed at a scale relevant to decision making.

- Even though the impact of climate change is widely understood globally, the exact effects at the watershed level are poorly understood. Recognizing local climate change impacts at a watershed level is sensibly imperative since adaptations are practised at the watershed level. The future climate change impacts on the water resources in the Tikur Wuha watershed is poorly understood.
- The SWAT model is widely used in climate and LU/LC changes impact assessments in Ethiopia and has an excellent performance in predicting climate change and water interaction.
- As far as rainfall distribution in Ethiopia is concerned, the main problem is not the amount, rather the variability. The spatiotemporal variability of rainfall is more important than total rainfall deficits for water-related issues in Ethiopia. Historically, climate variability has had a high impact on Ethiopian agricultural productivity and livelihood. Ethiopian rainfall is highly variable, both temporally and spatially, and must be analyzed at a watershed level rather than the whole. Trends in annual and seasonal rains are mostly sensitive to local scale climatic controls such as topography. Trend analysis studies in Ethiopia are not conclusive, and some are conducted at a macro scale, which needs more examination. Several studies investigated the meteorological trends in Ethiopia, however, there are no prior studies that investigated water resource management in the watershed in the study period considered.
- Soil erosion is one of the main problems upsetting water resources and land productivity in the study area. Soil erosion hazards and the main factors affecting soil loss are highly site-specific. A large amount of the total soil loss from a watershed originated from a small portion of the watershed areas. Managing this small portion of the watershed can significantly reduce both the onsite and offsite impacts of soil erosion. Since resources are scarce in developing countries like Ethiopia, implementing watershed management practices on the entire watershed is not practical. Therefore, recognizing erosion-prone areas for prioritizing sub-watershed based on the severity and

risks of soil erosion is indispensable for planning and implementing sustainable watershed management and wise use of resources. Many studies are conducted in Ethiopia on prioritising watersheds to implement SWC measures by considering the amount of soil loss. However, almost all are not prioritized based on sub-watershed (without delineating the sub-watershed). It is not practical to implement SWC measures, given that a watershed is a superlative unit for developing and managing the land and water resources.

- There are several methods for assessing soil erosion, but no one best universal method for evaluating soil erosion works everywhere. Methods have to be critically chosen depending on the assessment and applicability objectives because each is best at performing a particular purpose. If the intention is to predict the amounts of SLR under different SWC measures, the empirical models are efficient and effective. In contrast, the objective is to understand erosion mechanics; preference should be given to the physically-based water erosion models. USLE and its revised version (RUSLE) integrated with GIS and RS soil erosion assessment methods have been used in most countries and showed better performance. It is recommended for data-scarce areas. However, utilization of USLE/RUSLE in other areas requires adaptation to local conditions.

CHAPTER 3: STUDY AREA, DATASETS, AND RESEARCH METHODOLOGY

3.1 Description of the Study Area

The Tikur Wuha watershed location is between latitude 6° 48' 47" N to 7° 10' 58" N and longitude 38° 28' 28" E to 38° 43' 3" E in Southern Ethiopia (Figure 3.1). It falls into two administrative boundaries of the Sidama national regional state in the south and Oromia national regional state in the northern alignments. TWW has a catchment area of 681km². The Tikur Wuha river originates from the Wondo genet highlands. The Tikur Wuha river is 52km long and flows northwest toward Lake Hawassa in Ethiopia. Several streams characterize the drainage network of the TWW. All streams drain into the Cheleleka wetlands, which flow into Lake Hawassa through the Tikur Wuha river (the sole permanent river feeding Lake Hawassa). A river gauging station is located at Dato, near the outlet of the river. The topography ranges from 1668 to 2976 meters above the mean sea level (Figure 3.1). The considerable part of the study area (57.83%) is level to the gentle slope (0-8%) but bounded by steep mountains with hillier regions to the eastern part of the watershed. TWW is a sub-humid watershed in the Ethiopian highlands. Based on the rainfall data from four meteorological stations from 1978 to 2017, the average annual rainfall was 1071mm. Rainfall shows a bimodal pattern (Figure 3.2). The watershed receives about 47% of annual rainfall during the Kiremt season (June to September). The Belg season (February to May) and the dry season (October to January) subsidize 37% and 15% of the annual rain, respectively. The annual average daily temperature of the watershed is about 18.5°C (Figure 3.2). Four major soil types have been identified in the watershed: Andosols, Fluvisols, Luvisols, and Vertisols. Most of the watershed area is rain-fed agricultural land (primarily mixed perennial and annual cropping). Other LU/LCs in the watershed are grassland, shrubland, urban, and swampy. Because of population growth and urbanization, rapid LU/LC change in the watershed is observed. The issue of soil erosion is severe in the TWW. Water-related climate change impacts in the TWW are poorly understood. Hence, the comprehensive assessment of the effects of climate change and LU/LC change on water availability in the watershed is essential.

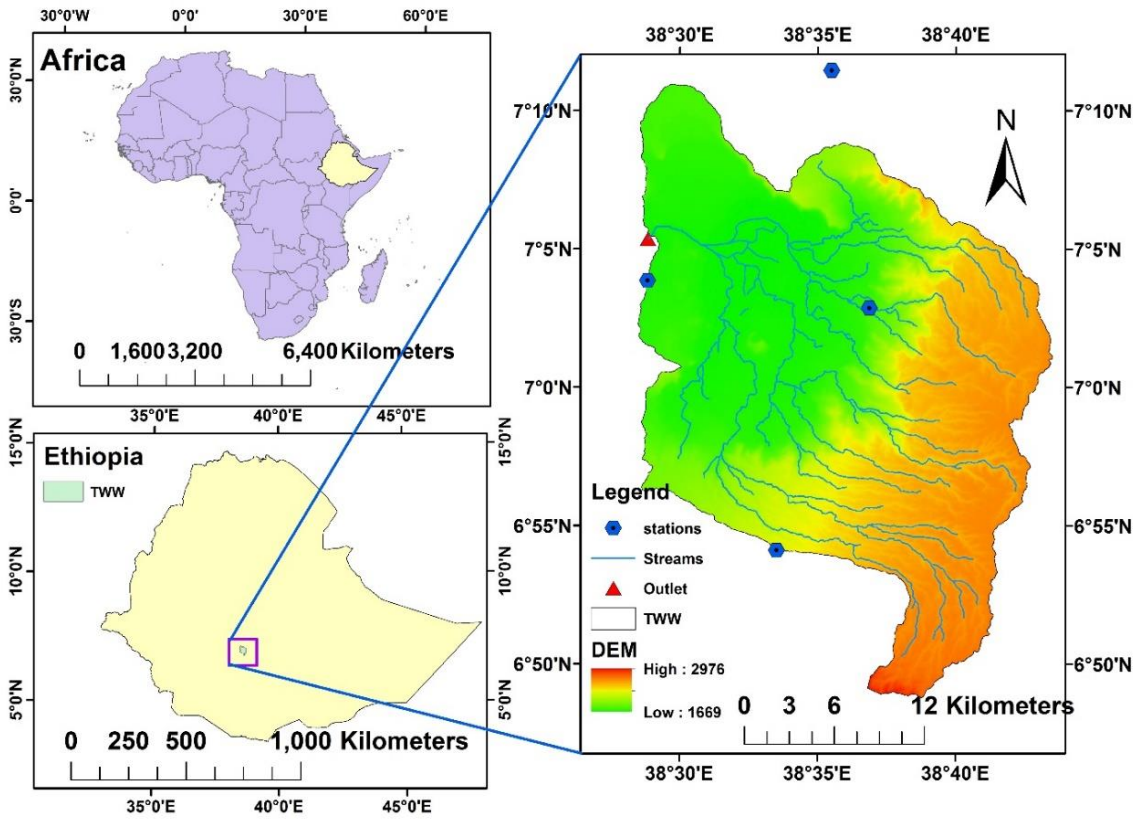


Figure 3.1. Location of Tikur Wuha watershed

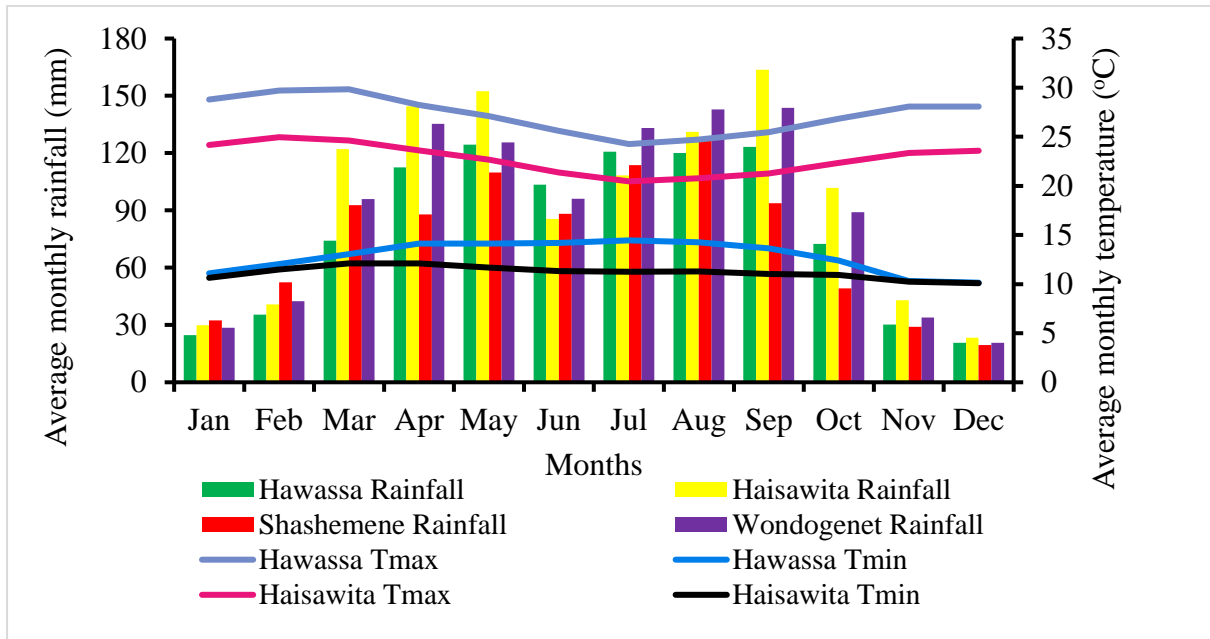


Figure 3.2. The 40 years average monthly rainfall and temperature of the TWW

3.2 Datasets for the Study

Both spatial and temporal data were used for the study. The spatial datasets are the Digital Elevation Model (DEM), LU/LC, and soil. Temporal data includes hydrological and meteorological data. Shuttle Radar Topography Mission (SRTM) DEM 30m resolution was downloaded from <https://earthexplorer.usgs.gov>. The path/row of the DEM is 38/6 and 38/7, and the acquisition date is 23-09-2014. The DEM was used for watershed delineation, sub-basin definition, and Hydrological Response Units (HRUs) setup. The topographic parameters of the studied watershed are also derived from the DEM. Figure 3.3 showed the DEM of the TWW.

Landsat Multispectral Scanner (MSS) for 1978, Landsat Thematic Mapper (TM) for 1988 and 1998, and Landsat Operational Land Imager and Thermal Infrared Sensor (OLI_TIRS) for 2017 were used for LU/LC change detection and to disclose the hydrological impacts of LU/LC dynamics in the study area. The images are downloaded from <https://earthexplorer.usgs.gov>. Landsat image data was selected due to its accessibility of adequately long period image series in the study watershed (year consistency across the TWW) to analyse LU/LC dynamics. The satellite images were taken in the same time frame in the dry season (November and December) under clear cloud cover conditions, and in the same vegetation season to negate vegetative effects on the change detection between pairs of images as well as to balance the bias from inter-annual variability of cloud cover. Clouds introduce significant noise to an image by obscuring the reflectance of radiation from Earth's surface materials. The details of the characteristics of the images used for classification are given in Table 3.1. A soil map was prepared from the FAO soil map for the study area. The soil's physical and chemical property parameters were derived from the digital soil map of the world soil database. Figure 3.4 displays the soil map of the study area. These spatial datasets and text files need to be prepared before running the hydrological model. The spatial datasets were created in the raster format, and the same projection was used for all maps.

The daily meteorological data are precipitation, minimum temperature, maximum temperature, wind speed, solar radiation, and relative humidity. The meteorological data from 1978 to 2017 were collected from the National Meteorology Service

Agency (NMSA) Ethiopia, South nation nationalities and people's regional state branch office at Hawassa. The number of stations is selected based on data availability, spatial representation, data length (years), and data records gaps. Four stations, Hawassa, Haisawita, Wondogenet, and Shashemene, were chosen based on the criteria. Hawassa station is a class one (synoptic) station. At Hawassa station, more than ten meteorological parameters are observed. Haisawita station is the third class station (ordinary station). Only three meteorological elements are found: maximum air temperature, minimum air temperature of the day, and total rainfall amount in 24 hours. Shashemene and Wondo genet stations are the fourth class stations (rainfall recording station). At these stations, only the total rainfall amount in 24 hours is observed. In all the stations, the rain gauges are non-recording type. Daily streamflow data from 1980 to 2002 was taken from the Ministry of Water, Irrigation and Energy in Ethiopia to calibrate and validate the SWAT model.

The bias-corrected daily minimum and maximum temperature and precipitation outputs from the Coordinated Regional Climate Downscaling Experiment (CORDEX) were obtained from GFZ (Geoforschungs Zentrum) German Research Centre for Geoscience for both historical (1960 to 1999) and future time horizons (2020 to 2099). CORDEX is a global collaborative project that aims to improve the awareness of regional downscaling of global climate scenarios and provide and develop comprehensive, regional climate information essential for vulnerability, impact, and adaptation studies at local and regional levels. Table 3.2 summarizes the type, source, and purpose of the data.

Table 3.1. The characteristics of Landsat images used for LU/LC change detection

Spacecraft Identifier	Sensors	Date of acquisition	Path-Row	Spatial resolution
LANDSAT 8	OLI/TIRS	12-Dec-2017	168-55	30m x 30m
LANDSAT 5	TM	24-Dec-1998	168-55	30m x 30m
LANDSAT 5	TM	10-Nov-1988	168-55	30m x 30m
LANDSAT 3	MSS	07-Nov-1978	181-55	57m x 57m

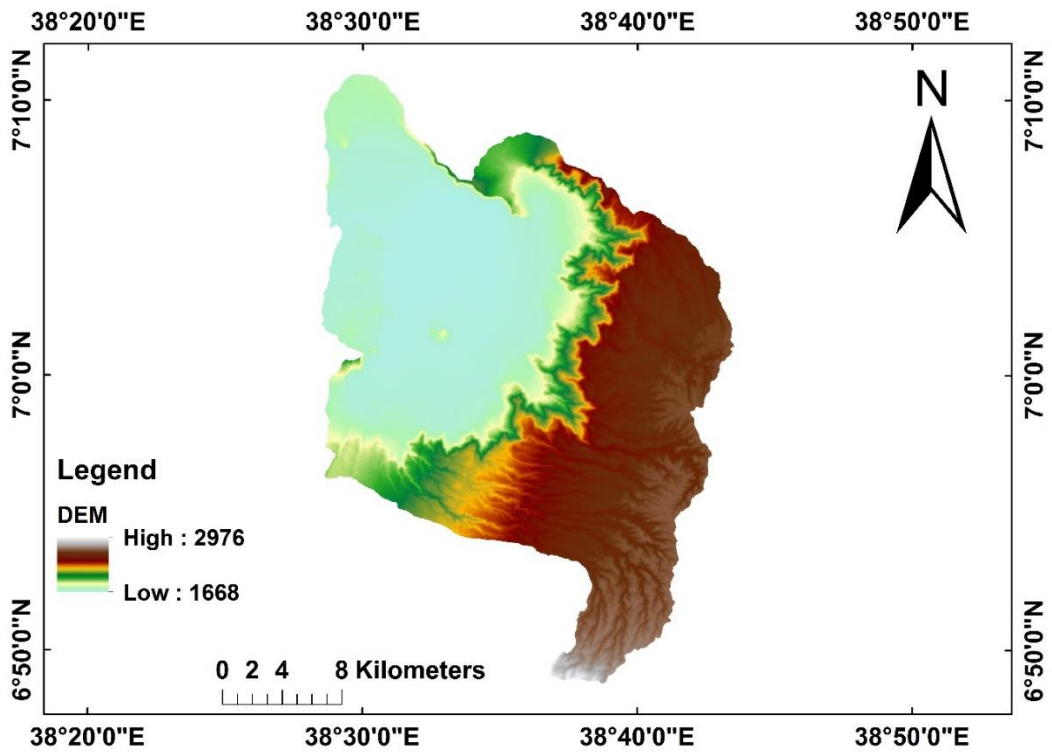


Figure 3.3. Digital elevation model of Tikur Wuha watershed

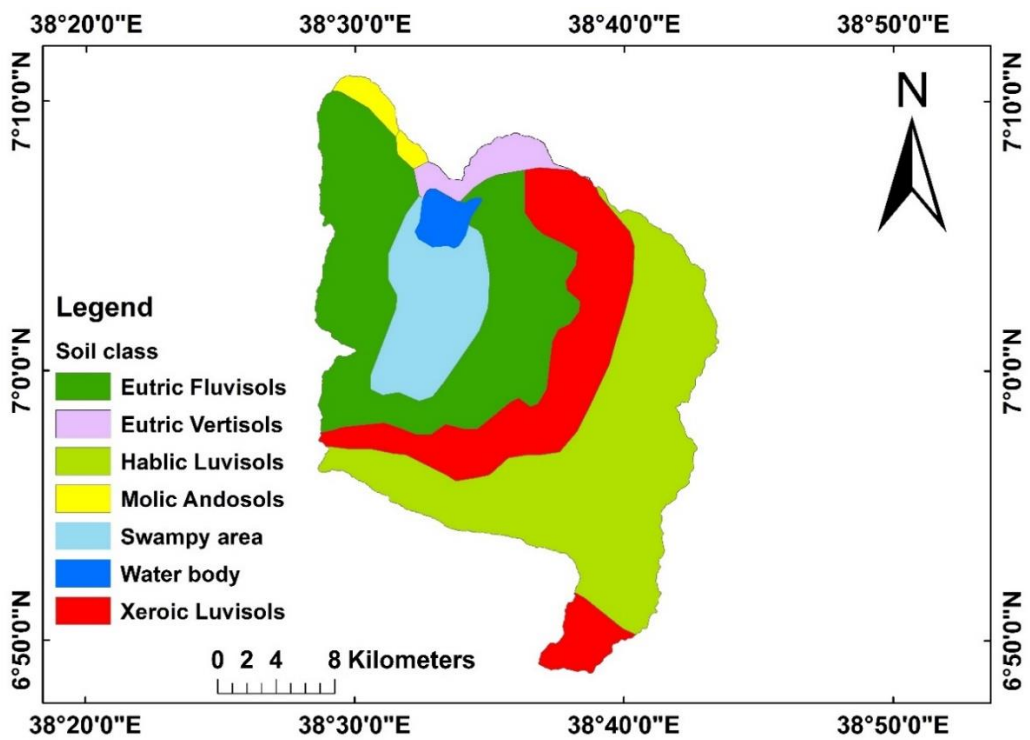


Figure 3.4. Soil class map of the Tikur Wuha watershed

Table 3.2. The type, source, and the purpose data

Types of Data	Period (Time)	Source	Purpose
Meteorological Data	1978 to 2017	NMSA, Ethiopia	Input for SWAT and USLE, and for trend analysis
Hydrological Data (Streamflow)	1980 to 2002	MoWIE, Ethiopia	For calibration and Validation
Spatial data (DEM)	2014	USGS	For watershed delineation, Input for both SWAT and USLE
Spatial data (Soil)		FAO	Input for both SWAT and USLE
Spatial data(LU/LC)	1978, 1988, 1998, and 2017	USGS	Input for both SWAT and USLE, LU/LC change detection
CORDEX data (T-max and T-min, and precipitation)	1960-1999 and 2020-2099	German Research Centre for Geoscience	Analysis of climate change impacts on hydro-meteorological variables

3.3 Research Methodology

This research has the climate change impact, LU/LC change effect, trend and variability analysis, and soil erosion portion. The Soil and Water Assessment Tool (SWAT) hydrological model was used to assess the hydrological response of climate and LU/LC change in TWW. The Mann-Kendall (MK) trend test was used to detect the trends of hydro-meteorological variables. The universal soil loss equation (USLE) was implemented to predict the soil loss rate and prioritize the sub-watersheds of TWW for soil and water conservation practices. Figure 3.5 presents the general methodology flow chart. The data processing and analysis methods for each objective are discussed independently under the topics from 3.3.1 to 3.3.4.

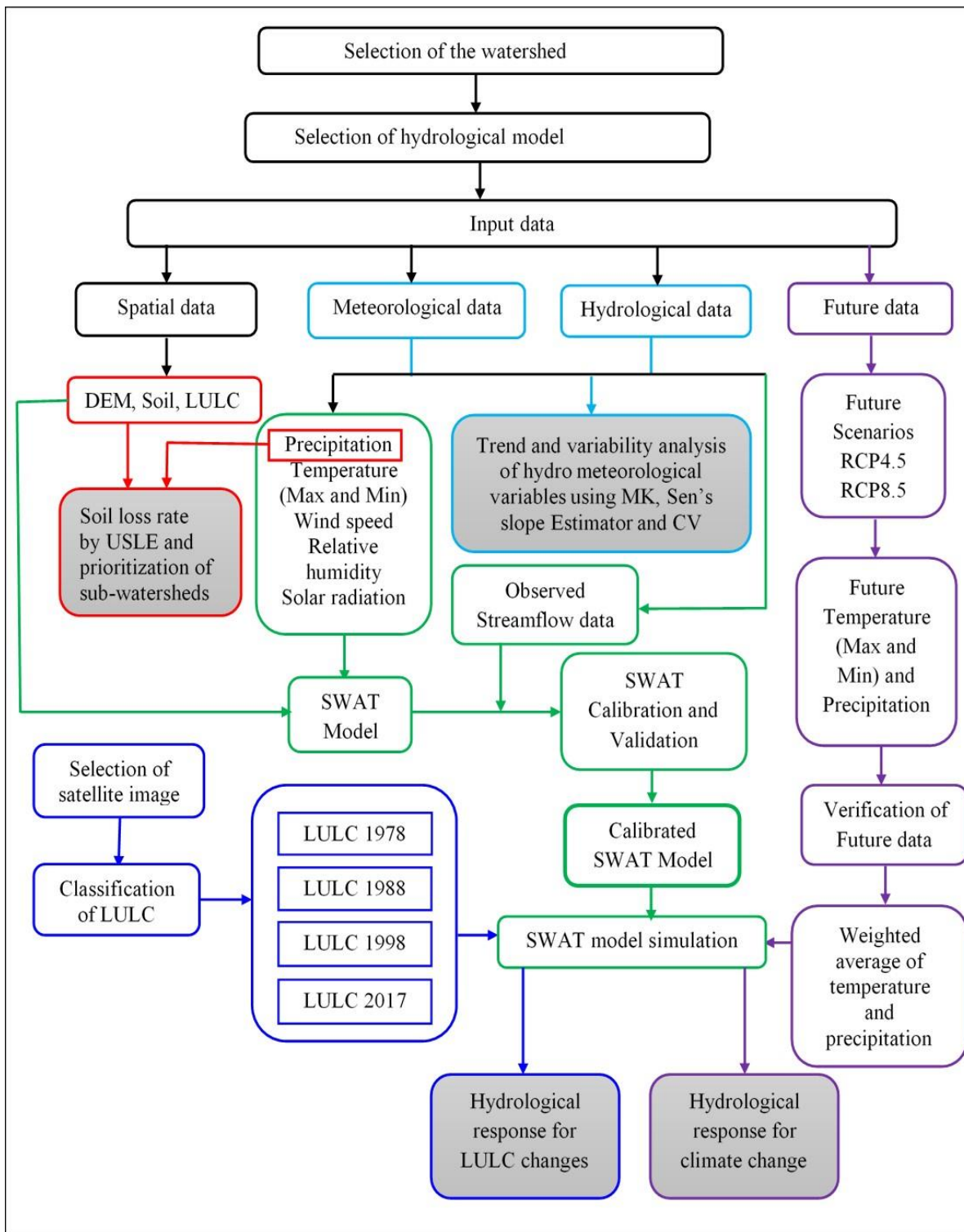


Figure 3.5. General methodology framework of the study

3.3.1 Methods for hydro-meteorological impacts of climate change

The following three steps have been followed to predict the potential impact of climate change on hydro-meteorological variables in TWW:

- i. The two most crucial climate elements, temperature (minimum and maximum) and precipitation, which affects water availability, were collected for both historical and future time based on RCP4.5 and RCP8.5 climate change scenarios; analysed and compared with the baseline/reference period.
- ii. The SWAT model was calibrated and validated based on observed streamflow data in TWW.
- iii. The potential impacts of climate change on streamflow was evaluated by using SWAT in the two future time slices, mid-century (2020 to 2059) and end century (2060 to 2099), compared with the reference period (1960 to 1999).

3.3.1.1 Selection and evaluation of climate scenarios

The accuracy of GCMs decreases at increasingly finer spatial and temporal scales, while impact studies' needs increase with higher resolution (Wigley et al. 1990; Xu 1999). The bias-corrected CORDEX output climate data were used for this study because GCM is inherently unable to represent local sub-grid-scale features. Since the multi-model ensemble approach better accounts for uncertainties involved with climate models, several climate models' usage of ensembles has become common (Kundzewicza et al. 2018). Besides, it is recommended that a range of possible climate scenarios be considered rather than a single best or average case climate scenario (Jose and Dwarakish 2020).

A performance indicator is a measure of any model to determine how well it simulates the observed data. It is very much necessary and recommended to have a detailed evaluation of model performance against observed datasets, which can help determine the best-performing models. NSE (Nash and Sutcliffe Efficiency) was used for this study (Nash and Sutcliffe 1970). For the performance evaluation of the climate models, monthly maximum and minimum temperature and yearly precipitation (1978–2001) at the Hawassa meteorological station were used. For further analysis, a weighted average of the five best models was used. A list of RCMs selected from multiple GCMs and used in the study is given in Table 3.3.

Table 3.3. List of RCMs from multiple GCMs used in the study

Institute ID	Institute name	Model ID (RCMs)	Driving model
CCCma	Canadian Center for Climate Modelling and Analysis	CCCma-RCM4	CCCma-CanESM2
DMI	Danish Meteorological Institute	DMI-HIRHAM5	ICHEC-EC-EARTH
KNMI	Koninklijk Netherlands Meteorological Institute	KNMI-RACMO22T	ICHEC-EC-EARTH
SMHI	Swedish Meteorological and Hydrological Institute	SMHI-RCA4	ICHEC-EC-EARTH
SMHI	Swedish Meteorological and Hydrological Institute	SMHI-RCA4	MPI-M-MPI-ESM-LR

For the most part, potential socio-economic and technological trends are inexplicable and might not be similar to historical shifts. Emissions levels will depend on the mitigation strategy that will be implemented in the future, influencing anthropogenic emissions. It is recommended that various potential scenarios be implemented, not a single best or average case (Vano et al. 2015; Kundzewicza et al. 2018). According to the RCP4.5 storyline, the population growth rate will decline, the economy will show steady growth, and tangible land-use regulations will be decided so that environmental protection is adequately valued. The RCP8.5 storyline, on the other hand, indicates that urban demands will increase with population growth linked to relatively low economic development, and society will focus more on development than on the protection of the environment (Kim et al. 2015). Each RCP trajectory is, therefore, the outcome of particular scenarios of socio-economic and technological growth. Thus, the choice of RCP plays a significant role in rightly predicting climate change's potential impacts. Of the four RCPs under the fifth Assessment Report (AR5) of IPCC, two of the most frequently used in climate change impact studies: the

mitigation scenario (RCP4.5) and the high-emission scenario (RCP8.5), were used for this study.

This study takes into account the reference period from 1960 to 1999. Future time horizons are established between 2020 and 2059 (mid-century) and between 2060 and 2099 (end of the century). A comparison was made between these time horizons and the reference period to determine the potential impacts of climate change on the hydro-meteorological variables. The projected climate variables were introduced in a SWAT model to evaluate future climate projections' hydrological impact in two horizons: mid-century and end century, focusing on the annual, seasonal, and monthly bases. All future hydrological predictions (average discharges of every 40 years) were compared with their baselines at monthly, yearly and seasonal scales.

3.3.1.2 Description and applicability of the SWAT hydrological model

The impact of climate and LU/LC change on streamflow was determined using the Soil and Water Assessment Tool (SWAT). Studies on the effects of climate change on water resources have been carried out in many parts of the world using different hydrologic models. The SWAT model is widely used in hydrologic modelling for an impact study of climate and LU/LC change. SWAT is a watershed scale, physically based, and semi-distributed hydrological model developed by the USDA suited to explain the relationship between input (soil, land use, topography, and weather) and output variables (sediment, water, and agrochemical yields) in agricultural watersheds over long periods (Arnold et al. 1998). SWAT divides watersheds into multiple sub-watersheds for modelling purposes, further divided into hydrologic response units (HRUs). HRUs represent percentages of the area within the sub-watershed that are identical in land use, slope, and soil type. The SWAT model's main advantage is that, unlike the other models, it does not require much calibration and can be used on ungauged watersheds. The SWAT Model outputs include all water balance components at each watershed level and are available daily, monthly, or annual time steps. SWAT can be used to simulate a single watershed or a system of multiple hydrologically connected watersheds.

The SWAT hydrological model was selected for this study to predict the climate and LU/LC change impact on streamflow due to its excellent performance in the country

for different hydro-climatic conditions and input data availability. In Ethiopia, SWAT has been calibrated, validated, and widely implemented. It has a good performance (has a fair degree of accuracy) to study the impact of climate and LU/LC change on water availability (Setegn et al. 2011; Dile et al. 2013; Wagesho et al. 2013; Serur and Sarma 2016). SWAT was also widely used in different parts of the world for a broad range of scales and environmental conditions to evaluate the potential impact of climate change on water resources (Changkun et al. 2015; Adhikari and Nejadhashemi 2016a, b; Basheer et al. 2016; Azari et al. 2016; Leta et al. 2016). Impact studies require the model to simulate a continuous process rather than a single event, and the SWAT model can predict long term sequences of flow. Also, it is freely available (open source) and compatible with ArcGIS. The SWAT model is limited in that it does not explicitly allow for the inclusion of spatial data as model inputs. Data must be processed into a form that the SWAT model can use. Geographic Information Systems (GIS) have been successfully integrated with the SWAT model to process the inputs and outputs. The ArcSWAT interface that works in the ArcGIS environment is the most popular one. ArcSWAT is freely available public domain software. The main components of SWAT are watershed delineation, creation of HRU, editing input, running SWAT, and visualization of results. SWAT simulates the hydrological cycle based on the water balance equation.

$$SW = SW_o + \sum_{i=1}^n (R_{day} - Q_{surf} - E_a - W_{seep} - Q_{gw}) \quad (3.1)$$

where SW is final soil water content (mm), SW_o is initial soil water content on day i (mm), t is time (days), R_{day} is the amount of the precipitation on day i (mm), Q_{surf} is the amount of surface runoff on day i (mm), E_a is the amount of evaporation on day i (mm), W_{seep} are the amount of percolation and bypass flow exiting the soil profile bottom on day i (mm), and Q_{gw} is the amount of return flow on day i (mm).

SWAT has different options for calculating the hydrological components in a watershed. In this study, the Penman-Monteith method was used to determine potential evapotranspiration. Surface runoff was estimated using the Soil Conservation Service's curve number method (Equation 3.2).

$$Q_{sur} = \frac{(R_{day} - 0.2S)^2}{(R_{day} + 0.8S)} \quad (3.2)$$

Where Q_{sur} is the daily surface runoff (mm), R_{day} is the rainfall depth for the day (mm), and S is the retention parameter (mm). The retention parameter (S) is given in Equation 3.3.

$$S = 25.4 \left(\frac{1000}{CN} - 10 \right) \quad (3.3)$$

S is the drainable volume of soil water per unit area of the saturated thickness (mm/day), CN is the curve number.

3.3.1.3 Preparation of weather generator parameters

The SWAT needs daily precipitation, minimum and maximum temperature, solar radiation, wind speed and relative humidity. Values for all these parameters may be read from records of measured data or generated. This study used station data for all weather variables. The weather data obtained for the stations in and near TWW had missed some of the variables. These missed values were filled with the weather generator utility in the SWAT model from weather generator parameters' values. This study used the *pcpSTAT* and *Dew02.exe* programs to prepare weather generator parameters based on forty years of data from the synoptic station (Hawassa station).

3.3.1.4 Preparation of LU/LC map

The LU/LC maps used to evaluate climate change impacts on streamflow were prepared using the Landsat Thematic Mapper (TM) for 1988 and 1998. The Landsat images were projected to the Universal Transverse Mercator (UTM) coordinate system (WGS 84 datum, UTM Zone 37 N). A supervised classification procedure was implemented for classification. Among different classification algorithms, the Maximum Likelihood Classification (MLC) algorithm was selected for supervised classification. ERDAS 2014 was employed for image classifications purposes and ArcGIS 10.3 for mapping purposes. For classification, seven LU/LC classes were established in the scheme as intensively cultivated (AGRR), moderately cultivated (AGRC), water (WATR), shrubland (RNGB), built-up (URHD), swampy (WETN), and grassland (RNGE). The categories specified in the LU/LC map were reclassified into SWAT land cover/crop types. The LU/LC map preparation details were given in topic 3.3.2.1, and the maps are shown in chapter five.

3.3.1.4 Calibration and validation of the model

Appropriate implementation of the SWAT model involves calibration and validation of the model against historical measured data. Model calibration involves correction/adjustment of model parameters and constants to reduce the deviation of model output from the observed data set. It estimates model parameters by comparing model estimations with measured values for the same condition. Model validation means that a model is acceptable for its intended application because it meets specified performance requirements (Rykiel 1996). Model validations involve running a model using input parameters determined during the calibration process. It is the process of determining that a particular model can make adequately accurate predictions (Refsgaard and Knudsen 1996). The accuracy of model predictions is usually tested by comparing predicted with measured values and applying some measure of goodness-of-fit. The result of model predictions can be compared with the measurements to ensure their validity. Therefore, calibration and validation were performed in this study using 23 (1980–2002) years of streamflow measured data. The data was separated into warm-up (1980–1982), calibration (1983-1995), and validation (1996–2002) periods. The prolonged calibration period (65%) with a LU/LC map within the calibration period (1988) was used to better parameterise the model. Calibration and validation were performed in SWAT-CUP 2012 version 5.1.4 using the Sequential Uncertainty Fitting (SUFI-2) algorithm, based on the SWAT-CUP user manual (Abbaspour 2013). SUFI-2 is a semi-automated calibration and uncertainty analysis algorithm that accounts for all uncertainty sources, including driving variable uncertainty, conceptual model, parameters, and measured data (Tang et al. 2012; Zhou et al. 2014; Vilaysane et al. 2015).

3.3.1.5 Model performance evaluation

The SWAT model performances were evaluated using Nash-Sutcliffe Efficiency (NSE), root-mean-square error to observation standard deviation ratio (RSR), coefficient determination (R^2), and per cent bias (PBIAS). NSE is a statistical indicator for evaluating the model's performance. It defines the relative size of the residual variance to the observed data variance (Nash and Sutcliffe 1970) and ranges from one to a large negative number; one indicates a perfect model (Equation 3.4).

RSR is the ratio of the root-mean-square error (RMSE) to the observation standard deviation, and it ranges from zero to a large positive number. The higher the RSR values, the lower the model performance; RSR has an optimum value of zero (Equation 3.5). The coefficient determination (R^2) is the magnitude of the linear relationship between the observed and the simulated values. R^2 varies from zero to one with higher values that display less error variation (Equation 3.6). PBIAS indicates the simulated result's tendency to overestimate or underestimate compared to the observed values (Equation 3.7) (Moriassi et al. 2007). The low-magnitude values of PBIAS indicate better model simulations. The optimal value of PBIAS is zero (Moriassi et al. 2007). According to Moriassi et al. (2007) recommendation, the model evaluation can be judged satisfactory if RSR is less or equal to 0.70, NSE greater than 0.50, and PBIAS less than +/-25% for streamflow. Table 3.4 summarizes statistical performance indicators for streamflow simulation with a monthly time step.

$$NSE = 1 - \frac{\sum_{i=1}^n (x_i - y_i)^2}{\sum_{i=1}^n (x_i - \bar{x})^2} \quad (3.4)$$

$$RSR = \frac{\left[\sqrt{\sum_{i=1}^n (x_i - y_i)^2} \right]}{\left[\sqrt{\sum_{i=1}^n (x_i - \bar{x})^2} \right]} \quad (3.5)$$

$$R^2 = \frac{[\sum_{i=1}^n (x_i - \bar{x}_i)(y_i - \bar{y}_i)]^2}{\sum_{i=1}^n (x_i - \bar{x}_i)^2 \sum_{i=1}^n (y_i - \bar{y}_i)^2} \quad (3.6)$$

$$PBIAS = \left[\frac{\sum_{i=1}^n (x_i - y_i) * (100)}{\sum_{i=1}^n (x_i)} \right] \quad (3.7)$$

Where x_i and y_i are observed and simulated values, respectively. n is the number of datasets.

Table 3.4. Overall performance ratings for a simulation with a monthly time step (Moriasi et al. 2007).

Performance rating	RSR	NSE	PBIAS (%) for streamflow
Very good	$0.00 < \text{RSR} \leq 0.50$	$0.75 < \text{NSE} \leq 1.00$	$\text{PBIAS} < \pm 10$
Good	$0.50 < \text{RSR} \leq 0.60$	$0.65 < \text{NSE} \leq 0.75$	$\pm 10 \leq \text{PBIAS} < \pm 15$
Satisfactory	$0.60 < \text{RSR} \leq 0.70$	$0.50 < \text{NSE} \leq 0.65$	$\pm 15 \leq \text{PBIAS} < \pm 25$
Unsatisfactory	$\text{RSR} > 0.70$	$\text{NSE} \leq 0.50$	$\text{PBIAS} \geq \pm 25$

The SWAT model was set up for TWW and run on a monthly time step. The calibrated SWAT model was run for both the reference period (1960 to 1999) and the future climate change scenarios for a period of mid-century (2020–2059) and end century (2060 to 2099) based on the 1998 LU/LC map. The SWAT model outputs were compared with the historical values/reference period monthly, seasonal, and yearly. The future precipitation, minimum temperature, and maximum temperature are also compared with the reference period (1960 to 1999) to recognize the impact of climate change on temperature and precipitation. Figure 3.6 summarizes the methodology for climate change's effects on hydro-meteorological variables.

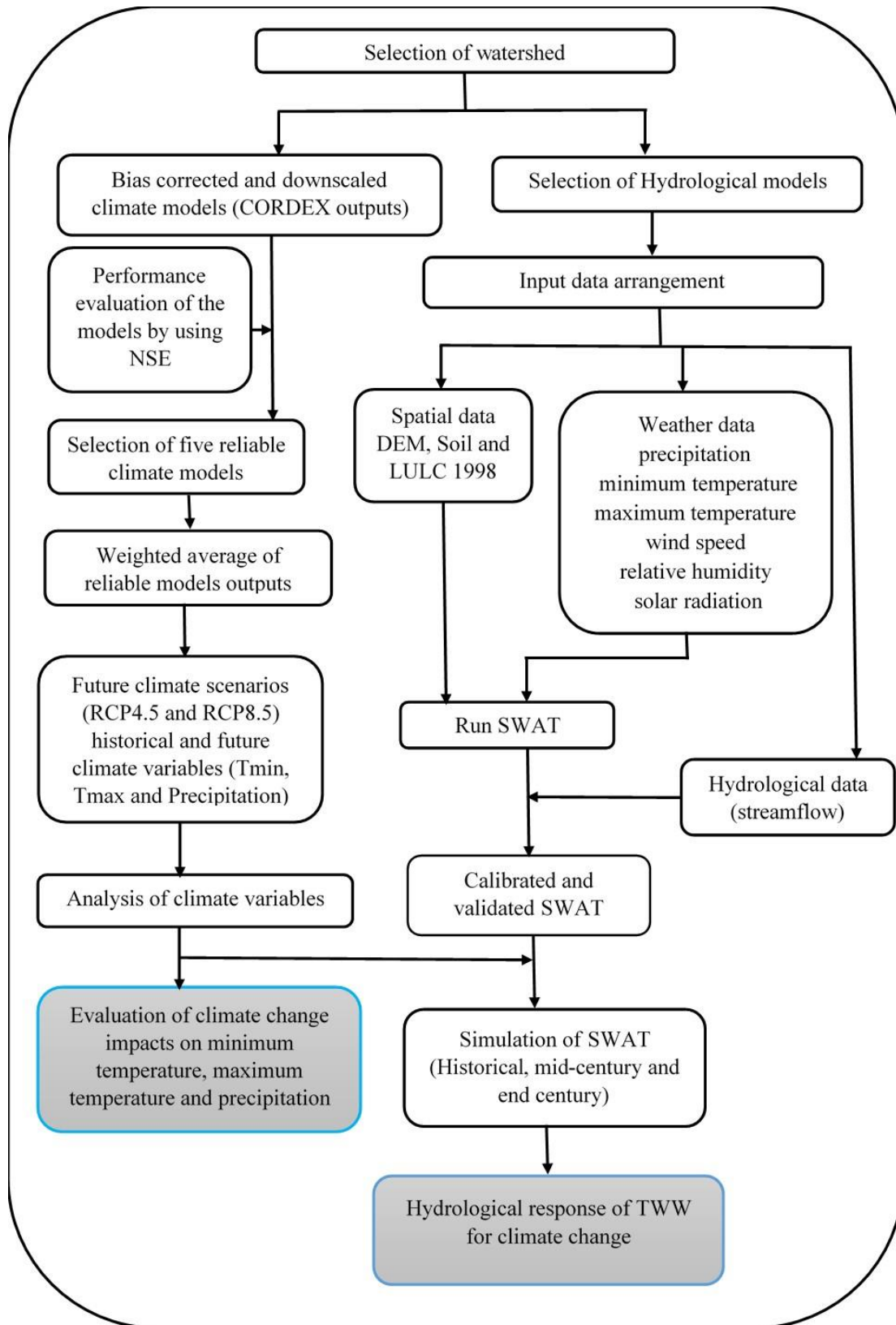


Figure 3.6. Methodology flow chart for climate change impacts on hydro-meteorological variables in TWW

3.3.2 Methods for land use/land cover change impacts

3.3.2.1 LU/LC change detection

Assessments of LU/LC change were done using four Landsat images; Landsat Multispectral Scanner (MSS) for 1978, Landsat Thematic Mapper (TM) for 1988 and 1998, and Landsat Operational Land Imager and Thermal Infrared Sensor (OLI_TIRS) for 2017. The images under clear cloud-cover conditions were collected from the USGS Centre for Earth Resources Observation and Science (<https://earthexplorer.usgs.gov/>). All Landsat images were projected to the Universal Transverse Mercator (UTM) coordinate system (WGS 84 datum, UTM Zone 37 N). A supervised classification procedure was implemented for classification. In supervised classification, the user supervises the pixel classification process. Supervised classification is based on the idea that a user can select sample pixels in an image representing specific classes and then direct the image processing software to use these training sites as references to classify all other pixels in the image. Training sites are selected based on the knowledge of the user. For this study, this is done by selecting 600 representative reference data from Google Earth images of the corresponding periods and experience of the user. Among different classification algorithms, the Maximum Likelihood Classification (MLC) algorithm was selected for supervised classification. MLC is the most common and widely used algorithm that assumes that the statistics for each class in each band are normally distributed and calculates the probability that a given pixel belongs to a specific category. Each pixel is assigned to the class with the highest probability (maximum likelihood).

As Lillesand elucidated, "*A classification is not complete until its accuracy is assessed*" (Lillesand 2015). In thematic mapping from remotely sensed data, the word accuracy is used to clarify the degree of "correctness" of a classification (Foody 2002). Therefore, classification accuracy is naturally taken to mean how the derived image classification agrees with reality or conforms to the truth. Therefore, accuracy assessment is a general term for comparing the classified image to geographical data considered accurate or ground truth data to determine the classification process's accuracy.

A confusion matrix (or error matrix) is the most widely used quantitative technique to assess the accuracy of classified images (Foody 2002). A confusion matrix is a row by column table with as many rows as columns that show the agreement between the classification result and a reference image. Each row of the table is reserved for one of the information or remote sensing classes the classification algorithm uses, whereas each column displays the corresponding ground truth classes in identical order. A confusion matrix is used to properly analyze the validity of each category, including the classification as a whole. The most common classification accuracy assessment approaches are expressing overall accuracy, producer's accuracy, and user's accuracy (Lillesand et al. 2004).

The producer's accuracy measures how accurately the analyst classified the image data by category (columns). Producer accuracy niceties the errors of omission. An error of omission results when a pixel is incorrectly classified into another category. It is an important measure because the producers of spatial data are interested in knowing how well a particular area on the Earth's surface can be mapped. Producers' accuracies are derived by dividing the number of properly classified pixels in each category (on the major diagonal) by the number of reference pixels used for that category.

User accuracy represents the possibility that a sample from the classified image actually represents that class on the ground. User accuracy specifics errors of commission. An error of commission indicates the probability that a pixel classified into a given category actually represents that category on the ground. User accuracy is vital for users of spatial data because users are principally interested in knowing how well the spatial data actually represents what can be found on the ground (Lillesand et al. 2004). The user accuracy is calculated by dividing the number of accurately classified samples of the relevant class by the total number of verified samples belonging to that class. Overall classification accuracy is the ratio of the number of correct classifications to the total number of samples evaluated. The overall accuracy constitutes the percentages of correctly classified classes lying along the diagonal in the confusion matrix. Accuracy assessment was employed regarding the corresponding Google Earth images to illustrate the representativeness of the

classified images on the ground. ERDAS 2014 was used for image classifications purposes and ArcGIS 10.3 for mapping purposes.

For classification, seven LU/LC classes were established in the scheme as intensively cultivated (AGRR), moderately cultivated (AGRC), water (WATR), shrubland (RNGB), built-up (URHD), swampy (WETN), and grassland (RNGE). Detailed explanations of the LU/LC types are given in Table 3.5. The categories specified in the LU/LC map were reclassified into SWAT land cover/crop types. LU/LC change analysis was carried out using the classified (1978, 1988, 1998, and 2017) states to demonstrate the LU/LC changes trend. To elucidate the extent of changes experienced between the subsequent periods, the per cent of change and rate of change was computed using Equation (3.8) and (3.9), respectively. The same method was employed by Gashaw et al. (2018).

$$\text{Percent of change} = \left(\frac{A-B}{B} \right) 100 \quad (3.8)$$

$$\text{Rate of change (Km}^2\text{/yr)} = \left(\frac{A-B}{T} \right) \quad (3.9)$$

A is the LU/LC area (Km²) in time two, B is the area of LU/LC (Km²) in time one, T is the time interval between A and B in years.

Table 3.5. Description LU/LC classes in Tikur Wuha watershed

No.	LU/LC Type	Explanation
1	Intensively cultivated	This unit includes mechanized and smallholder farms. Both are characterized by tilled and planted, bare crop fields, and limited areas temporarily left as fallow. (dominated by seasonal crops, such as Barley, Wheat, Teff, Maize, Pulses, Potatoes, Pepper)
2	Moderately cultivated	This unit is dominated by perennial crops, such as Khat (<i>Catha edulis</i>) and Coffee (<i>Coffea arabica</i>), Enset (<i>Ensete-ventricosum</i>), Sugar Cane
3	Water	Open water areas (Lake Cheleleka, Tikur Wuha river, and all watershed streams).
4	Shrubland	These areas are covered with shrubs, bushes, and small trees mixed with grasses.
5	Built-up	This unit describes urban areas of residential, commercial, industrial buildings, transportation infrastructures, an urban settlement with bare ground and roads.
6	Swampy	This unit labels the marshland area with topographic low where the water table is near or above the land surface.
7	Grassland	This unit refers to the areas dominated by grass with a low occurrence of shrubs. The grassy area used for communal grazing

3.3.2.2 *Methods for LU/LC change impacts on streamflow*

The impact of LU/LC change on streamflow was determined using the calibrated and validated SWAT version SWAT2012 hydrological model. The SWAT hydrological model is briefly discussed in topic 3.3.1.2. The different period LU/LC map (1978LU/LC, 1988LU/LC, 1998LU/LC and 2017LU/LC) with fixed DEM, soil and weather data was used to run the SWAT model. The streamflow from the simulation was compared and discussed. Figure 3.7 showed the methodology framework to determine the LU/LC change impacts on streamflow.

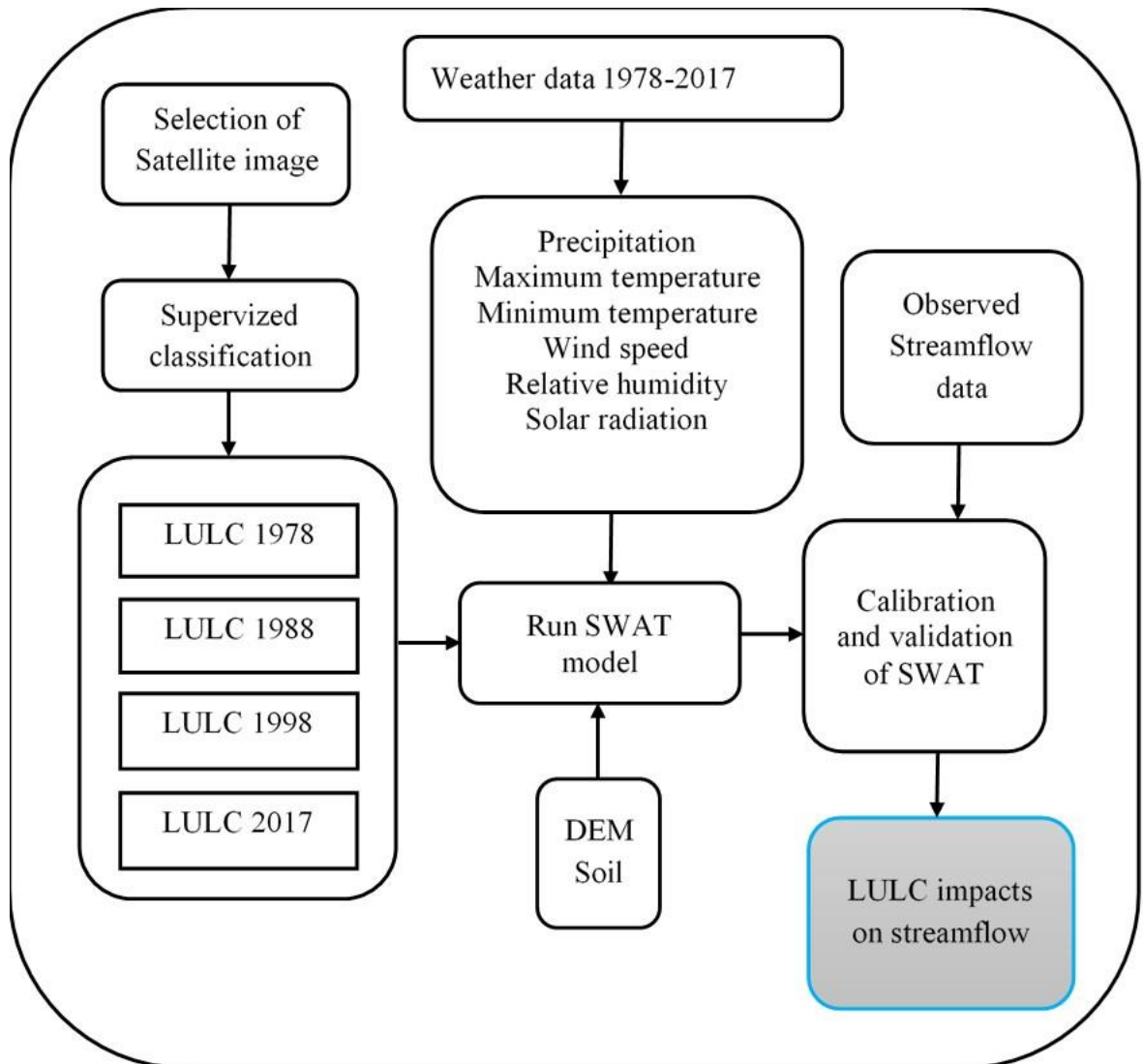


Figure 3.7. Methodology flow chart for LU/LC impacts on streamflow

3.3.3 Methods for variability and trend analysis of hydro-meteorological variables

The analysis of the trend can be done using either parametric or non-parametric tests. Parametric trend tests are more powerful than non-parametric ones, but they usually need distributed and independent data (Hamed and Rao 1998). The hydro-meteorological data is often non-normally distributed, censored, and missing data. If the data is not normally distributed, parametric methods result in invalid inferences and mislead the decision-makers. Major advantage of non-parametric tests compared to parametric tests is its advantage for non-normal distribution and quality-checked datasets. A non-parametric test is often referred to as a distribution-free or distribution

independent method. Several non-parametric methods are available for the trend detection of meteorological variables, but the Mann-Kendall (M-K) test is the widely used non-parametric approach for trend detection of hydro-meteorological time series such as precipitation and temperature (Hamed and Rao 1998; Yue et al. 2002). The M-K test is a non-parametric test, which tests for a trend in a time series without specifying whether the trend is linear or non-linear (Yue et al. 2002). Since there are probabilities of outliers existing in the data set, the non-parametric M-K test is advantageous because of its statistics based on the positive (+) or negative (-) signs, instead of the value of the random variable, and therefore, the trends recognized are less sensitive to outliers. The M-K test is widely used to detect trends of meteorological variables (Tabari et al. 2011). For this study, the non-parametric M-K test (Equation 3.10) with a 0.05 level of significance was used to detect the annual and seasonal trend of hydro-meteorological variables. The M-K trend test was used because it is robust, simple, can cope with missing values, and the data need not follow any specific distribution (Mann 1945; Kendall 1975). Besides supporting the M-K trend test results, linear trend lines are plotted for each station using Microsoft Excel®. Figure 3.8 summarizes the method adopted to analyze trends and variability of hydro-meteorological variables.

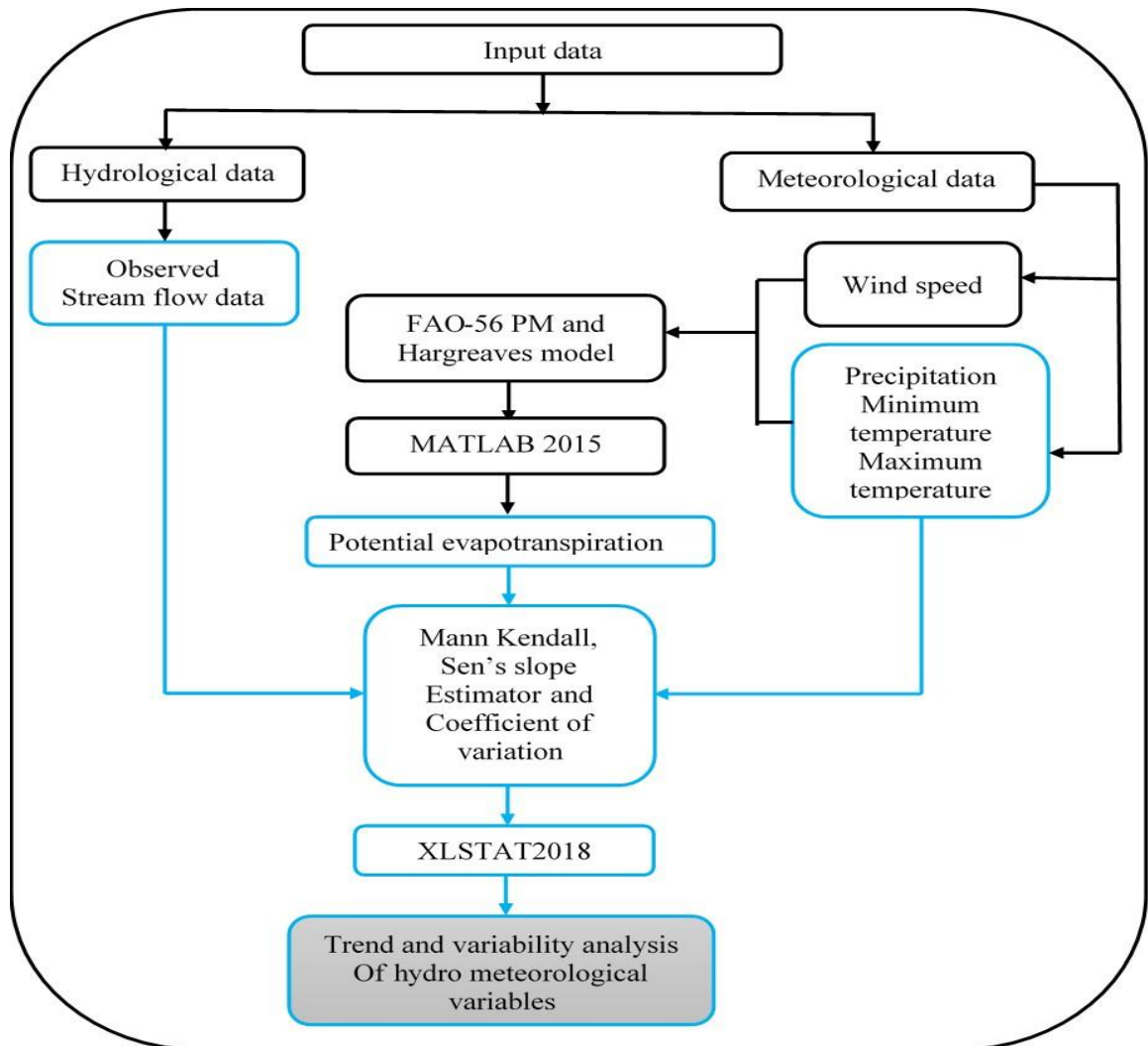


Figure 3.8. Methodology flow chart for trend and variability analysis of hydro-meteorological variables in TWW

The M-K test statistic ‘S’ is calculated based on Mann (1945) and Kendall (1975) using Equation 3.10. The statistic S is increased by one if a data value from a later time is higher than the data value from an earlier time. In contrast, S is decreased by one if the data value later is lower than that sampled earlier. The net result of all such increase and decrease yields the final value of S. The statistics S of Kendall's tau is given by Equation 3.11. The null hypothesis (H0) in this test assumes that there is no trend (S=0), and this is tested against the alternative hypothesis (Ha), which assumes that there is a trend (S0).

$$S = \sum_{i=1}^{n-1} \sum_{j=i+1}^n \text{sgn}(x_j - x_i) \quad (3.10)$$

The application of trend test is done to a time series x_i that is ranked from $i = 1, 2, \dots, n-1$ and x_j , which is ranked from $j = i + 1, i + 2, \dots, n$. Each of the data point x_i is taken as a reference point which is compared with the rest of the data point's x_j so that:

$$Sgn(X_j - X_i) = \begin{cases} +1 & \text{if } (X_j - X_i) > 0 \\ 0 & \text{if } (X_j - X_i) = 0 \\ -1 & \text{if } (X_j - X_i) < 0 \end{cases} \quad (3.11)$$

Where X_i and X_j are the annual values in years i and j ($j > i$), respectively.

Under the null hypothesis that X_i and X_j are independent and randomly ordered.

When the number of observations is more than 10 ($n \geq 10$), the statistic 'S' is approximately normally distributed, with the mean of S becomes 0 (Kendall 1975). In this case, the variance statistic is given as Equation 3.12.

$$Var(S) = \frac{n(n-1)(2n+5) - \sum_{j=1}^m t_j(t_j-1)(2t_j+5)}{18} \quad (3.12)$$

Where m is the number of tied groups in the data set, and t_j is the number of data points in the j^{th} tied group.

The standardized test statistics Z_s for the M-K test were computed by using Equation 3.13.

$$Z_s = \begin{cases} \frac{S-1}{\sigma} & \text{if } S > 0 \\ 0 & \text{if } S = 0 \\ \frac{S+1}{\sigma} & \text{if } S < 0 \end{cases} \quad (3.13)$$

Where, $\sigma = \sqrt{Var(S)}$

Z_s is used to judge the presence of the significance of any trend. Positive Z_s show an upward trend, and negative Z_s show a downwards trend for the period.

The parameter estimate of the slope was then tested for statistical significance using the probability value (*p-value*) at a 0.05 level of significance. A *p-value* of less than 0.05 shows a monotonic trend, and a *P-value* greater than 0.05 indicates no trend.

Since non-parametric tests are commonly designed to point out the existence but not the magnitude of a trend, the magnitude of the trend was estimated using Sen's Slope Estimator method (Sen 1968). Sen's slope estimator is a non-parametric approach and gives a robust estimate of the magnitude of a monotonic (increasing/decreasing) trend and is a widely used tool in quantifying a trend in hydro-meteorological time series.

In general, the slope β between two values of a time series x can be computed as Equation 3.14 (Sen 1968).

$$\beta = \frac{x_j - x_i}{j - i} \quad (3.14)$$

Where x_j and x_i are considered data values at time j and i ($j > i$), respectively.

A negative value of β indicates a downward trend, whereas a positive value of β indicates an upward trend.

The median of these N values of β is represented as Sen's estimator of the slope, calculated as Equation 3.15.

$$Q_{med} = \frac{\beta(N+1)}{2} \text{ if } N \text{ is odd, and } Q_{med} = \left\{ \beta \left(\frac{N}{2} \right) + \frac{\beta(N+2)}{2} \right\} / 2 \text{ if } N \text{ is even} \quad (3.15)$$

A positive value of Q_{med} indicates an upward or increasing trend and a negative value of Q_{med} gives a downward or decreasing trend in the time series.

Forty years (1978 to 2017), daily observed data were used for the analysis. The observed data of all the variables were tested for consistency and missing records. For temperature and streamflow, missing cases are filled using linear interpolation, and nearest neighbour values are used for rainfall. Similar methods were employed by Raju and Nandagiri (2017). Data analysis was undertaken using XLSTAT 2018 software and excel spreadsheet 2013.

Observed daily rainfall of four stations and temperature (T-max and T-min) from two stations are collected from NMSA branch office at Hawassa. Streamflow was obtained from MoWIE. Observed PET data is not available on TWW. For estimation and planning of water resources and to compute crop water use, determining PET is critical. An accurate estimate of PET is pertinent for hydrological and agricultural studies, especially under increasing water scarcity and changing climate (Allen et al. 1998). Due to the difficulty of obtaining accurate field measurements, evapotranspiration is commonly computed from weather data.

Many authors have proposed several models. Many of the models are subject to local calibration, thereby making them have limited global acceptance. Due to the higher performance of the FAO-56 Penman-Monteith (FAO-56 PM) model in different parts of the world when compared with other models, it has been accepted as the sole method of computing reference evapotranspiration (PET) from meteorological data (Allen et al. 1998). The FAO-56 PM model has been universally accepted as the

exclusive method for estimating reference evapotranspiration. The FAO-PM method was developed by defining the reference crop as a hypothetical crop with an assumed height of 0.12m, with a surface resistance of 70 sm^{-1} and an albedo of 0.23, closely resembling the evaporation from an extensive surface of green grass of uniform height, actively growing and adequately watered (Allen et al. 1998). In this study, the daily values of PET were computed using the FAO-56 PM method (Equation 3.16) and MATLAB software for the Hawassa station.

$$ET_o = \frac{0.408 \cdot \Delta \cdot (R_n - G) + \gamma \cdot \frac{900}{T+273} \cdot u_2 \cdot (e_s - e_a)}{\Delta + \gamma \cdot (1 + 0.34 \cdot u_2)} \quad (3.16)$$

Where,

ET_o = reference evapotranspiration rate/ (mm d^{-1}),

T = mean air temperature ($^{\circ}\text{C}$),

u_2 = wind speed (m s^{-1}) at 2 m above the ground.

R_n = net radiation at the crop surface, $\text{MJ m}^{-2} \text{d}^{-1}$;

G = soil heat flux density, $\text{MJ m}^{-2} \text{d}^{-1}$;

e_s = saturation vapour pressure, KPa;

e_a = actual vapour pressure, KPa;

$e_s - e_a$ = saturation vapor pressure deficit, KPa;

Δ = slope of the vapor pressure curve, $\text{KPa } ^{\circ}\text{C}^{-1}$;

γ = psychrometric constant, $\text{KPa } ^{\circ}\text{C}^{-1}$

In computing daily evapotranspiration using the FAO-56 PM model, five specific climate data are required: daily maximum and minimum air temperature, solar radiation, wind speed, and relative humidity. These data are not always available at all weather stations, especially in Ethiopia and most developing countries. Thus, using PET models that require a reduced set of climate data continues to be an important alternative in such cases. In most cases, only the maximum and minimum air temperatures are available. In such a situation, the procedure for estimating PET outlined in Allen et al. (1998) is used and has been found to produce acceptable results. The Hargreaves model has been recommended for the computation of PET when only the maximum and minimum air temperatures are available (Allen et al. 1998). In TWW, at Haisawita station (where limited climatic data is available, the

maximum and minimum air temperatures), PET was determined using the Hargreaves model (equation 3.17). The equation stated by Hargreaves and Samani (1982) and is given as:

$$ET_o = 0.0023 * (T_{max} - T_{min})^{0.5} * R_a \quad (3.17)$$

Where,

ET_o = reference evapotranspiration (mmd⁻¹),

T_{max} = maximum air temperature

T_{min} = minimum air temperature

R_a = the extra-terrestrial solar radiation (MJ m⁻² d⁻¹)

The Thiessen polygon method was employed to compute the average annual rainfall in the watershed (Chow 2010). The Thiessen method is generally more accurate than the arithmetic mean method. If there are n gauges in the watershed, the areal weighted average precipitation for the watershed is given by Equation 3.18.

$$\bar{P} = \frac{1}{A} \sum_{j=1}^n A_j P_j \quad (3.18)$$

Where,

\bar{P} is the weighted average of rainfall in the watershed

$A = \sum_{j=1}^n A_j$ is watershed area

A_j is the area within the watershed assigned to each station

P_j is the rainfall recorded at the jth gage

Variability analysis

This study has computed the inter-annual and seasonal variability of hydro-meteorological variables using the Coefficient of Variation (CV). A higher and lower value of seasonal and annual CV indicates greater and lesser variability, respectively. The value of CV was computed by using Equation 3.19.

$$CV = \left(\frac{\sigma}{\mu} \right) * 100 \quad (3.19)$$

Where μ is the mean rainfall, and σ is the standard deviation.

The CV is used to classify the degree of variability of rainfall events and is considered as less variability (CV < 0.20), moderate variability (0.20 < CV < 0.30), and high variability (CV > 0.30). The same CV value range was used in Ethiopia (Asfaw et al. 2018; Samy et al. 2019).

3.3.4 Methods for prediction of the soil loss rate

The USLE (Wischmeier and Smith 1978) and its revised version (RUSLE) (Renard et al. 1997) are widely used models for assessment of SLR (Ashiagbor et al. 2013; Maryam and Biswajeet 2014; Ganasri and Ramish 2016; Markose and Jayappa 2016; Rejari et al. 2016; Uddin et al. 2016; Yuan et al. 2016). USLE was mainly developed for conditions in the United States of America (USA). The use of USLE in other areas requires adaptation to the local situation. Thus, Hurni (1985) simplified the USLE by adapting the factors to conditions in Ethiopia based on long term measurements and experimental data from a large number of test plots in five Soil Conservation Research Project (SCRIP) stations, namely: Anjeni, Andit Tid, Gununo, Hunide Lafito and Mayabir in various slopes, soils, land uses, crops, and under several SWC treatments in different agro-climatic zones of Ethiopia and one additional station in Eritrea (Afdeyu). In various agro-climatic regions of Ethiopia, USLE coupled with GIS has been successfully and extensively applied for the estimation of the spatial variation of soil loss, and it has provided good results (Bewket and Teferi 2009; Brhane and Mokonen 2009; Sisay et al. 2014; Adugna et al. 2015; Ayalew 2015; Wolka et al. 2015; Fenta et al. 2016; Gelagay and Minale 2016; Gashaw et al. 2017). Therefore, the present study employed USLE (Equation 2.1) adopted for the Ethiopian condition (Hurni 1985) and coupled with a GIS tool to quantify the SLR of TWW. The details of the USLE factors are found in (Wischmeier and Smith 1978) and briefly described underneath. The following three steps were developed to estimate the SLR and recognition of the priority watershed and summarized in Figure 3.9.

- (i) It is generating the raster map of the necessary input parameters of USLE.
- (ii) The watershed SLR map was developed and classified into severity categories based on different criteria (based on soil erosion severity class, soil loss tolerance of the area, and average soil loss rate of the country).
- (iii) Prioritization of sub-watersheds for SWC practices based on the relative erosion status of the sub-watersheds

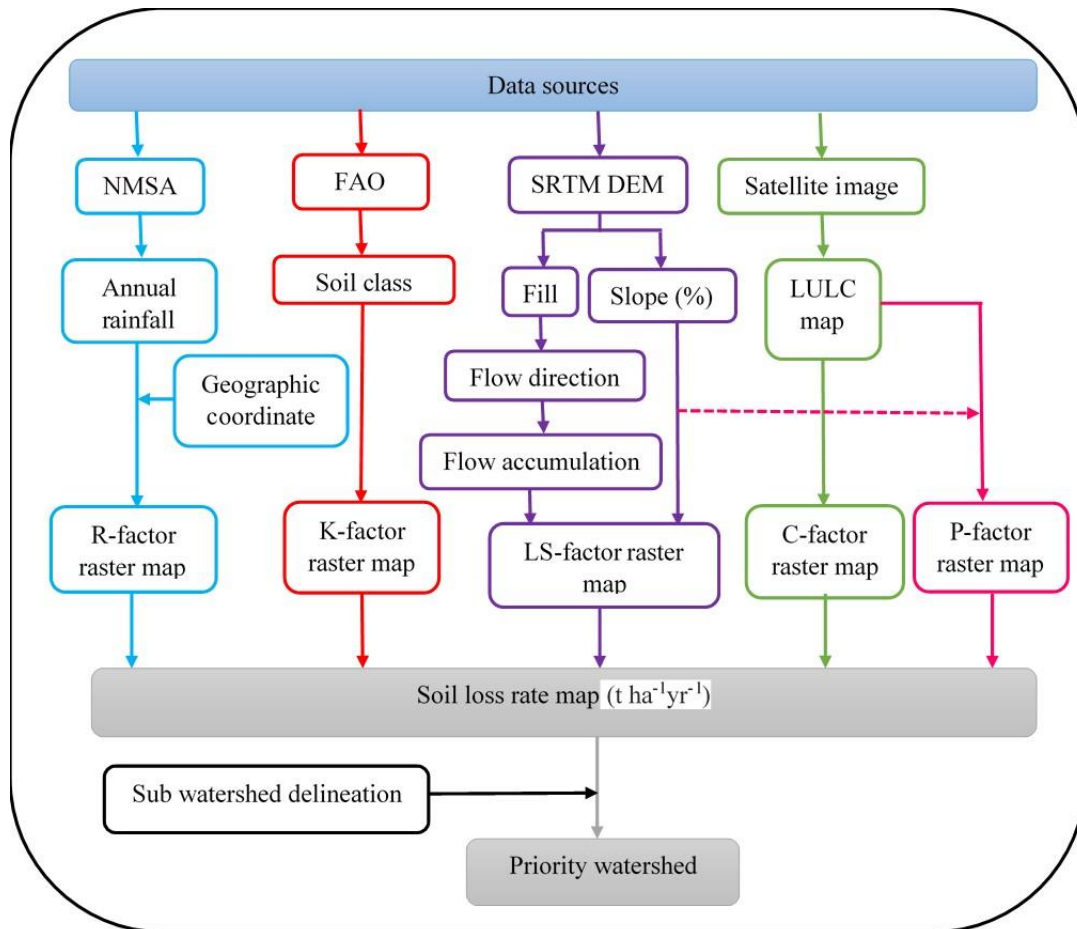


Figure 3.9. The framework for the modelling of SLR and prioritization of watersheds using the USLE

3.3.4.1 Rainfall erosivity factor (R-factor)

The R-factor is determined by the rainfall erosion index (EI₃₀). It is a measure of rainfall events (Wischmeier and Smith 1978). However, measured data like intensity and kinetic energy are not commonly obtainable in every area for the R-factor's precise determination (Lal and Humberto 2008). Researchers developed various equations for the R-factor computation based on average annual, monthly, and daily precipitations. However, those equations can not be applied to Ethiopia since they are valid for their elaborate areas. Also, extrapolating them to another place beyond the database from which they have been derived is not convincing. Due to the difficulty of direct determination of R-factor, as the intensity of the precipitation does not exist at the meteorological stations in the TWW, indirect methods developed by Hurni (1985) for Ethiopia based on average annual rainfall (Equation 3.20) are applied.

$$R = 0.56P - 8.12 \quad (3.20)$$

Where P is the average yearly precipitation in mm.

A similar method was employed by (Bewket and Teferi 2009; Amsalu and Mengaw 2014; Adugna et al. 2015; Ayalew 2015). The daily rainfall data for four stations in and near the watershed was collected from the national meteorological service agency, South Nation Nationality and People Regional State, Hawassa branch office. In developing countries like Ethiopia, meteorological stations are sparsely available. All the stations in and near the watershed that satisfy the criteria (The data availability, period of observation of data in the study area and gaps in data records are the criteria applied for the choice of used stations) were included. Nearest neighbour values filled the missing data.

The databases of the rainfall from four stations are for 40 years (1978 to 2017). The data were first aggregated into average annual rainfall amounts in the attribute table. The average yearly rainfall amounts of the four stations were entered as point values for the geo-referenced locations culminating in a point map. The point map was rasterized using the functions in ArcGIS 10.3 software. The rasterized rainfall point map was then used to develop a Thiessen map (rainfall map), with continuous surface annual rainfall values depicting different rainfall regimes in the study area. The annual rainfall map shows the spatial variation of annual rainfall in the watershed, and it was used to generate the R-factor raster map. The R-factor map was developed by using GIS-based on the annual rainfall map and Equation 3.20.

3.3.4.2 Soil erodibility factor (K-factor)

Soils vary in their vulnerability to erosion. This variation, due to the soil type itself, is called soil erodibility (Wischmeier and Smith 1978). Organic matter content, permeability, texture, and soil structure are the critical soil characteristics that control the K-factor. Typically, a soil type becomes less erodible with a decrease in silt fraction, regardless of whether the corresponding increase is in the sand or clay fraction (Wischmeier and Smith 1978). Determining K-factor values by directly measuring the erodibility factor is expensive and requires considerable time and equipment to execute. In this study, to determine the K-factor value, Hurni (1985) adapted K-factor estimations for various soil types for Ethiopian conditions were used. However, this value is in the US unit. It needs to adjust the values multiplied by a conversion factor to get the SI unit's values.

3.3.4.3 Slope length and slope steepness (LS-factor)

The LS-factor reflects the impact of topography on water erosion. Steeper slopes raise runoff velocities, and longer slopes allow for the accumulation of runoff. Both these results increased erosion potential. The steeper and prolonged the hill, the higher is the risk of erosion (Hudson 1995). The two factors have been determined separately. However, considering the two as a single topographic factor is convenient in field applications. Since each location's altitude defines topography within an area, altitude data stored in a DEM is the standard input for performing topographical operations in a raster format. The LS-factor can be used in a single index for this research, as shown in Equation 3.21, defined by (Wischmeier and Smith 1965), and derived from DEM.

$$LS = \left(\frac{x}{22.13} \right)^m (0.065 + 0.045s + 0.0065s^2) \quad (3.21)$$

Where x = the field slope length, can be determined by multiplying flow accumulation and the resolution of the DEM, s = slope gradient (%). The magnitude of m in Equation 3.21 does not mean the same for all places or conditions at a given site. m values vary from 0.2 – 0.5 subjects to the slope, as provided in Table 3.6 (Wischmeier and smith 1978).

Table 3.6. Relationship between slope in per cent and m-values

Slope (%)	greater than five	between three and five	between one and three	less than one
m-values	0.5	0.4	0.3	0.2

3.3.4.4 Cover and management factor (C-factor)

The C-factor is the ratio of soil loss from land with specific vegetation to the corresponding soil loss from continuous fallow (Wischmeier and Smith 1978). In estimating the C-factor, it is indispensable to know the LU/LC of the study area. The LU/LC map of the watershed was developed from the Landsat Operational Land Imager and Thermal Infrared Sensor (OLI_TIRS) image acquired on 12-December-2017 during the dry season. The details of the development of the LU/LC map are given in section 3.3.2.1. The C-factor value was determined for each LU/LC class of the TWW based on available literature recommendations in the Rift valley Lake Basin in Ethiopia (MoWR 2008) in the Ethiopian highlands (Hurni 1985), and other published literature.

3.3.4.5 Support practice factor (P-factor)

The P-factor gives the ratio between the soil losses expected for a specific soil conservation practice to that of up and downslope ploughing (Wischmeier and Smith 1978). The effects of supportive conservation methods such as terracing, contouring, tillage, cropping practices, in particular, and land management, in general, are significant in controlling SLR in a specific area. The magnitude of erosion declines with the installation of these methods. Supportive SWC practice decreases runoff amount and speed and encourages the deposition (Morgan 2005). In the TWW, an insignificant portion of the watershed has been cured with improved SWC intervention through the Safety Net Program and the government. Previously constructed works were reported as destroyed in many places due to the free grazing of cattle and a lack of maintenance (MoWR 2008). Hence, P-factor values from slope and land use classes were used in this study. Firstly, we developed the LU/LC map. The LU/LC map was reclassified into two categories that are agricultural land and non-agricultural land. At the same time, we reclassified the slope in per cent map into six classes. Then, using raster analysis in ArcGIS 10.3, we developed a P-factor raster map using the reclassified LU/LC map, slope in per cent map. Similar methods of determining P-factor values have been employed in earlier studies from several nations (Bewket and Teferi 2009; Adediji et al. 2010; Shiferaw 2011; Mulu and Dwarakish 2016).

CHAPTER 4: HYDRO-METEOROLOGICAL IMPACT ASSESSMENT OF CLIMATE CHANGE

4.1 General

As climate change impact is location-specific and varies seasonally and regionally, it should be examined at each watershed. This topic covers the validation of CORDEX data of five RCMs from multiple GCMs using observed and historical data of climate variables. It also discusses how the future temperature and precipitation will change in the mid and end of the century compared to baseline periods. Besides, it describes the potential impacts of climate change on streamflow in TWW for the mid and end century.

4.2 Validation of CORDEX Data with Observed Data

The performance of the bias-corrected CORDEX data was checked by using NSE. Validation was done based on 24 years' simulation from 1978 to 2001 (the common period for observed and historical data) monthly and yearly for temperature and precipitation, respectively. The results are presented in Table 4.1. The weight was given based on the performance of the models. The NSE of the five best models' minimum temperature output ranges from 0.66 to 0.83, whereas the maximum temperature output ranges from 0.61 to 0.78. The NSE of the precipitation of the five best models output ranges from 0.39 to 0.59. The NSE of the five selected models' weighted average is 0.85 and 0.84 for temperature and precipitation, respectively (Table 4.1). The result revealed that rainfall is less well simulated than temperature, the minimum temperature is better simulated than the maximum temperature, and the weighted average of selected models perform better than a single model in the Tikur wuha watershed. It is in agreement with previous studies (Fang et al. 2015; Legese 2017). RCMs/GCMs had better represent the temperature domain than the precipitation domain (Fang et al. 2015). Legese (2017) reported that precipitation exhibited a worse agreement than the temperature in Bale highlands in southern Ethiopia.

Table 4.1. The NSE values of the five selected and the weighted average of the RCMs

Model ID (RCMs)	Driving model	NSE		
		Minimum temperature	Maximum temperature	Precipitation
CCCma-RCM4	CCCma-CanESM2	0.69	0.62	0.45
DMI-HIRHAM5	ICHEC-EC-EARTH	0.66	0.61	0.39
KNMI-RACMO22T	ICHEC-EC-EARTH	0.83	0.78	0.52
SMHI-RCA4	ICHEC-EC-EARTH	0.79	0.71	0.59
SMHI-RCA4	MPI-M-MPI-ESM-LR	0.75	0.69	0.54
Weighted average		0.85	0.85	0.84

4.3 Description of statistical parameters of seasonal and annual climate variables

4.3.1 Description of statistical parameters of seasonal and annual climate variables of historical CORDEX outputs

The summary of the statistical parameters for precipitation, minimum temperature, and maximum temperature of the weighted average of historical CORDEX outputs are given in Table 4.2.

Table 4.2. Summary of statistical parameters for all variables of the weighted average historical CORDEX outputs (1960 to 1999)

Variables	Statistical parameters	Bega	Belg	Kiremt	Annual
Precipitation (mm)	Minimum	98.81	181.40	418.74	802.09
	Maximum	293.33	525.43	733.94	1330.19
	Average	169.13	366.92	542.60	1078.64
	CV	23.57	20.33	13.56	10.28
Minimum Temperature (°C)	Minimum	8.44	10.91	11.92	10.40
	Maximum	10.20	12.54	13.70	12.02
	Average	9.31	11.78	12.77	11.22
	CV	4.45	3.33	2.98	3.35
Maximum Temperature (°C)	Minimum	24.37	25.11	22.46	24.04
	Maximum	26.87	27.54	24.21	26.09

Average	25.79	26.40	23.37	25.18
CV	2.41	2.37	1.81	1.93

Note: CV = Coefficient of variation in percent

Annual precipitation has ranged from 802.09mm to 1330.19mm in the historical period, with an average of 1078.64mm. Rainfall during the Kiremt season ranges from 418.74mm to 733.94mm, with an average of 542.60mm. The average rainfall in Belg is 366.92mm, with a range of 181.40mm to 525.43mm. The average rainfall in the Bega is 169.13mm, with a range of 98.81mm to 293.33mm. The minimum monthly average precipitation was recorded in January, and the maximum monthly average rainfall is observed in May. The CV value of annual rainfall is 10.28% implies that the interannual variability of annual rainfall is less in the Historical period. Seasonally, rainfall variability is large in Bega and Belg compared to the Kiremt season.

Forty-year annual minimum temperature ranges from 10.40 °C to 12.02 °C with an average value of 11.22 °C. The average minimum temperature of Bega ranges from 8.44 °C to 10.20 °C with an average value of 9.31 °C. The average minimum temperature of Belg ranges from 10.91 °C to 12.54 °C with an average value of 11.78 °C. The average minimum temperature of Kiremt ranges from 11.92 °C to 13.70 °C, with an average value of 12.77 °C. The result showed that the average minimum temperature is greater in Kiremt (wet season) than in Belg and Bega (dry season). The weather is cold in the Bega than in Kiremt. CV values of seasonal minimum temperature also revealed that the minimum temperature variability is lower in Kiremt than Belg and Bega.

The forty-year annual maximum temperature ranges from 24.04 °C to 26.09 °C with an average value of 25.18 °C. In the Bega, the maximum temperature ranges from 24.37 °C to 26.87 °C, with an average value of 25.79 °C. In Belg, the maximum temperature ranges from 25.11 °C to 27.544 °C with an average value of 26.40 °C, whereas in Kiremt, the maximum temperature ranges from 22.46 °C to 24.21 °C with an average value of 23.37 °C. The maximum temperature is less in Kiremt than in Belg and Bega. The lowest yearly average maximum temperature was recorded in 1964, and the highest annual average maximum temperature was recorded in 1998.

4.3.2 Description of statistical parameters of seasonal and annual climate variables of mid-century CORDEX outputs

The summary of the statistical parameters for the weighted average precipitation, minimum temperature, and maximum temperature of mid-century CORDEX outputs are given in Table 4.3.

Table 4.3. Summary of statistical parameters for all variables of the weighted average mid-century CORDEX outputs (2020 to 2059)

Scenario	Variables	Statistical parameters	Bega	Belg	Kermit	Annual	
RCP4.5	Precipitation (mm)	Minimum	91.62	161.51	402.54	758.01	
		Maximum	267.40	475.58	696.12	1340.58	
		Average	182.69	341.45	567.75	1091.89	
		CV	22.29	21.60	12.19	10.09	
	Minimum Temperature (°C)	Minimum	10.08	12.41	13.10	12.06	
		Maximum	12.03	14.33	14.94	13.69	
		Average	11.12	13.39	13.91	12.81	
		CV	4.48	3.56	3.27	3.44	
	Maximum Temperature (°C)	Minimum	25.66	26.70	23.91	25.60	
		Maximum	28.29	29.36	26.27	27.77	
		Average	27.19	28.03	24.93	26.71	
		CV	2.45	2.56	2.27	2.19	
	RCP8.5	Precipitation (mm)	Minimum	92.76	166.16	421.58	832.75
			Maximum	356.27	539.40	739.57	1303.79
			Average	198.93	332.65	582.47	1114.05
			CV	28.33	22.31	13.03	10.29
Minimum Temperature (°C)		Minimum	10.06	12.42	12.12	12.03	
		Maximum	12.99	14.75	15.36	14.22	
		Average	11.38	13.69	14.14	13.07	
		CV	6.33	4.96	4.64	4.96	
Maximum Temperature (°C)		Minimum	24.97	26.17	23.27	25.22	

Temperature (°C)	Maximum	29.53	29.26	26.40	28.13
	Average	26.94	27.95	24.98	26.61
	CV	3.64	3.15	2.89	2.97

Note: CV = Coefficient of variation in percent

In mid-century, the average annual rainfall ranges from 758.01mm to 1340.58mm, with an average value of 1091.89mm for the case of the RCP4.5 scenario. It ranges from 832.75mm to 1303.79mm, with an average value of 1114.05mm for the RCP8.5 scenario. In the Belg season, the rainfall varies from 161.51mm to 475.58mm for RCP4.5, and it ranges from 166.16mm to 539.40mm for the RCP8.5 scenario. In the Kiremt season, the rainfall varies from 402.54mm to 696.12mm for RCP4.5, and it ranges from 421.58mm to 739.57mm for the RCP8.5 scenario. The Belg and Kiremt average rainfall are 341.45mm and 567.75mm for RCP4.5. The average rainfall of Belg and Kiremt is 332.65mm and 582.47mm for RCP8.5. The CV values uncover that the rainfall variability is relatively high in Bega and Belg than Kiremt and annual variability for RCP4.5 and RCP8.5 scenarios in mid-century. This implies that the variability of precipitation is higher in the dry season than in the wet season. The maximum monthly rainfall will appear in July and August, whereas the minimum monthly rainfall will appear in January and December.

In mid-century, the Bega season minimum temperature ranges from 10.08 °C to 12.03 °C with an average value of 11.12 °C for the RCP4.5 °C scenario, and it varies from 10.06 °C to 12.99 °C with an average value of 11.38 °C for the RCP8.5 scenario. The Belg season minimum temperature ranges from 12.41°C to 14.33 °C with an average value of 13.39 °C for the RCP4.5 scenario, and it varies from 12.42 °C to 14.75 °C with an average value of 13.69 °C for the RCP8.5 scenario. The Kiremt season average minimum temperature is 13.91 °C and 14.14 °C for RCP4.5 and RCP8.5 scenarios. The annual average daily minimum temperature is 12.81 °C and 13.07 °C for the RCP4.5 and RCP8.5 scenarios. The minimum temperature is less in the dry season than in the wet season in the study area.

The maximum temperature ranges from 25.66 °C to 28.29 °C, 26.70 °C to 29.36 °C, 23.91 °C to 26.27 °C, and 25.60 °C to 27.77 °C for the Bega, Belg, Kiremt and annual, respectively for the RCP4.5 scenario. Whereas for the RCP8.5 scenario, it ranges

from 24.97 °C to 29.53 °C, 26.17 °C to 29.26 °C, 23.27 °C to 26.40 °C, and 25.22 °C to 28.13 °C for the Bega, Belg, Kiremt and annual, respectively. The yearly average maximum temperature is 26.71 °C and 26.61 °C for RCP4.5 and RCP8.5, respectively. The average maximum temperature in the RCP4.5 scenario is 27.19 °C, 28.03 °C, and 24.93 °C for the Bega, Belg, and Kiremt. It is 26.94 °C, 27.95 °C, and 24.98 °C in the RCP8.5 scenario for the Bega, Belg, and Kiremt, respectively. In contrast to the minimum temperature, the maximum temperature is less in the wet season than in the dry season. The variability of the minimum temperature is higher than the maximum temperature. Seasonally, the CV values disclose that the temperature variability is relatively lower in Kiremt and Belg than in the Bega.

4.3.3 Description of statistical parameters of seasonal and annual climate variables of end century CORDEX outputs

The summary of the statistical parameters for the weighted average precipitation, minimum temperature, and maximum temperature of end century CORDEX outputs are given in Table 4.4.

Table 4.4. Summary of statistical parameters for seasonal and annual climate variables of the weighted average of end century CORDEX outputs (2060 to 2099)

Scenario	Variables	Statistical parameters	Bega	Belg	Kermit	Annual
RCP4.5	Precipitation (mm)	Minimum	113.32	198.46	445.33	931.41
		Maximum	339.33	478.13	745.52	1403.51
		Average	200.73	349.59	584.50	1134.82
		CV	26.31	19.38	13.43	9.61
	Minimum Temperature (°C)	Minimum	11.34	13.42	14.15	13.16
		Maximum	12.61	15.18	15.61	14.29
		Average	12.02	14.29	14.79	13.70
		CV	2.81	2.52	2.07	1.90
	Maximum Temperature (°C)	Minimum	27.51	28.11	24.78	26.95
		Maximum	29.22	29.85	26.87	28.28
		Average	28.28	29.06	25.87	27.73

		CV	1.38	1.63	1.84	1.09
RCP8.5	Precipitation (mm)	Minimum	147.48	192.04	505.51	1026.41
		Maximum	424.15	668.59	899.80	1552.25
		Average	247.89	374.78	639.58	1262.25
		CV	25.11	22.66	15.01	10.80
Temperature (°C)	Minimum	Minimum	12.20	14.72	15.01	14.12
		Maximum	15.65	17.41	18.18	17.06
		Average	14.01	16.18	16.16	15.61
		CV	6.43	4.89	5.31	5.38
Temperature (°C)	Maximum	Minimum	28.54	29.25	25.89	27.96
		Maximum	32.69	33.18	29.63	31.65
		Average	30.17	31.12	27.70	29.65
		CV	3.78	3.36	3.66	3.36

Note: CV = Coefficient of variation in percent

In the end century, the annual rainfall ranges from 931.41mm to 1403.51mm, with an average value of 1134.82mm for the case of RCP4.5. Whereas for the case of RCP8.5, it ranges from 1026.41mm to 1552.25mm with an average value of 1262.25mm. In the Kiremt season, the precipitation ranges from 445.33mm to 745.52mm and 505.51mm to 899.80mm for RCP4.5 and RCP8.5 scenarios. The average Kiremt rainfall is 584.50mm and 639.58mm for the RCP4.5 and RCP8.5 scenarios, respectively. The average rainfall in Bega and Belg is 200.73mm and 349.59mm for the RCP4.5, and it is 247.89mm and 374.78mm for the RCP8.5 scenario. The seasonal and annual rainfall is higher for RCP8.5 compared to RCP4.5. Like mid-century, the maximum average monthly rainfall will be in July and August, and the minimum average monthly rainfall is in December and January. The CV values uncovered that the rainfall variability is high in Bega and Belg season relative to the Kiremt season.

For RCP4.5 in end century, the minimum temperature ranges from 11.34 °C to 12.61 °C (Bega), 13.42 °C to 15.18 °C (Belg), 14.15 °C to 15.61 °C (Kiremt), and 13.16 °C to 14.29 °C (annual). The average minimum temperature is 12.02 °C, 14.29 °C, 14.79 °C, and 13.70 °C for Bega, Belg, Kiremt, and annual. For the case of RCP8.5 at the end

century, the minimum temperature ranges from 12.20 °C to 15.65 °C, 14.72 °C to 17.41 °C, 15.01 °C to 18.18 °C, and 14.12 °C to 17.06 °C for Bega, Belg, Kiremt, and annual. The average minimum temperature will be 14.01 °C, 16.18 °C, 16.16 °C, and 15.61 °C, for Bega, Belg, Kiremt, and annual, respectively. At the end century, the minimum temperature is less in the Bega than Belg and Kiremt for both RCP4.5 and RCP8.5 scenarios. The result revealed that both the variability and size of the minimum temperature are relatively high for RCP8.5 than RCP4.5.

The Bega season maximum temperature ranges from 27.51 °C to 29.22 °C with an average value of 28.28 °C for the RCP4.5 scenario, whereas it ranges from 28.54 °C to 32.69 °C with an average value of 30.17 °C for the RCP8.5 °C scenario. The Belg season maximum temperature ranges from 28.11 °C to 29.85 °C with an average value of 29.06 °C for RCP4.5, and it goes from 29.25 °C to 33.18 °C with an average value of 31.12 °C for the RCP8.5 scenario. The Kiremt season maximum temperature varies from 24.78 °C to 26.87 °C with an average value of 25.87 °C for the RCP4.5, and it ranges from 25.89 °C to 29.63 °C with an average value of 27.70 °C for the RCP8.5 scenario. In the end century, the maximum annual average temperature will be 27.73 °C and 29.65 °C for RCP4.5 and RCP8.5 scenarios, respectively. In contrast to minimum temperature, the maximum temperature is relatively high in Bega and Belg than in Kiremt. The result revealed that both the variability and size of the maximum temperature is relatively high for RCP8.5 compared to RCP4.5.

4.4 Climate Change Impacts on Precipitation, Minimum and Maximum Temperature

4.4.1 Climate change impacts on precipitation

The summary of the average values and per cent of change in precipitation on the monthly, seasonal, and yearly bases is given in Table 4.5. The variation of rainfall in historical, mid, and end century are demonstrated in Figure 4.1. The per cent of change in precipitation for mid and end century for both scenarios on a monthly basis are shown in Figure 4.2.

Table 4.5. Summaries of the average values and per cent of change of precipitation in mid and end century compared to the historical period

Months	Average values					Per cent of change in precipitation in mid and end century compared to the historical period			
	Historical	MID4.5	MID8.5	END4.5	END8.5	MID4.5	MID8.5	END4.5	END8.5
Jan	18.96	17.28	18.36	22.78	29.20	-8.85	-3.13	20.15	54.03
Feb	31.79	37.53	35.25	36.75	47.16	18.06	10.88	15.59	48.35
Mar	63.31	62.11	64.96	67.36	70.00	-1.89	2.61	6.41	10.57
Apr	126.57	119.69	113.69	116.46	121.64	-5.44	-10.18	-7.99	-3.89
May	145.25	122.12	118.75	129.02	135.98	-15.92	-18.24	-11.18	-6.38
Jun	114.53	118.37	116.16	107.78	127.57	3.35	1.43	-5.89	11.39
Jul	142.44	151.15	162.02	160.31	185.42	6.11	13.74	12.54	30.17
Aug	142.92	151.84	165.69	168.68	177.31	6.24	15.93	18.02	24.06
Sep	142.70	146.40	138.60	147.73	149.28	2.59	-2.87	3.52	4.61
Oct	90.20	103.85	104.14	102.27	123.65	15.14	15.46	13.39	37.09
Nov	38.52	39.88	49.76	50.82	61.86	3.54	29.18	31.94	60.61
Dec	21.46	21.68	26.67	24.86	33.17	1.03	24.27	15.86	54.60
Bega	169.13	182.69	198.93	200.73	247.89	8.02	17.62	18.68	46.57
Belg	366.92	341.45	332.65	349.59	374.78	-6.94	-9.34	-4.72	2.14
Kiremt	542.60	567.75	582.47	584.50	639.58	4.64	7.35	7.72	17.87
Yearly	1078.64	1091.89	1114.05	1134.82	1262.25	1.23	3.28	5.21	17.02

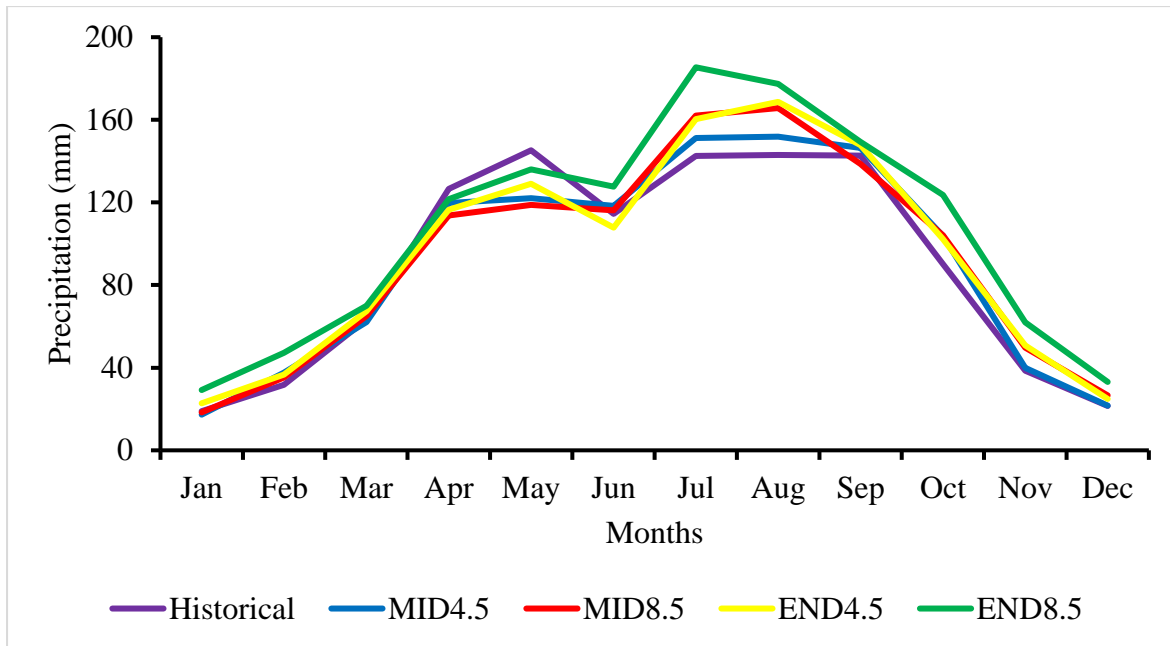


Figure 4.1. Intra annual variation of precipitation in TWW in the historical, mid and end century for RCP4.5 and RCP8.5 climate change scenario

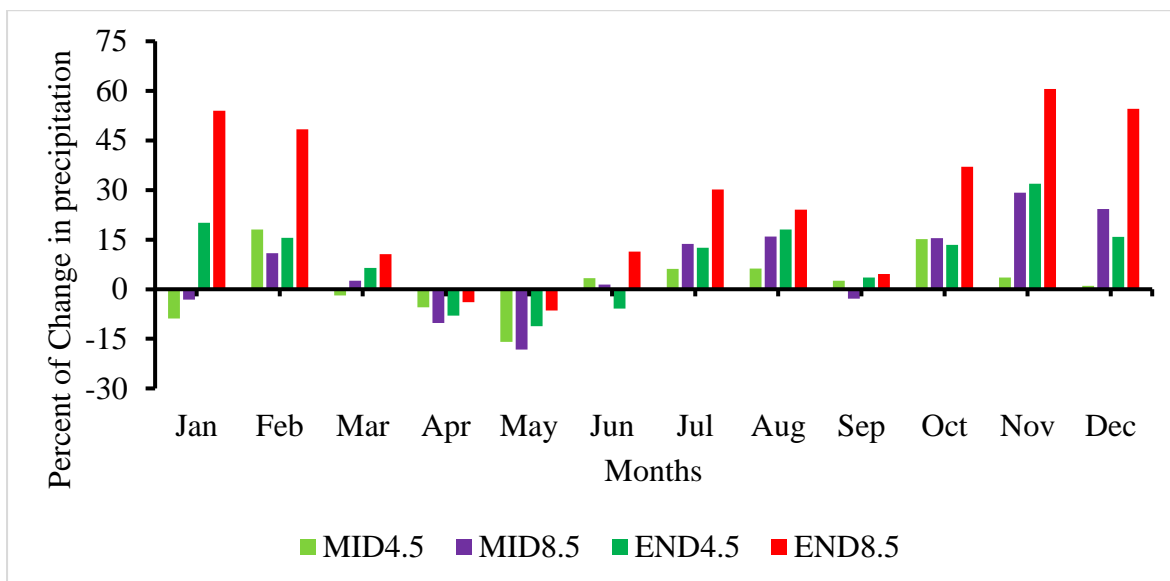


Figure 4.2. Per cent of change in precipitation in TWW in the mid and end century for RCP4.5 and RCP8.5 climate change scenario compared to the Historical period

In mid-century, the Belg rainfall reduced by 6.94% and 9.34% for RCP4.5 and RCP8.5, respectively, compared to the reference period. At the same time, the Kiremt season rainfall increased by 4.64% and 7.35% for RCP4.5 and RCP8.5 scenarios compared to the reference period. The annual rainfall shows a slight increase of

1.23% for RCP4.5 and 3.28% for RCP8.5. The Bega rainfall increases by 8.02% for the RCP4.5 and by 17.62% for the RCP8.5 scenario. At the end century, the rainfall increased in all seasons and both scenarios except Belg. The Belg season rainfall reduced by 4.72% for RCP4.5, rising by 2.14% for RCP8.5 compared to the baseline period. The Kiremt season rainfall increased by 7.72% for RCP4.5 and 17.87% for RCP8.5 in the end century compared to the baseline period. Compared to the baseline period, the yearly average rainfall increased by 5.21% for RCP4.5 and 17.02% for RCP8.5 in the end century. The Bega season rainfall increased in both scenarios.

In general, the study revealed that the Bega, Kiremt, and annual rainfall increased in both mid and end century for all scenarios. Whereas, the Belg rainfall decreased for all cases except for RCP8.5 in the end century. The rainfall increased more in the end century than mid-century. The increase in precipitation is higher in the Bega compared to Belg and Kiremt season. No significant change in variability is observed in rainfall in the study area. It is uncertain whether rainfall will rise/drop in Ethiopia, and its projections vary between -25% and +30% by the 2050s (USAID 2016). Although it varies in both magnitude and direction, precipitation shows an increasing trend in the future in the Lake Tana watershed in northern Ethiopia (Gebre and Ludwing 2015; Nigatu et al. 2016). Nigatu et al. (2016) observed the increase in the annual rainfall noticeably up to 37% in the future relative to (1981 to 2010). In the Blue Nile river basin in northern Ethiopia, the average annual rainfall increased in the future ranging from 2.1% to 43.8% (Mekonnen and Disse 2018). Chaturvedi et al. (2012) used eighteen GCMs outputs under CMIP5 to project rainfall for overall India. They found that even if the more considerable spatial variation is observed, rainfall increases from 4% to 5% and 6% to 14% for 2021-2050 and 2070-2099, respectively, compared to baseline time (1961 to 1990). In Kerala, India's humid tropics, Raneesh and Santosh (2011) reported that for the southwestern monsoon period, there is a decrease in rainfall by 11.5% for the A2 scenario and by 8.79% for the B2 scenario from 2071 to 2100 compared to the baseline period (1981-2010). Based on the RCP8.5 climate change scenario, in the 2050s (2041–2060), the annual rainfall increase in Malawi up to 24.6% at a country level compared to (1981–2000) (Adhikari and Nejadhashemi 2016a). It increases up to 30.7% at the country level in

Tanzania by 2050s compared to the 1990s (1980 to 1999) (Adhikari and Nejadhashemi 2016b).

4.4.2 Climate change impacts on the minimum and maximum temperature

A summary depicting how the temperature changes in the mid-and end-century with both RCP4.5 and RCP8.5 scenarios are presented in Table 4.6. The difference is calculated based on the baseline period.

Table 4.6. Summaries of the change in minimum and maximum temperature in mid and end century for RCP4.5 and RCP8.5 climate change scenario compared to the historical period

Climate scenario	Season	Mid-century (2020 to 2059)		End century (2060 to 2099)	
		Change in T-min (°C)	Change in T-max (°C)	Change in T-min(°C)	Change in T-max (°C)
RCP4.5	Bega	1.81	1.40	2.71	2.49
	Belg	1.61	1.63	2.51	2.66
	Kiremit	1.14	1.56	2.02	2.50
	Annual	1.59	1.53	2.48	2.55
RCP8.5	Bega	2.07	1.15	4.70	4.38
	Belg	1.91	1.55	4.40	4.72
	Kiremit	1.37	1.61	3.86	4.33
	Annual	1.85	1.43	4.39	4.47

Note: T-min = minimum temperature, T-max = maximum temperature

The yearly average minimum temperature increases in the mid-century by 1.59 °C for RCP4.5 and 1.85 °C for RCP8.5 relative to the baseline period. Compared to the baseline period, the average maximum annual temperature increased by 1.53 °C for RCP4.5 and 1.43 °C for RCP8.5. Seasonally, the average minimum temperature increased by 1.81 °C, 1.61 °C, and 1.14 °C for the Bega, Belg, and Kiremt, respectively, for the RCP4.5 climate change scenario. It increased by 2.07 °C, 1.91 °C, and 1.37 °C for Bega, Belg, and Kiremt, respectively, for the RCP8.5. Compared to the baseline period, the average maximum temperature increases by 1.40 °C, 1.63 °C, and 1.56 °C for the Bega, Belg, and Kiremt, respectively, for RCP4.5 the baseline

period. For the RCP8.5 scenario, it increased by 1.15 °C, 1.55 °C, and 1.61 °C for Bega, Belg, and Kiremt, respectively.

In the end century, the average annual minimum temperature increased by 2.48 °C and 4.39 °C for the RCP4.5 and RCP8.5 scenario, respectively, compared to the baseline period. Compared to the baseline period, the average yearly maximum temperature increased by 2.55 °C for the RCP4.5 and 4.47 °C for the RCP8.5. Seasonally, the average minimum temperature increased by 2.71 °C, 2.51 °C, and 2.02 °C for the Bega, Belg, and Kiremt, respectively, for the RCP4.5 scenario. For RCP8.5, it increased by 4.70 °C, 4.40 °C, and 3.86 °C for Bega, Belg, and Kiremt, respectively. The average maximum temperature also increased by 2.49 °C, 2.66 °C, and 2.50 °C for Bega, Belg, and Kiremt, respectively, for the RCP4.5 scenario. For the RCP8.5, the maximum temperature increased by 4.38 °C, 4.72 °C, and 4.33 °C, respectively, for Bega, Belg, and Kiremt seasons.

Figure 4.3 indicate the monthly, seasonal and yearly average maximum temperature of historical, mid and end century for RCP4.5 and RCP8.5 climate change scenarios. For the RCP8.5, the mean temperature rises to a greater degree at the end of the century. Figure 4.4 depicts historical, mid-century, and end-of-century average minimum temperatures for RCP4.5 and RCP8.5 climate change scenarios. For RCP8.5, the minimum temperature rises to a greater degree at the end century. Figure 4.5 showed the yearly average daily minimum and maximum temperature in the future for RCP4.5 and RCP8.5 climate change scenarios. The result of the study is in agreement with the previous reports in Ethiopia. Most GCMs and regional projections of climate models in Ethiopia agreed that the yearly average temperature is estimated to rise by between 1-2°C (USAID 2016), between 1.4 °C and 2.9 °C (Cochrane and Singh 2017) by 2050. The temperature increases in all months and seasons in the Lake Tana watershed in northern Ethiopia (Gebre and Ludwing 2015). Serur and Sarma (2016) also reported that both the minimum and maximum temperatures will increase in southern Ethiopia in the future. In the Lake Tana watershed in Ethiopia, Nigatu et al. (2016) observed an increase in the mean monthly maximum temperature noticeably up to 3.0 °C from 2071 to 2100 relative to (1981 to 2010). Whereas the mean monthly maximum temperature increased up to 3.9 °C from 2080 to 2100. In

Ethiopia's Blue Nile river basin, the annual average maximum temperature increased up to 4.3 °C, and the average annual minimum temperature increased up to 4.1 °C at the end of the 21st century (Mekonnen and Disse 2018). Setegn et al. (2011) analysed future temperatures in Ethiopia's Lake Tana basin. They found that from 2070 to 2100, the temperature increased by 2 °C-4.4 °C and 2.2 °C-4.9 °C in the wet and dry period, respectively, compared to the baseline period (1980-2000). Chaturvedi et al. (2012) used eighteen GCMs and all four climate change emission scenarios under CMIP5 to project surface temperature for overall India. They found that, under the no policy scenario, the mean surface temperature increases in the range of 1.7 to 2°C and 3.3 to 4.8 °C for the period of (2021 to 2050) and (2070 to 2099), respectively compared to baseline time (1961 to 1900). In Kerala, India's humid tropics, Raneesh and Santosh (2011) reported that, for the southwestern monsoon period in the A2 emission scenario, there is an increase in temperature by 2 °C from 2071 to 2100 compared to the baseline period (1981-2010). For the same period in the B2 scenario, the temperature increased by 1%. Shrestha et al. (2016) estimated the potential climate change effect on Nepal's Indrawati River basin's temperature. They used RCP4.5 and RCP8.5 scenarios under one regional climate model and two GCMs. They found that the area's average ensemble temperature will continuously rise and increase by 2.5 °C to 4.9 °C by the end of the 21st century compared to the reference period (1981 to 2005).

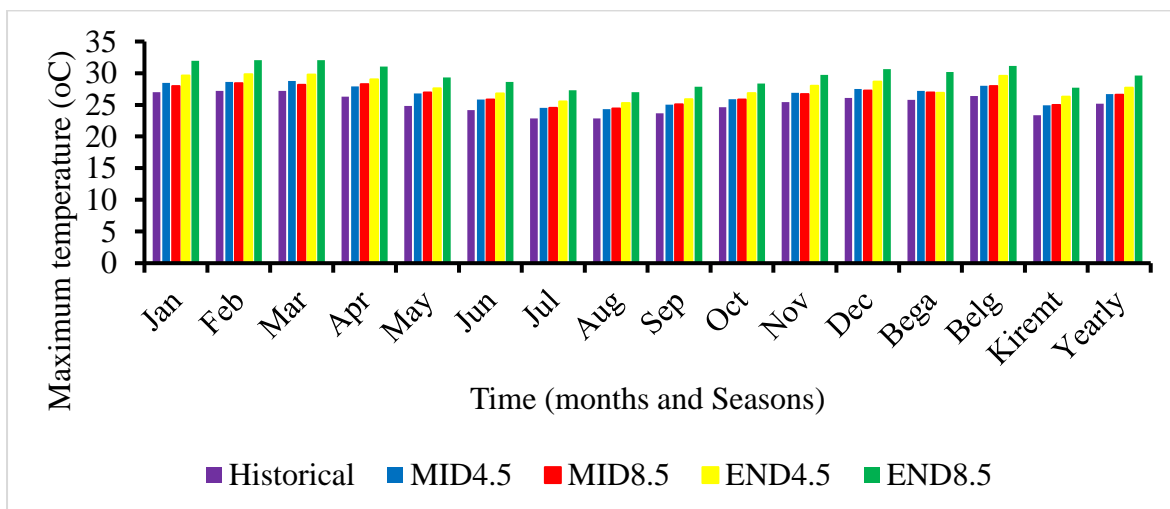


Figure 4.3. Monthly, seasonal, and yearly average maximum temperature of historical, mid and end century for RCP4.5 and RCP8.5 climate change scenarios

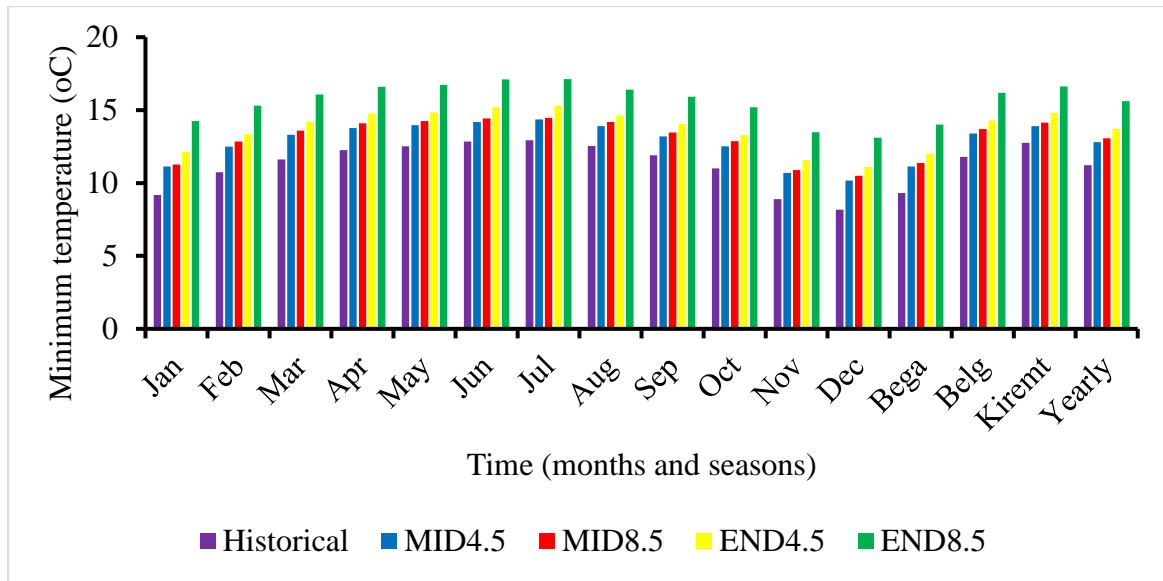


Figure 4.4. Monthly, seasonal, and yearly average minimum temperature of historical, mid and end century for RCP4.5 and RCP8.5 climate change scenarios

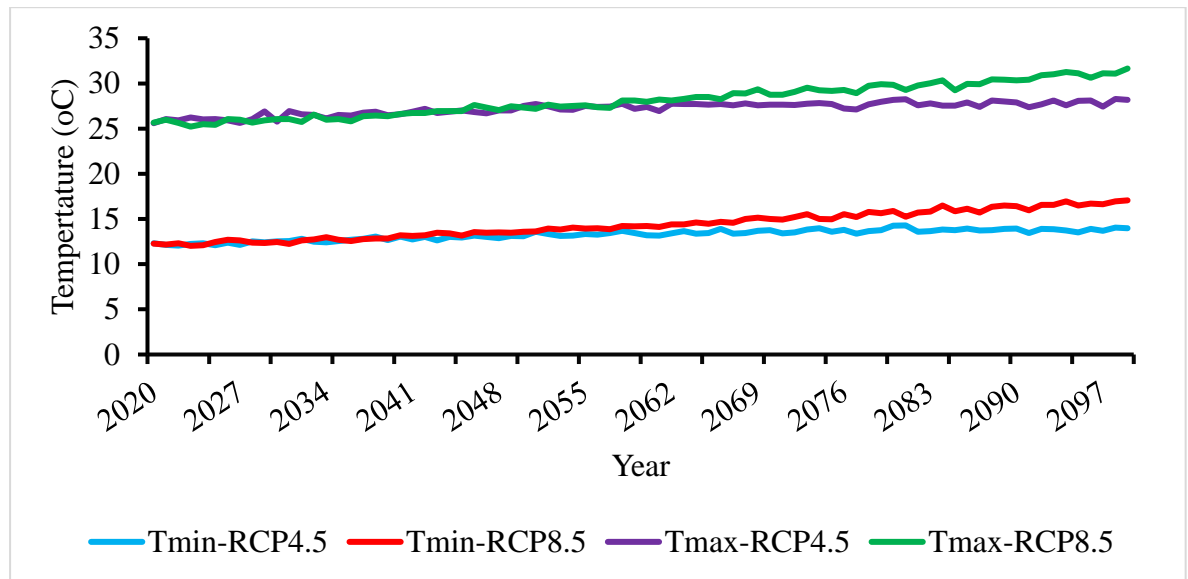


Figure 4.5. Yearly average minimum and maximum temperature in the future for RCP4.5 and RCP8.5 climate change scenario

4.5 Calibration Validation and Model Performance Evaluation

The SWAT hydrological model was calibrated and validated using observed streamflow data based on monthly databases. The LU/LC 1988 (during the calibration period) LU/LC map was used for model calibration due to its being in the calibration period. From January 1980 to December 1982, it was treated as a "warm-up" period to

stabilize the model. Model calibration was performed using simulated and observed streamflow data from January 1983 to December 1995 and model validation data from January 1996 to December 2002. Figure 4.6 demonstrates the graphical comparison of measured and simulated streamflow for calibration periods (1983-1995) and validation (1996-2002). Figure 4.7 and Figure 4.8 show the scatter plots of simulated and observed monthly average daily flow for the calibration and validation period. Table 4.7 provides the statistical performance indices. The results showed that the simulated streamflow was well correlated with the streamflow observed, with a correlation coefficient equal to 0.77 for the calibration and 0.85 for the validation period. The Nash–Sutcliffe efficiency (NSE) of the SWAT was 0.68 for calibration and 0.64 for the validation period. In general, the result revealed that the SWAT model had performed well in simulating the hydrological impacts of climate changes in the study area.

Table 4.7. Statistical performance indicator of SWAT for TWW with the different objective function

Statistical Indicator	Calibration	Validation	Performance Rating	
			Calibration	Validation
NSE	0.68	0.64	Good	Satisfactory
RSR	0.60	0.63	Good	Good
R ²	0.77	0.85	Acceptable	Acceptable
PBIAS	10.43	1.79	Good	Very Good

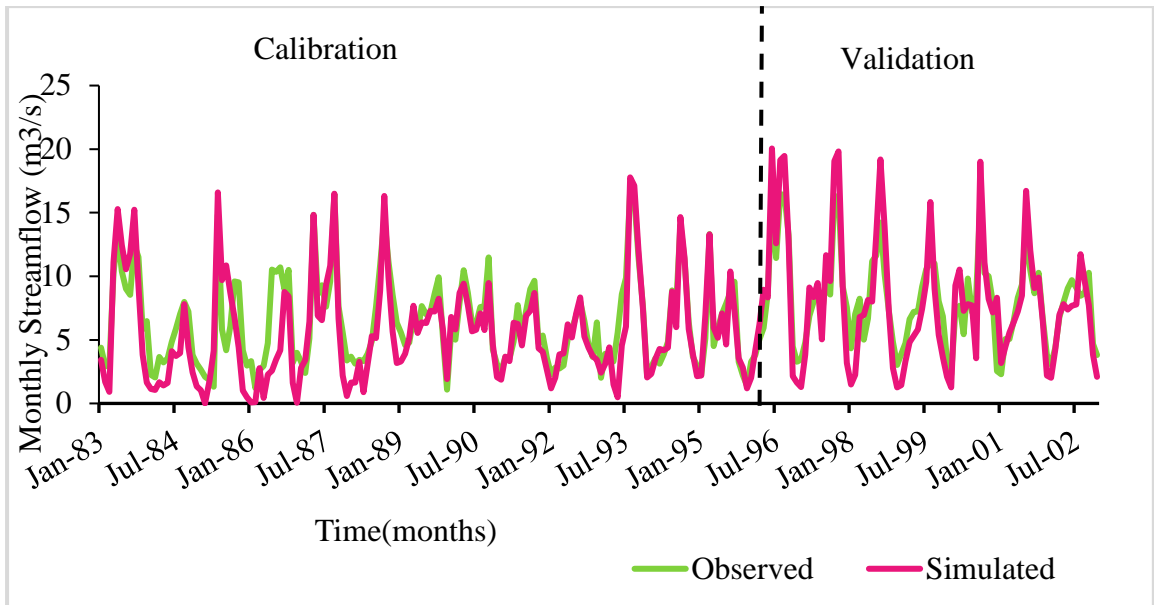


Figure 4.6. Simulated and observed streamflow for calibration and validation period

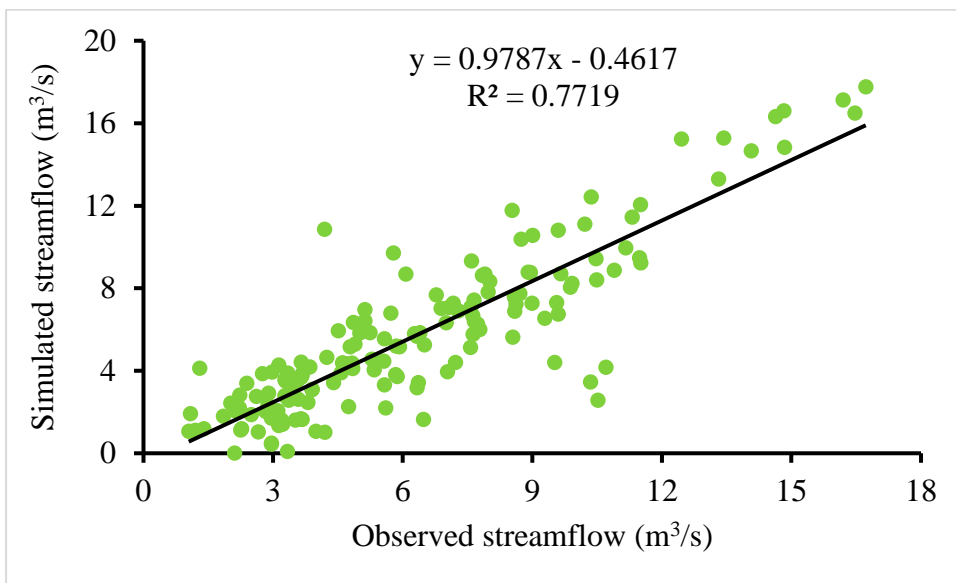


Figure 4.7. Scatter plots of simulated and observed monthly average daily flow for calibration period.

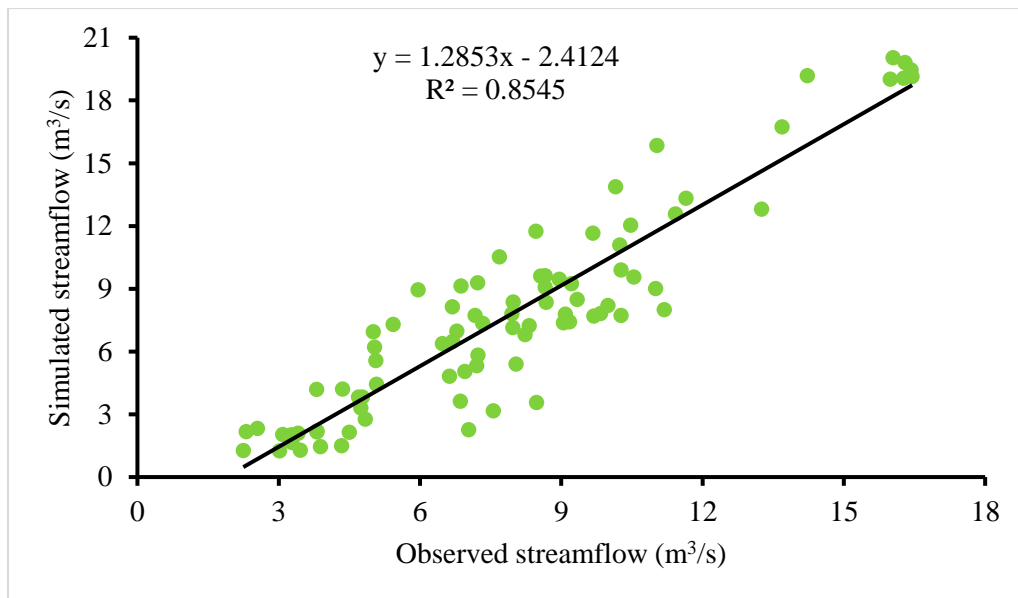


Figure 4.8. Scatter plots of simulated and observed monthly average daily flow for the validation period.

4.6 Climate Change Impacts on Streamflow

The summary of the average values and per cent of change in streamflow on the monthly, seasonal, and yearly bases is given in Table 4.8. The monthly variation of average streamflow in historical, mid, and end centuries are demonstrated in Figure 4.9. The per cent of change in monthly streamflow for the mid and end century for both scenarios is shown in Figure 4.10.

Table 4.8. Summaries of the average values and per cent of change of streamflow in mid and end century compared to the historical period

Months	Average Streamflow (m ³ /s)					Per cent of change in streamflow (m ³ /s) compared to the historical period			
	Historical	MID4.5	MID8.5	END4.5	END8.5	MID4.5	MID8.5	END4.5	END8.5
Jan	0.76	0.84	0.96	1.12	1.47	11.22	26.42	47.12	93.89
Feb	1.60	1.00	1.25	1.24	1.86	-37.46	-21.95	-22.68	16.28
Mar	4.78	3.13	3.74	3.48	4.11	-34.52	-21.86	-27.18	-14.09
Apr	9.14	5.86	5.91	6.22	7.50	-35.95	-35.38	-31.92	-18.00

May	10.76	8.80	9.04	8.15	10.82	-18.22	-15.99	-24.20	0.57
Jun	15.42	15.43	17.32	15.94	19.93	0.09	12.31	3.36	29.23
Jul	18.04	18.87	21.05	21.04	23.50	4.59	16.66	16.64	30.26
Aug	19.58	21.34	21.33	21.36	22.98	8.99	8.92	9.09	17.37
Sep	17.48	18.79	18.71	18.88	20.73	7.52	7.08	8.06	18.60
Oct	10.98	12.34	12.92	13.15	14.71	12.31	17.60	19.74	33.94
Nov	5.38	5.99	6.36	6.53	8.04	11.27	18.20	21.31	49.32
Dec	1.47	1.60	1.96	2.08	2.70	8.50	33.00	40.87	82.96
Bega	4.65	5.19	5.55	5.72	6.73	11.66	19.36	22.98	44.72
Belg	6.57	4.70	4.98	4.77	6.07	-28.52	-24.16	-27.34	-7.60
Kiremt	17.63	18.61	19.60	19.31	21.78	5.55	11.18	9.51	23.56
Yearly	9.62	9.50	10.04	9.93	11.53	-1.22	4.45	3.29	19.88
Dry	4.75	3.54	3.81	3.71	4.74	-25.55	-19.86	-21.83	-0.21
Wet	14.48	15.46	16.28	16.15	18.31	6.76	12.43	11.54	26.47

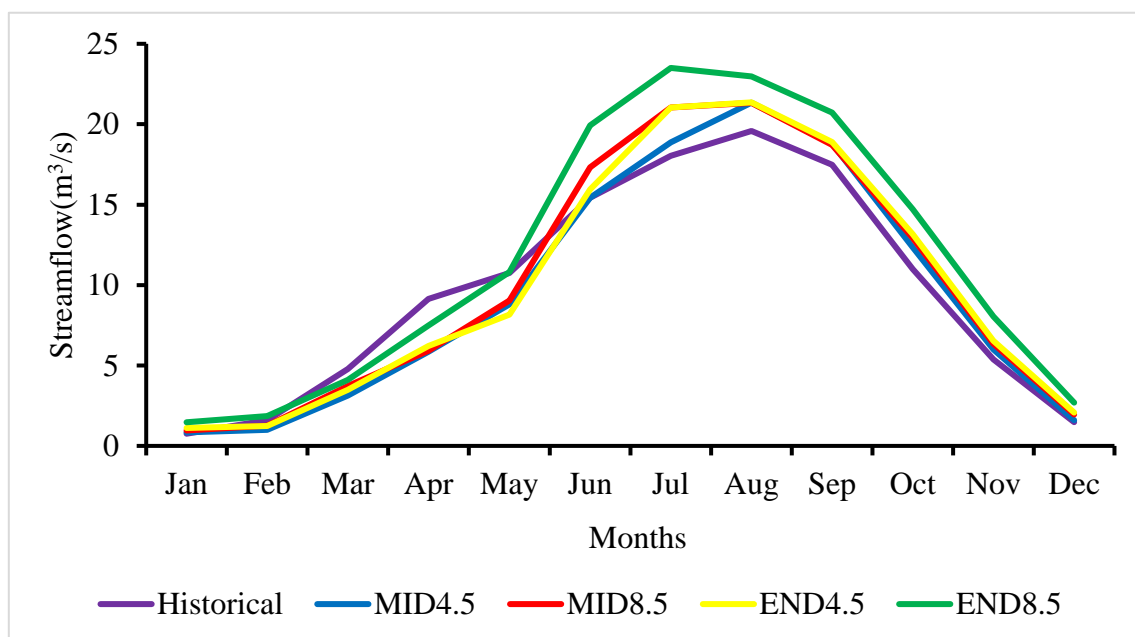


Figure 4.9. The monthly variation of average streamflow in historical, mid, and end century

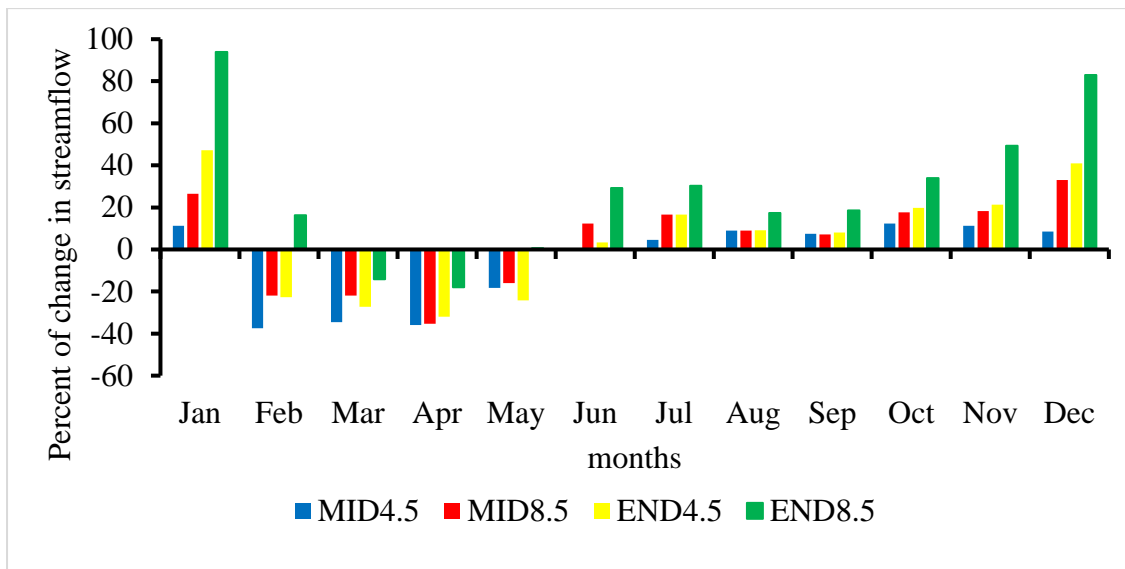


Figure 4.10. Per cent of change of average streamflow in the future compared to the reference period

In all cases, the Belg season streamflow will be reduced in the future compared to the baseline time. The reduction in streamflow in the Belg season is related to the decrease in the Belg rainfall in the future in the area. In mid-century, the Belg streamflow reduced by 28.52% for the RCP4.5 and 24.16% for the RCP8.5 climate change scenario. In the end century, the Belg streamflow reduced by 27.34% and 7.60% for the RCP4.5 and RCP8.5 scenarios. Whereas the Kiremt season streamflow increased in the future in both scenarios compared to the baseline period. In mid-century, the Kiremt streamflow increased by 5.55% and 11.18% for the RCP4.5 and RCP8.5, respectively. In the end century, the Kiremt streamflow increased by 9.51% and 23.56%, respectively. The annual average streamflow in TWW disclosed that the streamflow increased in all cases except a slight reduction in the RCP4.5 scenario in mid-century. It increased by 4.45% for the RCP8.5 scenario in mid-century. In the end century, the yearly average streamflow increased by 3.29% and 19.88% for the RCP4.5 and RCP8.5 scenarios, respectively. The monthly average streamflow shows a reduction from February to May and increased in all other months. In TWW in Ethiopia, the average Bega streamflow increased in the future in all cases. In mid-century, the Bega streamflow increased by 11.66% and 19.36% for the RCP4.5 and RCP8.5 scenarios, respectively. In the end century, the Bega season streamflow increased by 22.98% for RCP4.5 and 44.72% for the RCP8.5 climate change scenario

compared to the reference period. Climate change affects the streamflow in the study watershed by increasing the wet season flow and reducing the dry season flow.

An increase in water availability in the rainy and transitional seasons, whereas a decline in the dry season is also reported in southern Ethiopia (Serur and Sarma 2016). In the Weyib watershed of south Ethiopia, based on a single GCM (CanESM2) output, Serur and Sarma (2016) identified the annual average daily streamflow increased in 3.98-20.40% for RCP4.5 and 9.18-24.49% for RCP8.5 climate change scenario. Studies suggest a 30% decrease in the runoff on several Nile tributaries by 2050 (USAID 2016). In the Lake Tana watershed in northern Ethiopia, Gebre and Ludwing (2015) identified that the average yearly runoff might raise about +55.7% (RCP 4.5) and +74.8% (RCP 8.5) for the period of (2035-2064), and by +73.5% (RCP 4.5) and +127.4% (RCP 8.5) for the period (2071-2100) as compared to the baseline period (1960 to 2005). In the same watershed, Nigatu et al. (2016) reported that the streamflow increased up to 28% from 2071 to 2100. Whereas, Setegn et al. (2011) observed a statistically significant decline in streamflow magnitude from 2070 to 2100 compared to 1980-2000 in the Lake Tana basin. In the Blue Nile river basin in northern Ethiopia, runoff showed an increasing trend within the period (2040 to 2069) compared to (1961 to 1990) (Kim and Kaluarachchi 2009). Whereas Dile et al. (2013) reported, the basin discharge is decreased from 2010 to 2039 and increase from 2070 to 2100. Wagesho et al. (2013) examined the climate change impacts on Blate and Hare watersheds' runoff in southern Ethiopia. The increase in the streamflow varies from -4% to 18% and -4% to 14% for Hare and Blate River basins, respectively, during the simulation period (2081 to 2090) compared to the baseline period (1990-1999). Abraham et al. (2018) revealed a high water availability reduction in the future in the Katar and Meki sub-watersheds of Lake Ziway in southern Ethiopia. They reported that annual runoff depth was reduced by up to 19.45% and 20.28% in Katar and Meki sub-watersheds, respectively, by 2080s (2071 to 2099) compared to the base period (1980 to 2005). Another study in the same watershed by Zeray et al. (2006) also indicates that the watershed's water resource is greatly affected by climate change in the future. They used B2A and A2A scenarios and SWAT to analyze the future interaction between climate change and water resources in the Lake Ziway watershed. They reported that the average inflow volume to Lake Ziway decreases notably by

about 19.47% and 27.43% for A2A and B2A scenarios, respectively, from 2001 to 2099 relative to 1981-2000. A study carried out by Chaemiso et al. (2016) in the Omo-Gibe basin in southern Ethiopia indicated that the surface water availability is declining within the dry period and rising within the wet period in the future (the 2030s and 2090s) relative to the base period (1980 to 2005). In Kerala, India's humid tropics, Raneesh and Santosh (2011) reported that, for the southwestern monsoon period in the A2 emission scenario, streamflow decrease by and 7.53%, and in the B2 scenario, streamflow decreased by 4.62% from 2071 to 2100 compared to 1981 to 2010. Adhikari and Nejadhashemi (2016a) assessed the impact of global change on water resources in Malawi using six GCMs, based on RCP8.5. The runoff increases by 7.5% to 50% at the country level from 2041 to 2060 compared to 1981-2000. At the sub-basin level, the north's annual runoff increases and declines in the south part of the country. Furthermore, Adhikari and Nejadhashemi (2016b) used the same GCMs and emission scenarios to evaluate the effect of global warming on water resources in Tanzania by the 2050s. A significant increase in surface runoff (18.3 to 104.8%) was reported for the wet seasons. Overall, the sub-basin, watershed, and country levels revealed an increase in Tanzania's water resources during the wet seasons in the 2050s (2040-2059) compared to the 1990s (1980 to 1999).

The climate change influence on streamflow in the Gorganroud basin in Iran was studied by Mahmood et al. (2016). They found an increase in streamflow of 9.5%, 2.8% and 5.8% for the B1, A2, and A1F1 emission scenarios, respectively, by 2050s (2040-2069) compared to the baseline period (1971 to 2000). Zhu et al. (2016) used the RCP2.6, RCP4.5, and RCP8.5 emission scenarios to predict climate change's influence on the water resources of the Yellow river basin in China. They found a considerable reduction of water resources up to 30% in the early and mid-21st century (up to 2080) relative to the reference period (1962 to 2005). Changkun et al. (2015) analysed the climate change effect on streamflow in Central Asia's Chu river basin. They found that in the short (1916-2045) and far future (2066-2096) periods, a general reduction trend was recognized in mean annual runoff in streamflow (-27.7% to - 6.6%), snow (-21.4% to 1.1%) and glacier (-26.6% to -1%) compared to the reference period (1966-1995).

There are two general approaches to controlling the undesirable impacts of ongoing climate change: mitigation and adaptation, slowing down GHG emissions, and reducing their consequences, respectively. Concerning water resource and crop production, adaptation measures consist of using varieties and drought-resistant crops, using water-efficient irrigation techniques like drip irrigation, implementing water harvesting technology, and adjusting crop calendars (Bates et al. 2008). Hadgu et al. (2015) point out that alteration in crop type/variety, watershed management measures, crop diversifications, an adjustment in planting calendar, and water-efficient irrigation practices are adaptation measures that have been implemented in Tigray regional state in Northern Ethiopia. Another report by Atreya et al. (2005) showed that the above-listed adaptations strategies are commonly implemented by farmers in Ethiopia's central Rift valley.

4.7 Closure

In general, the study revealed that the Bega, Kiremt, and annual rainfall increased in both the mid and end century for all scenarios. Whereas, the Belg rainfall decreased in all cases except for RCP8.5 in the end century. The rainfall increased more in the end century than in the mid-century. The increase in precipitation is higher in the Bega compared to Belg and Kiremt season. No significant change in variability was observed in rainfall in the study area. Both the average minimum and maximum temperature increased for all scenarios and time horizons. In all cases, the Belg season streamflow will be reduced in the future compared to the baseline time. The reduction in streamflow in the Belg season is related to the decrease in Belg rainfall in the future in the area. Whereas the Kiremt season streamflow increased in the future in both scenarios compared to the baseline period. The annual average streamflow in TWW disclosed that the streamflow increased in all cases except a slight reduction in the RCP4.5 scenario in mid-century. Climate change affects the streamflow in the study watershed by increasing the wet season flow and reducing the dry season flow.

CHAPTER 5: HYDROLOGICAL RESPONSES TO LAND USE/LAND COVER CHANGE

5.1 General

This section provides insight into the LU/LC change dynamics from 1978 to 2017 in the Tikur Wuha watershed. It also provides the LU/LC change impacts on streamflow.

5.2 LU/LC Change Detection

5.2.1 Classification accuracy assessment

The LU/LC map of the Tikur Wuha watershed from 1978 to 2017 was developed using four historical Landsat satellite images, and a maximum likelihood supervised classification algorithm to a satisfactory level of accuracy. The results of the assessment identified the presence of seven LU/LC classes in the TWW. The LU/LC includes intensively cultivated, moderately cultivated, swampy, built-up, shrubland, water, and grassland. The accuracy of the classified maps was assessed by a set of 600 points based on Google Earth and the user's experience. The summary of the accuracy report of the four classified images is given in Table 5.1.

Table 5.1. Summary of accuracy assessment of LU/LC

LU/LC Map	Accuracy (%)	URHD	RNGE	AGRR	WETN	AGRC	RNGB	WATR	Overall accuracy
1978	User acc.	78.57	81.45	73.85	79.59	75.51	75.71	74.67	77.50
	Prod. acc.	72.37	80.80	72.73	80.41	80.43	72.60	78.87	
1988	User acc.	86.30	81.55	84.55	84.88	82.65	78.33	74.29	82.17
	Prod. acc.	79.75	81.55	86.92	82.95	81.82	77.05	82.54	
1998	User acc.	85.19	86.92	86.67	83.78	86.49	79.03	81.94	84.83

	Prod.								
	acc.	83.64	86.11	86.67	83.78	84.96	79.03	86.76	
	User								
2017	acc.	90.28	89.47	87.60	84.06	88.69	86.11	82.14	87.33
	Prod.								
	acc.	87.84	87.63	89.08	84.06	87.18	84.93	90.20	

Note: URHD = Built up, RNGE = Grassland, AGRR = Intensively Cultivated, WETN = Swampy, AGRC = Moderately Cultivated, RNGB = Shrubland, WATR = Water, User acc. = user's accuracy and Prod. acc. = producer's accuracy

Accuracy assessment with the help of Google Earth samples has yielded agreeable results (Table 5.1). The accuracy assessment results for 1978, 1988, 1998, and 2017 LU/LC maps showed an overall accuracy of 77.50%, 82.17%, 84.83%, and 87.33%, respectively. Overall accuracy is a descriptive statistic computed by dividing the total sum of correctly classified by the total number of reference pixels in the error matrix (Lillesand 2015). The producer's accuracy ranges from 72.37% to 90.20%, and the user's accuracy varies from 73.85% to 90.28% for the different categories in the study period. Producer accuracy measures how much of the land in each category were classified correctly (it measures the proportion of the land base correctly classified). User accuracy measures the proportion of each thematic map class which is correct. The higher the proportion of the pixels within the user and producer accuracies for the individual class in question, the more accurate the classified maps are. All producer's accuracy, user's accuracy, and overall accuracy for 1978 are relatively less than 1988, 1998, and 2017. The reason may be due to the low resolution of the 1978 images compared to images acquired in 1988, 1998, and 2017. The quality of Google Earth image is also relatively less for 1978. The accuracy of the classified LU/LC types depends on the images' quality and spectral contents, and ground truth data quality (Lillesand et al. 2004).

5.2.2 The magnitude of LU/LC changes

Figures 5.1 to 5.4 illustrates the LULC map for the Tikur Wuha watershed during 1978, 1988, 1998, and 2017 respectively. Table 5.2 revealed the size (spatial extent) and percentage of the area covered by each LU/LC class to the watershed area. The

LU/LC classes (Table 5.1) extracted from the classification indicated that grassland was the most dominant LU/LC class in 1978. Grassland occupied 38.49 % (262.07 km²) in 1978 and diminished to 20.79% in 2017. However, in all other years, cultivated land (a combination of intensively and moderately cultivated) was the most dominant LU/LC class in the study period. Cultivated land occupied 32.82%, 46.82%, 50.34%, and 56.99% in 1978, 1988, 1998, and 2017, respectively. The study area is predominantly cultivated land.

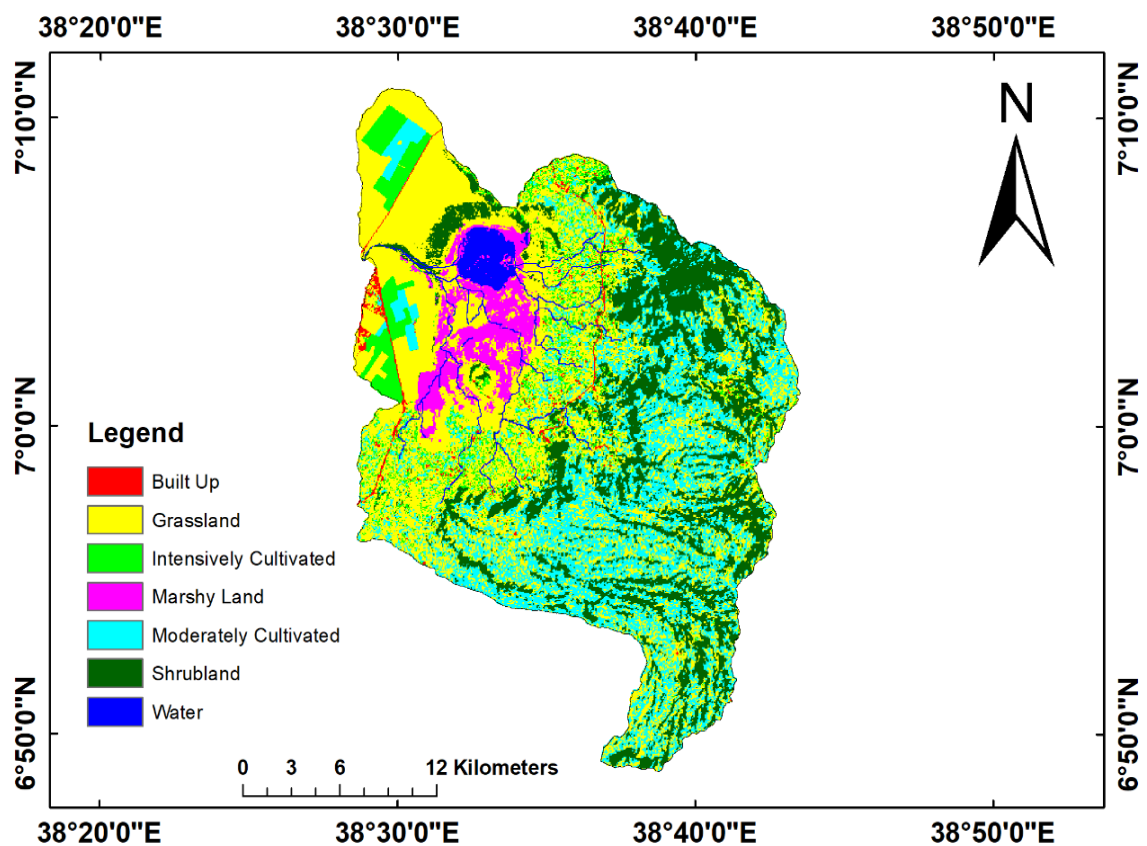


Figure 5.1. LU/LC map of the Tikur Wuha watershed in 1978

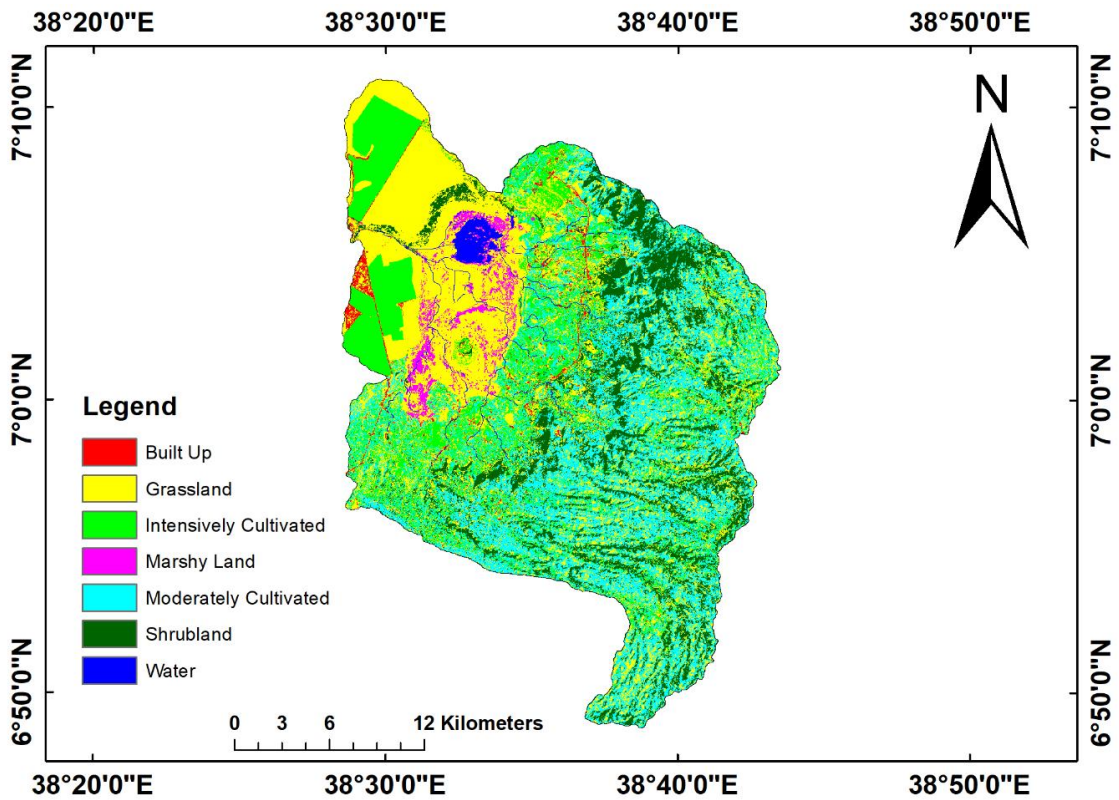


Figure 5.2. LU/LC map of the Tikur Wuha watershed in 1988

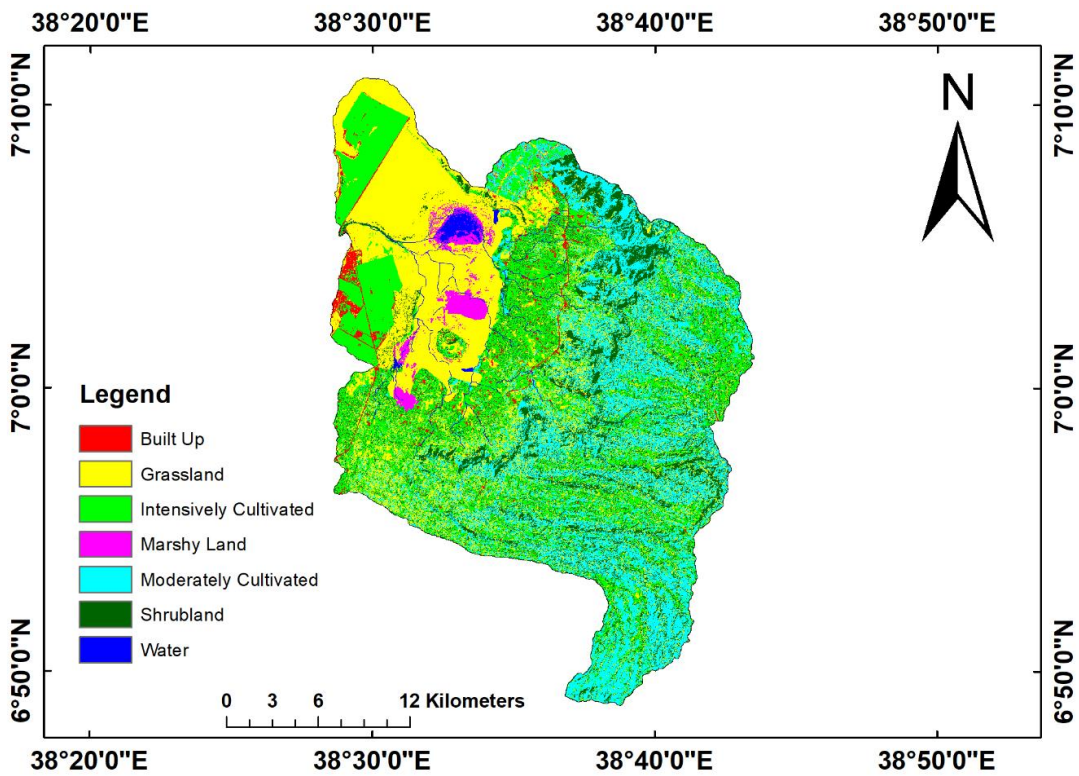


Figure 5.3. LU/LC map of the Tikur Wuha watershed in 1998

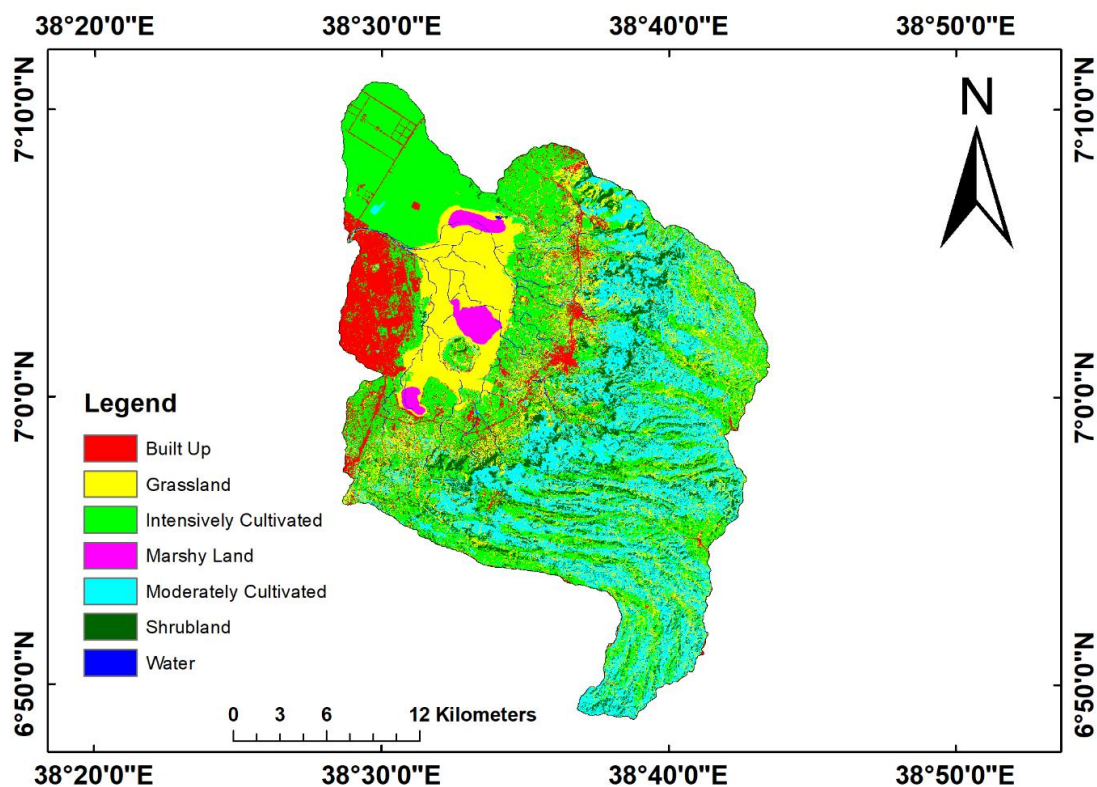


Figure 5.4. LU/LC map of the Tikur Wuha watershed in 2017

Table 5.2. The areal extent of LU/LC classes in the Tikur Wuha watershed in 1978, 1988, 1998 and 2017

LU/LC Type	1978		1988		1998		2017	
	Area (Km ²)	Area (%)	Area (Km ²)	Area (%)	Area (Km ²)	Area (%)	Area (Km ²)	Area (%)
URHD	8.11	1.19	9.94	1.46	14.73	2.16	65.16	9.57
RNGE	262.07	38.49	213.11	31.30	190.71	28.01	141.58	20.79
AGRR	49.18	7.22	116.66	17.13	170.85	25.09	217.32	31.92
WETN	31.52	4.63	14.12	2.07	11.57	1.70	10.14	1.49
AGRC	167.47	24.60	202.12	29.69	171.94	25.25	170.70	25.07
RNGB	144.13	21.17	114.85	16.87	112.71	16.55	71.38	10.48
WATR	18.40	2.70	10.08	1.48	8.37	1.23	4.60	0.68
Total	680.88	100.00	680.88	100.00	680.88	100.00	680.88	100.00

Note: URHD = Built-up, RNGE = Grassland, AGRR = Intensively Cultivated, WETN = Marshy, AGRC = Moderately Cultivated, RNGB = Shrubland and WATR = Water

A significant amount of LU/LC changes occurred in the Tikur Wuha watershed in the study period. Among the other land classes, the area under built-up and intensively cultivated shows continuously an increasing trend in the study period. Built-up area increased from 8.11Km² (1.19%) in 1978, to 14.73 Km² (2.16%) in 1998, and to 65.16 Km² (9.57%) in 2017. During the whole analysis period, there was a net gain of 57.05 Km². A rapid per cent change in built-up areas during the 1998 to 2017 period was observed. The expansion of Hawassa town (the regional capital city) and the recently introduced industry zone in the watershed are the main reasons for the fast growth in the built-up area in the watershed. Intensively cultivated land covered 49.18 Km² (7.22%) in 1978 was increased to 116.66 Km² (17.13%), in 1988, 170.85Km² (25.09%) in 1998 and to 217.32 Km² (31.92%) in 2017. The population growth and the decline of land productivity may be the possible reasons for such changes. Grassland showed a continuous decline in the entire period considered. Grassland declined from 38.49% in 1978 to 20.79% in 2017.

Similarly, shrubland was reduced by nearly 50% during the entire study period. It diminished from 21.17% in 1978 to 10.48% in 2017. The water body was reduced from 18.40 Km² in 1978 to 4.60 Km² in 2017. It is mainly due to the continuous decrease and vanishing of Lake Cheleleka in the Tikur Wuha watershed. The reduction and disappearance of Lake Cheleleka in the watershed with time was reported (WWDSE 2001; Dadi 2013 and Wondrade 2014). The swampy area was also reduced from 31.52 Km² to 10.14 Km² from 1978 to 2017.

The expansion of cultivated and built-up areas and the withdrawal of shrubland, grassland, swampy, and water body were observed in the watershed during the entire study period. The finding of this study coincides with other research findings in Ethiopia. In Ethiopia, it was recorded that cultivated land was rapidly expanding to highly steep areas at the cost of the forest (Zelege and Hurni 2001; Maitima et al. 2009, Getachew and Melesse 2012, Chakilu and Moges 2017). Expansion of cultivated land and build up area at the expense of shrubland and grassland was observed in Tekeze Dam watershed (Welde and Gebremariam 2017), in Adanssa Watershed (Gashaw et al. 2018), in Ketar watershed (Tufa et al. 2015), Melka Kuntie watershed (Getahun and Van Lanen 2015) in a different part of Ethiopia. In the Dano watershed of West Africa, Yira et al. (2016) reported a decrease in Savannah and

increased cultivated land and a build-up area. A significant expansion of urban area within a short period (1990 to 2006) were observed in the Yom watershed in Thailand (Petchprayoon et al. 2010). In Nepal's Bagmati River watershed, built-up areas were increased by 6%, whereas the forest, shrubland, grassland, cropland, open field, and the water body decreased from 2000 to 2010 (Pokhrel 2018).

5.2.3 Rate, per cent, and trend of LU/LC change

Rate, per cent, and trend of change of each LU/LC were summarized in Table 5.3. Figure 5.5 showed the trends in LU/LC change for each class. Figure 5.6 demonstrates the rate of change in LU/LC in the Tikur Wuha watershed.

Table 5.3. LU/LC per cent of changes with respect to the original area of each class and rate of changes from 1978 to 2017 in the Tikur Wuha watershed

LU/LC Type	1978 to 1998		1998 to 2017		1978 to 2017	
	Per cent of change	Rate of change (Km ² /yr)	Per cent of change	Rate of change (Km ² /yr)	Per cent of change	Rate of change (Km ² /yr)
URHD	81.57	0.33	342.27	2.65	703.02	1.46
RNGE	-27.23	-3.57	-25.76	-2.59	-45.98	-3.09
AGRR	247.40	6.08	27.20	2.45	341.89	4.31
WETN	-63.29	-1.00	-12.36	-0.08	-67.83	-0.55
AGRC	2.67	0.22	-0.72	-0.07	1.93	0.08
RNGB	-21.80	-1.57	-36.67	-2.18	-50.48	-1.87
WATR	-54.50	-0.50	-45.04	-0.20	-74.99	-0.35

Note: URHD = Built-up, RNGE = Grassland, AGRR = Intensively Cultivated, WETN = Marshy, AGRC = Moderately Cultivated, RNGB = Shrubland and WATR = Water

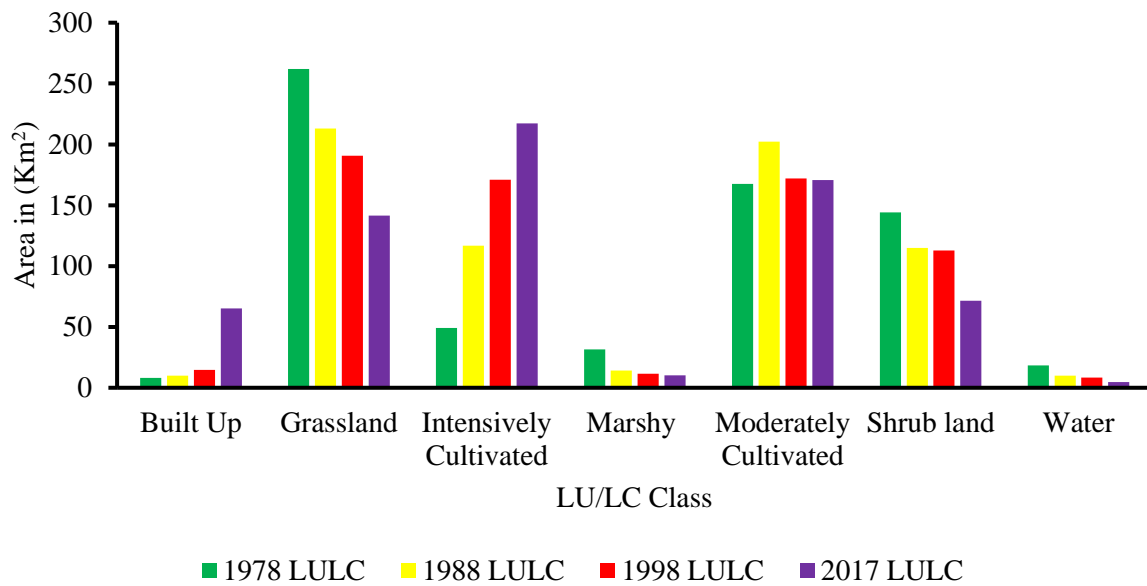


Figure 5.5. LCLU change trend from the year 1978 to 2017 in Tikur Wuha watershed

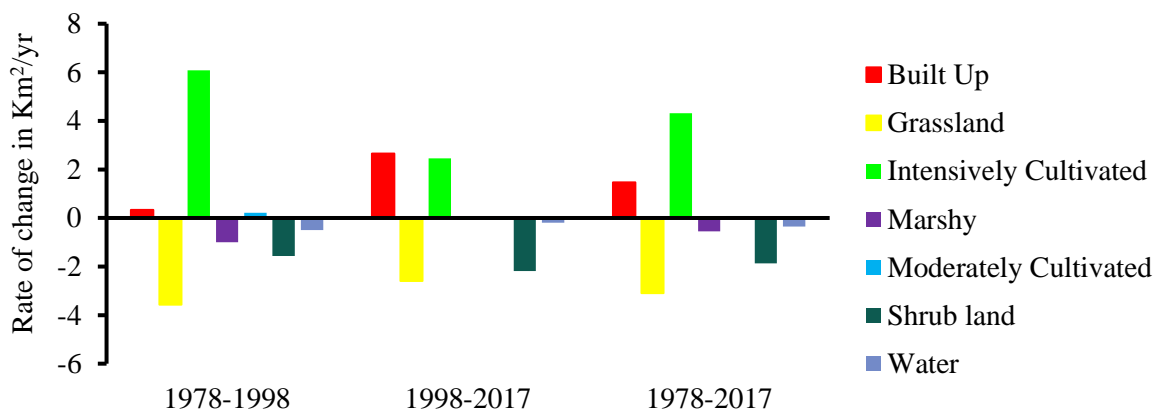


Figure 5.6. Rate of change of LU/LC (km^2/yr) in Tikur Wuha watershed

The expansions of cultivated and built-up areas and the withdrawal of shrubland, grassland, swampy, and water body were observed in the watershed during the entire study period. The annual expansion rate (Km^2/yr) of the built-up area was 0.33 Km^2/yr and 2.65 Km^2/yr from 1978 to 1998 and 1998 to 2017, respectively. The result reveals that the rate of gaining of the built-up area between 1998 and 2017 was high compared to 1978 and 1998. The intensively cultivated land change rate was 6.08 Km^2/yr and 2.45 Km^2/yr from 1978 to 1998 and 1998 to 2017, respectively. It discloses that the rate of gaining intensively cultivated land between 1978 and 1998 was high compared to the period between 1998 and 2017. Over the entire study period, the rate of change of intensively farmed land (4.31 Km^2/yr) is higher than the

rate of change of the built-up area (1.46 Km²/yr). However, when we come to the per cent of change, the built-up area increased by 703.02%, and intensively cultivated land increased by 341.89% over the entire study period. The moderately cultivated land shows an increasing trend in the 1978 to 1998 period with 2.67% (0.22 Km²/yr); and a decreasing trend in the 1998 to 2017 period with 0.72% (0.07 Km²/yr). However, it shows an expansion over the study period with a rate of 0.08 Km²/yr. All the other LU/LC types were shown a decreasing trend during the study period in the watershed. Shrubland declined at 1.57 Km²/yr from 1978 to 1998 and 2.18 Km²/yr from 1998 to 2017. The annual rate of grassland change was -3.57 Km²/yr from 1978 to 1998 and -2.59 Km²/yr from 1998 to 2017. It showed a decreasing trend over the entire study period by 3.09 Km²/yr. The rate of contraction of grassland was high from 1978 to 1998 compared to 1998 to 2017. The rate of contraction of shrubland was low from 1978 to 1998 compared to 1998 to 2017. The water body and swampy area showed a decreasing trend in the watershed with a rate of 0.35 Km²/yr and 0.55 Km²/yr, respectively. The water body lost 74.99% of the area during the study period, and the swampy area lost 67.83% of its size during the study period (Table 5.3, Figures 5.5, and 5.6).

5.3 Hydrological Responses to Land Use/Land Cover Change

The SWAT hydrological model was calibrated and validated using observed streamflow data based on monthly databases. The statistical performance indices of the model are discussed under section 4.5. The SWAT model performed well. The summary of the result of LU/LC change impacts on streamflow in TWW is presented in Table 5.4, and the intera annual variation of streamflow in TWW is demonstrated in Figure 5.7.

Table 5.4. The monthly, seasonal, and yearly average and per cent of change in streamflow (m³/s) in different LU/LC

	1978	1988	1998	2017	Per cent of Change in Streamflow			
					1978-1988	1978-1998	1978-2017	1988-1998
Months	LU/LC	LU/LC	LU/LC	LU/LC				
Jan	1.39	1.43	1.48	1.59	2.57	6.53	14.41	7.40

Feb	1.85	2.13	2.25	2.49	14.95	21.59	34.63	10.72
Mar	3.13	3.55	3.79	4.16	13.38	21.07	32.86	9.74
Apr	4.18	4.51	4.58	4.81	7.75	9.57	15.00	4.95
May	4.65	4.62	4.63	4.89	-0.60	-0.50	5.11	5.65
Jun	4.54	4.93	4.56	4.85	8.55	0.44	6.81	6.34
Jul	5.40	5.99	6.07	6.54	11.00	12.45	21.16	7.74
Aug	8.37	8.71	9.42	9.94	3.96	12.43	18.75	5.62
Sep	8.74	9.44	9.66	9.98	7.99	10.50	14.16	3.31
Oct	6.65	7.23	7.05	7.28	8.74	5.97	9.40	3.24
Nov	3.57	4.07	3.80	3.84	13.88	6.49	7.65	1.10
Dec	1.70	1.99	1.82	1.82	16.71	6.50	6.67	0.16
Bega	3.33	3.68	3.54	3.63	10.50	6.24	9.11	2.70
Belg	3.45	3.70	3.81	4.09	7.18	10.39	18.35	7.20
Kiremt	6.76	7.27	7.43	7.83	7.44	9.80	15.74	5.41
Annual	4.52	4.88	4.92	5.18	8.12	9.07	14.77	5.23
Dry flow	3.01	3.04	2.78	3.29	0.79	-7.61	9.29	18.30
Wet flow	6.21	6.73	6.76	7.07	8.29	8.80	13.84	4.63

Note: Dry flow (December-May) and Wet flow (June-November)

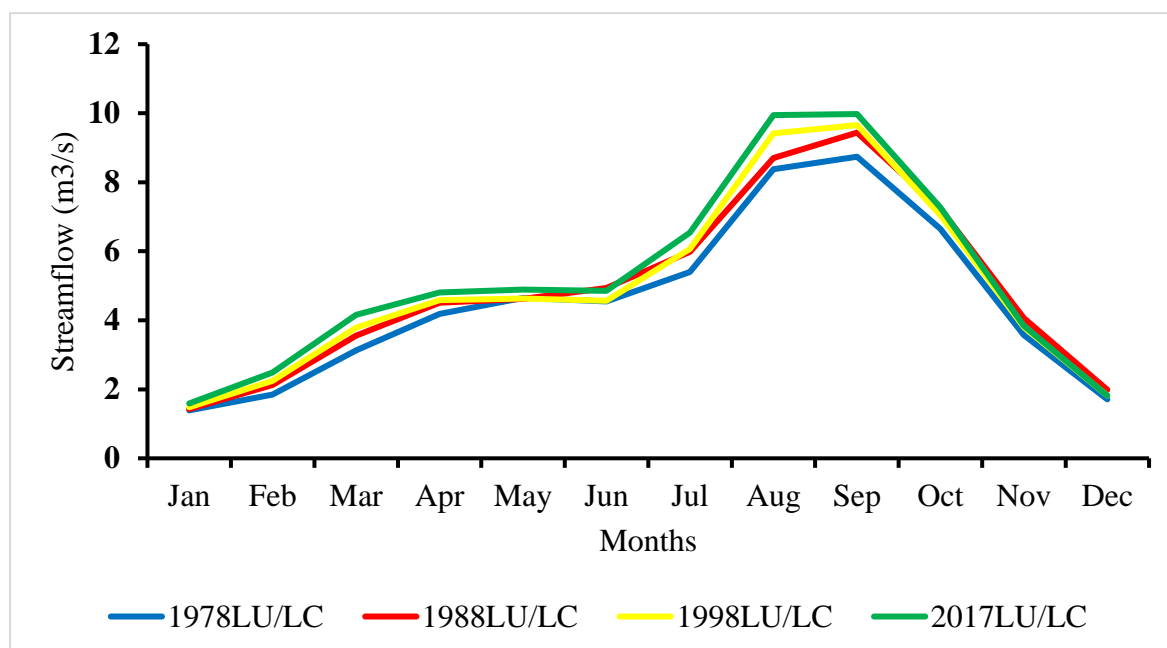


Figure 5.7. Intra annual variation of streamflow for the year 1978 to 2017

During the wet season, the average watershed streamflow increased from 6.21 m³/s in 1978 to 6.76 m³/s in 1998. In contrast, it increased from 6.76 m³/s in 1998 to 7.07 m³/s in 2017. Wet flow increased by 8.29%, 8.80%, and 4.63% between 1978 and 1988, 1978 and 1998, and 1998 and 2017. The wet season flow had generally risen from 6.21 m³/s in 1978 to 7.07 m³/s in 2017 by 13.84%. During the dry season, the average watershed streamflow decreased from 3.01 m³/s in 1978 to 2.78 m³/s in 1998. It was reduced by 7.61%. In comparison, it increased from 2.78 m³/s in 1998 to 3.29 m³/s in 2017 by 18.30%. The dry season flow had generally risen from 3.01 m³/s in 1978 to 3.29 m³/s in 2017. It was increased by 9.29%. The results show that the average annual streamflow increased by 8.12%, 9.07%, 14.77% between 1978 and 1988, 1978 and 1998, and 1978 and 2017 (Table 5.4). The maximum flow is observed during August and September at the end of the Kiremt Season in the watershed. The Kiremt season flow increased by 9.80% during the first half of the study period (1978-1998) and by 5.41% in the second half (1998-2017). It increased by 15.74% in 2017 compared to 1978. The observed changes in the streamflow have resulted from LU/LC changes involving reducing shrubland and grassland, expanding cultivation, and the built-up area in the TWW.

The result is in agreement with studies elsewhere in Ethiopia (Bewket and Sterk 2005; Getachew and Melesse 2012; Getahun and Van Lanen 2015; Tufa et al. 2015; Chakilu and Moges 2017; Gashaw et al. 2018; Welde and Gebremariam 2017), Africa (Yira et al. 2016), China (Yang et al. 2014), Pakistan (Younis and Ammar 2018), Thailand (Petchprayoon et al. 2010) and Nepal (Pokhrel 2018). Babar and Ramesh 2015 have stated that the conversion of forests to agricultural areas and increased built-up areas from 2003 to 2013 have affected India's Nathravathi river basin. Increased streamflow is expected in the watershed involving reducing shrubland and grassland during the expansion of cultivation and built-up. Typically, LU/LC change is influenced by human activities rather than natural events. Currently, agricultural expansion, fuelwood consumption, industry zone expansion, and urbanization are human-made activities, which cause LC/LU changes in TWW. Such changes can have a significant impact on the hydrology of the watershed. In general, the LU/LC changes, which had occurred from 1978 to 2017, had increased the annual streamflow by 14.77%. The result revealed that the LU/LC change had a dominant role in the watershed's

hydrological responses. This indicates an immediate need to control the LU/LC to ensure water availability in the watershed.

5.4 Closure

A significant amount of LU/LC changes occurred in the TWW in the study period. The expansion of cultivated and built-up areas and the withdrawal of shrubland, grassland, swampy, and water body were observed in the watershed during the entire study period. In general, the LU/LC changes, which occurred from 1978 to 2017, increased the annual streamflow by 14.77%. The result revealed that the LU/LC change had a dominant role in the watershed's hydrological responses. This indicates an immediate need to control the LU/LC to ensure water availability in the watershed.

CHAPTER 6:TREND AND VARIABILITY OF HYDRO-METEOROLOGICAL VARIABLES

6.1 General

In this section, the trend and variability of hydro-meteorological variables of TWW in southern Ethiopia have been presented and discussed. Many meteorological trend analyses studies have been conducted in Ethiopia, but no previous study was conducted with this study period in the watershed. This study attempts to fill this gap. The study used daily rainfall, maximum temperature, minimum temperature, and PET from 1978 to 2017 and streamflow from 1980 to 2002. The M-K trend test and Sen's slope estimator were used to examine the trend and magnitude of the changes, respectively. Also, the CV value was computed for variability analysis. PET was estimated by FAO-56 PM and Hargreaves models.

6.2 Rainfall Variability and Trend

Rainfall is one of the primary input climate variables for water resource planning and hydrological analysis. Table 6.1 describes the complete information about the four rain gauge stations used for the study. For the total yearly average rainfall and both Belg and Kiremt rainfall season, the lowest rainfall occurred at Shashemene in the northern portion of the watershed, while the highest annual average rainfall occurred over Haisawita in the southern portion of the watershed. Both yearly and seasonal rainfall depicted an increasing trend from the northern part to the watershed's southern part. Figure 6.1 describes the 40 years average annual rainfall of each station. Figure 6.2 shows the seasonal variation of precipitation in the TWW. The rainfall system in TWW is a bimodal type (Figure 6.2), where the primary rainy season (Kiremt) is led by a minor rainy season (Belg). In the study area, the contribution of Kiremt seasons for the total annual rainfall was very high across stations. The Belg rainfall also contributes a substantial amount to the total yearly rainfall of stations. For the case of TWW, 46.54%, 37.75%, and 15.75% of the annual rain are subsidized from Kiremt, Belg, and Bega rainfall, respectively (Figure 6.2). The variability of annual rainfall was lowest compared to the seasonal variations. Rainfall variability was highest for Bega (dry season) compared to Belg and Kiremt. The 40 years mean monthly rainfall

analysis uncovered that the minimum average monthly rainfall was recorded in December in all the measuring stations, whereas September received the maximum average rain in all the stations except Shashemene. Shashemene received the maximum average rainfall in August (Tables 6.2 to 6.5).

Table 6.1. Features of stations for measured rainfall

Station name	Latitude	Longitude	Altitude (m)	Area (km ²)	area in %	Average annual precipitation (mm)
Hawassa	7 ⁰ 3'51''	38 ⁰ 28'50''	1701	136.28	20.02	962.33
Haisawita	6 ⁰ 54'7''	38 ⁰ 33'32''	2249	209.94	30.83	1146.37
Shashemene	7 ⁰ 11'27''	38 ⁰ 35'30''	1943	32.28	4.74	894.58
wondogenet	7 ⁰ 2'52''	38 ⁰ 36'53''	1770	302.38	44.41	1087.29

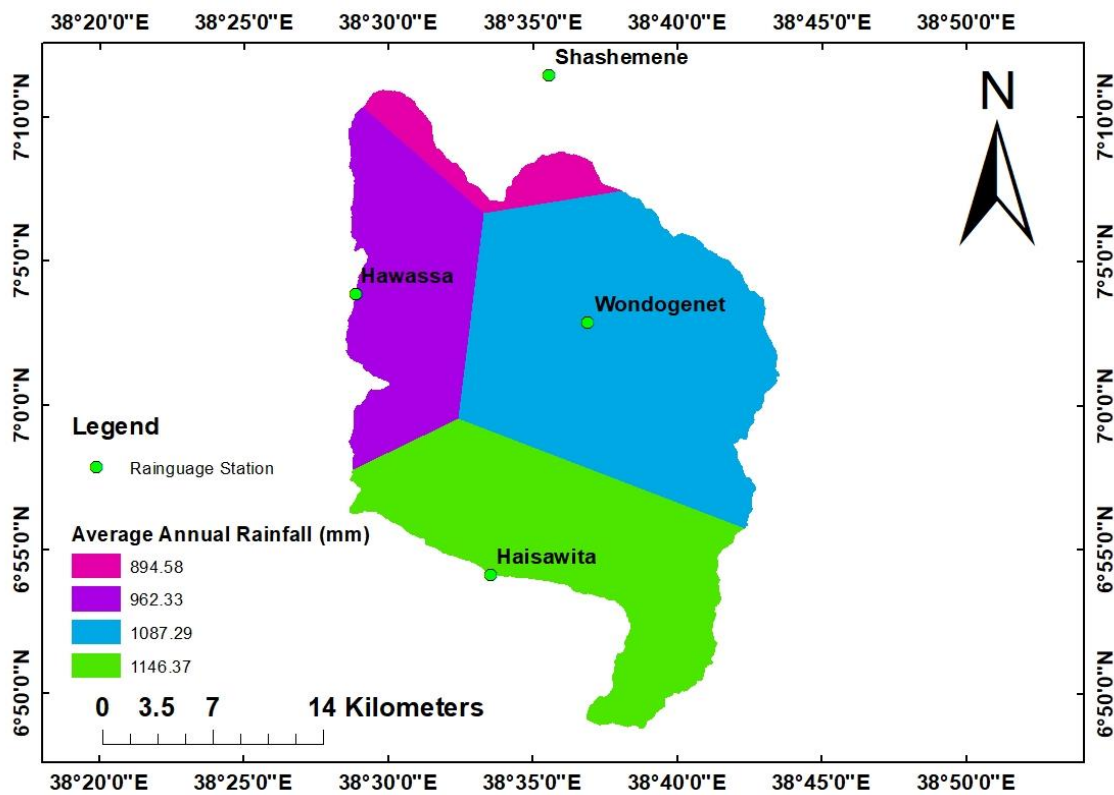


Figure 6.1. Average annual rainfall (mm) of each rain gauge station in TWW (1978-2017)

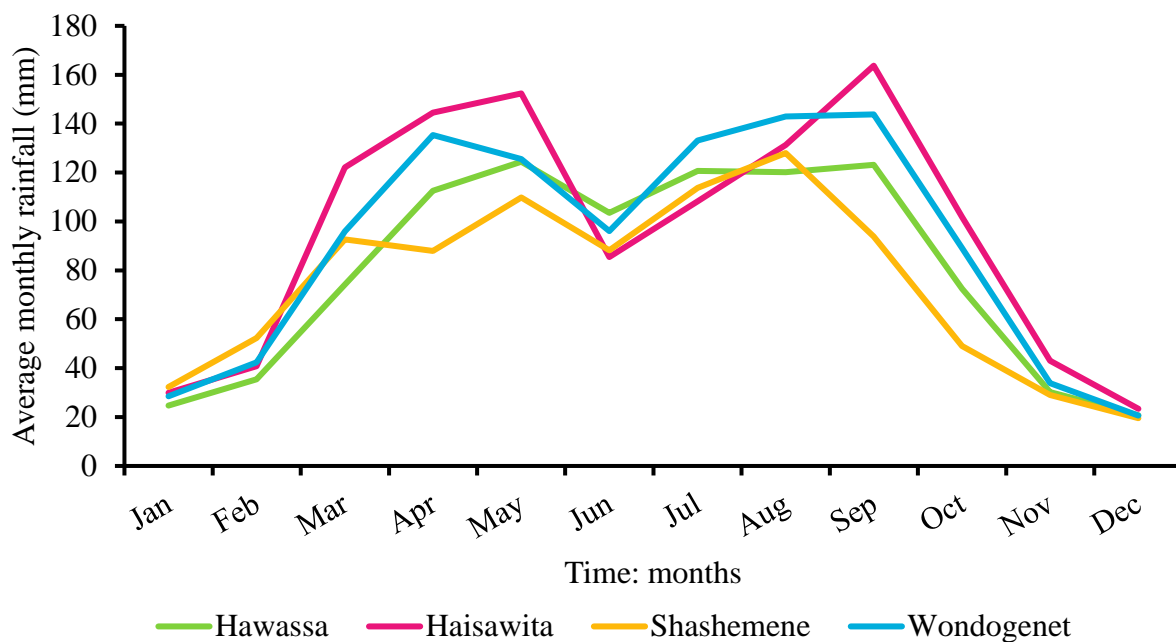


Figure 6.2. Seasonal distribution of rainfall in the watershed (1978-2017)

The M-K trend test results of Hawassa station shown, there is no statistically significant trend in all months, seasons, and the annual rainfall during the study period at a 0.05 level of significance. Nevertheless, insignificant rising and declining trends are observed at the Hawassa station of TWW (Table 6.2). Results revealed that annual rainfall showed negligible change for the study period. It increased only at the rate of 7.2 mm/decade. The yearly rainfall at Hawassa station varies from 670.90mm to 1197.90mm, with an average of 962.33mm. At this station minimum, monthly average rainfall was recorded during December, and the maximum monthly average rainfall was observed during May. 48.59% of the annual rainfall is contributed during the Kiremt season, and the rest, 36.02% and 15.39%, were subsidized from Belg and Bega seasons, respectively. Relatively less rainfall variability is observed in annual rainfall (CV=0.14), moderate variability in Kiremt (CV= 0.23) and Belg (CV=0.27) season, and high variability in dry (CV=0.47) season. Although in all the stations' understudy, annual rainfall was classified under low variability. Relatively less rainfall variability was observed at Hawassa compared to other stations (Tables 6.2 to 6.5). Belg season rainfall variability at Hawassa was moderate, while other stations showed high variability. A high variation of rainfall has been observed in the dry

season (October–January). This result indicates that the rain in the dry season is highly inconsistent and uncertain. Nevertheless, it is recognized that the dry season contributes nearly 15% of the annual rainfall. Figure 6.3 supports the M-K trend test and shows the interannual precipitation variability at Hawassa station in TWW.

Table 6.2. Summary statistics of Hawassa rainfall (1978-2017)

Variable	μ	σ	CV	τ	p-value	Sen's slope	Trend nature	Trend sig.
Oct	72.52	43.45	0.592	-0.08	0.49	-0.41	Negative	Not Sig.
Nov	30.20	32.68	1.068	0.14	0.21	0.28	Positive	Not Sig.
Dec	20.69	30.19	1.441	0.05	0.64	0.03	Positive	Not Sig.
Jan	24.74	27.96	1.116	0.11	0.34	0.08	Positive	Not Sig.
Feb	35.44	37.15	1.035	-0.13	0.24	-0.49	Negative	Not Sig.
Mar	74.16	42.63	0.568	0.05	0.63	0.28	Positive	Not Sig.
Apr	112.60	51.00	0.447	-0.12	0.28	-0.69	Negative	Not Sig.
May	124.43	58.40	0.463	0.11	0.33	0.97	Positive	Not Sig.
Jun	103.56	45.50	0.434	-0.10	0.38	-0.48	Negative	Not Sig.
Jul	120.71	37.10	0.303	0.06	0.62	0.26	Positive	Not Sig.
Aug	120.09	36.94	0.304	-0.01	0.96	-0.01	Negative	Not Sig.
Sep	123.21	46.94	0.376	-0.03	0.77	-0.18	Negative	Not Sig.
Bega	148.14	70.07	0.467	0.10	0.36	1.03	Positive	Not Sig.
Belg	346.62	93.35	0.266	0.04	0.74	0.57	Positive	Not Sig.
Kiremt	467.57	107.03	0.226	-0.03	0.77	-0.30	negative	Not Sig.
Annual	962.33	140.70	0.144	0.04	0.75	0.72	Positive	Not Sig.

Where μ =average; σ =standard deviation; CV= Coefficient of variance; τ = Kendall's tau; Not Sig. = not significant

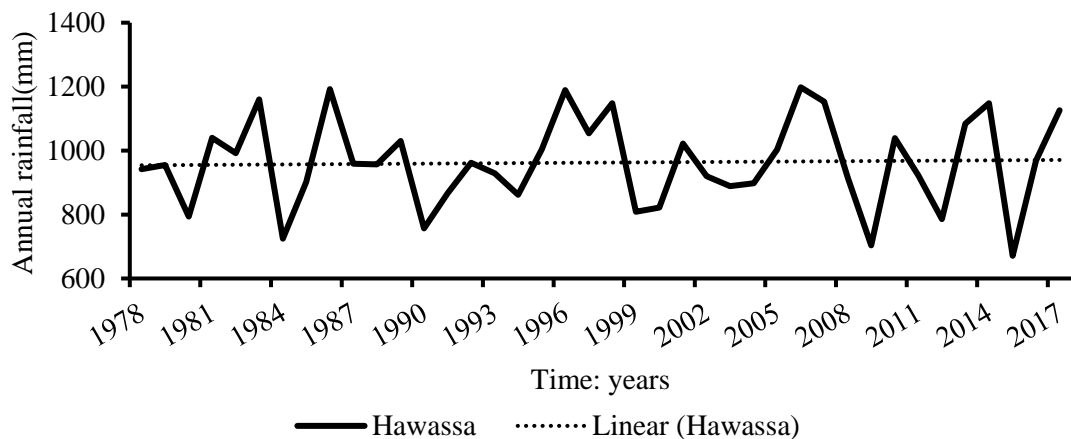


Figure 6.3. Trend and interannual variability of annual rainfall Hawassa (1978 -2017)

At Haisawita station, there is no statistically significant increasing/decreasing trend in all the months, seasons, and annual rainfall. Notwithstanding, rainfall shows an insignificant decreasing trend in Belg, Kiremt, and yearly rainfall at a rate of 16.8, 3.0, and 10.4 mm per decade, respectively (Table 6.3). The relatively maximum annual average rainfall was recorded at Haisawita station compared to other stations. The annual rainfall ranges from 810.10mm to 1494.90mm, with an average value of 1146.37mm. The Kiremt season contributes 42.62% of annual rainfall, with the remaining 40.09% and 17.27% coming from the Belg and Bega seasons, respectively. At this station minimum, monthly average rainfall was recorded during December, and the maximum monthly average rainfall was observed during September. Even though the CV value of all the months and seasons varies from moderate to high, annual rainfall is less variable (CV=0.17) at the station. Seasonally, Kiremt and Belg showed moderate variability, whereas the Bega showed a very high rainfall variability. Figure 6.4 strengthens the non-significant decreasing trend and shows the interannual variability of annual rainfall at Haisawita station.

Table 6.3. Summary statistics of Haisawita rainfall (1978-2017)

Variable	μ	σ	CV	τ	p-value	Sen's slope	Trend nature	Trend sig.
Oct	101.79	55.29	0.54	0.08	0.46	0.58	Positive	Not Sig.
Nov	42.97	28.43	0.65	0.12	0.26	0.50	Positive	Not Sig.

Dec	23.38	25.35	1.07	-0.12	0.30	-0.19	Negative	Not Sig.
Jan	29.89	33.90	1.12	0.01	0.92	0.00	positive	Not Sig.
Feb	40.77	31.65	0.77	-0.18	0.10	-0.72	Negative	Not Sig.
Mar	122.05	60.91	0.49	-0.10	0.36	-0.70	Negative	Not Sig.
Apr	144.52	62.02	0.42	-0.04	0.69	-0.32	Negative	Not Sig.
May	152.35	73.97	0.48	0.10	0.36	1.27	Positive	Not Sig.
Jun	85.47	42.01	0.49	-0.06	0.62	-0.19	Negative	Not Sig.
Jul	108.27	48.33	0.44	-0.08	0.46	-0.29	Negative	Not Sig.
Aug	131.21	49.45	0.37	0.01	0.90	0.12	Positive	Not Sig.
Sep	163.70	47.03	0.28	0.02	0.90	0.14	Positive	Not Sig.
Bega	198.03	71.34	0.36	0.11	0.32	1.20	Positive	Not Sig.
Belg	459.69	141.11	0.30	-0.08	0.45	-1.68	Negative	Not Sig.
Kirmt	488.65	111.07	0.22	-0.02	0.84	-0.30	Negative	Not Sig.
Annual	1146.37	199.65	0.17	-0.04	0.75	-1.04	Negative	Not Sig.

Where μ =average; σ =standard deviation; CV= Coefficient of variance; τ = Kendall's tau; Not Sig. = not significant

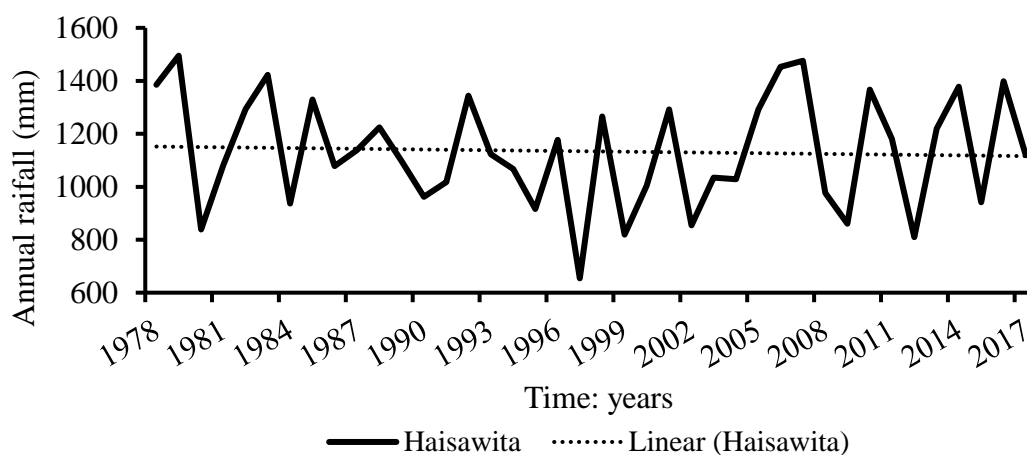


Figure 6.4. Trend and interannual variability of annual rainfall Haisawita

The maximum reduction rate is noticed at Shashemene station. Unlike other stations in TWW, the results of the M-K trend test at Shashemene station indicated a statistically significant decreasing trend at 0.05 significance level in both Belg and annual rainfall and a non-significant decreasing trend in Kiremt season (Table 6.4). The yearly rainfall at the station reduces at a rate of 49.3mm per decade. It is a

relatively high rate compared to other stations and areal weighted average annual rainfall. It is noted that this reduction in the annual rainfall was caused by a decline in the Belg season in the northern part of the watershed. Shashemene received a relatively minimum yearly average rainfall. Annual precipitation ranges from 627.80mm to 1234.20mm, with an average value of 894.58mm. 47.51% of the yearly rainfall is contributed during the Kiremt season, and the rest 38.15% and 14.54% were subsidized from Belg and Bega seasons, respectively. In terms of variability, both Kiremt and annual rainfall depict less variability (CV= 0.18), whereas rainfall is highly unpredictable with high CV values in Bega and Belg seasons. Compared to other stations, Kiremt rainfall at Shashemene exhibits relatively less variability. Figure 6.5 also supports the results obtained from the M-K trend test. At this station minimum, monthly average rainfall was recorded during December, and the maximum monthly average rainfall was observed during July.

Table 6.4. Summary statistics Shashemene rainfall (1978-2017)

Variable	μ	σ	CV	τ	<i>p</i> - value	Sen's slope	Trend nature	Trend sig.
Oct	49.11	43.65	0.88	0.25	0.03	1.60	Positive	Sig.
Nov	29.09	30.91	1.05	0.21	0.06	0.61	Positive	Not Sig.
Dec	19.54	21.62	1.09	-0.06	0.57	-0.04	Negative	Not Sig.
Jan	32.35	40.51	1.24	-0.23	0.05	-0.68	Negative	Sig.
Feb	53.19	51.74	0.96	-0.17	0.12	-1.02	Negative	Not Sig.
Mar	90.18	67.67	0.74	-0.26	0.02	-1.90	Negative	Not Sig.
Apr	89.29	54.90	0.61	-0.13	0.26	-0.77	Negative	Not Sig.
May	108.61	48.69	0.44	-0.02	0.84	-0.16	Negative	Not Sig.
Jun	88.95	41.69	0.46	-0.13	0.23	-0.70	Negative	Not Sig.
Jul	113.37	36.13	0.31	0.17	0.12	0.82	Positive	Not Sig.
Aug	128.10	41.99	0.32	-0.04	0.72	-0.18	Negative	Not Sig.
Sep	94.55	50.36	0.53	0.12	0.27	0.80	Positive	Not Sig.
Bega	130.08	68.08	0.52	0.16	0.15	1.42	Positive	Not Sig.
Belg	341.27	118.49	0.34	-0.35	0.00	-4.46	negative	Sig.

Kiremt	424.97	77.40	0.18	-0.01	0.95	-0.04	Negative	Not Sig.
Annual	894.58	159.19	0.18	-0.23	0.04	-4.93	Negative	Sig.

Where, μ =average; σ =standard deviation; CV = Coefficient of variance; τ = Kendall's tau; Sig. = Significant at 0.05 confidence level; Not Sig. = not significant

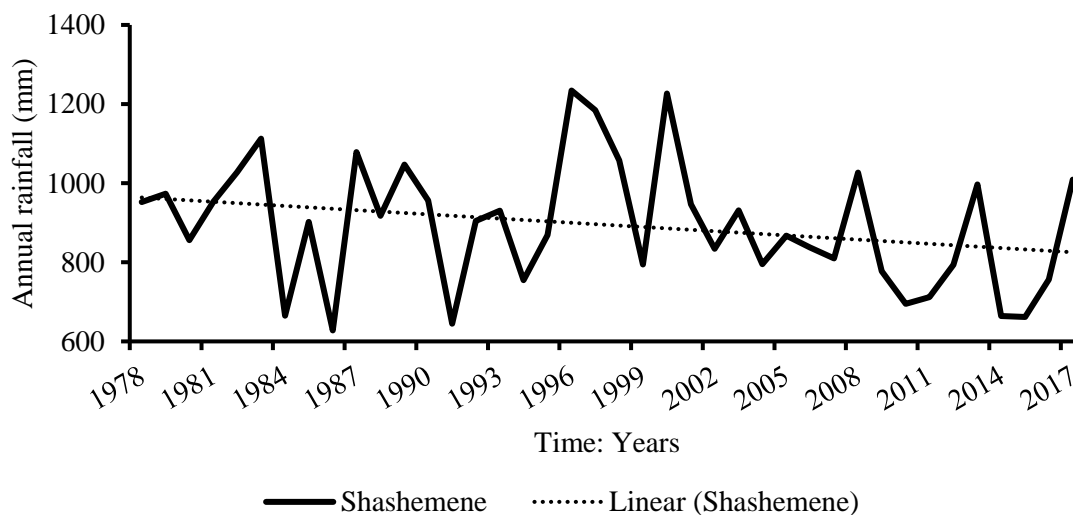


Figure 6.5. Trend and interannual variability of annual rainfall Shashemene

The Wondogent station showed a statistically insignificant downward trend in all the months except August for all seasons and annual rainfall (Table 6.5). Except for yearly and Kiremt rainfall, rainfall exhibited a high variability at Wondogent (Eastern part of the watershed) in all the months and seasons. At this station minimum, monthly average rainfall was recorded during December, and the maximum monthly average rainfall was observed during August. The Kiremt season contributes 47.44% of annual rainfall, with the remaining 36.73% and 15.83% subsidized from the Belg and Bega seasons, respectively. Annual precipitation ranges from 644.30mm to 1423.90mm, with an average of 1087.29mm at Wondogenet for the study period. Yearly rainfall variability was less compared to seasonal rainfall variability. While seasonal rainfall variability is high in Belg and Bega, annual and Kiremt rainfall variability is less to moderate, with CV values of 0.18 and 0.24, respectively. Figure 6.6 displays a decreasing trend and interannual variability of precipitation at the station.

Table 6.5. Summary statistics of Wondogenet Precipitation (1978-2017)

Variable	μ	σ	CV	τ	<i>p</i> -value	Sen's slope	Trend nature	Trend sig.
Oct	89.14	57.00	0.63	-0.13	0.25	-0.82	Negative	Not Sig.
Nov	33.85	39.27	1.15	-0.05	0.68	-0.08	Negative	Not Sig.
Dec	20.61	21.77	1.04	-0.13	0.23	-0.23	Negative	Not Sig.
Jan	28.51	31.21	1.08	-0.02	0.85	0.00	Negative	Not Sig.
Feb	42.44	41.82	0.97	-0.17	0.12	-0.77	Negative	Not Sig.
Mar	95.98	53.97	0.56	-0.14	0.21	-1.01	Negative	Not Sig.
Apr	135.38	65.73	0.48	-0.09	0.42	-0.80	Negative	Not Sig.
May	125.54	65.17	0.51	-0.03	0.77	-0.22	Negative	Not Sig.
Jun	96.07	51.48	0.53	-0.21	0.06	-1.27	Negative	Not Sig.
Jul	133.09	67.64	0.50	-0.05	0.63	-0.34	Negative	Not Sig.
Aug	142.92	47.13	0.33	0.11	0.32	0.69	Positive	Not Sig.
Sep	143.78	40.59	0.28	-0.06	0.59	-0.44	Negative	Not Sig.
Bega	172.11	90.12	0.52	-0.06	0.58	-0.72	Negative	Not Sig.
Belg	399.33	131.24	0.32	-0.18	0.10	-3.21	Negative	Not Sig.
Kiremt	515.85	126.49	0.24	-0.01	0.92	-0.18	Negative	Not Sig.
Annual	1087.29	194.21	0.18	-0.14	0.20	-3.54	Negative	Not Sig.

Where μ =average; σ =standard deviation; CV= Coefficient of variance; τ = Kendall's tau; Not Sig. = not significant

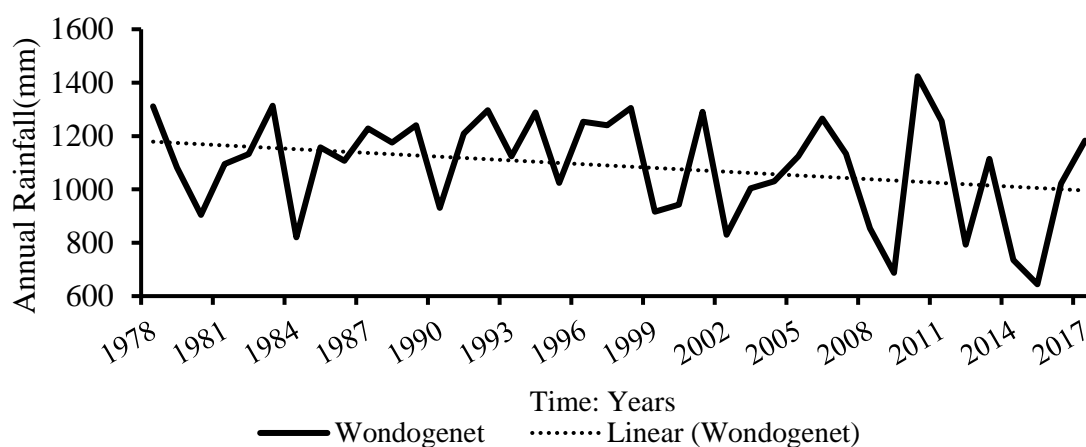


Figure 6.6. Trend and interannual variability of annual rainfall Wondogenet

The annual rainfall varies from 747.89mm to 1321.87mm at the watershed level, with a weighted average of 1071.35mm. The results depicted no statistically significant trend at the 0.05 level of confidence in the areal weighted average rainfall in TWW. However, the watershed's annual rainfall exhibited an insignificant declining trend of 20.8 mm/decade (Table 6.6). In general, there was no statistically significant change in yearly weighted average rainfall throughout the studied period in the watershed. This finding agrees with the report of the NMSA of Ethiopia. They reported that from 1951 to 2005, the annual rainfall average from 42 rain gauge stations over the entire country remained almost constant. Also, Bega rainfall showed more variability than Belg and Kiremt (NMSA 2007).

Overall the findings from this study are in close agreement with prior studies that analysed the rainfall trends in Ethiopia. The spatiotemporal dynamics of rainfall in Ethiopia were investigated by Cheung et al. (2008). They used historical rain gauge data from 134 stations in 13 basins from 1960 to 2002. They stated no notable change in the yearly rainfall at the country and watershed level in Ethiopia. Although there is a significant decline in Kiremt season rainfall in the country's central and southwestern parts, the Belg rainfall shows an insignificant increment with higher variability. Wagesho et al. (2013) examined the variability of seasonal and annual rainfall over Ethiopia based on 0.5° resolution gridded monthly rainfall data (381 grid points) for the duration of 1951 to 2000. The yearly and Kiremt rainfall showed significant decreasing trends in Ethiopia's western and northern portions, whereas an increasing annual rainfall trend was detected in a small area in eastern parts of Ethiopia.

Statistically, insignificant trends were observed in most regions (77%) of Ethiopia. In Ethiopia's highlands, Alemayehu and Bewket (2017) measured monthly rainfall trends (1883 to 2013). They found that both the Kiremt and annual rainfall show statistically insignificant rising trends, while Belg rainfall shows significant declining trends. Since 1982, yearly and Kiremt rainfall in southern, eastern, and south-western Ethiopia has decreased significantly (Seleshi and Zanke 2004). Admassu and Seid (2006) assessed the trend of rainfall over Ethiopia from 1973 to 2002. They reported that the annual total rainfall exhibits a statistically significant declining trend while

Belg rainfall does not show any significant trend in the analysis period. Abrha and Simhadri (2015) analyzed the monthly, seasonal, and annual rainfall trends in southern Tigray for 34 years (1978 to 2012). They reported a statistically significant increase in Kiremt rainfall in the area, while Belg rainfall exhibits an insignificant declining trend. Annual rainfall does not show any significant change in the area for the period. In West Africa (Benin), no significant annual rainfall trends were noticed from 1940 to 2015 (Ahokpossi 2018). Annual, seasonal, and monthly rainfall trends were examined in 30 subregions in India over the 1871–2005 years by Kumar et al. (2010). They concluded that rainfall exhibited a decreasing trend for the annual and monsoon season on the country's scale, whereas it showed an increasing trend in other seasons.

Figure 6.7 supports the decreasing but statistically insignificant trends of average annual rainfall in the TWW. The CV value is relatively low (CV=0.15), indicating no substantial annual yearly average rainfall variability in the watershed for the study period. In general, rainfall exhibited high variability in the Bega and Belg seasons, moderate variability in the Kiremt season, and annual rainfall showed less variability. In the Woleka watershed of Ethiopia, Asfaw et al. (2018) reported that the Kiremt and annual rainfall had declined significantly at a rate of 15mm and 13mm per/decade, respectively. As well, highly variable and erratic, but an insignificant declining trend of Belg rainfall was noted.

Table 6.6. Summary statistics of the areal weighted average annual rainfall of TWW (1978-2017)

Variable	μ	σ	CV	τ	<i>p</i> - value	Sen's slope	Trend nature	Trend sig.
Weighted average rainfall	1071.35	161.19	0.15	-0.13	0.26	-2.08	Negative	Not Sig.

Where μ =average; σ =standard deviation; CV= Coefficient of variance; τ = Kendall's tau

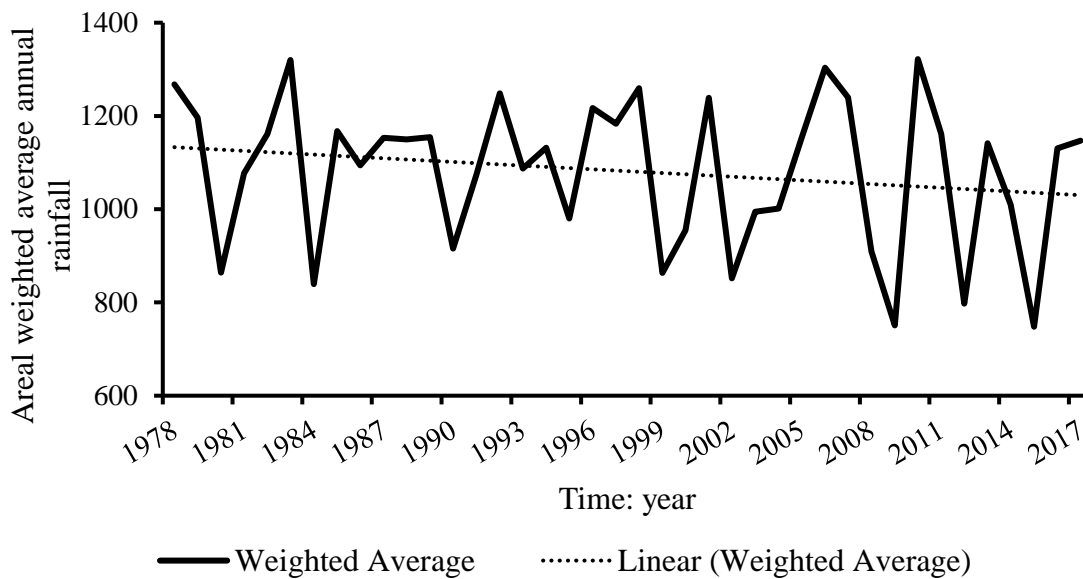


Figure 6.7. Trend and interannual variability of the areal weighted average annual rainfall of TWW

6.3 Temperature Variability and Trend

Temperature is the principal element of climate and usually helps to perceive the variation of climate. Temperature impacts the hydrological processes in a watershed. Trend analysis of temperature in TWW was conducted with daily minimum and maximum temperature data from 1978-2017. The result discovered a significantly rising trend for both minimum and maximum temperatures. The minimum temperature showed a more significant rising trend than the maximum at both stations (Hawassa and Haisawita). An increasing trend of both minimum and maximum monthly temperature at the Woleka watershed in Ethiopia was noted by Asfaw et al. (2018).

Figure 6.8 manifests Intra annual variation of temperature in TWW. The monthly average daily maximum temperature was relatively high in Bega and Belg at both stations and less in Kiremt. In contrast, the monthly average daily minimum temperature is higher in Kiremt compared to other seasons. The highest monthly average maximum daily temperature at both stations occurred during February, whereas the highest monthly average minimum daily temperature occurred during July and March, at Hawassa and Haisawita, respectively. Also, the lowest monthly

average maximum daily temperature occurred at both stations during July, whereas the lowest monthly average minimum daily temperature occurred during December.

Figure 6.9 illustrates the interannual variation in annual average minimum and maximum daily temperatures. Yearly average maximum daily temperature ranges from 21.67⁰C to 24.86⁰C with an average of 22.76⁰C at Haisawita station, and it ranges from 25.36⁰C to 28.56⁰C with an average of 27.22⁰C at Hawassa station. On the other hand, the yearly average minimum daily temperature varies from 10.31⁰C to 11.98⁰C, with an average value of 11.18⁰C at Haisawita station. It varies from 10.63⁰C to 14.89⁰C, with an average of 12.83⁰C at Hawassa station during the study period. In both cases, the temperature in Hawassa is higher than that of Haisawita. This implies that the watershed is warmer in the west and northwest portions than the south and southwest portions. Local increases and variability in temperature affect soil moisture and evapotranspiration. It, in turn, has associations to decide appropriate crop types and cropping calendars in the area.

Figure 6.10 markedly discloses that there has been a warming trend in the annual minimum and maximum temperature during the study period in the watershed. The M-K trend test revealed that seasons and yearly average daily minimum and maximum temperature exhibited a statistically significant rising trend in all seasons and annual average daily minimum and maximum temperature. The monthly average daily minimum, and maximum temperature also showed a statistically significant rising trend except for November, December and January for the case of maximum temperature. It is found that both the minimum and the maximum temperature have been increased intensely from 1978 to 2017. The average minimum temperature increased more rapidly than that of the average maximum temperature in TWW. The yearly average of daily minimum temperature in TWW has been rising by 0.36⁰C and 0.6⁰C per decade at Haisawita and Hawassa station, respectively (Table 6.7 and Table 6.8). Averaged over 40 stations in the country over the last 55 years (1951-2005) indicated that the temperature had been shown a warming trend due to ongoing climate change. The minimum temperature in Ethiopia has been increasing by about 0.37 ⁰C per decade (NMSA 2007). Nearly the same result is found at Haisawita station in TWW. The yearly average daily maximum temperature increases with the

magnitude of 0.4 and 0.45⁰C per decade at Hawassa and Haisawita stations, respectively (Table 6.8 and Table 6.10). Although both minimum and maximum temperatures showed an increasing trend, their variability is considerably less in all months, seasons, and years (Tables 6.7 to 6.10).

The result of the temperature trend analysis is consistent with the results of previous researchers in the country. In the Ethiopian context, several researchers have reported an increase in temperature. Jury and Funk (2013) evaluated the long-term (1948 to 2006) temperature trend over Ethiopia. They observed that the temperature increases (0.3 °C per ten years) across most of Ethiopia. A rise in temperature and PET were recognized in Belg throughout 1987-2007 in Ethiopia's highlands (Resoll 2011). Both the maximum and minimum temperatures exhibited a statistically significant warming trend across Ethiopia's central highlands from 1981 to 2011, as Alemayehu and Bewket (2017) testified. Variability and trend of the seasonal and yearly temperature of the UBNRB in Ethiopia were investigated from 1981 to 2010 by Mengistu et al. (2014). Annually, both the minimum and maximum temperatures exhibited a statistically significant warming trend in the area except in the basin's small western side. In general, they concluded that the mean maximum temperature is augmented at a lower speed than that of the minimum temperature, and there is no statistically significant trend in yearly precipitation in the Basin.

In Africa (IPCC 2014) and worldwide (Rosmann et al. 2016), temperature data sets have shown an increasing trend. On a global scale, the rise in temperatures is undeniable. Xu et al. (2004) detected a rising trend in temperature in China from 1955 to 2000. A recent study by Forootan (2019) shows an increasing trend in temperature in the central part of Iran. A rising temperature was detected in India (Kumar et al. 2010; Wani et al. 2017).

From the present trend analysis, it can be concluded that there is a tendency to increment in temperature. It may occur because of the effect of global change. The increasing trend in temperature can lead to weather extremes like a drought in the watershed. Therefore, it is recommended that temperature variability be monitored to reduce its adverse impacts on the watershed's productivity.

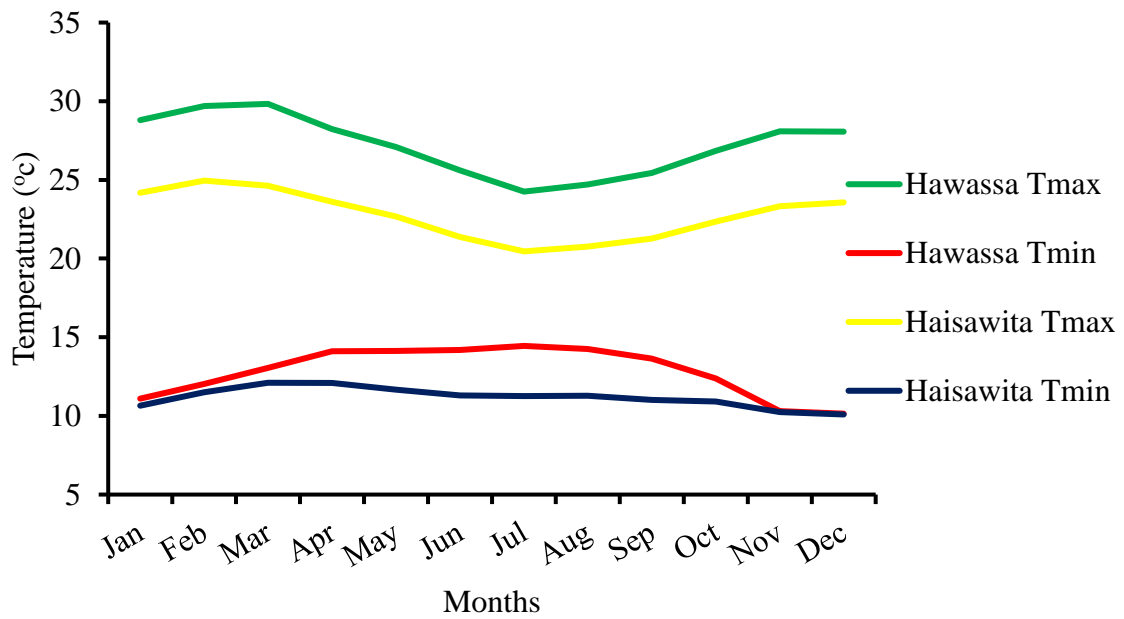


Figure 6.8. Trend and intra-annual variability of temperature in TWW

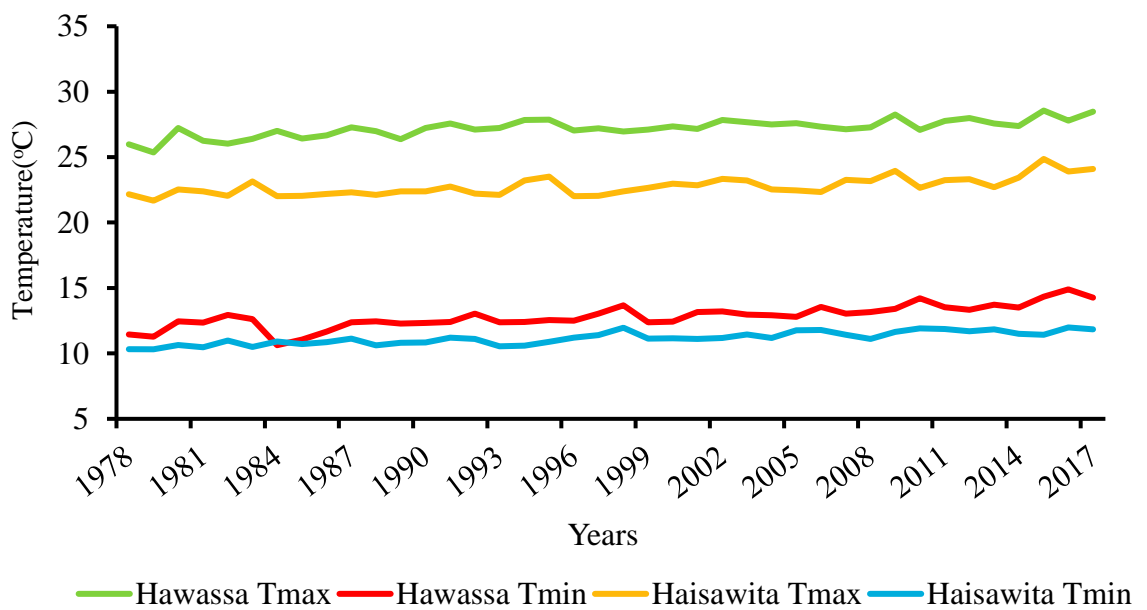


Figure 6.9. Trend and Interannual variability of temperature in TWW

Table 6.7. Summary statistics of Hawassa minimum temperature (1978-2017)

Variable	μ	σ	CV	τ	p-value	Sen's slope	Trend nature	Trend sig.
Oct	12.39	1.55	0.12	0.46	< 0.0001	0.08	Positive	Sig.
Nov	10.31	1.78	0.17	0.54	< 0.0001	0.10	Positive	Sig.
Dec	10.14	1.71	0.17	0.36	0.00094	0.08	Positive	Sig.
Jan	11.09	1.61	0.14	0.31	0.00463	0.07	Positive	Sig.
Feb	12.04	1.57	0.13	0.24	0.02876	0.05	Positive	Sig.
Mar	13.04	1.37	0.10	0.32	0.00358	0.05	Positive	Sig.
Apr	14.11	0.93	0.07	0.30	0.00567	0.03	Positive	Sig.
May	14.13	1.04	0.07	0.46	< 0.0001	0.06	Positive	Sig.
Jun	14.19	0.81	0.06	0.48	< 0.0001	0.05	Positive	Sig.
Jul	14.45	0.97	0.07	0.59	< 0.0001	0.05	Positive	Sig.
Aug	14.26	0.83	0.06	0.62	< 0.0001	0.06	Positive	Sig.
Sep	13.65	0.91	0.07	0.65	< 0.0001	0.07	Positive	Sig.
Bega	10.98	1.25	0.11	0.61	< 0.0001	0.09	Positive	Sig.
Belg	13.33	0.99	0.07	0.37	0.00054	0.04	Positive	Sig.
Kiremt	14.14	0.76	0.05	0.71	< 0.0001	0.06	Positive	Sig.
Annual	12.82	0.89	0.07	0.67	< 0.0001	0.06	Positive	Sig.

Where, μ =average; σ =standard deviation; CV= Coefficient of variance; τ = Kendall's tau; Sig. = Significant at 0.05 confidence level

Table 6.8. Summary statistics of Hawassa maximum temperature (1978-2017)

Variable	μ	σ	CV	τ	p-value	Sen's slope	Trend nature	Trend sig.
Oct	26.837	1.009	0.037	0.32	0.00372	0.04	Positive	Sig.
Nov	28.082	0.983	0.035	0.18	0.10578	0.02	Positive	Not Sig.
Dec	28.070	0.782	0.027	0.10	0.38218	0.01	Positive	Not Sig.
Jan	28.799	0.847	0.029	0.23	0.03298	0.03	Positive	Sig.
Feb	29.696	1.266	0.042	0.32	0.00305	0.05	Positive	Sig.
Mar	29.833	1.365	0.045	0.28	0.00943	0.05	Positive	Sig.

Apr	28.223	1.494	0.052	0.37	0.00083	0.07	Positive	Sig.
May	27.084	0.873	0.032	0.35	0.00122	0.04	Positive	Sig.
Jun	25.606	0.948	0.037	0.42	0.00011	0.05	Positive	Sig.
Jul	24.255	1.041	0.042	0.60	< 0.0001	0.07	Positive	Sig.
Aug	24.708	0.807	0.032	0.48	< 0.0001	0.05	Positive	Sig.
Sep	25.450	0.831	0.032	0.38	0.00037	0.04	Positive	Sig.
Bega	27.947	0.695	0.025	0.27	0.01245	0.02	Positive	Sig.
Belg	28.709	0.907	0.031	0.50	< 0.0001	0.06	Positive	Sig.
Kiremt	25.005	0.779	0.031	0.58	< 0.0001	0.05	Positive	Sig.
Annual	27.220	0.672	0.024	0.56	< 0.0001	0.04	Positive	Sig.

Where μ =average; σ =standard deviation; CV= Coefficient of variance; τ = Kendall's tau; Not Sig. = not significant; Sig. = significant at 0.05 confidence level

Table 6.9. Summary statistics of Haisawita minimum temperature (1978-2017)

Variable	μ	σ	CV	τ	p-value	Sen's slope	Trend nature	Trend sig.
Oct	10.923	0.640	0.058	0.438	< 0.0001	0.034	Positive	Sig.
Nov	10.236	0.665	0.064	0.538	< 0.0001	0.041	Positive	Sig.
Dec	10.090	0.643	0.063	0.250	0.02308	0.020	Positive	Sig.
Jan	10.642	0.867	0.080	0.405	0.000167	0.043	Positive	Sig.
Feb	11.495	0.917	0.079	0.374	0.000541	0.039	Positive	Sig.
Mar	12.106	0.845	0.069	0.371	0.000759	0.029	Positive	Sig.
Apr	12.088	0.689	0.056	0.386	0.000453	0.036	Positive	Sig.
May	11.676	0.739	0.062	0.357	0.001198	0.034	Positive	Sig.
Jun	11.304	0.738	0.064	0.507	< 0.0001	0.043	Positive	Sig.
Jul	11.254	0.626	0.055	0.652	< 0.0001	0.042	Positive	Sig.
Aug	11.274	0.584	0.051	0.353	0.001354	0.023	Positive	Sig.
Sep	11.021	0.638	0.057	0.614	< 0.0001	0.041	Positive	Sig.
Bega	10.473	0.512	0.048	0.585	< 0.0001	0.034	Positive	Sig.
Belg	11.841	0.617	0.051	0.446	< 0.0001	0.035	Positive	Sig.
Kiremt	11.213	0.537	0.047	0.651	< 0.0001	0.036	Positive	Sig.
Annual	11.176	0.488	0.043	0.649	< 0.0001	0.036	Positive	Sig.

Where μ =average; σ =standard deviation; CV= Coefficient of variance; τ = Kendall's tau; Sig. = significant at 0.05 confidence level

Table 6.10. Summary statistics of Haisawita maximum temperature

Variable	μ	σ	CV	τ	p-value	Sen's slope	Trend nature	Trend sig.
Oct	22.348	1.027	0.045	0.304	0.005754	0.043	Positive	Sig.
Nov	23.333	1.055	0.045	0.205	0.063793	0.024	Positive	Not Sig.
Dec	23.577	0.751	0.031	0.036	0.754742	0.003	Positive	Not Sig.
Jan	24.171	0.918	0.037	0.104	0.345273	0.010	Positive	Not Sig.
Feb	24.956	1.281	0.051	0.300	0.006109	0.049	Positive	Sig.
Mar	24.630	1.478	0.059	0.402	0.000265	0.074	Positive	Sig.
Apr	23.610	1.221	0.051	0.364	0.000781	0.057	Positive	Sig.
May	22.678	0.945	0.041	0.241	0.028474	0.030	Positive	Sig.
Jun	21.372	1.004	0.046	0.341	0.001938	0.045	Positive	Sig.
Jul	20.457	1.023	0.049	0.315	0.00387	0.046	Positive	Sig.
Aug	20.758	0.884	0.042	0.426	< 0.0001	0.035	Positive	Sig.
Sep	21.263	1.001	0.047	0.526	< 0.0001	0.056	Positive	Sig.
Bega	23.357	0.710	0.030	0.226	0.040992	0.021	Positive	Sig.
Belg	23.969	0.884	0.036	0.531	< 0.0001	0.055	Positive	Sig.
Kiremt	20.963	0.869	0.041	0.469	< 0.0001	0.045	Positive	Sig.
Annual	22.763	0.692	0.030	0.521	< 0.0001	0.041	Positive	Sig.

Where μ =average; σ =standard deviation; CV= Coefficient of variance; τ = Kendall's tau; Not Sig. = not significant; Sig.= significant at 0.05 confidence level

6.4 Streamflow Variability and Trend

Historical streamflow data is the most critical factor in planning and designing water resource projects. The decisions on water resources management and policies could be affected by recognizing a trend in streamflow. As a contribution to evaluating streamflow in the Ethiopian highlands in semi-humid areas, monthly, seasonal and annual discharge trends were recognized for one station at the outlet in the downstream parts of the TWW. Table 6.11 depicted that yearly streamflow showed a

statistically significant increasing trend in TWW. Twenty-three years' average monthly maximum streamflow was recorded during October, and the average monthly minimum streamflow was measured during February. The Tikur Wuha River's streamflow has increased by as much as 21.16MCM per decade in the watershed.

A decrease in streamflow in the absence of a significant rainfall trend resulting from human interventions was detected in Iran (Forootan 2019) and China (Xu et al. 2004; Wang et al. 2009). Wang et al. (2009) study the impact and relative importance of climate variations and human activities on China's runoff. They concluded that human activities such as change of LU/LC have relatively more impacts on runoff than climate. A report from Nepal shows the annual rainfall displaying an increasing trend, whereas runoff displays a decreasing trend (Pal et al. 2017). Casimiro et al. (2012) also detected the change in runoff from 1969 to 2004 in Peru with no rainfall variation. They believed anthropogenic activities might have changed runoff in the region. In Ethiopia, Mulu and Dwarakish (2016) noticed an increase in streamflow by about 10.9% from 2001 to 2008 compared to 1993 to 2000 due to a change in LU/LC. Streamflow is affected by several factors, such as rainfall variability and human interventions (Hassaballah et al. 2017). As stated above, human intervention, especially LU/LC change, plays a significant role in these changes.

From the investigation results, we noticed that the streamflow shows a rising trend without a precipitation trend. Previous studies in the area associated the increasing runoff pattern with a significant change in LU/LC in the watershed resulting from urbanization and deforestation. There was a small lake (Lake Cheleleka, 12 km²) in the upstream portion of the watershed. Lake Cheleleka was filled with silt through time due to soil erosion, and it changed into marshland and grassland. The water previously stored in Lake Cheleleka flows to the Tikur Wuha River (Water Works Design and Supervision Enterprise [WWDSE] 2001; Gebreegziabher 2004; MoWR 2008). In addition to these, there are many discharges of wastewater from several newly constructed industries in the river's urban sites. It may be one of the reasons for the increasing trend of streamflow in TWW. Recently built urban drainage toward the river from Hawassa city is maybe another reason for the increments in streamflow of

TWW. However, the increasing streamflow trend without the corresponding increase in rainfall in the study area needs further investigation.

Tikur Wuha River is the only permanent river that fed Lake Hawassa. It subsidizes an average of 78.483MCM of water per year to the Lake (Table 6.11). The trend and variability of the streamflow and runoff of the Tikur Wuha River directly link with the water balance and lake level rise of Lake Hawassa. Previous studies about the water balance of Lake Hawassa and Lake level reported that the level of the lake Hawassa showed an increasing trend (WWDSE 2001; Gebreegziabher 2004; MoWR 2008). They associated it with climate change, land-use change, and lake sedimentation due to water erosion. Streamflow and runoff variability were very high during the Belg season and moderated in all other seasons. Interannual variability was moderate during the study period. Streamflow is affected by several factors, such as rainfall variability and human interventions (Mulu and Dwarakish 2016; Hassaballah et al. 2017). Figure 6.10 displayed the increasing trend and interannual variability of streamflow in the study area.

Table 6.11. Summary statistics of streamflow TWW (1978-2017)

Variable	μ	σ	CV	τ	<i>p</i>-value	Sen's slope	Trend nature	Trend sig.
Oct	10.318	2.033	0.193	0.130	0.403319	0.062	Positive	Not Sig.
Nov	8.143	2.729	0.328	0.594	< 0.0001	0.339	Positive	Sig.
Dec	7.009	3.018	0.421	0.650	< 0.0001	0.369	Positive	Sig.
Jan	5.686	2.895	0.498	0.731	< 0.0001	0.362	Positive	Sig.
Feb	4.368	2.429	0.544	0.660	< 0.0001	0.250	Positive	Sig.
Mar	4.543	2.452	0.528	0.621	< 0.0001	0.249	Positive	Sig.
Apr	4.776	2.364	0.484	0.549	0.000138	0.205	Positive	Sig.
May	6.496	2.373	0.357	0.518	0.000364	0.261	Positive	Sig.
Jun	7.318	2.610	0.349	0.455	0.002032	0.209	Positive	Sig.
Jul	7.667	2.254	0.288	0.478	0.001103	0.182	Positive	Sig.
Aug	8.503	2.115	0.243	0.281	0.064601	0.119	Positive	Not Sig.
Sep	9.342	1.992	0.209	0.063	0.672503	0.034	Positive	Not Sig.

Bega	31.157	9.283	0.291	0.684	< 0.0001	1.207	Positive	Sig.
Belg	20.183	8.700	0.422	0.605	< 0.0001	0.955	Positive	Sig.
kiremt	32.829	7.615	0.227	0.383	0.010247	0.533	Positive	Sig.
Annual	78.483	20.271	0.253	0.684	< 0.0001	2.116	Positive	Sig.

Where, μ =average; σ =standard deviation; CV= Coefficient of variance; τ = Kendall's tau; Not Sig. = not significant; Sig. = significant at 0.05 confidence level

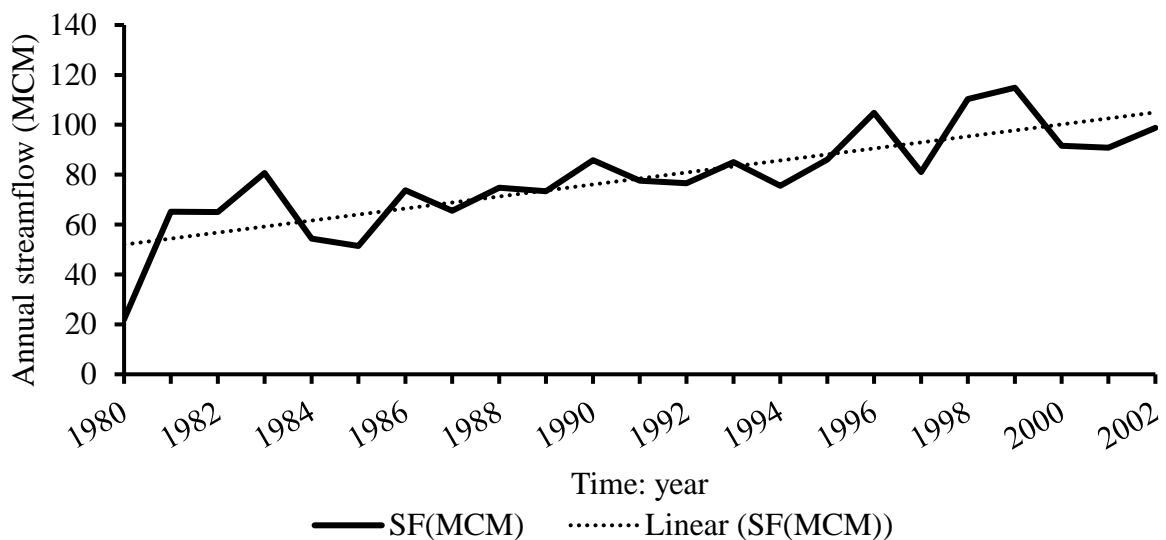


Figure 6.10. Trend and inter-annual variability of streamflow and runoff in TWW

6.5 PET Variability and Trend

The variability and trend analysis of the PET was carried out in the watershed. The results are presented in Table 6.12 and Table 6.13. At Hawassa, there is no statistically significant trend in annual and seasonal PET. However, it showed an insignificant increasing trend for annual, Belg, and Kiremt seasons and a decreasing trend for the dry season (Table 6.12). A statistically significant rising trend was detected during July, whereas insignificant increasing and decreasing trends were observed in all other months. PET increases at a 5.03, 2.44, and 6.48 mm/decade rate during annual, Kiremt and Belg, respectively.

At Haisawita, except for two months in the dry season (December and January), PET exhibits an increasing trend in all the other months. It showed insignificant increments

in the Bega and Kiremt seasons, whereas in Belg, it displayed a statistically significant rising trend. Annual PET exhibited a statistically significant increasing trend by the magnitude of 20.74 mm per decade (Table 6.13). In general, PET shows a rising tendency in the TWW. The magnitude of the trend points out that the increment rate of PET was more rapid at Haisawita than at Hawassa. The increasing trend in PET may be due to the rising temperature in the study period. A slight difference in PET at different stations (Hawassa and Haisawita) in TWW may arise from the different methods employed in computing the PET, and it may be from the slight temperature difference. Figure 6.11 presents both the trend and variability of PET in TWW in the study area. Very less PET variability with a CV value of less than 7% was observed in both stations' months and seasons. Interannual variability is also very less.

Table 6.12. Summary statistics Hawassa PET (1978-2017).

Variable	μ	σ	CV	τ	<i>p</i> - value	Sen's slope	Trend nature	Trend sig.
Oct	121.150	6.746	0.055	0.026	0.826	0.019	Positive	Not Sig.
Nov	119.950	6.566	0.054	-0.179	0.106	-0.133	Negative	Not Sig.
Dec	120.588	5.541	0.045	-0.249	0.024	-0.166	Negative	Not Sig.
Jan	126.666	6.231	0.049	-0.085	0.452	-0.075	Negative	Not Sig.
Feb	126.892	8.124	0.063	0.108	0.336	0.156	Positive	Not Sig.
Mar	144.793	9.334	0.064	0.044	0.703	0.075	Positive	Not Sig.
Apr	129.916	8.776	0.067	0.256	0.020	0.279	Positive	Not Sig.
May	125.624	6.092	0.048	0.046	0.685	0.029	Positive	Not Sig.
Jun	111.973	5.213	0.046	0.118	0.291	0.081	Positive	Not Sig.
Jul	106.902	5.607	0.052	0.249	0.024	0.181	Positive	Sig.
Aug	112.338	4.527	0.040	0.133	0.232	0.082	Positive	Not Sig.
Sep	113.619	4.266	0.037	-0.064	0.571	-0.041	Negative	Not Sig.
Bega	488.355	18.647	0.038	-0.159	0.153	-0.391	Negative	Not Sig.
Belg	527.225	21.364	0.040	0.213	0.054	0.648	Positive	Not Sig.
Kiremt	444.831	14.007	0.031	0.154	0.167	0.244	Positive	Not Sig.
Annual	1460.411	39.895	0.027	0.097	0.385	0.503	Positive	Not Sig.

Where μ =average; σ =standard deviation; CV= Coefficient of variance; τ = Kendall's tau; Not Sig. = not significant; Sig. = significant at 0.05 confidence level

Table 6.13. Summary statistics of Haisawita PET (1978-2017)

Variable	μ	σ	CV	τ	p-value	Sen's slope	Trend nature	Trend sig.
Oct	120.539	7.786	0.064	0.167	0.134	0.128	Positive	Not Sig.
Nov	118.446	6.606	0.055	0.064	0.571	0.063	Positive	Not Sig.
Dec	120.362	5.179	0.042	-0.041	0.720	-0.031	Negative	Not Sig.
Jan	125.450	6.802	0.054	-0.062	0.586	-0.053	Negative	Not Sig.
Feb	123.974	8.903	0.071	0.177	0.111	0.232	Positive	Not Sig.
Mar	138.374	10.019	0.071	0.336	0.002	0.426	Positive	Sig.
Apr	127.783	8.727	0.067	0.251	0.022	0.269	Positive	Sig.
May	123.614	7.674	0.061	0.063	0.568	0.073	Positive	Not Sig.
Jun	109.173	6.981	0.063	0.141	0.206	0.150	Positive	Not Sig.
Jul	106.937	7.595	0.070	0.133	0.232	0.133	Positive	Not Sig.
Aug	112.135	6.504	0.057	0.228	0.039	0.179	Positive	Sig.
Sep	113.209	6.444	0.056	0.295	0.007	0.225	Positive	Sig.
Bega	484.797	19.264	0.039	0.044	0.703	0.125	Positive	Not Sig.
Belg	513.745	23.711	0.046	0.356	0.001	1.095	Positive	Sig.
Kiremt	441.454	23.315	0.052	0.177	0.111	0.567	Positive	Not Sig.
Annual	1439.996	52.549	0.036	0.279	0.011	2.074	Positive	Sig.

Where μ =average; σ =standard deviation; CV= Coefficient of variance; τ = Kendall's tau; Not Sig. = not significant; Sig. = Significant at 0.05 confidence level

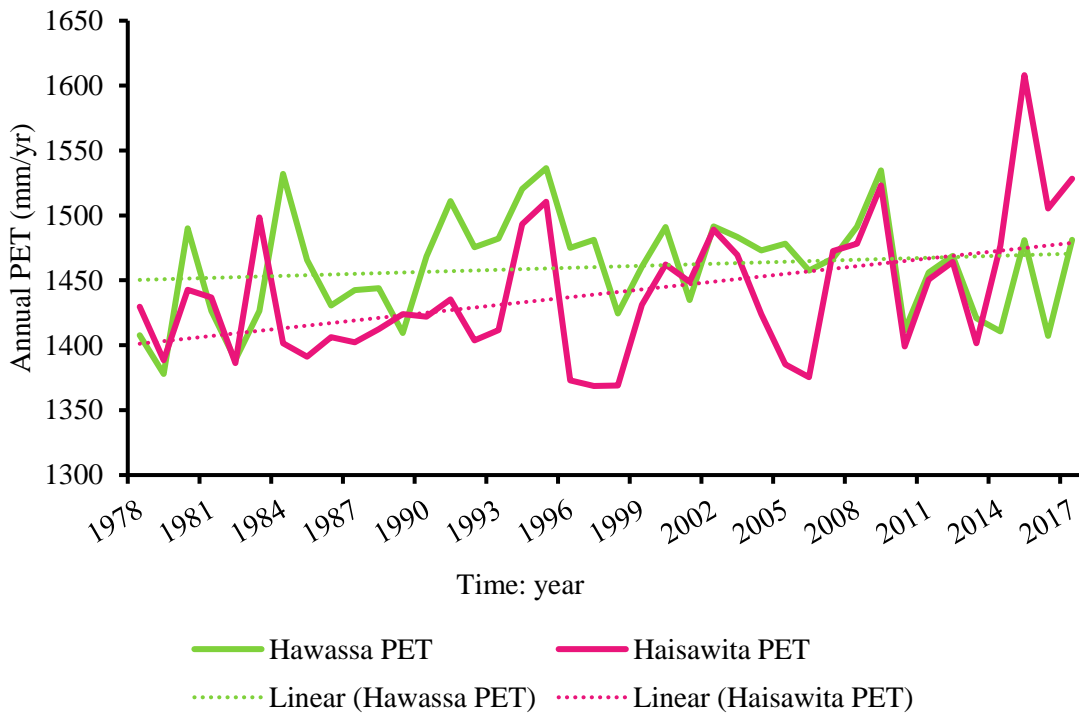


Figure 6.11. Trend and interannual variability of PET in TWW

6.6 Closure

From the present trend analysis result, it can be concluded that there is no statistically significant trend at the 0.05 level of confidence in the average annual rainfall in TWW. However, the watershed's annual rainfall exhibited an insignificant declining trend. The results depicted markedly disclose that there has been a warming trend in the minimum and maximum temperature during the study period in the watershed. The average minimum temperature raised more rapidly than that of the average maximum temperature. The streamflow was found to be increased by as much as 21.16MCM per decade in the watershed. PET exhibits an increasing tendency in the TWW.

CHAPTER 7: WATERSHED PRIORITIZATION FOR CONSERVATION ACTIVITIES

7.1 General

In this section, the USLE factors are determined, and the corresponding raster maps were developed. The average soil loss rate was estimated, and SLR was reclassified. The priority watersheds were recognized for SWC activities based on the magnitude of the SLR. The detail of the dataset and methodology employed was found in chapter three.

7.2 USLE Factors Determined

7.2.1 R-factor

Based on the rainfall data from four meteorological stations in and near the watershed for 40 years from 1978 to 2017, the yearly average rainfall was 1071.35mm. The annual rainfall and rainfall erosivity of the area and each station's contribution to TWW are summarized in Table 7.1. Figure 7.1 indicates the 40 years average yearly rainfall amount and its spatial variation in the TWW. Figure 7.2 displays the spatial variation of the R-factor of TWW.

The R-factor ranges from 530.78 MJ mm ha⁻¹ hr⁻¹yr⁻¹ to 633.85 MJ mm ha⁻¹ hr⁻¹yr⁻¹ with an average value of 591.84 MJ mm ha⁻¹ hr⁻¹yr⁻¹. It is highest at Haisawita and relatively low at Shashemene. This value of the R-factor is less compared to the report by Andriyanto et al. 2015. Andriyanto et al. 2015 reported R-factor from 980 to 1439 MJ MJ mm ha⁻¹ hr⁻¹yr⁻¹ in the Kalikato watershed in Indonesia. This significant difference in R-factor arises from the high yearly average rainfall value of 2509mm in the area. The result is high compared to Brhane and Mekonen 2009. They reported R-factor 357 MJ mm ha⁻¹ hr⁻¹yr⁻¹ at Medego Watershed, Northern Ethiopia.

Table 7.1. Annual rainfall and the R-factor of TWW

Station name	Altitude (m)	Latitude	Longitude	Area (km ²)	Area (%)	Yearly average rainfall (mm)	R-factor
Hawassa	1701	7°03'	38°28'	136.28	20.02	962.33	530.78
Haisawita	2249	6°54'	38°33'	209.94	30.83	1146.37	633.85
Shashemene	1943	7°11'	38°35'	32.28	4.74	894.58	492.84
Wondogenet	1770	7°20'	38°36'	302.38	44.41	1087.29	600.76
Average						1071.35	591.84

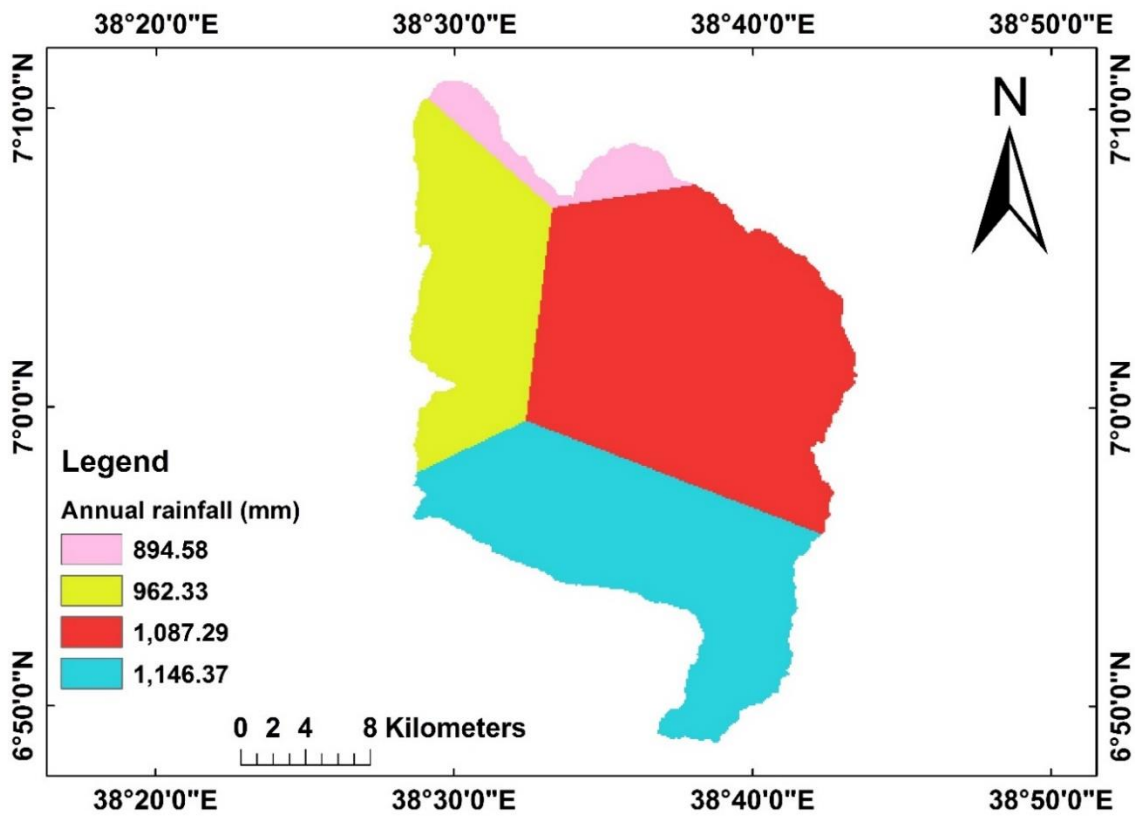


Figure 7.1. Annual rainfall map of TWW

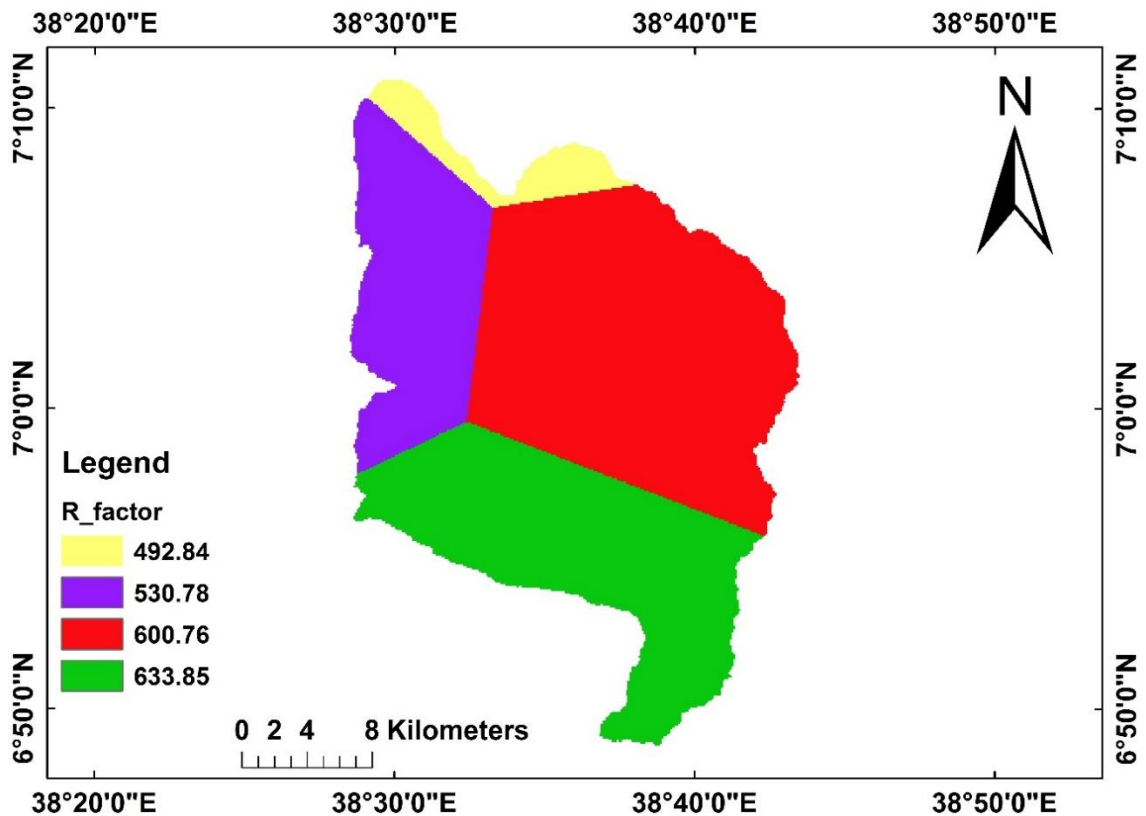


Figure 7.2. Rainfall erosivity map of TWW

7.2.2 K-factor

Table 7.2 revealed the K-factors for each soil class with the corresponding soil type with a percentage of the area in TWW. Figure 7.3 displays the value of the K-factor and its spatial pattern in the TWW. The K-factor of TWW ranges from 0.000 to 0.026 t hr MJ⁻¹mm⁻¹. Panagos et al. (2012) assessed the K-factor for Europe, relying on 22,000 soil samples collected within Europe. They found that the K-factor of USLE ranges from 0.013 to 0.087 t hr MJ⁻¹mm⁻¹, with a mean of 0.041 t hr MJ⁻¹mm⁻¹ in the SI unit. The K-factor values in China are concentrated in the ranges between 0.0229 and 0.0457 t hr MJ⁻¹mm⁻¹, with an average of 0.0321 in the SI unit (Wang et al. 2016). The K-factor of TWW is in the range of other results elsewhere (Panagos et al. 2012; Wang et al. 2016). Compared to studies in Ethiopia (Bewket and Teferi 2009; Brhane and Mekonen 2009; Amsalu and Mengaw 2014), the K-factor value is relatively less. Both Bewket and Teferi (2009) and Amsalu and Mengaw (2014) reported K-factors ranging from 0.15 to 0.25 t hr MJ⁻¹mm⁻¹ in Ethiopia. Brhane and Mekonen (2009) revealed the K-factor ranging from 0.15 to 0.30 t hr MJ⁻¹mm⁻¹ at Medego Watershed,

Northern Ethiopia. Ashiagbor et al. 2013, showed the K-factor values up to 0.351 t hr MJ⁻¹ mm⁻¹ in Guana, Africa. This difference in values resulted from using the K-factor value without converting it to the SI unit.

Table 7.2. K-factor values in SI unit and the corresponding area

Soil Type	Area (km ²)	Area (%)	K-factor (U.S. unit)	K-factor (SI metric unit)
Water body	11.94	1.75	0.00	0.000
Swampy area	67.05	9.85	0.00	0.000
Hablic Luvisols	233.54	34.30	0.09	0.012
Xeroic Luvisols	135.25	19.86	0.11	0.015
Eutric Vertisols	18.99	2.79	0.15	0.020
Eutric Fluvisols	203.64	29.91	0.18	0.024
Molic Andosols	10.47	1.54	0.20	0.026

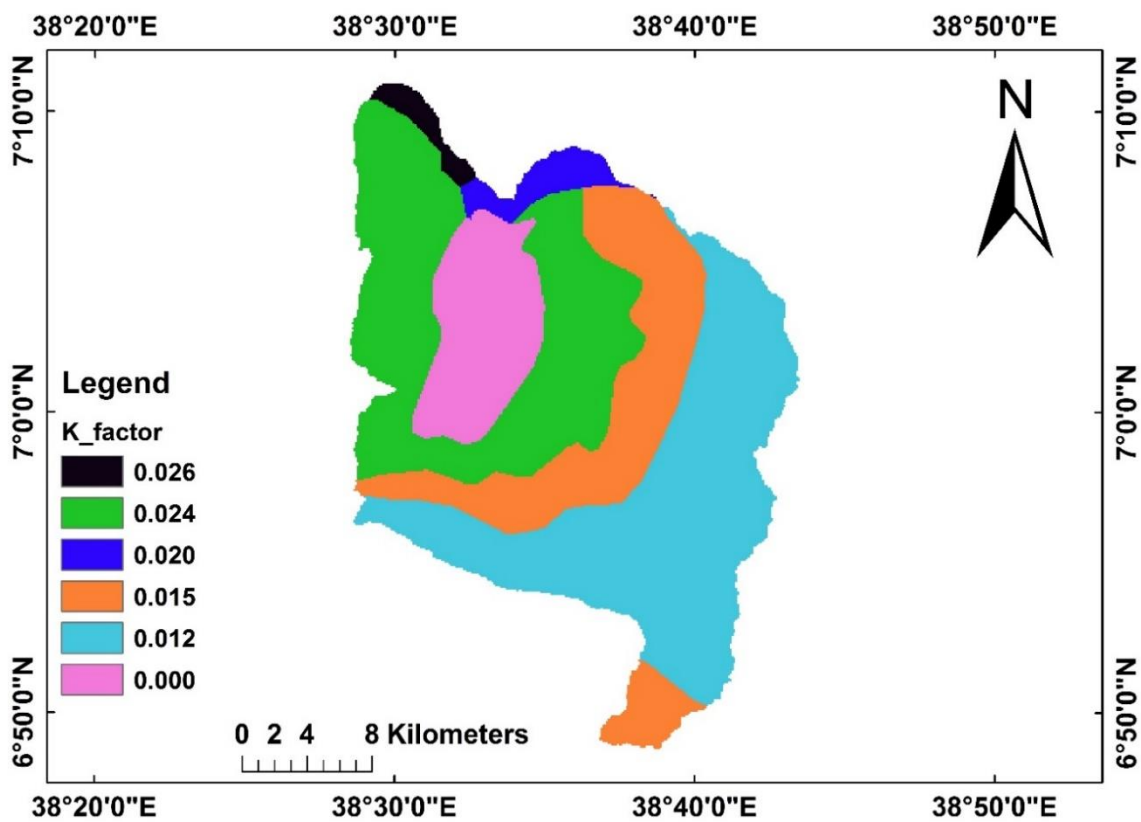


Figure 7.3. K-factor map of TWW

7.2.3 LS-factor

The LS-factor is presented in Table 7.3 and displayed as a map (Figure 7.4). It varies from zero to greater than 60. A significant part of the area (41.05%) have LS-factor less than one, and almost half of the watershed (51.94 %) have LS-factor between one and 60. A small portion of the watershed (7.01%) have an LS-factor value greater than 60. Bewket and Teferi 2009 also reported that the LS-factor ranges from zero to greater than 100 in the Chemoga watershed in the Ethiopian highlands. The LS-factor reflects the impacts of topography on water erosion. Steeper slopes can favour higher runoff velocities, whereas longer slopes favour runoff accumulation. Both these factors can lead to an increase in soil erosion. The steeper and prolonged the hill, the higher is the risk of erosion (Hudson 1995). The higher LS-factor are observed in the steeper slope area in the study watershed.

Table 7.3. The LS-factor values and the corresponding area

LS-factor values	0 -0.5	0.5 -1.0	1.0 - 10	10 - 30	30 - 60	> 60
Area (km ²)	230.25	49.28	203.04	102.25	48.37	47.69
Area (%)	33.81	7.24	29.82	15.02	7.10	7.01

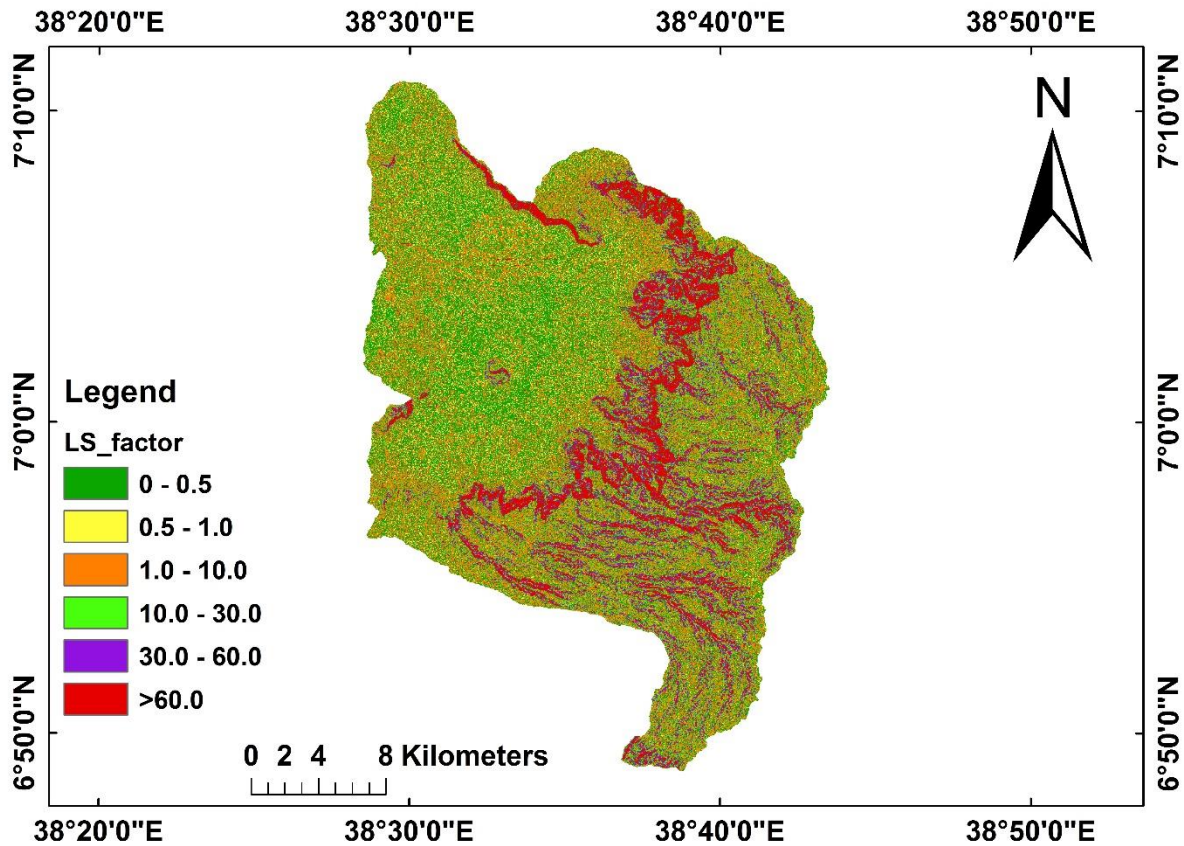


Figure 7.4. LS-factor map of TWW

7.2.4 C-factor

The C-factor is the ratio of soil loss from land with specific vegetation to the corresponding soil loss from continuous fallow (Wischmeier and Smith 1978). The 2017 LU/LC class map was used to develop the C-factor map. Most of the watershed area (56.99%) is cultivated land. Other LU/LCs in the watershed are grassland, shrubland, urban, and swampy. The forest in the study area is too small to be mapped (Figure 7.5). Each LU/LC class's C factor values were allocated based on literature recommendations in the Rift valley Lake Basin in Ethiopia (MoWR 2008) and Ethiopian highlands (Table 7.4). The C-factor map was developed and depicted in Figure 7.5. The C-factor of TWW ranges from zero to one, and it is in the range of studies elsewhere. Bewket and Teferi 2009 reported that the C-factor ranges from 0.01 to 0.60 in the Ethiopian highlands.

Table 7.4. Adopted cover and management factor values for different LU/LC in the TWW

LU/LC	Area (km ²)	Area (%)	C-factor values	References
Intensively cultivated	217.32	31.92	0.25	Hurni 1985; MoWR 2008
Moderately cultivated	170.70	25.07	0.15	Hurni (1985); MoWR 2008
Built up	65.16	9.57	0.01	Haregeweyn <i>et al.</i> 2017
Shrub land	71.38	10.48	0.10	MoWR 2008
Grassland	141.58	20.79	0.05	MoWR 2008; Hurni (1985)
Marshy	10.14	1.49	0.00	MoWR 2008
Water	4.60	0.68	1.00	Yesuph and Dagnev(2019)

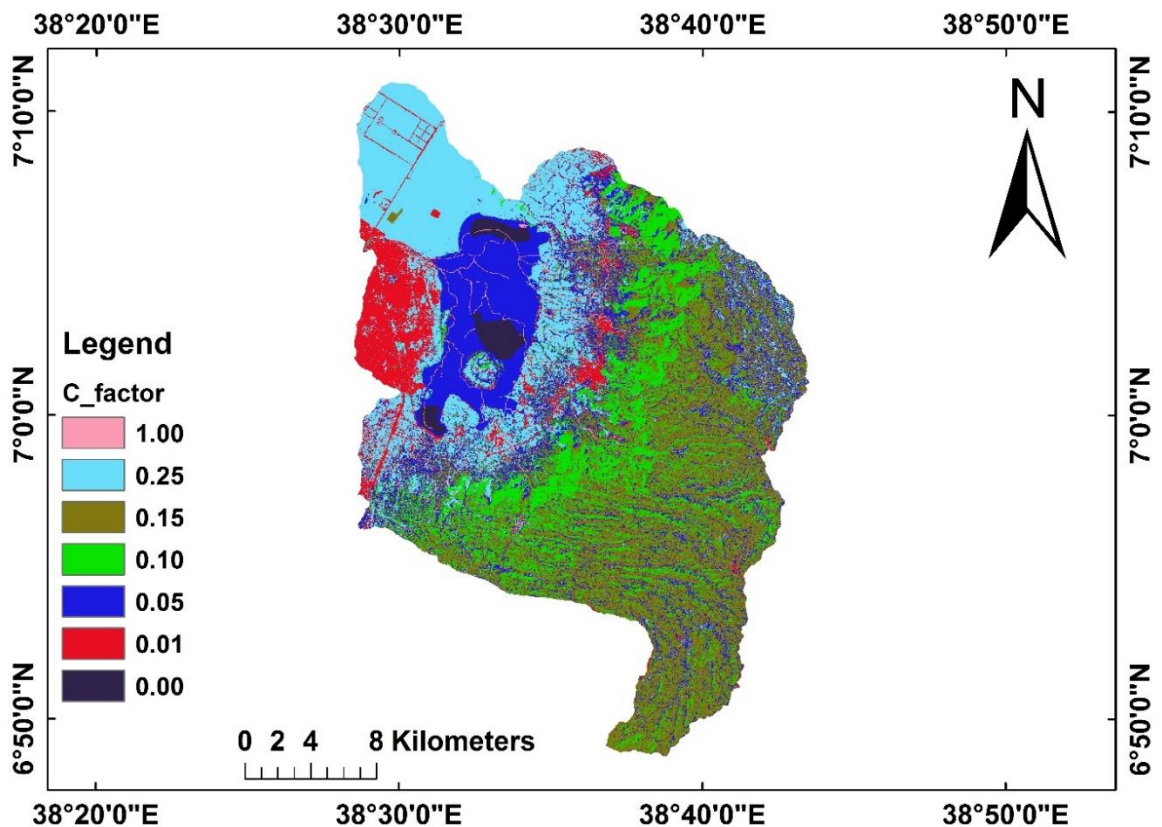


Figure 7.5. Cover and management factor map of the TWW

7.2.5 P-factor

The P-factor gives the ratio between the soil loss expected for a particular soil conservation practice to that with up-and down-slope ploughing (Wischmeier and Smith 1978). The p-factor raster map was developed based on the LU/LC and slope of the watershed. The P-factor values are given in Table 7.5 and depicted in Figure 7.6. The P-factor of the watershed ranges from 0.11 to one, and it is in the range of studies elsewhere in Ethiopia (Bewket and Teferi 2009; Shiferaw 2011; Ayalew 2015; Mulu and Dwarakish 2016).

Table 7.5. P-factor values

Land-use class	Slope class in per cent	P-factor
Agricultural land	Zero to five	0.10
	Five to ten	0.12
	Ten to twenty	0.14
	Twenty to thirty	0.19
	Thirty to fifty	0.25
	Fifty to hundred	0.33
Non-agricultural land	All	1.00

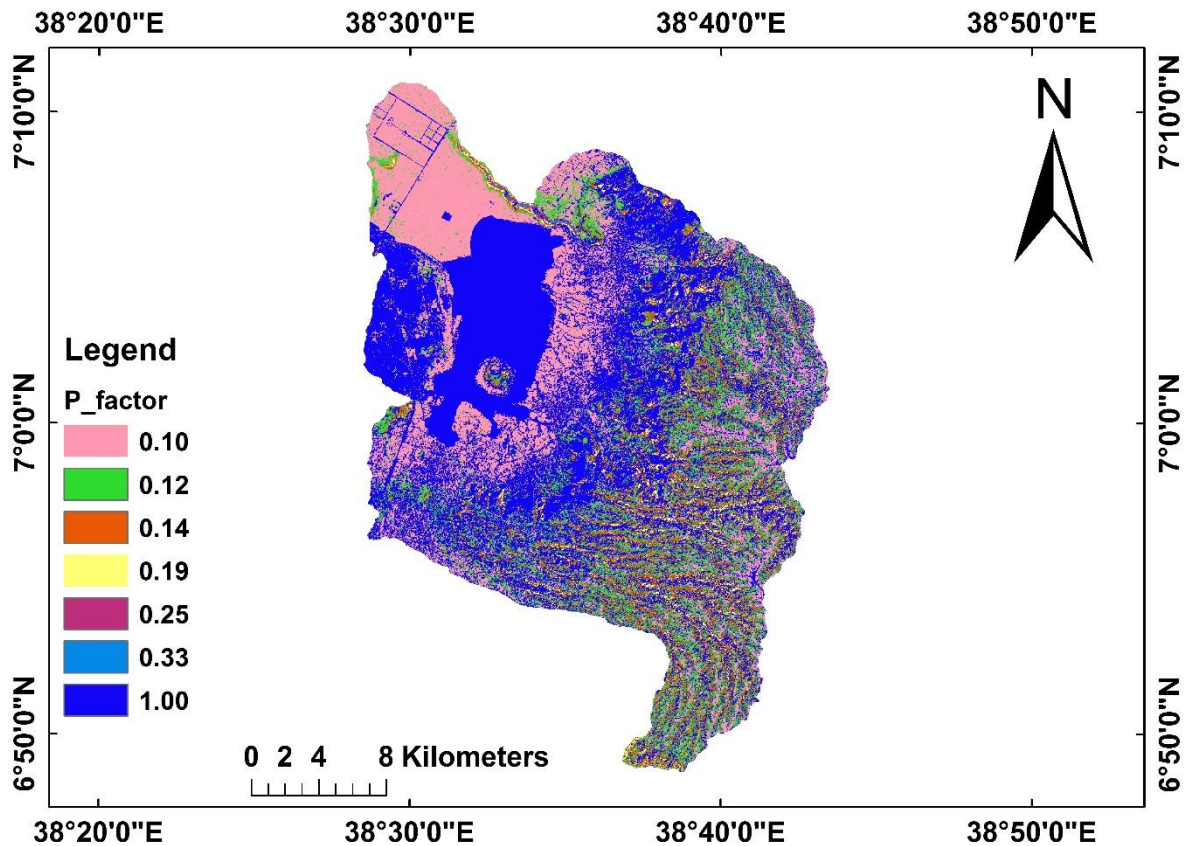


Figure 7.6. Supporting practice factor map

7.3 The Soil Loss Rate of Tikur Wuha Watershed

The SLR of TWW was predicted by using USLE. It is computed by map algebra under the raster calculation of ArcGIS 10.3. The predicted SLR was classified based on severity class (Table 7.6) and depicted in Figure 7.7.

It is necessary to validate the model by comparing the model output with numerical data independently derived from experiments or observations of the environment. Nevertheless, for this purpose, measured data should be available. Usually, it is challenging to get observed data for calibration and validation of water erosion models in a developing country. It is a problem that model validators often face in a developing country. In the case of no measured data for calibration and validation of the model, and if the purpose is for prediction of soil loss for watershed management (execution of the SWC), researchers usually make a comparison of the result with published data with similar watershed results (validating the results of model

estimation through comparison of erosion rates with reported measured values in the literature) (Bewket and Teferi 2009; Brhane and Mekonen 2009; Meshesha et al. 2012; Wolka et al. 2015; Fanta et al. 2016; Gashaw et al. 2017). Confidence is gained by knowing that the model has performed well in applications to monitored areas of similar soil, slope, and vegetation conditions to which it is applied. Also, researchers used limited field data by measuring for a short period from in situ experimental plot (Olivares et al. 2011; Andriyanto 2015), data from field experiments which were established for another purpose (Ubierna et al. 2009; Fanta et al. 2016), critical observation in the field (through qualitative erosion surveys by visual estimation of erosion status) (Bewket and Teferi 2009; Brhane and Mekonen 2009; Meshesha et al. 2012; Fanta et al. 2016; Yuan et al. 2016), and soil loss tolerance of the country with the respective agro-climatic zone for comparison of the results (Brhane and Mekonen 2009; Meshesha et al. 2012; Sujaul et al. 2012; Yuan et al. 2016), and a combination of the above. For many applications, it may be sufficient to show that a model predicts the correct location (spatial variation) of erosion and sedimentation.

Land managers and policymakers are more interested in the spatial distribution of soil erosion risk than in the absolute value of soil erosion loss (Ashiagbore et al. 2013). If the model is used to explain erosion processes (for scientific purposes), experimental data should be used for validation. Due to the absence of observed sediment data specific to the study area, approaches described by Ketema and Dwarakish (2019) were used to ensure the applicability of the USLE in TWW. The results were compared with similar studies across the Ethiopian highlands and in the Rift valley lake basins. The result was also linked to soil loss tolerance (SLT) and Ethiopia's average SLR.

The SLR of TWW was ranged from 0.00 to greater than 45 t ha⁻¹yr⁻¹ with the mean value of 14.13 t ha⁻¹yr⁻¹. It resulted in the gross soil loss of 962083 t yr⁻¹ in the entire watershed (from 68088 ha). The average SLR of TWW is found within the range of the SLR in areas having the same agro-climatic zone in Ethiopia (Bewket and Teferi 2009; Brhane and Mokonin 2009; Amsalu and Mengaw 2014; Senti et al. 2014; Sisay 2014; Ayalew 2015a,b; Gashaw et al. 2017; Belaynehi et al. 2019). These studies discovered that SLR ranged from 9.10 t ha⁻¹yr⁻¹ to 93 t ha⁻¹yr⁻¹. The average SLR of

TWW is comparable with the annual mean SLR of Ethiopia ($12 \text{ t ha}^{-1}\text{yr}^{-1}$) (Hurni 1988).

Table 7.6. SLR class of TWW based on severity class

SLR class ($\text{t ha}^{-1}\text{yr}^{-1}$)	Area in km^2	Area in %	Severity class
0 - 5	534.43	78.49	Very slight
5 - 10	40.41	5.93	Slight
10 - 25	43.33	6.36	Moderate
25 - 45	23.17	3.41	Severe
> 45	39.54	5.81	Very severe

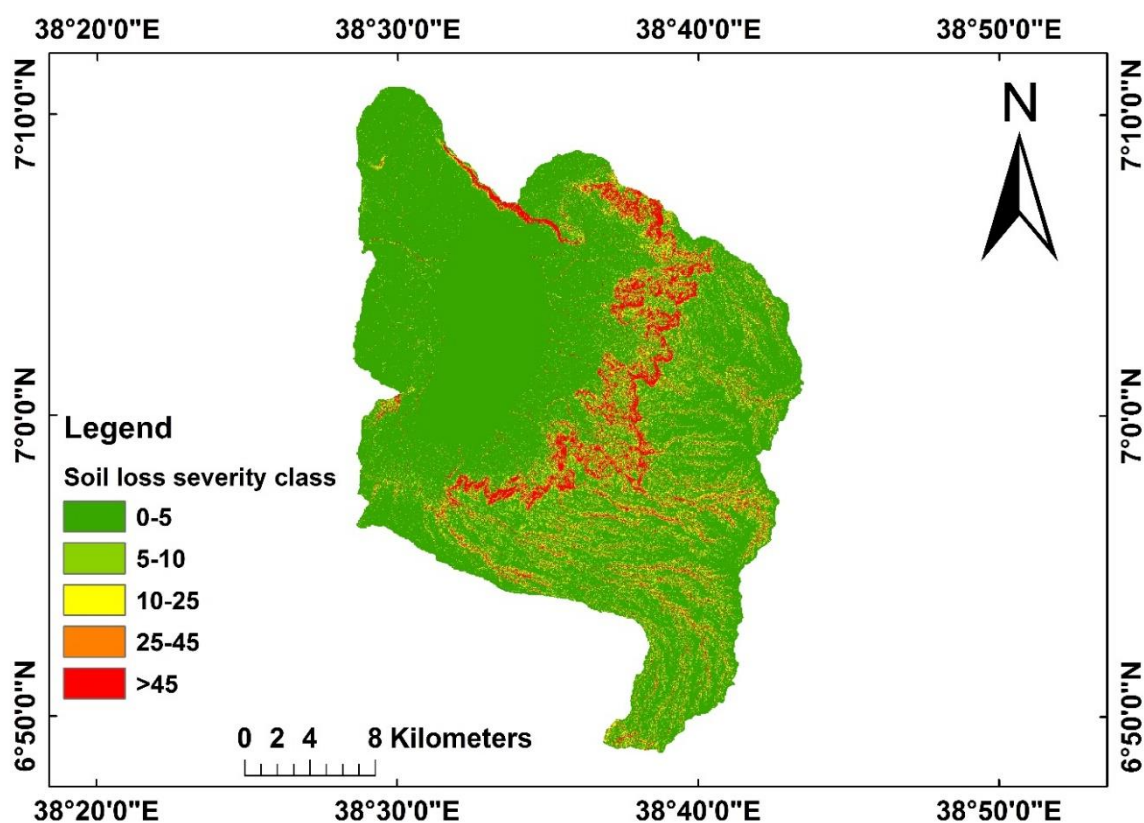


Figure 7.7. SLR class map of TWW based on severity class

Although the result of the study is found to be in the range of results reported in Ethiopia, the estimated mean annual SLT is relatively lower than the estimates in other watersheds (Bewket and Teferi 2009; Amsalu and Mengaw 2014; Senti et al.

2014; Sisay 2014; Gashaw et al. 2017; Belaynehi et al. 2019). This is because previous studies in Ethiopia used K-factor values in U.S. units. It results in overestimating the SLR and misleading the decision-makers. The major problem in water erosion assessment in Ethiopia is the misuse of K-factor values. This study used corrected K-factor values in TWW in Ethiopia. Besides, the majority of the study watershed (57.83%) is flat to the gentle slope (0-8%).

The result of the study found that a small portion of the watershed (9.22% of the study area) is suffering from severe and very severe SLR ($> 25 \text{ t ha}^{-1}\text{yr}^{-1}$). The majority of the watershed (78.49% of the TWW) are classified under very slight ($< 5 \text{ t ha}^{-1}\text{yr}^{-1}$) potential erosion risk (Table 7.6; Figure 7.7). The finding of this study matches the results carried out in Ethiopia and elsewhere in different parts of the world. Studies point out that, within the watershed, small erosion hot spot areas are the source of a large amount of soil loss and sediment load (Setegn et al. 2009; Maryam and Biswajeet 2014; Adriyanto et al. 2015; Ayalew 2015; Gelagay and Minale 2016; Markose and Jayappa 2016; Rejari et al. 2016; Yuan et al. 2016; Gashaw et al. 2017). The spatial pattern of the classified SLR map (Figure 7.7) shows areas with severe and very severe SLR are found in the east, northeast, and southeast portion of the TWW. Managing this small portion of the watershed can significantly improve its productivity of the watershed.

Also, the SLR was classified based on the SLT of the country, specific to the study watershed. The SLT of Ethiopia varies from $2\text{-}22 \text{ t ha}^{-1}\text{yr}^{-1}$ (Hurni 1988). The value of SLT depends on the agro-climatic zone. Based on annual rainfall and altitude, the agro-climatic region of the TWW is Weynadega and Dega. It implies that the SLT of TWW varies from 6 to $12 \text{ t ha}^{-1}\text{yr}^{-1}$. The average SLR of TWW ($14.13 \text{ t ha}^{-1}\text{yr}^{-1}$) is beyond the maximum SLT of the watershed. The implication is that there is a need to execute proper SWC measures to reduce the extent of SLR from TWW below the minimum SLT value, protect Lake Hawassa from sedimentation and pollution, and increase the agricultural productivity of TWW. Table 7.7 and Figure 7.8 show the area having a SLR higher than the maximum SLT of the study watershed and having a SLR less than the area's minimum SLT. 14.41% of the watershed have a SLR higher than the maximum SLT.

Table 7.7. Soil loss rate class based on soil loss tolerance (SLT) of the TWW

SLR class (t ha ⁻¹ yr ⁻¹)	Area in km ²	Area in %	Severity class
0 - 6	545.14	80.06	Low
6 - 12	37.61	5.53	Medium
> 12	98.13	14.41	High

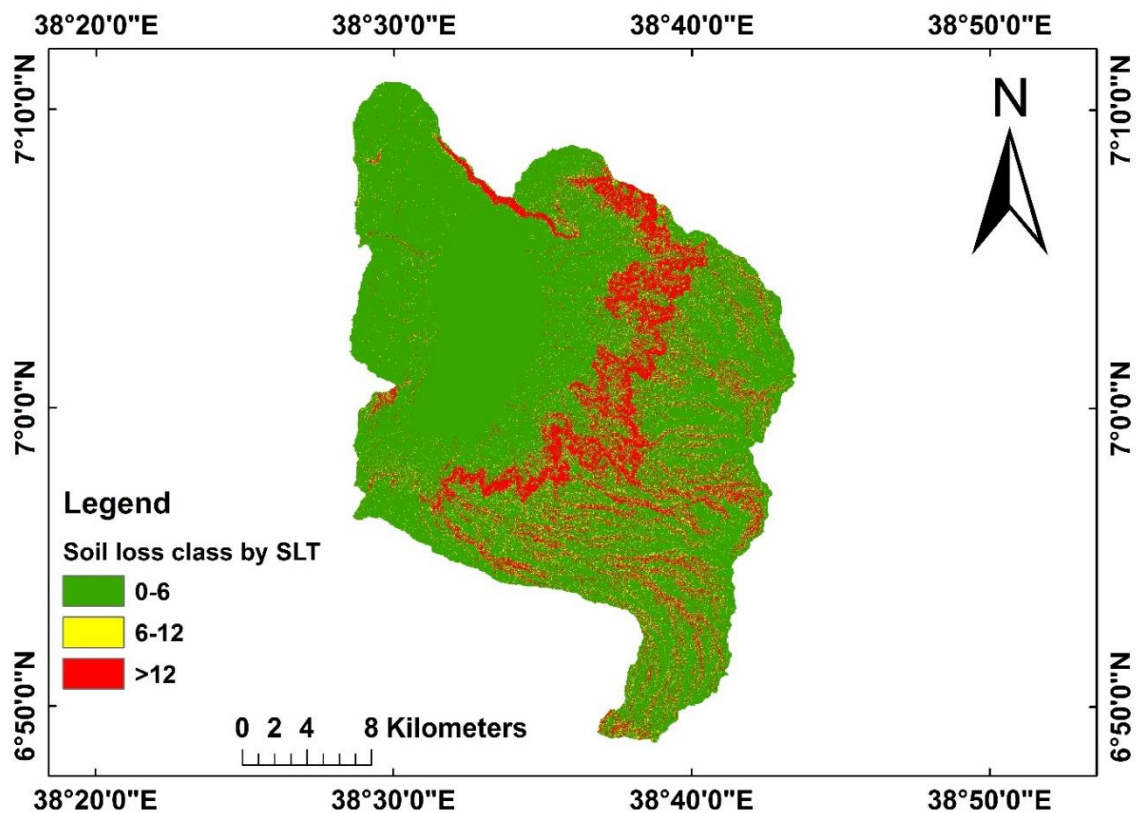


Figure 7.8. Soil loss rate class based on SLT of the area

Moreover, the SLR of TWW was classified into two levels based on Ethiopia's average soil erosion. Reports from Ethiopia (Hurni 1988) show that the average SLR nationwide was estimated to be 12 t ha⁻¹yr⁻¹. Even though most of the area (85.59%) have SLR below the country's average (Table 7. 8) SLR, the average SLR of the watershed is higher than the average SLR of the country. This also uncovers that there is a need to implement SWC practices in the TWW. Figure 7.9 showed the watershed portion having a SLR higher than the average SLR of the country.

Table 7.8. Soil loss rate class based on the average value of soil erosion of Ethiopia

Soil loss rate class($t\ ha^{-1}yr^{-1}$)	Area in km^2	Area in %	severity class
0 - 12	582.75	85.59	Low to medium
> 12	98.13	14.41	high

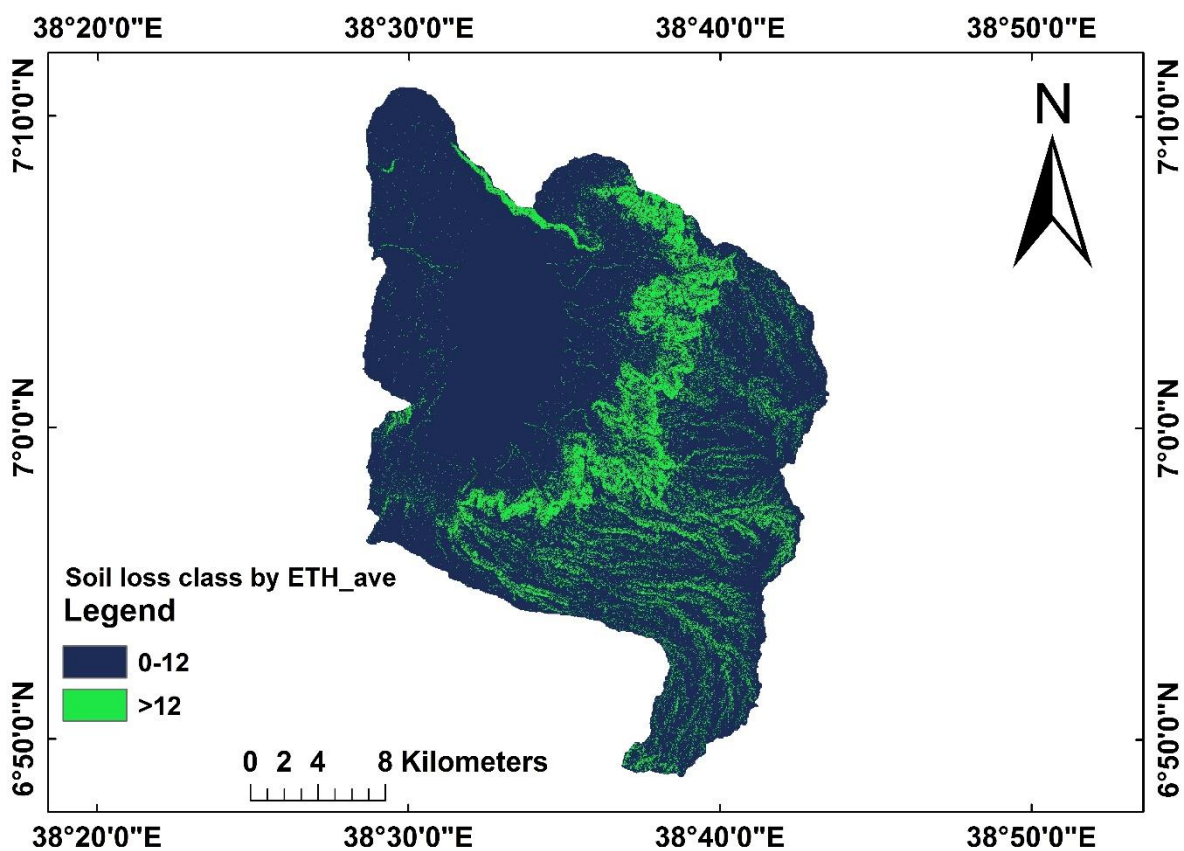


Figure 7.9. Soil loss rate class based on Ethiopia average SLR

7.4 Prioritization of Sub-watersheds for SWC Based on SLR

It is not practicable to take the whole watershed area at a time for its SWC practice. Thus, the entire watershed is divided into several sub-watersheds. The purpose is to identify priority watersheds to plan and implement SWC practices. The TWW has been divided into seven sub-watersheds to prioritize the sub-watersheds. The area of each sub-watershed is ranges from $37.07\ km^2$ to $199.03\ km^2$, which is considered a functional working area for the execution of SWC practices. The average SLR was

estimated for each watershed (Figure 7.10). The ranking of the watersheds was done in decreasing order. A watershed with the highest average yearly SLR value was ranked first, and the lowest was last (Table 7.9).

Table 7.9. Priority watersheds for SWC based on the SLR

Sub-watersheds	Area (Km ²)	Area (%)	Average SLR (t ha ⁻¹ yr ⁻¹)	Rank	Priority class
SW_1	96.26	14.14	19.11	2	High
SW_2	100.65	14.78	19.06	3	High
SW_3	75.18	11.04	19.86	1	High
SW_4	87.13	12.80	16.96	4	High
SW_5	199.03	29.23	10.41	5	Medium
SW_6	37.07	5.44	0.66	7	Low
SW_7	85.56	12.57	8.94	6	Medium

The study results revealed that all the sub-watersheds in TWW except SW_6 are needs implementation of SWC practices. Watershed SW_3 (19.86 t ha⁻¹yr⁻¹) was ranked first, followed by SW_1, SW_2, and SW_4, respectively. These watersheds are found on the eastern side of TWW and having relatively steep slope sides (Figure 7.10). The implication is that topography is the dominant factor affecting SLR in the study watershed (Figure 7.4 and 7.10). The lowest average SLR was generated from SW_6 (0.66 t ha⁻¹ yr⁻¹).

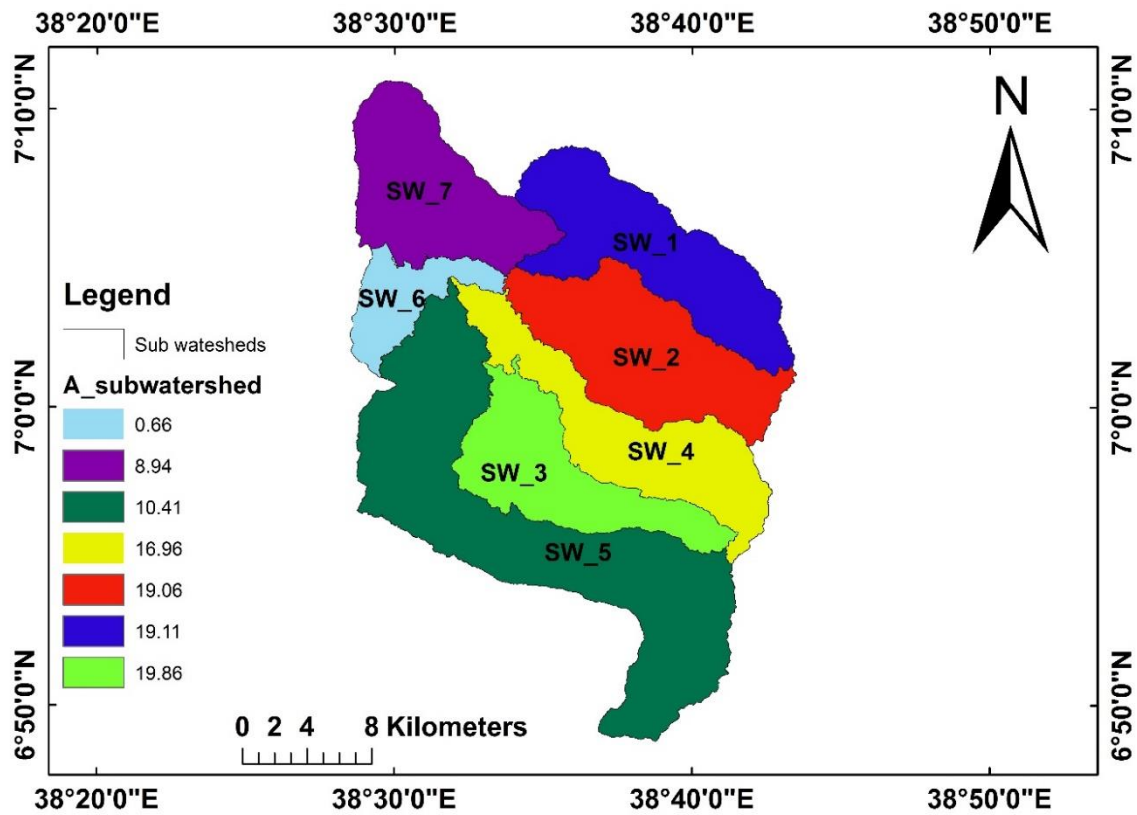


Figure 7.10. The average SLR of sub-watersheds in TWW

The TWW was categorized into three prioritization classes; high, medium, and low (Table 7.9 and Figure 7.11). The final priority map (Figure 7.11) was developed. Figure 7.11 shows, SW_3, SW_1, SW_2, and SW_4, were categorized as high priority (priority) sub-watersheds in the TWW that need immediate SWC measures to reduce soil loss from the watershed. SW_6 at the downstream side was low priority, whereas SW_5 and SW_6 were classified as medium priority (second priority) watersheds. The sub-watershed with high priority subsidize more to SLR. Therefore, the top priority should be given to them during the planning and execution of SWC practices in TWW.

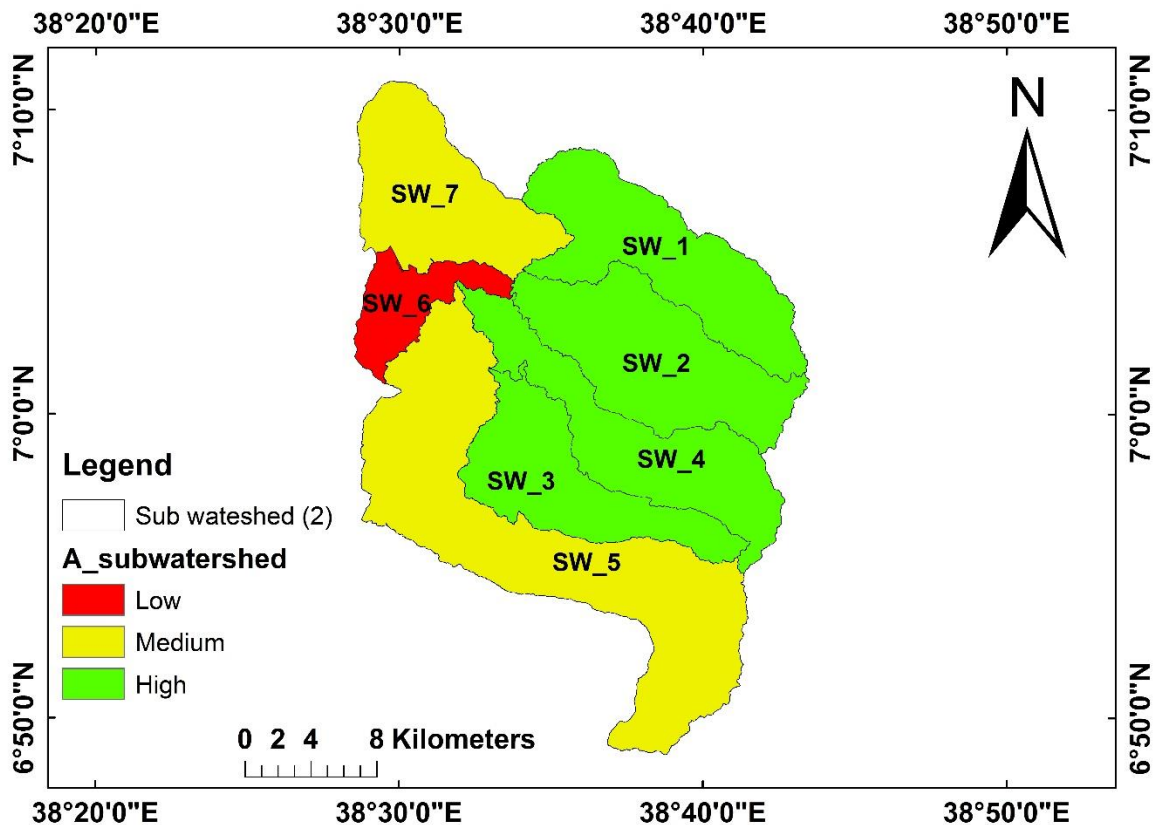


Figure 7.11. Priority watersheds for planning and implementation SWC practices in TWW

7.5 Closure

The average soil loss rate of TWW is $14.13 \text{ t ha}^{-1}\text{yr}^{-1}$. The study found that a small portion of the watershed is suffering from severe and very severe SLR. The average SLR of TWW is beyond the maximum SLT of the watershed. Also, the average SLR of the watershed is higher than the average SLR of the country. The implication is that there is a need to execute proper SWC measures to reduce the extent of SLR from TWW below the minimum SLT value. The sub-watershed with high priority subsidize more to SLR. The study results revealed that the sub-watersheds on the eastern side of TWW and having relatively steep slope sides are affected by severe erosion. Therefore, the top priority should be given to them during the planning and execution of SWC practices in TWW.

CHAPTER 8: CONCLUSIONS AND RECOMMENDATIONS

The weighted average of validated CORDEX data from multiple GCMs was used to identify how future temperature and precipitation will change and simulate the potential impacts of climate change on streamflow in TWW for the mid and end of the century. The performance of the bias-corrected CORDEX data was checked by using NSE. The result revealed that precipitation exhibited a worse agreement than the temperature in the study area. The minimum temperature was better simulated than the maximum temperature, and the weighted average of selected models performed better than a single model in the Tikur wuha watershed. The SWAT model was used to simulate the streamflow. The SWAT model has performed well in simulating the hydrological impacts of climate changes in the study area. The study found that the Bega, Kiremt, and annual rainfall increased in the mid and end of the century for all scenarios. In contrast, rainfall in Belg decreased in all cases except RCP8.5 by the end of the century. Rainfall increased faster at the end of the century than it did in the middle. The increase in precipitation is higher in the Bega compared to Belg and Kiremt season. No significant change in variability was observed in rainfall in the study area. In the mid-century, the annual average daily minimum temperature has increased by 1.59 °C for RCP4.5 and 1.85 °C for RCP8.5 relative to the baseline period. Compared to the baseline period, the annual average daily maximum temperature increased by 1.53 oC for RCP4.5 and 1.43 oC for RCP8.5. In the end century, the yearly average daily minimum temperature increased by 2.48 °C and 4.39 °C for RCP4.5 and RCP8.5, respectively, compared to the baseline period. Compared to the baseline period, the annual average daily maximum temperature increased by 2.55 °C for the RCP4.5 and 4.47 °C for the RCP8.5. The average yearly streamflow in TWW increased in all cases except a slight reduction in the RCP4.5 scenario in mid-century. It increased by 4.45% for the RCP8.5 scenario in mid-century. In the end century, the yearly average streamflow increased by 3.29% and 19.88% for the RCP4.5 and RCP8.5 scenarios, respectively. In general, the result revealed that average streamflow increased in the wet season and decreased in the dry season in all cases in the future because of climate change. It agrees with other reports in Ethiopia. The increase in streamflow may increase flooding, and a decrease in

streamflow may result in draught unless proper watershed management activities are implemented to cope with the climate change in the study area.

This study examined LU/LC dynamics and their impact on streamflow over 40 years in the Tikur Wuha watershed in southern Ethiopia. The results of the assessment identified the presence of seven LU/LC classes in the TWW. The LU/LC includes intensively cultivated, moderately cultivated, swampy, built-up, shrubland, water, and grassland. Grassland was the most dominant LU/LC class in 1978, but the study area is predominantly cultivated land in all other times. The accuracy assessment results for 1978, 1988, 1998, and 2017 LU/LC maps showed an overall accuracy of 77.50%, 82.17%, 84.83%, and 87.33%, respectively. It can be inferred from the study that a significant shift has occurred in LU/LC in the TWW over the study period. There has been a steady expansion of cropland and built-up and the withdrawal of shrubland, swampy, water body, and grassland during the 1978-2017 periods. Intensively cultivated land and the built-up area were expanded at a rate of 4.31 Km²/yr and 1.46 Km²/yr, respectively, over the entire study period. Shrubland, waterbody, grassland, and swampy show a decreasing trend with rates of 1.87 Km²/yr, 0.35 Km²/yr, 3.01 Km²/yr, and 0.55 Km²/yr, respectively. The possible reasons for the increase in built-up and cultivated land and the decrease of other LU/LC categories in the study period could be the increased demand for farmland, the expansion of Hawassa town, and the newly established industry zone due to the increase in population in the study area. The finding of this study coincides with other research findings in Ethiopia. The LU/LC changes, which occurred from 1978 to 2017, increased the annual streamflow by 14.77%. The streamflow increased in all seasons and all the months in the watershed. The result revealed that the LU/LC change had a dominant role in the watershed's hydrological responses. This indicates an immediate need to control the LU/LC to ensure water availability in the watershed.

Evaluation of the variability and trend of hydro-meteorological variables is required to notice the historical change and future predictions. This study includes both variability and trend analysis of hydro-meteorological variables using 40 years (1978-2017) observed data in TWW. For the annual, Belg, and Kiremt, the minimum rainfall was observed at Shashemene in the northern portion of the watershed, whereas the

maximum rainfall occurred at Haisawita in the southern portion of the watershed. The rainfall system in TWW is a bimodal type. In the study area, the contribution of Kiremt seasons to the total annual rainfall was very high across stations. The Belg rainfall also contributes a considerable amount. At the watershed level, the yearly rainfall ranges from 747.89mm to 1321.87mm. The weighted areal average value is 1071.35mm. The results depicted that there is no statistically significant trend in the areal weighted average rainfall in TWW. However, the watershed's annual rainfall exhibited an insignificant declining trend with a magnitude of 20.8 mm/decade. In general, rainfall exhibited high variability in the Bega and Belg seasons, moderate variability in the Kiremt season, and annual rainfall exhibited less variability. The 40 years average monthly rainfall analysis uncovered that the lowest average rainfall was observed in all the measuring stations in December, whereas September received the highest average rainfall in all the stations except Shashemene. Shashemene received the maximum average rainfall in August. A significant falling trend was detected at Shashemene (northern part of the watershed) and insignificant declining rainfall tendencies in Haisawita and Wondogenet. Nevertheless, at Hawassa, annual rainfall showed an insignificant rising trend only at the rate of 7.2 mm/decade. Generally, the study found less interannual rainfall variability across the studied stations than the seasonal rainfall. There was a high rainfall variability during the dry season (Bega) and a relatively moderate and less variability during the Belg and Kiremt seasons. The finding of the study markedly discloses that there has been a rising trend in the annual average of daily maximum and minimum temperature in the last 40 years in the watershed. In all the seasons, annual and months, average daily maximum and minimum temperature exhibited a statistically significant warming trend. It has been found that both the minimum and the maximum temperature have been increased intensely from 1978 through 2017. The average minimum temperature increased more rapidly than that of the average maximum temperature in TWW. The yearly average of daily minimum temperature in TWW has been increasing by 0.36 °C and 0.60 °C every ten years at Haisawita and Hawassa station, respectively. A rising trend of temperature and a declining rainfall trend in the watershed may reduce available water for crop production. The increase in temperature in the watershed may raise the possibility of extreme weather events. Therefore, it is recommended that temperature

variability be monitored to reduce its adverse impacts on the watershed's productivity. The streamflow of the Tikur Wuha River was found to be increased by 21.16 MCM per decade in the watershed. The strictly increasing trend of streamflow without the corresponding increase of rainfall in the study area resulted from LULC change. Streamflow variability was very high during the Belg season and moderated in all other seasons. Interannual variability was moderate during the study period. Since Tikur Wuha River is the sole permanent river feeding Lake Hawassa, the increasing trend and variation have many consequences. Therefore, the variation of streamflow should be carefully monitored. In general, PET exhibits a rising tendency in the TWW. The nature of the trend-line indicates that the increment rate of PET was more at Haisawita than Hawassa. The increasing trend in PET is allied to the increasing temperature in the study period. A slight difference in PET at different stations (Hawassa and Haisawita) in TWW may arise from the different methods employed in computing the PET, and it may be from the slight temperature difference. The findings could have vital implications for the management of water resources at the watershed scale. The increase in temperature and the variability of rainfall affect soil moisture. It, in turn, has associations to decide appropriate crop types and cropping calendars in the area. There was a serious need to begin effective adaptation measures in the TWW. Stakeholders should be involved in implementing mitigation and adaptation techniques to reduce the undesirable impacts on the watershed. It is recommended that approaches intended in the agricultural area take the trend and variability of temperature and precipitation into consideration in TWW. Farmers usually use indigenous water harvesting technologies, water conservation strategies, adjusting planting dates (cropping calendars), and mixed cropping systems to tackle global change and variability in the Ethiopian highlands. Changes in crop type/variety, watershed management measures, crop diversification, a shift in planting calendar, and water-efficient irrigation practices are common adaptation measures used throughout Ethiopia. Also, this study is based on observed data in the watershed; it is needed to conduct an investigation based on forecasted data to realize how the hydro-meteorological variables will vary in the future and be affected by global change. It is also recommended to extend the study to more stations to conclude at a regional level.

Planning and implementation of SWC measures are required to reverse the effect of soil loss and for sustainable agricultural production. Recognition of priority watersheds is very critical in identifying the sub-watersheds needing preferential SWC practices. This study quantitatively assessed and mapped SLR in TWW and identified the priority watersheds using USLE. The average SLR of the watershed ($14.13 \text{ t ha}^{-1}\text{yr}^{-1}$) is larger than the maximum SLT of the watershed and higher than the country's average SLR. The implication is that there is a need to plan and execute proper SWC methods in the watershed to decline the extent of SLR from TWW below the minimum SLT value and protect the Lake Hawassa from sedimentation and pollution increase the productivity of TWW. The result of the study found that the majority of the watershed (78.49% of the watershed) are classified under low ($< 5 \text{ t ha}^{-1} \text{ yr}^{-1}$) SLR. A small portion of the watershed (9.22%) is suffering from severe and very severe SLR ($>25 \text{ t ha}^{-1}\text{yr}^{-1}$). Managing this small portion of the watershed can significantly increase the productivity of the area. A large amount of SLR originated from a small part of the southeast, east, and northeast part of the watershed. Severe and very severe SLR were detected in the steep slope portion of the TWW. The implication of this is, the slope is the dominant factor affecting SLR in the study watershed. The findings of the study are comparable to those made by other studies at the same agro-climatic condition in Ethiopia at the watershed level. The generated SLR maps concerning sub-watersheds are used to identify areas where corrective actions should be commenced. The TWW in Ethiopia has been divided into seven sub-watersheds. SWC methods must be carried out, prioritising four sub-watersheds (SW_3, SW_1, SW_2, and SW_4), falling under the top priority zone in the watershed. The sub-watershed with high priority subsidize more to SLR. Therefore, top priority should be given to them during the planning and execution of SWC practices in TWW.

REFERENCES

- Abbaspour, K. C. (2013). SWAT-CUP 2012. SWAT Calibration and uncertainty program—a user manual.
- Abraham, T., Woldemicheala, A., Muluneha, A., and Abateb, B. (2018). “Hydrological Responses of Climate Change on Lake Ziway Catchment, Central Rift Valley of Ethiopia.” *Journal of Earth Science and Climate Change*, 9(6), 1-16.
- Abbrha, M. G. and Simhadri, S. (2015). “Local Climate Trends and Farmers’ Perceptions in Southern Tigray, Northern Ethiopia.” *International Journal of Environment and Sustainability*, 4(3), 11-28.
- Andriyanto, C., Sudarto, S., & Suprayogo, D. (2015). “Estimation of soil erosion for a sustainable land use planning: RUSLE model validation by remote sensing data utilization in the Kalikonto watershed.” *Journal of Degraded and Mining Lands Management*, 3(1), 459-468.
- Adediji, A., Tukur, A. M. and Adepoju, K. A. (2010). “Assessment of revised universal soil loss equation (RUSLE) in Katsina area, Katsina state of Nigeria using remote sensing (RS) and geographic information system (GIS).” *Iranica Journal of Energy & Environment*, 1(3), 255-264.
- Adhikari, U., and Nejadhashemi, A.P. (2016a). “Impacts of Climate Change on Water Resources in Malawi.” *Journal of Hydrologic Engineering*, 21(11), 1-13.
- Adhikari, U., and Nejadhashemi, A.P. (2016b). “Multiscale Assessment of the Impacts of Climate Change on Water Resources in Tanzania.” *Journal of Hydrologic Engineering*, 22(2), 1-13.
- Adinarayana, J. (2003). “Spatial decision support system for identifying priority sites for watershed management schemes.” *In a first interagency conference on research in the watersheds (ICRW)*, 405–408, Arizona, Benson.
- Admassu, S. and Seid, A. H. (2006). “Analysis of rainfall trend in Ethiopia.” *Ethiopian Journal of Science and Technology*, 3(2), 15-30.

- Adugna, A., Abegaz, A. and Cerdà, A. (2015). "Soil erosion assessment and control in Northeast Wollega, Ethiopia." *Solid Earth Discuss*, 7, 3511–3540.
- Ahmed, M. H. (2016). "Climate change adaptation strategies of maize producers of the Central Rift Valley of Ethiopia." *Journal of Agriculture and Rural Development in the Tropics and Subtropics*, 117(1), 175-186.
- Ahokpossi, Y. (2018). "Analysis of the rainfall variability and change in the Republic of Benin (West Africa)." *HYDROLOGY SCI J.*, 63(15-16), 2097-2123.
- Alemayehu, A. and Bewket, W. (2017). "Local spatiotemporal variability and trends in rainfall and temperature in the central highlands of Ethiopia." *Physical Geography*, 99(2), 85-101.
- Alemu, Y. T. (2015). "Flash Flood Hazard in Dire Dawa, Ethiopia." *Journal of Social Sciences and Humanities*, 1(4), 400-414.
- Allen, R. G., Pereira, L. S., Raes, D. and Smith, M. (1998). "FAO Irrigation and drainage paper No. 56. Rome" *Food and Agriculture Organization of the United Nations*, 56(97), 1-156.
- Amsalu, T. and Mengaw, A. (2014). "GIS-Based Soil Loss Estimation Using RUSLE Model: The Case of Jabi Tehinan Woreda, ANRS, Ethiopia." *Natural Resources*, 5, 616-626.
- Andriyantou, C., Sudarto and Suprayogo, D. (2015). "Estimation of soil erosion for a sustainable land use planning: RUSLE model validation by remote sensing data utilization in the Kalikontowatershed." *Journal of degraded and mining lands management*, 3(1), 459- 468.
- Arnold, J. G, Srinivasan, R., Muttiah, R.S. and Williams, J.R. (1998). "Large-area hydrologic modelling and assessment part I: Model development." *Journal of the American Water Resources Association*, 34(1), 73-89.
- Asfaw, A., Simane, B., Hassen, A., and Bantider, A. (2018). "Variability and time series trend analysis of rainfall and temperature in north-central Ethiopia: A case study in Woleka sub-basin." *Weather and climate extremes*, 19, 29-41.

- Ashiagbor, G., Forkuo¹, E.k, Laari, P. and Aabeyir, R. (2013). “Modeling Soil Erosion Using RUSLE and GIS Tools.” *International journal of remote sensing & geoscience*, 2(4).
- Atreya, K., Sharma, S. and Bajracharya, R. M. (2005). “Minimization of soil and nutrient losses in maize-based cropping systems in the mid-hills of central Nepal.” *kathmandu University Journal of Science, Engineering and Technology*, 1(1).
- Awulachew, S. B., Yilma, A. D., Loulseged, M., Loiskandl, W., Ayana, M., Alamirew, T. (2007). “Water Resources and Irrigation Development in Ethiopia.” *International Water Management Institute [IWMI Working Paper 123]*, 1-78.
- Ayalew, G. (2015a). “A Geographic Information System Based Soil Loss Estimation in Lalen Watershed for Soil Conservation Planning, Highlands of Ethiopia.” *Journal of Dynamics in Agricultural Research*, 2 (3), 31-39.
- Ayalew, G. (2015b). “A Geographic Information System Based Soil Loss and Sediment Estimation in Zingin Watershed for Conservation Planning, Highlands of Ethiopia.” *World Applied Sciences Journal*, 33 (1), 69-79.
- Azari, M., Moradi, H.R., Saghafian, B. and Faramarzi, M. (2016). “Climate change impacts on streamflow and sediment yield in the North of Iran.” *Hydrological Sciences Journal*, 61(1), 123-133.
- Babar, S., & Ramesh, H. (2015). “Streamflow response to land use–land cover change over the Nethravathi River Basin, India.” *Journal of Hydrologic Engineering*, 20(10), 1-11.
- Basheer, A. K., Haishen, L., Abubaker, O., Abubaker, B. A., and Abdelgader, A. M. S. (2016). “Impacts of climate change under CMIP5 RCP scenarios on the streamflow in the Dinder River and ecosystem habitats in Dinder National Park, Sudan.” *Hydrology and Earth System Science*, 20, 1331–1353.
- Bates, B.C., Kundzewicz, Z.W., Wu, S., and Palutikof, J.P. Eds. (2008). “Climate Change and Water.” *Technical Paper of the Intergovernmental Panel on Climate Change. IPCC Secretariat*, Geneva, 1-210.

- Bayramov, E., Buchroithner, M. F., and McGurty, E. (2013). "Differences of MMF and USLE Models for Soil Loss Prediction along BTC and SCP pipelines." *Journal of Pipeline Systems Engineering Practice*, 4 (1), 81-96.
- Beach, T. (1987). "A Review of Soil Erosion Modelling," In *Design for a Water-Resources GIS* (pp. 9-1-10–32). Water resource research centre university of Minnesota.
- Belayneh, M., Yirgu, T., and Tsegaye, D. (2019). "Potential soil erosion estimation and area prioritization for better conservation planning in Gumara watershed using RUSLE and GIS techniques." *Environmental Systems Research*, 8(1), 1-17.
- Bekele, W. (2003). "Economics of soil and water conservation: Theory and an empirical application to subsistence farming in the eastern Ethiopian highlands." Doctoral dissertation, Swedish University of Agricultural Sciences, Uppsala.
- Berhane, GM., Gebreyohannes, T., Martens, K. and Walraevens, K. (2016). "Overview of Micro-Dam Reservoirs (MDR) in Tigray (Northern Ethiopia): Challenges and Benefits." *Journal of African Earth Sciences*, 123, 210-222.
- Berhanu, B., Seleshi, Y., & Melesse, A. M. (2014). "Surface water and groundwater resources of Ethiopia: potentials and challenges of water resources development." In *Nile River Basin* (pp. 97-117). Springer, Cham.
- Bewket, W. (2002). "Land cover dynamics since the 1950s in Chemoga watershed, Blue Nile basin, Ethiopia." *Mountain research and development*, 22(3), 263-269.
- Bewket, W., and Conway, D. (2007). "A note on the temporal and spatial variability of rainfall in the drought-prone Amhara region of Ethiopia." *International Journal of Climatology*, 27(11), 1467-1477.
- Bewket, W. and Sterk, G. (2005). "Dynamics in land cover and its effect on streamflow in the Chemoga watershed, Blue Nile basin, Ethiopia." *Hydrological processes*, 19(2), 445-458.
- Bewket, W., and Teferi, E. (2009). "Assessment of Soil Erosion Hazard and Prioritization for Treatment at the Watershed Level: Case Study in the Chemoga

Watershed, Blue Nile Basin, Ethiopia.” *Land degradation and development*, 20, 609–622.

Brhane, G. and Mekonen, K. (2009). “Estimating Soil Loss Using Universal Soil Loss Equation (USLE) for Soil Conservation planning at Medego Watershed, Northern Ethiopia.” *Journal of American Science*, 5 (1), 58-69.

Bridges, EM. and Oldeman, LR. (1999). “Global assessment of human-induced soil degradation.” *Journal of Arid Soil and Rehabilitation*, 13(4), 319-325.

Casimiro, W. S. L., Ronchail, J., Labat, D., Espinoza, J. C., and Guyot, J. L. (2012). “Basin-scale analysis of rainfall and runoff in Peru (1969–2004): Pacific, Titicaca and Amazonas drainages.” *HYDROLOGY SCI J.* 57(4): 625-642.

Chaemiso, S. E., Abebe, A. and Pingale, S. M. (2016). “Assessment of the impact of climate change on surface hydrological processes using SWAT: a case study of Omo-Gibe River basin, Ethiopia.” *Modeling Earth Systems and Environment*, 2(205), 1-15.

Chakilu, G. G., and Moges, M. A. (2017). “Assessing the Land Use/Cover Dynamics and its Impact on the Low Flow of Gumara Watershed, Upper Blue Nile Basin, Ethiopia.” *Hydrology Current Research*, 7(268).

Chakraborty, S., Pandey, R. P., Chaube, U. C. and Mishra, S. K. (2013). “Trend and variability analysis of rainfall series at Seonath River Basin, Chhattisgarh (India).” *International Journal of Applied Sciences and Engineering Research*, 2(4), 425-434.

Changkun, M. A., Lin, S., Shiyin, L., Ming’an, S. and Yi, L. (2015). “Impact of climate change on the streamflow in the glacierized Chu River Basin, Central Asia.” *Journal of Arid Land*, 7 (4), 501–513.

Chaturvedi, R.K., Joshi, J., Jayaraman, M., Bala, G., and Ravindranath, N. H. (2012). “Multi-model climate change projections for India under representative concentration pathways.” *Current Science*, 103(7), 791-802.

Cheung, W. H., Senay, G. B., and Singh, A. (2008). “Trends and spatial distribution of annual and seasonal rainfall in Ethiopia.” *International Journal of Climatology*, 28(13), 1723- 1734.

Chow, V.T. (2010). *Applied hydrology*. Tata McGraw-Hill Education, 1-243.

- Coca, D.A., and Nilca, M.I. (2016). “Quantitative assessment of soil erosion using GIS empirical methods in the upper catchment of Bârsa River.” *Geo Patterns*, 1 (2), 13-17.
- Cochrane, L., and Singh, R. (2017). “Climate services for resilience: the changing roles of NGOs in Ethiopia.” *Building Resilience and Adaptation to Climate Extremes and Disasters*, Macmillan London, 1-31.
- Conway, D. (2000). “Some aspects of climate variability in the northeast Ethiopian highlands, Wollo and Tigray.” *Ethiopian journal of science*, 23 (2), 139–161.
- Dadi, M. (2013). “The impact of sedimentation and climate variability on the hydrological status of Lake Hawassa, South Ethiopia.” Doctoral Dissertation, University of Bonn, Bonn.
- Dessie, G., & Christiansson, C. (2008). “Forest decline and its causes in the south-central rift valley of Ethiopia: Human impact over a one hundred year perspective.” *Journal of the Human Environment*, 37(4), 263-271.
- Dile, Y.T., Berndtsson, R. and Setegn, S. G. (2013). “Hydrological Response to Climate Change for Gilgel Abay River, in the Lake Tana Basin - Upper Blue Nile Basin of Ethiopia.” *PLoS ONE*, 8(10), 1-13.
- Dorosh, P., and Rashid, S. (Eds.). (2013). “Food and agriculture in Ethiopia: Progress and policy challenges.” University of Pennsylvania Press, 1-41.
- Dumenu, W. K. and Obeng, E. A. (2016). “Climate change and rural communities in Ghana: Social vulnerability, impacts, adaptations and policy implications.” *Environmental Science and Policy*, 55, 208–217.
- Eckelmann, W., Baritz, R., Bialousz, S., Bielek, P., Carre, F., Houšková, B., Jones, R.J.A... Zupan, M. (2006). “Common Criteria for Risk Area Identification according to Soil Threats.” *European Soil Bureau Research Report No.20*, EUR 22185 EN, 1-94.
- Eshetu, G., Johansson, T. P., Garedew, W., and Yisahak, T. (2018). “Climate Variability and Small-Scale Farmer Adaptation Strategy in Setema-Gatira Area of

Jimma, Southwestern Ethiopia.” *American journal of biological and environmental statistics*, 4(1), 1-9.

Ethiopian Panel on Climate Change (EPCC). (2015a). “First Assessment Report, Summary of Reports for Policy Makers.” *the Ethiopian Academy of Sciences, Addis Ababa, Ethiopia*, 1-92.

Ethiopian panel on Climate Change (EPCC). (2015b). “First Assessment Report, An Assessment of Ethiopia’s Policy and Institutional Frameworks for Addressing Climate Change.” *the Ethiopian Academy of Sciences, Addis Ababa, Ethiopia*, 1-88.

Fang, G., Yang, J., Chen, Y. N., & Zammit, C. (2015). “Comparing bias correction methods in downscaling meteorological variables for a hydrologic impact study in an arid area in China.” *Hydrology and Earth System Sciences*, 19(6), 2547-2559.

FAO. (2011). “The state of the world’s land and water resources for food and agriculture (SOLAW): Managing systems at risk.” *Food and Agriculture Organization of the United Nations, Rome and Earthscan, London*, 1-308.

Fathizad, H., Karimi, H., and Alibakhshi, S. M. (2014). “The estimation of erosion and sediment by using the RUSLE model and RS and GIS techniques (Case study: Arid and semi-arid regions of Doviraj, Ilam province, Iran).” *International Journal of Agriculture and Crop Sciences*, 7 (6), 304-314.

Fazzini, M., Bisci, C., and Billi, P. (2015). “The climate of Ethiopia.” In *Landscapes and landforms of Ethiopia* (pp. 65-87). Springer, Dordrecht.

Fenta, A.A, Yasuda, H., Shimizu, K., Haregeweyn, N. and Negussie, A. (2016). “Dynamics of Soil Erosion as Influenced by Watershed Management Practices: A Case Study of the Agula Watershed in the Semi-Arid Highlands of Northern Ethiopia.” *Environmental Management*, 58, 889–905.

Foody, G. M. (2002). “Status of land cover classification accuracy assessment.” *Remote sensing of environment*, 80(1), 185-201.

Forootan, E. (2019). “Analysis of trends of hydrologic and climatic variables.” *Soil and Water Research*, 14(3), 163-171.

- Foster, G. R., McCool, D. K., Renard, K. G. and Moldenhauer, W. C. (1981). "Conversion of the universal soil loss equation to SI metric units." *Journal of Soil and Water Conservation*, 36(6), 355-359.
- Funk, C., Rowland, J., Eilerts, G., Kebebe, E., Biru, N., White, L., and Galu, G. (2012). "A climate trend analysis of Ethiopia." *US Geological Survey, Fact Sheet*, 3053.
- Gambella Region Disaster Prevention and Preparedness Agency. (2007). "Report on Emergency Disaster Study." Gambella, Ethiopia.
- Ganasri, B.P., and Ramesh, H. (2016). "Assessment of soil erosion by RUSLE model using remote sensing and GIS - A case study of Nethravathi Basin." *Geoscience Frontiers*, 7, 953 - 961.
- Getachew, H. E., and Melesse, A. M. (2012). "The impact of land-use change on the hydrology of the Angereb Watershed, Ethiopia." *International Journal of Water Sciences*, 1, 1-7.
- Gashaw, T., Tulu, T., and Argaw, M. (2017). "Erosion risk assessment for prioritization of conservation measures in Geleda watershed, Blue Nile basin, Ethiopia." *Environmental Systems Research*, 6 (1), 1-14.
- Gashaw, T., Tulu, T., Argaw, M., and Worqlul, A. W. (2018). "Modelling the hydrological impacts of land use/land cover changes in the Andassa watershed, Blue Nile Basin, Ethiopia." *Science of the Total Environment*, 619, 1394-1408.
- Gebre, H., Kindie, T., Girma, M., and Belay, K. (2013). "Trend and variability of rainfall in Tigray, northern Ethiopia: analysis of meteorological data and farmers' perception." *Academia Journal of Agricultural Research*, 1(6), 088-100.
- Gebre, S. L., and F. Ludwig. (2015). "Hydrological Response to Climate Change of the Upper Blue Nile River Basin: Based on the IPCC Fifth Assessment Report (AR5)." *Journal of Climatology and Weather Forecasting*, 3 (1). 1-15.
- Gebreegziabher, Y. (2004). "Assessment of the Water Balance of Lake Awassa Catchment, Ethiopia," M.Sc Thesis, International Institute for Geo-information Science and Earth Observation, Enschede, The Netherlands.

- Gebrehiwot, T., and van der Veen, A. (2013). "Assessing the evidence of climate variability in the northern part of Ethiopia." *Journal of development and agricultural economics*, 5(3), 104-119.
- Gelagay, H. S. (2016). "RUSLE and SDR Model-Based Sediment Yield Assessment in a GIS and Remote Sensing Environment; A Case Study of Koga Watershed, Upper Blue Nile Basin, Ethiopia." *Hydrology Current Research*, 7 (2), 1-7.
- Gelagay, H. S. and Minale, A.S. (2016). "Soil loss estimation using GIS and Remote sensing techniques: A case of Koga watershed, Northwestern Ethiopia." *Journal of International Soil and Water Conservation Research*, 4, 126 - 136.
- Getachew, H. E., and Melesse, A. M. (2012). "The impact of land-use change on the hydrology of the Angereb Watershed, Ethiopia." *International Journal of Water Sciences*, 1, 1-7.
- Getahun, Y. S., and Van Lanen, H. A. J. (2015). "Assessing the impacts of land use-cover change on the hydrology of Melka Kunturie subbasin in Ethiopia, using a conceptual hydrological model." *Hydrology: Current Research*, 6(3), 1-11.
- Gissila, T., Black, E., Grimes, D. I. F., and Slingo, J. M. (2004). "Seasonal forecasting of the Ethiopian summer rains." *International Journal of Climatology: A Journal of the Royal Meteorological Society*, 24(11).
- Hadgu, G., Tesfaye, K., Mamo, G., and Kassa, B. (2015). "Farmers' climate change adaptation options and their determinants in Tigray Region, Northern Ethiopia." *African Journal of Agricultural Research*, 10(9), 956-964.
- Hallegatte, S., Bangalore, M., Bonzanigo, L., Fay, M., Kane, T., Narloch, U., Rozenberg, J., Treguer, D., and Vogt-Schilb, A. (2016). "Shock Waves: Managing the Impacts of Climate Change on Poverty." *Climate Change and Development Series*, Washington, DC: World Bank publications.
- Hamed, K. H., and Rao, A. R. (1998). "A modified Mann-Kendall trend test for autocorrelated data." *Journal of hydrology*, 204(1-4), 182-196.

Haregeweyn, N., Poesen, J., Wit, J De., Haile M., Govers, G. and Deckers, S. (2006). “Reservoirs in Tigray (Northern Ethiopia): Characteristics and Deposition Problems.” *Land Degradation and Development*, 17 (2), 211-230.

Haregeweyn, N. B., Melesse, A., Tsunekawa, M., Tsubo, D., Meshesha and Balana, B. B. (2012). “Reservoir sedimentation and its mitigating strategies: a case study of Angereb reservoir (NW Ethiopia).” *Journal of Soils Sediments: Springer*, 12, 291-305.

Haregeweyn, N., Tsunekawa, A., Poesen, J., Tsubo, M., Meshesha, D. T., Fenta, A. A., and Adgo, E. (2017). “Comprehensive assessment of soil erosion risk for better land use planning in river basins: a Case study of the Upper Blue Nile River.” *Science of the Total Environment*, 574, 95-108.

Hargreaves, G. H., and Samani, Z. A. (1982). “Estimating potential evapotranspiration.” *Journal of the Irrigation and Drainage Division*, 108(3), 225-230.

Haregeweyn N, Tsunekawa A, Poesen J, Tsubo M, Meshesha D T, Fenta A A, dgo E .(2017). “Comprehensive assessment of soil erosion risk for better land use planning in river basins: a Case study of the Upper Blue Nile River.” *Science of the Total Environment*, 574: 95-108.

Hassaballah, K., Mohamed, Y., Uhlenbrook, S., and Biro, K. (2017). “Analysis of streamflow response to land use and land cover changes using satellite data and hydrological modelling: a case study of Dinder and Rahad tributaries of the Blue Nile (Ethiopia–Sudan).” *Hydrol. Earth Syst. Sci.* 21(10), 5217.

High-Level Panel of Experts (HLPE). (2015). “Water for food security and nutrition. A report by the High-Level Panel of Experts on Food Security and Nutrition of the Committee on World Food Security.” Rome, 2015.

Holden, E., Linnerud, K., and Banister, D. (2014). “Sustainable development: Our Common Future revisited.” *Global Environmental Change*, 26, 130-139.

Hudson, N. (1995). “Soil conservation.” (Third Edn.). B.T. Batsford, London, 391pp.

- Hurni, H. (1985). "Erosion-productivity-conservation systems in Ethiopia." *Proceedings of 4th International Conference on Soil Conservation*, Maracay, Venezuela, 3-9 November 1985, 654-674.
- Hurni, H. (1988). "Degradation and conservation of the resources in the Ethiopian highlands." *Mountain Research and Development*, 8 (2/3): 123-130.
- IPCC, (2007). "Climate Change 2007: Synthesis Report. Contribution of Working Groups I, II, and III to the Fourth Assessment Report of the Intergovernmental Panel on Climate Change." [Core Writing Team, Pachauri, R.K, and Reisinger, A. (Eds.)]. IPCC, Geneva, Switzerland, 104 pp.
- IPCC, (2014). "Climate Change 2014: Mitigation of Climate Change. Contribution of Working Group III to the Fifth Assessment Report of the Intergovernmental Panel on Climate Change." [Edenhofer, O., R. Pichs-Madruga, Y. Sokona, E. Farahani, S. Kadner, K. Seyboth, A. Adler, I. Baum, S. Brunner, P. Eickemeier, B. Kriemann, J. Savolainen, S. Schlömer, C. von Stechow, T. Zwickel and J.C. Minx (Eds.)]. Cambridge University Press, Cambridge, United Kingdom, and New York, NY, USA, 1454pp.
- International Hydropower Association (IHA). (2017). "Hydropower Status Report," 84pp.
- Jose, D. M., and Dwarakish, G. S. (2020). "Uncertainties in predicting impacts of climate change on hydrology in basin scale: a review." *Arabian Journal of Geosciences*, 13(19), 1-11.
- Jury, M. R., and Funk, C. (2013). "Climatic trends over Ethiopia: regional signals and drivers." *International Journal of Climatology*, 33(8), 1924-1935.
- Kebede, W., Tefera, M., Habitamu, T., Alemayehu, T. (2014). "Impact of Land Cover Change on Water Quality and Stream Flow in Lake Hawassa Watershed of Ethiopia." *Agricultural Sciences*, 5, 647-659.
- Kendall, M.G. (1975). "Rank Correlation Methods." Fourth Edition, Charles Griffin, London.

- Ketema, A., and Dwarakish, G. S. (2019). "Water erosion assessment methods: a review." *ISH Journal of Hydraulic Engineering*, 1-8.
- Kim, U., and Kaluarachchi, J. J. (2009). "Climate Change Impacts on Water Resources in the Upper Blue Nile River Basin, Ethiopia." *Journal of the American Water Resources Association*, 45(6), 1361-1378.
- Kim, K. B., Kwon, H. H., & Han, D. (2015). "Bias correction methods for regional climate model simulations considering the distributional parametric uncertainty underlying the observations." *Journal of Hydrology*, 530, 568-579.
- Kiros, G., Shetty, A., & Nandagiri, L. (2016). "Analysis of variability and trends in rainfall over northern Ethiopia." *Arabian Journal of Geosciences*, 9(6), 451.
- Kothyari, U. C. (2012). "Soil erosion and sediment yield modelling." *ISH Journal of Hydraulic Engineering*, 14(1), 84-103.
- Kumar, V., Jain, S. K., and Singh, Y. (2010). "Analysis of long-term rainfall trends in India." *HYDROLOGY SCI J.* 55(4): 484-496.
- Kundzewicz, Z. W., Krysanova, V., Benestad, R. E., Hov, Ø., Piniewski, M., & Otto, I. M. (2018). "Uncertainty in climate change impacts on water resources." *Environmental Science & Policy*, 79, 1-8.
- Lal, R. and Humberto, B. (2008). "Principles of Soil Conservation and Management." The Ohio State University, Columbus. OH, USA.
- Legese, W. (2017). "Climate Change Indication and Projection Over Bale Highlands, Southeastern Ethiopia." *J Climatol Weather Forecasting*, 5(212), 10-4172.
- Leta, O. T., El-Kadi, A. I., Dulaib, H., and Ghazal, K. A. (2016). "Assessment of climate change impacts on water balance components of Heeia watershed in Hawaii." *Journal of Hydrology: Elsevier. Regional Studies*, 8, 182–197.
- Lillesand, T., Kiefer, R. W., and Chipman, J. (2004). "Remote sensing and image interpretation." Fifth Eds. John Wiley & Sons, United States of America. 1-812.
- Lillesand, T., Kiefer, R. W., and Chipman, J. (2015). "Remote sensing and image interpretation." Seventh Eds. John Wiley & Sons, United States of America. 1-770.

- Mahmood, A., Moradi, H. R., Saghafian, B., and Faramarzi, M. (2016). "Climate change impacts on streamflow and sediment yield in the North of Iran." *Hydrological Sciences Journal*, 61(1), 123-133.
- Maitima, J. M., Mugatha, S. M., Reid, R. S., Gachimbi, L. N., Majule, A., Lyaruu, H.,...and Mugisha, S. (2009). "The linkages between land-use change, land degradation and biodiversity across East Africa." *African Journal of Environmental Science and Technology*, 3(10), 310-325.
- Mamuye, M., and Kebebew, Z. (2018). "Review on impacts of climate change on watershed hydrology." *Journal of Environment and Earth Science*, 8(1), 91-99.
- Mann, H. B. (1945). "Nonparametric tests against trend." *Econometrica: Journal of the Econometric Society*, 13(3), 245-259.
- Markose, V. J. and Jayappa, K.S. (2016). "Soil loss estimation and prioritization of sub-watersheds of Kali River basin, Karnataka, India, using RUSLE and GIS." *Environmental Monitoring and Assessment*, 188(4), 225.
- Maryam, K. and Biswajeet, P. (2014). "Spatio-temporal assessment of soil erosion at Kuala Lumpur metropolitan city using remote sensing data and GIS." *Geomatics, Natural Hazards and Risk*, 5 (3), 252-270.
- Mbaye, M.L., Hagemann, S., Haensler, A., Stacke, T., Gaye, A.T., and Afouda, A. (2015). "Assessment of Climate Change Impact on Water Resources in the Upper Senegal Basin (West Africa)." *American Journal of Climate Change*, 4 (01), 77-93.
- Mekasha, A., Tesfaye, K., and Duncan, A. J. (2014). "Trends in daily observed temperature and precipitation extremes over three Ethiopian eco-environments." *International Journal of Climatology*, 34(6), 1990-1999.
- Mekonnen, D.F. and Disse, M. (2018). "Analyzing the future climate change of Upper Blue Nile River Basin (UBNRB) using statistical downscaling techniques." *Journal of Hydrology Earth System Science*, 22(4), 2391-2408.
- Mengistu, D., Bewket, W., and Lal, R. (2014). "Recent spatiotemporal temperature and rainfall variability and trends over the Upper Blue Nile River Basin, Ethiopia." *International Journal of Climatology*, 34(7), 2278-2292.

- Meshesha, D. T., Tsunekawa, A., Tsubo, M., & Haregeweyn, N. (2012). Dynamics and hotspots of soil erosion and management scenarios of the Central Rift Valley of Ethiopia. *International Journal of Sediment Research*, 27(1), 84-99.
- Mondal, A., Khare, D., and Kundu, S. (2018). “A comparative study of soil erosion modelling by MMF, USLE, and RUSLE.” *Geocarto International*, 33(1), 89-103.
- Morgan, R. P. C. (2005). “Soil erosion and conservation”, Third Edition, published by Blackwell Publishing Ltd.
- Merritt, W. S., Letcher, R.A. and Jakeman, A.J. (2003). “A review of erosion and sediment transport models.” *Environmental Modelling and Software*, 18, 761-799.
- Moriasi, D. N., Arnold, J. G., Van Liew, M. W., Blingner, R. L., Harmel, R. D. and Veith. T. L. (2007). “Model evaluation guidelines for systematic quantification of accuracy in watershed simulations.” *American Society of Agricultural and Biological Engineers*, 50 (3), 885–900.
- Mosello, B., Calow, R., Tucker, J., Parker, H., Alamirew, T., Kebede, S. ... and Gudina, A. (2015). “Building adaptive water resources management in Ethiopia.” London: Overseas Development Institute, 1-100.
- MoWR. (2002). “Water sector development program main report volume II.” *Ministry of Water Resources, Federal Democratic Republic of Ethiopia*, Addis Ababa, 1-170.
- MoWR. (2008). “The Federal Democratic Republic of Ethiopia, Ministry of Water Resources: Rift Valley Lakes Basin Integrated Resources Development Master Plan Study Project. Phase 1 Report: Lake Hawassa Sub-basin Integrated Watershed Management Prefeasibility Study. Part 1 and 2. Halcrow Group Limited and Generation Integrated Rural Development (GIRD) Consultants.” Addis Ababa. Unpublished document
- MoWR and GW-MATE. (2011). “Ethiopia: a strategic framework for managed groundwater development”, Addis Ababa, 1-60.

Mulu, A. and Dwarakish, G.S. (2016). "Hydrological effects of land use /land cover changes on streamflow at Gilgel Abay River Basin, Upper Blue Nile, Ethiopia." *IJEE*, 9 (5): 1881-1886.

National Meteorological Services Agency (NMSA). (2007). "Climate change national adaptation program of action (NAPA) of Ethiopia." *National Meteorological Services Agency, Ministry of Water Resources, Federal Democratic Republic of Ethiopia, Addis Ababa*, 96pp.

NMSA. (2013). "Meteorological data and climatology directorate annual climate bulletin for the year 2013." 15pp.

Nash, J.E. and Sutcliffe, J.V. (1970). "River Flow Forecasting through Conceptual Model. Part 1-A Discussion of Principles." *Journal of Hydrology*, 10, 282-290.

Nigatu, Z.M., Rientjes, T., and Haile, A.T. (2016). "Hydrological Impact Assessment of Climate Change on Lake Tana's Water Balance, Ethiopia." *American Journal of Climate Change*, 5(1), 27-37.

Olivares, B., Verbist, K., Lobo, D., Vargas, R., and Silva, O. (2011). "Evaluation of the USLE model to estimate water erosion in an Alfisol." *Journal of soil science and plant nutrition*, 11(2), 72-85.

Osman, M., Sauerborn, P. (2002). "A preliminary assessment of characteristics and long-term variability of rainfall in Ethiopia - the basis for sustainable land use and resource management. In: Conference on International Agricultural Research for Development." Witzenhausen, October 9-11, 2002.

Pal, A. B., Khare, D., Mishra, P. K., & Singh, L. (2017). "Trend analysis of rainfall, temperature and runoff data: a case study of Rangoon watershed in Nepal." *Int J Students' Res Technol Manag*, 5(3), 21-38.

Panagos, P., Meusburger, K., Alewell, C., and Montanarella, L. (2012). "Soil erodibility estimation using LUCAS point survey data of Europe." *Environmental Modelling & Software*, 30, 143-145.

- Petchprayoon, P., Blanken, P. D., Ekkawatpanit, C., and Hussein, K. (2010). "Hydrological impacts of land use/land cover change in a large river basin in central–northern Thailand." *International Journal of Climatology*, 30(13), 1917-1930.
- Pokhrel, B. K. (2018). "Impact of Land Use Change on Flow and Sediment Yields in the Khokana Outlet of the Bagmati River, Kathmandu, Nepal." *Hydrology*, 5(2), 22.
- Raju, B. K., and Nandagiri, L. (2017). "Analysis of historical trends in hydro-meteorological variables in the upper Cauvery Basin, Karnataka, India." *Current Science*, 112(3), 577-587.
- Raneesh, K. Y. and Santosh, G. T. (2011). "A study on the impact of climate change on streamflow at the watershed scale in the humid tropics." *Hydrological Sciences Journal*, 56(6), 946-965.
- Refsgaard, J.C. and Knudsen, J. (1996). "Operational validation and intercomparison of different types of hydrological models." *Water Resources Research*, 32 (7), 2189-2202.
- Renard, K. G., Foster, G. R., Weesies, G. A., McCool, D. K. and Yoder, D. C. (1997). "Predicting Soil Erosion by Water: A Guide to Conservation Planning with the Revised Universal Soil Loss Equation (RUSLE)." *Agricultural Handbook No. 703*, US Department of Agriculture, Washington DC, 407pp.
- Rejani, R., Rao, K. V., Osman, M., Rao, C. S., Reddy, K. S., Chary, G. R., & Samuel, J. (2016). "Spatial and temporal estimation of soil loss for the sustainable management of a wet semi-arid watershed cluster." *Environmental monitoring and assessment*, 188(3), 143.
- Ringler, C., Bryan, E., Hassan, H., Alemu, T., and Hillesland, M. (2011). "How can African Agriculture Adapt to Climate Change: Insights from Ethiopia and South Africa." Washington, DC, 46pp.
- Robinson, S., Strzepek, K. and Cervigni, R. (2013). "The Cost of Adapting to Climate Change in Ethiopia: Sector-Wise and Macro-Economic Estimates." *Ethiopian strategy support program II, working paper 53*, 26pp.

- Rosell, S., and Holmer, B. (2007). "Rainfall change and its implications for Belg harvest in South Wollo, Ethiopia." *Physical Geography*, 89(4), 287-299.
- Rosell, S. (2011). "Regional perspective on rainfall change and variability in the central highlands of Ethiopia." *Applied Geography*, 31(1), 329-338.
- Rosmann, T., Domínguez, E., and Chavarro, J. (2016). "Comparing trends in hydrometeorological average and extreme data sets around the world at different time scales." *Journal of Hydrology: Regional Studies*, 5, 200-212.
- Rykiel, Jr. E. J. (1996). "Testing ecological models: the meaning of validation." *Ecological Modeling*, 90 (3), 229-244.
- Sadeghi, S. H. R. and Mizuyama, T. (2007). "Applicability of the Modified Universal Soil Loss Equation for prediction of sediment yield in Khanmirza watershed, Iran." *Hydrological Sciences Journal*, 52(5), 1067-1075.
- Samy, A., Ibrahim, M. G., Mahmod, W. E., Fujii, M., Eltawil, A. and Daoud, W. (2019). "Statistical Assessment of Rainfall Characteristics in Upper Blue Nile Basin over the period from 1953 to 2014." *Water*, 11(3), 468.
- Seleshi, Y., and Zanke, U. (2004). "Recent changes in rainfall and rainy days in Ethiopia." *International journal of climatology*, 24(8), 973-983.
- Sen, P. K. (1968). "Estimates of the regression coefficient based on Kendall's tau." *Journal of the American statistical association*, 63(324), 1379-1389.
- Senti, E.T., Tufa, B. W. and Gebrehiwot, K. A. (2014). "Soil erosion, sediment yield and conservation practices assessment on Lake Haramaya Catchment." *World Journal of Agricultural Sciences*, 2 (7), 186-193.
- Serur, A.B., and Sarma, A. K. (2016). "Impact of Climate Change on Water Availability in the Weyib River Basin, South-eastern Ethiopia." *International Journal of Innovative Research in Science, Engineering and Technology*, 5(6), 1-9.
- Setegn, S. G., Dargahi, B., Srinivasan, R. and Melesse, A. M. (2010). "Modelling of Sediment Yield From Anjeni-Gauged Watershed, Ethiopia Using SWAT Model." *Journal of the American Water Resources Association*, 46 (3), 514-526.

Setegn, S. G., Rayner, D., Melesse, A. M., Dargahi, B. and Srinivasan, R. (2011). "Impact of climate change on the hydroclimatology of Lake Tana Basin, Ethiopia." *Water resource researches*, 47(4), 1-13.

Setegn, S. G., Srinivasan, R., Dargahi, B. and Melesse, A. M. (2009). "Spatial delineation of soil erosion vulnerability in the Lake Tana Basin, Ethiopia." *Journal of Hydrological Processes*, 23 (26), 3738–3750.

Shi, P., Ma, X., Chen, X., Qu, S., and Zhang, Z. (2013). "Analysis of variation trends in precipitation in an upstream catchment of Huai River." *Mathematical Problems in Engineering*, 2013, 1-13.

Shiferaw, A. (2011). "Estimating soil loss rates for soil conservation planning in the Borena woreda of South Wollo highlands, Ethiopia." *Journal of Sustainable Development in Africa*, 13 (3), 87-106

Shiferaw, B. and Holden, S. T. (2001). "Farm-level benefits to investments for mitigating land degradation: empirical evidence from Ethiopia." *Environment and Development Economics*, 6(3), 335-358.

Shrestha, S., Manish, S. and Babel, M. S. (2016). "Modelling the potential impacts of climate change on hydrology and water resources in the Indrawati River Basin, Nepal." *Environmental Earth Science*, 75 (4), 1-13.

Shretha, S., Bach, T.V. and Pandey, V.P. (2016). "Climate change impacts on groundwater resources in Mekong Delta under representative concentration pathways (RCPs) scenarios." *Environmental Science and Policy*, 61, 1–13.

Sisay, A., Chalie, N., Girmay, Z., Takele, G., and Tolera, A. (2014). "Landscape-scale Soil Erosion Modeling and Risk Mapping of Mountainous areas in Eastern Escarpment of Wondo Genet Watershed, Ethiopia." *International Research Journal of Agricultural Science and Soil Science*, 4 (6), 107-116.

Spaeth, KE. JR., Pierson, FR. B. JR., Weltz, M. A. and Blackburn, W. H. (2003). "Evaluation of USLE and RUSLE estimated soil loss on rangeland." *Journal of range management*, 56 (3), 234-246.

- Sonneveld, B.G.J.S., Keyzer, M.A. and Albersen, P.J. (1999). "A non-parametric analysis of qualitative and quantitative data for erosion modelling: A case study for Ethiopia." *In: Sustaining the global farm. Selected papers of the International Soil Conservation Organization Conference*, pp. 979-993. West Lafayette, Indiana: Purdue University.
- Sujaul, I. M., Barzani, G. M., Ismail, B. S., Sahibin, A. R., and Ekhwan, T. M. (2012). "Estimation of the rate of soil erosion in the tasik chini catchment, Malaysia using the RUSLE model integrated with the GIS." *Australian Journal of Basic and Applied Sciences*, 6(12), 286-296.
- Tabari, H., Somee, B. S., and Zadeh, M. R. (2011). "Testing for long-term trends in climatic variables in Iran." *Atmospheric Research*, 100(1), 132-140.
- Taddese, G. (2001). "Land degradation: a challenge to Ethiopia." *Environmental management*, 27(6), 815-824.
- Tadege, A. (2007). "Climate change national adaptation program of action (NAPA) of Ethiopia." *National Meteorological Services Agency, Ministry of Water Resources, Federal Democratic Republic of Ethiopia*, Addis Ababa, 96pp.
- Tamene, L., Park, S. J., Dikau, R. and Vlek, P. L. G. (2006). "Analysis of factors determining sediment yield variability in the highlands of northern Ethiopia." *Geomorphology*, 76(1-2), 76-91.
- Tang, F.F., Xu, H.S. and Xu, Z.X. (2012). "Model calibration and uncertainty analysis for runoff in the Chao River Basin using sequential uncertainty fitting." *Procedia Environmental Sciences*, 13, 1760-1770.
- Taye, M. T., Ntegeka, V., Ogiramoi, N. P., and Willems, P. (2011). "Assessment of climate change impact on hydrological extremes in two source regions of the Nile River Basin." *Hydrology and Earth System Sciences*, 15(1), 209-222.
- Tiwari, A.K., Rissa, LM. Nearing, M.A. (2000). "Evaluation of WEPP and its comparison with USLE and RUSLE." *American Society of Agricultural Engineers*, 45 (5), 1129-1135.

Tufa, D. F., Abbulu, Y., and Rao, G. S. (2015). "Hydrological Impacts due to Land-Use and Land-Cover Changes of Ketar Watershed, Lake Ziway Catchment, Ethiopia." *International Journal of Civil Engineering and Technology*, 6(10), 36-45.

Ubierna, S. G., Martínez, M. A. C. and Ibarra, J. M. N. (2009). "USLE, RUSLE, and WEPP models use in mining restores hillslopes." In *Advances in studies on desertification: contributions to the International Conference on Desertification in memory of Professor Jo* (pp. 263-266). Universidad de Murcia.

Uddin, K., Murthy, M. S. R., Wahid, S. M. and Matin, M. A. (2016). "Estimation of Soil Erosion Dynamics in the Koshi Basin Using GIS and Remote Sensing to Assess Priority Areas for Conservation." *The public library of Science (PLoS) ONE*, 11(3), 1-19.

United States Departments of Agriculture (USDA). (2011). "National Agronomy Manual." *Natural resource conservation Service, 190-V-NAM, fourth Ed.*, February 2011 part 501. Washington, DC.

USAID. (2016). "Climate change risk in Ethiopia", *Country fact sheet*, 5pp.

Vano, J. A., Kim, J. B., Rupp, D. E., & Mote, P. W. (2015). "Selecting climate change scenarios using impact-relevant sensitivities." *Geophysical Research Letters*, 42(13), 5516-5525.

Vicuña, S., McPhee, J. and Garreaud, R. D. (2012). "Agriculture Vulnerability to Climate Change in a Snowmelt-Driven Basin in Semiarid Chile." *Journal of water resources planning and management*, 138 (5), 431-441.

Vilaysane, B., Takara, K., Luo, P., Akkharath, I. and Duan, W. (2015). "Hydrological stream flow modelling for calibration and uncertainty analysis using SWAT model in the Xedone river basin, Lao PDR." *Procedia Environmental Sciences*, 28, 380-390.

Wagesho, N., Jain, M. K. and Goel, N. K. (2013). "Effect of climate change on runoff generation: Application to Rift Valley Lakes Basin of Ethiopia." *Journal of Hydrologic Engineering*, 18(8), 1048-1063.

- Wagesho, N., Goel, N. K. and Jain, M. K. (2013). "Temporal and spatial variability of annual and seasonal rainfall over Ethiopia." *Hydrological Sciences Journal*, 58(2), 354-373.
- Wagner, P. D., Kumar, S., and Schneider, K. (2013). "An assessment of land-use change impacts on the water resources of the Mula and Mutha Rivers catchment upstream of Pune, India." *Hydrology and Earth System Sciences*, 17(6), 2233-2246.
- Wang, G., Xia, J., & Chen, J. (2009). Quantification of effects of climate variations and human activities on runoff by a monthly water balance model: A case study of the Chaobai River basin in northern China. *Water resources research*, 45(7), 1-12.
- Wang, B., Zheng, F., and Guan, Y. (2016). "Improved USLE-K factor prediction: A case study on water erosion areas in China." *International Soil and Water Conservation Research*, 4(3), 168-176.
- Wani, J. M., Sarda, V. K., & Jain, S. K. (2017). "Assessment of trends and variability of rainfall and temperature for the district of Mandi in Himachal Pradesh, India." *Slovak Journal of Civil Engineering*, 25(3), 15-22.
- WCED. (1987). "Our Common Future." Oxford: *Oxford University Press*, 300pp.
- Weldegebriel, Z. B. and Prowse, M. (2013). "Climate-Change Adaptation in Ethiopia: To What Extent Does Social Protection Influence Livelihood Diversification?" *Development Policy Review*, 31, 35-56.
- Welde, K. and Gebremariam, B. (2017). "Effect of land use land cover dynamics on the hydrological response of watershed: A case study of Tekeze Dam watershed, northern Ethiopia." *International Soil and Water Conservation Research*, 5(1), 1-16.
- Wigley, T. M. L., Jones, P. D., Briffa, K. R., & Smith, G. (1990). "Obtaining sub-grid-scale information from coarse-resolution general circulation model output." *Journal of Geophysical Research: Atmospheres*, 95(D2), 1943-1953.
- Williams, J.R. (1975). "Sediment-yield prediction with Universal Equation using runoff energy factor." 244-252 pp. In: *Present and Prospective Technology for*

Predicting Sediment Yield and Sources, United States Department of Agriculture. ARS- S40, Washington, D.C.

Wischmeier, W. H. and Smith D. D. (1965). "Predicting rainfall-erosion losses from cropland east of the Rocky Mountains." *Agricultural Handbook No. 282*: United States Department of Agriculture. Washington, D.C.

Wischmeier, W. H. and Smith, D. D. (1978). "Predicting rainfall erosion losses: a guide to conservation planning." *Agricultural Handbook No. 537*: United States Department of Agriculture. Washington, D.C, 67pp.

Wolanchu, K. W. (2012). "Watershed Management: An Option to Sustain Dam and Reservoir Function in Ethiopia." *Journal of Environmental Science and Technology*, 5 (5), 262-273.

Wolka, K., Tadesse, H., Garedew, E. and Yimer, F. (2015). "Soil erosion risk assessment in the Chaleleka wetland watershed, Central Rift Valley of Ethiopia." *Environmental Systems Research, a springer open journal*, 4 (5), 1-12.

Wondyrade, N. (2014). "GIS-based mapping of land cover changes utilizing multi-temporal remotely sensed image data in Lake Hawassa Watershed, Ethiopia." *Environmental Monitoring and Assessment*, 186 (3), 1765-1780.

World Bank. (2006). "Ethiopia: Managing water resources to maximize sustainable growth." Washington, DC, 119Pp.

World Bank. (2009). "Making development climate-resilient: A World Bank Strategy for Sub-Saharan Africa." *Report No. 46947-AFR*, Washington DC, The World Bank.

World Food Program (WFP). (2006). "Extensive flooding in Ethiopia: WFP update." United Nations WFP, Fighting Hunger Worldwide, 5pp.

WWDSE. (2001). "The study of lake Awassa level, lake Awassa study, and design project." *Water Works Design and Supervision Enterprise*, Addis Ababa.

Xu, Z. X., Chen, Y. N., & Li, J. Y. (2004). "Impact of climate change on water resources in the Tarim River basin." *Water Resources Management*, 18(5), 439-458.

Xu, C. Y. (1999). "Climate change and hydrologic models: A review of existing gaps and recent research developments." *Water Resources Management*, 13(5), 369-382.

- Yang, X., Ren, L., Liu, Y., Jiao, D., and Jiang, S. (2014). "Hydrological response to land use and land cover changes in a sub-watershed of West Liaohe River Basin, China." *Journal of arid land*, 6(6), 678-689.
- Yesuph, A. Y. and Dagne, A. B. (2019). "Soil erosion mapping and severity analysis based on the RUSLE model and local perception in the Beshillo Catchment of the Blue Nile Basin, Ethiopia." *Environmental Systems Research*, 8(1), 17.
- Yira, Y., Diekkrüger, B., Steup, G., and Bossa, A. Y. (2016). "Modeling land-use change impacts on water resources in a tropical West African catchment (Dano, Burkina Faso)." *Journal of Hydrology*, 537, 187-199.
- Younis, S. M. Z., and Ammar, A. (2018). "Quantification of the impact of changes in land use land cover on hydrology in the upper Indus Basin, Pakistan." *The Egyptian Journal of Remote Sensing and Space Science*, 21(3), 255-263.
- Yuan, L.F., Yang, G.S., Zhang Q.F. and Li, H.F. (2016). "Soil Erosion Assessment of the Poyang Lake Basin, China: Using USLE, GIS, and Remote Sensing." *Journal of Remote Sensing and GIS*, 5 (3), 1-12.
- Yue, S., Pilon, P. and Cavadias, G. (2002). "Power of the Mann–Kendall and Spearman's rho tests for detecting monotonic trends in hydrological series." *Journal of hydrology*, 259(1-4), 254-271.
- Zeleke, G. and Hurni, H. (2001). "Implications of land use and land cover dynamics for mountain resource degradation in the North-western Ethiopian highlands." *Mountain research and development*, 21(2), 184-191.
- Zeray, L., Roehrig, J. and Chekol, D. A. (2006). "Climate change impact on Lake Ziway watershed water availability, Ethiopia." In *Conference on International Agricultural Research for Development*, 1-4.
- Zhou, J., Liu, Y., Guo, H. and He, D. (2014). "Combining the SWAT model with sequential uncertainty fitting algorithm for streamflow prediction and uncertainty analysis for the Lake Dianchi Basin, China." *Hydrological Processes*, 28(3), 521-533.

Zhu, Y., Lin, Z., Wang, J., Zhao, Y. and He, F. (2016). "Impacts of climate changes on water resources in the Yellow River Basin, China." *12th International Conference on Hydro informatics, HIC. Procedia Engineering*, 154, 687-695.

LIST OF PUBLICATIONS

The following papers are published in journals/conference proceedings from the present study.

Publication in journals

1. Ketema, A. and Dwarakish, G. S. (2019). “Water erosion assessment methods: a review.” *ISH Journal of Hydraulic Engineering*, 1-8. DOI:10.1080/09715010.2019.1567398.
2. Ketema, A. and Dwarakish, G. S. (2020). “Trend and variability of hydro-meteorological variables of Tikur Wuha watershed in Ethiopia.” *Arabian journal of geoscience*, 13 (142), 1 - 20. DOI: 10.1007/s12517-020-5139-9.
3. Ketema, A. and Dwarakish, G. S. (2020). “Prioritization of sub-watersheds for conservation measures based on soil loss rate in Tikur Wuha watershed, Ethiopia.” *Arabian Journal of Geosciences*, 13(19), 1-16. DOI: 10.1007/s12517-020-06054-7.
4. Ketema, A. and Dwarakish, G. S. (2021). “Hydro-meteorological impact assessment of climate change on Tikur Wuha watershed in Ethiopia.” *Sustainable Water Resources Management*, 7(66), 1-20. DOI: 10.1007/s40899-021-00547-3.

International conference papers

1. Ketema, A. and Dwarakish, G. S. (2018). “Climate change impacts on water resource in Ethiopia.” *In Book of abstracts Hydro-2018 international conference (Hydraulics, Water Resources, and Coastal Engineering) NITP*, December 19-21, 2018, NIT Patna, India, pp 89.
2. Ketema, A. and Dwarakish, G. S. (2019). “Rainfall variability in Tikur Wuha Watershed, Ethiopia.” *In pros. Hydro-2019 international conference (Hydraulics, Water Resources, and Coastal Engineering) Osmania University*, December 18-20, 2019, Volume II, 3283 -3293. (ISBN-978-93-8935-484-3). Hyderabad, India.

Book Chapter

1. Ketema A. and Dwarakish, G. S. (2021) “Climate change impacts on water resource in Ethiopia.” *Jha et al. (eds.), In Book, Climate change impact on water resource, Water Science and Technology Library, Vol. 98, 62 – 69pp, Springer Nature, Switzerland AG Gewerbestrasse 11, 6330, Switzerland.*
https://doi.org/10.1007/978-3-030-64202-0_5



Name: Abiot Ketema

Date of Birth: 29-04-1980

Address: Hawassa University, Institute of Technology, Department of Biosystems Engineering, Hawassa Ethiopia, P.O. Box 05

Contact Details:

Mobile: +251916867171

+251904769596

E-mail: Ketemaabiot80@gmail.com

Professional Education:

Ph.D., Water Resources and Ocean Engineering

Thesis title: "Simulation of the hydrological impacts of climate and land use/cover change on Tikur Wuha watershed in Ethiopia"

National Institute of Technology Karnataka, India, 2021

Master of Science, Soil and Water Conservation Engineering, Hawassa University, Institute of Technology, Hawassa, 2012

Bachelor of Education in Physics, Dilla University, Department of Physics, Dilla, 2007

Diploma of Physics Education, Hawassa College of Teachers Education, Hawassa, 2003

Publications: Four journal papers, two conference proceedings, and one book chapter